



HAL
open science

Design of original vegetable oil-based cyclic carbonates and amines towards Poly(HydroxyUrethane)s

Océane Lamarzelle

► **To cite this version:**

Océane Lamarzelle. Design of original vegetable oil-based cyclic carbonates and amines towards Poly(HydroxyUrethane)s. Polymers. Université de Bordeaux, 2016. English. NNT: 2016BORD0267. tel-02003488

HAL Id: tel-02003488

<https://theses.hal.science/tel-02003488>

Submitted on 1 Feb 2019

HAL is a multi-disciplinary open access archive for the deposit and dissemination of scientific research documents, whether they are published or not. The documents may come from teaching and research institutions in France or abroad, or from public or private research centers.

L'archive ouverte pluridisciplinaire **HAL**, est destinée au dépôt et à la diffusion de documents scientifiques de niveau recherche, publiés ou non, émanant des établissements d'enseignement et de recherche français ou étrangers, des laboratoires publics ou privés.

THÈSE PRÉSENTÉE
POUR OBTENIR LE GRADE DE
DOCTEUR DE
L'UNIVERSITÉ DE BORDEAUX

ÉCOLE DOCTORALE DES SCIENCES CHIMIQUES

SPÉCIALITÉ: Polymères

Par Océane LAMARZELLE

**Design of original vegetable oil-based cyclic carbonates
and amines towards Poly(HydroxyUrethane)s**

**Conception de carbonates cycliques originaux et d'amines issus d'huiles
végétales pour la synthèse de Poly(HydroxyUréthane)s**

Sous la direction de : Pr. Henri, CRAMAIL

Co-encadrant : Dr. Etienne, GRAU

Soutenance prévue le 01 décembre 2016

Membres du jury :

M. ANDRIOLETTI, Bruno
M. DETREMBLEUR, Christophe
M. MICHAUD, Guillaume
M. TATON, Daniel
M. CRAMAIL, Henri
M. GRAU, Etienne
Mme. HILLAIRET, Caroline
M. CHOLLET, Guillaume

Professeur, Université Claude Bernard Lyon 1
Chercheur confirmé, Université de Liège
Docteur, Bostik
Professeur, Université de Bordeaux
Professeur, Université de Bordeaux
Docteur, Université de Bordeaux
Docteur, PIVERT
Docteur, ITERG

Rapporteur
Rapporteur
Examineur
Président du jury
Directeur de thèse
Co-encadrant
Invitée
Invité

*Happiness is not a station you arrive at,
but a manner of traveling...*

Margaret Lee Runbeck

Remerciements

Les travaux de thèse que j'ai menés pendant trois ans n'auraient jamais vu le jour sans l'aide de nombreuses personnes que je tiens à remercier.

Tout d'abord, je tiens à exprimer ma reconnaissance à M. Christophe Detrembleur, Chercheur confirmé à l'Université de Liège et à M. Bruno Andrioletti, Professeur à l'Université de Lyon 1 qui ont accepté de rapporter ces travaux de thèse, ainsi qu'à M. Daniel Taton, Professeur à l'Université de Bordeaux, pour avoir accepté de présider mon jury de thèse. Je tiens également à remercier M. Guillaume Michaud, Manager R&D chez Bostik, d'avoir apporté son point de vue industriel à ces travaux de thèse.

Je tiens particulièrement à exprimer ma gratitude à l'ensemble des membres du jury pour l'échange riche et instructif que nous avons eu lors de ma soutenance de thèse.

Je souhaiterais remercier la SAS PIVERT (*Picardie Innovation Végétales Enseignements et Recherches Technologiques*), organisme financier de ce projet de thèse ainsi que nos partenaires de l'ITERG (Centre technique et industriels des huiles et des corps gras), sans qui cette thèse ne se serait pas aussi bien déroulée. Je tiens à remercier plus particulièrement Caroline Hillairet, Chef de projet à la SAS PIVERT, Guillaume Chollet, Chef de projet à l'ITERG pour leur aide dans ces travaux et pour le bon relationnel entretenu tout au long de cette thèse.

Un très grand merci à Henri Cramail qui m'a donné l'opportunité de continuer le sujet de thèse de Lise Maisonneuve et d'y apporter ma touche personnelle. Merci pour la confiance que vous m'avez accordée pendant ces trois ans afin de représenter nos travaux dans de grands congrès internationaux et dans des journaux scientifiques. Merci pour les nombreuses discussions scientifiques (ou non-scientifiques), pour votre réconfort dans les moments difficiles et pour l'accompagnement dont vous avez fait preuve après ma soutenance, afin que je puisse trouver un emploi correspondant à mes attentes.

Un immense merci à Etienne Grau qui m'a encadrée tout au long de mes travaux de thèse. Ton aide a été pour moi très précieuse et je considère que cette thèse a pu voir le jour grâce à notre collaboration quotidienne. Comme tu l'as si bien dit lors de ma soutenance, les 1500 fois (et bien plus encore...) où j'ai frappé à ta porte (après avoir fait la queue bien sûr), m'ont permis de trouver des réponses, du réconfort et de la motivation dans les moments de doutes !!! Tu es un des seuls à avoir pu calmer mon stress parfois un peu excessif... Je me souviendrai toujours des idées « gavé cheloues » d'expériences du vendredi soir que tu nous suggérais mais qui malheureusement pour nous, ne marchaient pas souvent ... ! Bref !! Merci et encore merci !!! (Retiens tes larmes stp ^^ !)

Je tiens à souligner la participation de mes stagiaires de Licence et Master à ces travaux : Je remercie plus particulièrement Coraline Mattei pour l'optimisation de la synthèse d'amines sous air, Sergio Maldonado pour son travail sur la catalyse des NIPU et Alina Bordea pour sa forte implication dans le projet #SavOcé pour la synthèse de NIPU à partir de vanilline.

Je tiens également à exprimer ma reconnaissance à l'ensemble du personnel permanent du LCPO, notamment à Catherine, Dominique, Bernadette, Claude et Loïc qui participent quotidiennement au bon fonctionnement du laboratoire. Je remercie aussi tous les experts du LCPO qui nous aident et

permettent le fonctionnement optimal des appareils de mesures. Un grand merci à Gégé et Cédric pour leur gestion de la salle thermique et des TGA capricieuses, à Nico et Amélie pour les analyses SEC, à Eric pour la chromatographie flash (grande capricieuse également) et une dédicace spéciale à Anne-Laure pour m'avoir formée pendant de nombreuses heures à la technique RMN et pour avoir décrypté avec moi les spectres NIPU aux mille et un pics... ! Merci encore pour tous tes conseils avisés et pour toutes les discussions qu'on a pu avoir toutes les deux ☺

Je tiens à exprimer ma gratitude à Alain Soum et Cédric Le Coz, qui dès la classe prépa m'ont accueillie au LCPO pour un stage sur les plastiques biodégradables et m'ont ainsi transmis leur passion pour la chimie et la physico-chimie des polymères.

Je remercie toute la famille LCPO, doctorants, post-doctorants et stagiaires avec qui j'ai partagé de nombreux moments durant ces trois ans et qui sont, pour certains, devenus plus que des collègues ! Je remercie tout particulièrement mon binôme de prépa/école/thèse, dit Geogeo la patate, qui m'a très clairement supportée pendant 8 ans et surtout pendant ces trois dernières années !! T'es une machine Chouch et je suis très contente d'avoir pu partager cette expérience avec un fou comme toi. Certes ton rire ne me manquera pas, mais ta folie OUI !! 'La vie est une fête', ça c'est toi qui me l'as enseigné et je ne l'oublierai pas! Merci aussi à la grosse Lulu et au ptit keum Alex qui nous ont suivis tout au long de cette aventure de folichons, en France, en Espagne ou au Canada!!

Un très grand merci aux 'originels' dit également #, Lamberto et Garbouille, qui sont devenus de grands copains et qui m'ont énormément apporté dans mon quotidien au labo ! Merci encore pour tous les gars, j'avais beau être de l'école, vous n'avez pas hésité à m'accueillir dans votre cercle fermé de chimistes de la fac ! Une big dédicace au labo N1-36 (Best team ever: Lélé+PL+Geogeo+Océ) où on a pu pratiquer moult choses autres que de la chimie : le tabouret, la maniaquerie, la vaisselle, le rire, le Moscato show, la danse, le chant ('Hey nobody, loves me better than youuuuuuuuu'), les potins, la dermatologie, la dégustation d'huiles et j'en passe... Merci pour tous ces bons moments au labo mais aussi pour tous ceux passés à l'extérieur ☺ Merci Berto pour ces grands moments en DLS et en TEM et pour toutes les discussions plus ou moins intelligentes que nous avons eues!! Je n'ai qu'une (ou deux) choses à dire : Mouuuuuuu!!! Merci Ptit Sav', QP(PT), Martin, Boris et Fiona pour ces instants inoubliables dans le bureau de la folie (#SavOcé #horoscope #20minutes #labanqueducafé #çasentlafrite #feedly #GIF #mécanismemcpba), ça risque d'être bizarro dans mon futur bureau sans vous !!

Un grand merci à tous ceux que je n'ai pas encore cités : ElectroBrand, Hélène (#pauseclopede18h), Benji, Lucie, Bakka, Arthur, Ségo, Anna, Compiler, Ariane, Jeremie, Quentin, Audrey, Kévin, Olivia, Paul, Winnie, Edgar, Déborah, Julie, Dounia, Blandine, Estelle, Elise, Maud, Lise, Thomas, Prakash, Laurence, Amol, Loïc et bien d'autres encore ...

Enfin, je remercie de tout mon cœur tous mes amis qui m'ont soutenue pendant mes 8 ans d'étude ainsi que ma famille qui a toujours été d'un grand soutien malgré l'incompréhension complète de mon sujet de thèse ☺ ... (« Ma fille fait des polymères... !! »)

Et le meilleur pour la fin ...Un énorme MERCI à Kim (Chat) qui est resté à mes côtés sur cette longue route dont la thèse a fait partie, et sans qui je n'en serais pas là aujourd'hui tant sur le plan professionnel que personnel... Merci de m'avoir ramenée dans l'instant présent lorsque je m'en éloignais <3 ☺

General Table of Contents

List of abbreviations.....	11
Scientific Productions	12
Résumé	13
General Introduction	23
Chapter 1: State of the art: Towards isocyanate- and phosgene-free Poly(hydroxyurethane)s	29
Table of contents	30
Introduction	31
1. Routes towards bio-based amines	32
1.1. Synthesis of amines: generalities	33
1.2. Aerobic alcohol oxidation for the amine production.....	35
1.2.1. Alcohol oxidation into aldehyde intermediates	36
1.2.2. One-pot alcohol oxidation into nitrile intermediates	39
1.3. Amines from renewable resources	42
2. Cyclic carbonate syntheses	44
2.1. Synthesis of 5-membered cyclic carbonates (5CC).....	44
2.2. Synthesis of 6- to 8-membered cyclic carbonates (6CC- 8CC).....	47
2.3. Synthesis of bis-cyclic carbonates (bCC).....	49
3. Studies on the model cyclic carbonate/amine reaction	52
3.1. Mechanism of cyclic carbonate aminolysis.....	52
3.2. Kinetic and reaction conditions	53
3.3. Effect of the chemical structure of the amine.....	54
3.4. Effect of the substituent and size of the cyclic carbonate.....	55
3.5. Selectivity and by-products	57
3.6. Additives and catalysts for the cyclic carbonate/amine reaction.....	59
4. Thermoplastic Poly(hydroxyurethane)s (TPHUs)	61
4.1. Syntheses of PHUs and related molar masses	68
4.2. Selectivity and side reactions	70
4.3. Different reactivity for specific monomers	72
4.4. Thermo-mechanical properties and thermal stability of TPHUS	75
4.5. Towards bio-based PHUs	77
4.5.1. Vegetable oil-based cyclic carbonates to PHUs	77
4.5.2. Other bio-based cyclic carbonates to PHUs	81

Conclusions	83
References	84

Chapter 2: Bio-based amine synthesis through alcohol oxidation or thiol-ene “click” chemistry..... **91**

Table of contents	92
--------------------------------	-----------

Introduction	93
---------------------------	-----------

1. Bio-based amine synthesis via alcohol oxidation into nitrile..... **94**

1.1. Bio-based alcohol oxidation into nitrile under oxygen	95
1.2. Optimized oxidation of bio-based alcohols into nitrile under air	96
1.2.1. Copper catalyst screening	96
1.2.2. Copper ligand screening	98
1.2.3. Effect of temperature and pressure	99
1.2.4. Optimized system applied to other substrates	101
1.3. Heterogeneization of the catalysis: supported-TEMPO and Cu(0)	102
1.3.1. Supported catalysis using TEMPO-Si	102
1.3.2. Cu(0) additive	106
1.4. Bio-based diamines synthesis	108

2. Fatty acid-based amine via thiol-ene “click” chemistry..... **110**

2.1. Synthesis of fatty acid-based dienes.....	110
2.2. Thiol-ene coupling of fatty acid-based dienes with cysteamine.HCl.....	111

3. Comparison of the two routes..... **114**

Conclusions	117
--------------------------	------------

References	118
-------------------------	------------

Experimental and Supporting Information	119
--	------------

Chapter 3: Activated fatty acid- and glycerol-based cyclic carbonates towards Poly(hydroxyurethane)s synthesis..... **129**

Table of contents	130
--------------------------------	------------

Introduction	131
---------------------------	------------

1. Activated fatty acid-based cyclic carbonates towards PHUs..... **132**

1.1. Synthesis of activated lipidic cyclic carbonates.	132
1.1.1. Ether-activated monomers from epichlorohydrin	133
1.1.2. Ester-activated monomers from glycerol carbonate	135

1.1.3. Comparison between the two routes.....	136
1.2. Kinetic measurements and reactivity comparison.....	137
1.2.1. Comparison between activations.....	138
1.2.2. Impact of different parameters influencing the kinetics.....	140
1.2.3. Side reactions, by-products and selectivity.....	143
1.3. Poly(hydroxyurethane)s synthesis.....	146
2. Diglycerol dicarbonate as an activated monomer for PHUs.....	153
2.1. Monomer synthesis and characterization.....	154
2.1.1. Diglycerol carbonation toward DGDC.....	154
2.1.2. Characterization and properties.....	155
2.2. Poly(hydroxyurethane) synthesis and applications.....	158
2.2.1. DGDC-based PHUs with tunable properties varying diamine nature.....	158
2.2.2. PHUs from DGDC with different purity grade.....	162
2.2.3. DGDC-based copolymers.....	164
Conclusions.....	168
References.....	170
Experimental and Supporting Information.....	172

Chapter 4: Fatty acid-based sulfur-activated cyclic carbonates via thiol-ene “click” chemistry towards PHUs and post-functionalization..... 191

Table of contents.....	192
Introduction.....	193
1. Sulfur-activated cyclic carbonate synthesis and characterization.....	195
1.1. Sulfur-activated lipidic 5CC synthesis.....	195
1.2. Reactivity of sulfur-activated cyclic carbonates.....	198
1.3. Sulfone-activated CC and reactivity toward aminolysis.....	200
2. PHUs from sulfur-activated monomers: synthesis and post-functionalization.....	203
2.1. PHUs from sulfur activated monomers.....	203
2.2. Post-functionalization of sulfur-containing PHUs.....	207
2.2.1. Sulfonation.....	208
2.2.2. Sulfonium salts synthesis.....	211
Conclusions.....	214
References.....	215
Experimental and Supporting Information.....	216

Chapter 5: Potential solutions for the enhancement of cyclic carbonate reactivity towards amines: Catalysis and ‘ultra’-activated monomers	227
Table of contents	228
Introduction	229
1. Towards the catalysis of the cyclic carbonate-amine polyaddition	230
1.1. Screening of catalysts on the system DGDC-6cDA.....	230
1.2. Catalysis applied on lipidic activated-CC	235
2. ‘Ultra’-activated methyl acrylate-based cyclic carbonates towards PHUs and Poly(hydroxyurethane-amide-ester)s	236
2.1. Cyclic carbonates synthesis from methyl acrylate	237
2.1.1. <i>GECA synthesis</i>	237
2.1.2. <i>GECA and fatty acid-based monomer synthesis</i>	238
2.2. Kinetic study on GECA-based cyclic carbonate and side reactions.....	241
2.3. Polymerization of GECA and derivatives	245
2.3.1. <i>PHUs synthesis from GECA-based monomers</i>	245
2.3.2. <i>Poly(hydroxyurethane-amide-ester)s from GECA</i>	246
Conclusions	252
References	253
Experimental and Supporting Information	254
General Conclusions and Perspectives	263
Materials and Methods	267

List of abbreviations

Techniques:

COSY: Correlation Spectroscopy
DEPT: Distortionless Enhanced Polarization Transfer
DLS: Dynamic Light Scattering
DMA: Dynamic Mechanical Analysis
DSC: Differential Scanning Calorimetry
ESI: ElectroSpray Ionization
FTIR: Fourier Transformed InfraRed
GC: Gas Chromatography
HMBC: Heteronuclear Multiple Bond Correlation
HPLC: High Performance Liquid Chromatography
HSQC: Heteronuclear Single Quantum Coherence
MALDI-TOF: Time-Of-Flight Mass Spectrometer with Matrix-Assisted Laser Desorption/Ionization
NMR: Nuclear Magnetic Resonance
SEC: Size Exclusion Chromatography
TEM: Transmission Electron Microscopy
TGA: ThermoGravimetric Analysis
TOCSY: TOtal Correlation Spectroscopy
UV: Ultra-Violet

Chemicals

bpy: bipyridine
CALB: *Candida Antarctica* Lipase B
CDCl₃: deuterated chloroform
Cys.HCl: cysteamine hydrochloride
DABCO: 1,4-diazabicyclo[2.2.2]octane
DBTL: dibutyltin dilaurate
DBU: 1,8-diazabicyclo[5.4.0]undec-7-ene
DCM: dichloromethane
DETA: diethylenetriamine
DMAC: dimethylacetamide
DMAP: 4-dimethylaminopyridine
DMC: dimethyl carbonate
DMPA: 2,2-dimethoxy-2-phenylacetophenone
DMF: dimethylformamide
DMSO: dimethylsulfoxide
EDA: ethylene diamine
Et₃N: triethylamine
EtOH: ethanol
HCl: hydrochloric acid
HFIP: hexafluoroisopropanol
HMDA: hexamethylenediamine
IPDA: isophorone diamine
mCPBA: *meta*-chloroperbenzoic acid
MeCN: acetonitrile
MeOH: methanol
p-(Me)bpy: 4,4'-dimethyl-2,2'-bipyridyl
MTBD: 7-methyl-1,5,7-triazabicyclo[4.4.0]dec-5-ene

NMI: N-methylimidazole
PEG: polyethylene glycol
PPG: polypropylene glycol
PTMO: poly(tetramethylene oxide)
TBABr: tetrabutylammonium bromide
TBAI: tetrabutylammonium iodide
TBD: 1,5,7-triazabicyclododecene
TCB: 1,2,4-trichlorobenzene
TEMPO: 2,2,6,6-tetramethyl-1-piperidinyloxy, free radical
TFA: trifluoroacetic acid
THF: tetrahydrofuran
TMC: trimethylene carbonate
TU: thiourea

Characteristic parameters

Đ: dispersity
DP_n: polymerization degree
ΔH: enthalpy
E_a: activation energy
k_{app}: apparent reaction rate constant
M_n: number average molar mass
M_w: mass average molar mass
PDI: polydispersity index (in DLS)
RT: room temperature
T: temperature
T_{5%}: temperature corresponding to 5 w.% loss
T_g: glass transition temperature
T_m: melting temperature

Polymerization techniques

ADMET: acyclic diene metathesis
ROP: ring-opening polymerization

Others

bCC: bis-cyclic carbonate
bxCC: x-membered bis-cyclic carbonate
CC: cyclic carbonate
xCC: x-membered cyclic carbonate
ESI†: Experimental and Supporting Information
HU: hydroxyurethane
NIPU: Non-Isocyanate Polyurethanes
PA: polyamides
PHU: poly(hydroxyurethane)
PLA: poly(lactic acid)
PS: polystyrene
PU: polyurethane
TPHU: thermoplastic poly(hydroxyurethane)
TPU: thermoplastic polyurethane

Scientific Productions

Publications and patents

- O. Lamarzelle, P.-L. Durand, A.-L. Wirotius, G. Chollet, E. Grau, H. Cramail, Activated lipidic cyclic carbonates for non-isocyanate polyurethane synthesis, *Polymer Chemistry*, **2016**, 7, 1439-1451
- L. Maisonneuve, O. Lamarzelle, E. Rix, E. Grau, H. Cramail, Isocyanate-Free Routes to Polyurethanes and Poly(hydroxy Urethane)s, *Chemical Reviews*, **2015**, 115 (22), 12407–12439
- G. Hibert, O. Lamarzelle, L. Maisonneuve, E. Grau, H. Cramail, Bio-based aliphatic primary amines from alcohols through the ‘Nitrile route’ towards non-isocyanate polyurethanes, *European Polymer Journal*, **2016**, 82, 114-121.

Communications

Posters

O. Lamarzelle, E. Grau, H. Cramail, *Activated lipidic cyclic carbonates for NIPU synthesis*

- **17^{ième} journée Ecole Doctorale des Sciences Chimiques (EDSC)**, Talence, April 16 (2015)
- **International Symposium on Ionic Polymerization (IP15)**, Bordeaux, July 5-10 (2015)
- **Warwick Polymer Conference 2016**, Warwick, England, July 11-14 (2016)

Oral Presentations

O. Lamarzelle, E. Grau, H. Cramail, *Activated lipidic cyclic carbonates for NIPU synthesis*

- **3rd International Symposium on Green Chemistry**, La Rochelle, May 3-7 (2015)
- **JIP-JEPO 2015**, San Sebastian, Spain, September 14-18 (2015)
- **Colloc FGL 2016**, « Chimie et Procédés du Végétal », Montpellier, January 27-29 (2016)

O. Lamarzelle, L. Maisonneuve, E. Grau, H. Cramail, *Fully bio-based Non-isocyanate Polyurethanes (NIPU) via cyclic carbonate/amine route.*

N.I.C.E., “The 3rd International Conference on Bioinspired and Biobased Chemistry & Materials”, Nice, October 16-19 (2016)

Résumé

Conception de nouveaux carbonates cycliques et amines issus d'huiles végétales pour la synthèse de poly(hydroxyuréthane)s

Cette thèse porte sur la synthèse de carbonates cycliques et d'amines à partir d'huiles végétales, utilisés comme monomères pour l'obtention de poly(hydroxyuréthane)s thermoplastiques plus respectueux de l'environnement.

Les polymères représentent une importante classe de matériaux trouvant d'innombrables applications dans des domaines tels que l'emballage, l'automobile, le bâtiment, les sports et loisirs, l'industrie textile, etc. Selon *Plastic Europe*, la production mondiale a atteint 311 millions de tonnes en 2014 ¹ dont 39.5% alloués au domaine de l'emballage. De plus, la production de plastique utilise 7% du pétrole produit sur une année.² Cependant, la raréfaction des ressources fossiles ainsi que la fluctuation du prix du baril de pétrole représentent un frein majeur à la pérennité de la production de polymères synthétiques. Au regard du « Développement Durable » et de la limitation des émissions de gaz à effet de serre, des efforts sont actuellement engagés afin de remplacer les ressources pétrolières par des matériaux d'origine renouvelable. Dans ce contexte, la biomasse est considérée comme l'unique ressource de carbones renouvelables disponible sur Terre. Le temps de régénération de ce carbone renouvelable est évalué en dizaines d'années contrairement à celui issu des ressources fossiles qui se compte en quelques millions d'années !³

Ces dix dernières années, de nombreux chercheurs ont synthétisé des « plastiques » bio-sourcés, afin de répondre aux besoins futurs qui sont en adéquation avec une chimie plus durable. Plus particulièrement, l'utilisation de la biomasse comme plateforme pour la synthèse de polymères 'verts' a été envisagée suivant deux stratégies : (i) la modification chimique de bio-polymères disponibles tels que la cellulose, la lignine ou l'amidon,⁴ (ii) la synthèse de polymères à partir de monomères issus de la déconstruction ou de l'extraction de la biomasse.⁵⁻⁷

Parmi les bio-ressources disponibles, les huiles végétales représentent une plateforme d'intérêt pour le développement de nouveaux synthons, précurseurs de polymères bio-sourcés. En effet, la raffinerie de ces huiles conduit à l'obtention de glycérol et d'esters d'acides gras.

Ces derniers contiennent une densité importante de fonctions telles que des insaturations, des esters ou des alcools qui peuvent être directement utilisés ou dérivatisés pour la synthèse de monomères.

Parmi les différents « plastiques » disponibles, les Polyuréthanes (PUs) représentent une classe importante de polymères de spécialité. Ils sont principalement utilisés dans la synthèse de mousses flexibles ou rigides ainsi que dans la formulation d'adhésifs. La voie classique d'accès aux polyuréthanes est la polyaddition entre (poly)alcools et (poly)isocyanates (Schéma 1). Cette synthèse est hautement compétitive d'un point de vue industriel du fait de la disponibilité des précurseurs et de la grande sélectivité de la réaction.⁸ Pour ce faire, plusieurs catalyseurs sélectifs de la réaction alcool/isocyanate tels le dilaurate de dibutyl étain (DBTL) ou les additifs à base de mercure sont couramment utilisés pour la synthèse de PUs. Depuis la mise en place de la norme REACH, la recherche académique ainsi que les industries chimiques se doivent de remplacer les composés chimiques et les procédés dangereux par des alternatives plus « vertes ». De ce fait, les isocyanates qui sont directement produits à partir d'un gaz toxique, le phosgène, doivent être substitués. Pour atteindre cet objectif, de plus en plus de groupes de recherche focalisent leurs investigations sur des voies d'accès à des polyuréthanes, sans employer de phosgène ni d'isocyanate. Les polyuréthanes sans isocyanate peuvent par exemple être synthétisés par transuréthanisation de carbamates et d'alcools ou par copolymérisation d'aziridines et de dioxyde de carbone.

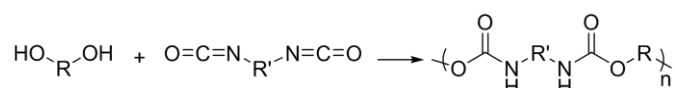


Schéma 1- Synthèse de polyuréthanes via la polyaddition entre diols et diisocyanates.

La polyaddition de (poly)carbonates cycliques à 5 chaînons et de (poly)amines (Schéma 2) est une des voies les plus étudiées et peut être des plus prometteuses pour la synthèse de polyuréthanes plus durables.⁹ L'aminolyse des carbonates cycliques conduit à la formation d'hydroxyuréthanes possédant des groupements hydroxyle pendants. La structure inhérente des PHUs leur confère des propriétés d'hydrophilicité et permet également une post-fonctionnalisation générant de nouvelles propriétés.

Le principal inconvénient de la polyaddition carbonate/amine est la faible réactivité des carbonates cycliques à 5 chaînons vis-à-vis des amines, amenant à l'obtention de PHUs de faibles masses molaires, présentant des propriétés thermo-mécaniques insuffisantes. En effet,

la cinétique de polymérisation n'est pas assez rapide et n'est donc pas compétitive en comparaison à la voie alcool/isocyanate. De plus, les conversions en fonctions carbonates sont généralement incomplètes et entraînent la présence de monomères résiduels dans les matériaux. Ce phénomène est directement lié à la stabilité et au manque de réactivité des carbonates cycliques à 5 chaînons. Un des exemples les plus révélateurs est celui des carbonates cycliques issus d'acides gras synthétisés à partir de l'époxydation/carbonatation des insaturations. En effet, ces derniers sont stabilisés par l'effet électronique inductif positif des chaînes aliphatiques situées en α des cycles, réduisant ainsi leur réactivité¹⁰ et nécessitant des conditions de polymérisation plus rudes ($T > 130^\circ\text{C}$, 1 semaine).

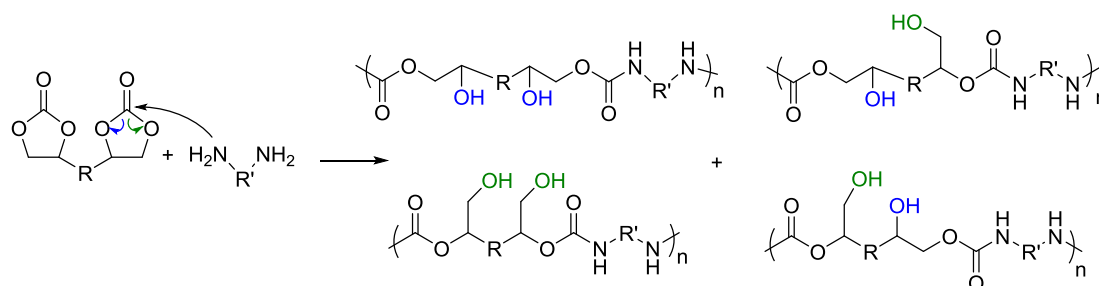


Schéma 2- Synthèse de poly(hydroxyuréthane) via la polyaddition de diamines et de bis-carbonates cycliques.

Plusieurs solutions ont été proposées pour contourner ce problème. Premièrement, la synthèse de carbonates cycliques à 6, 7 and 8 chaînons a permis l'obtention de monomères possédant une tension de cycle plus élevée et donc une meilleure réactivité vis-à-vis des amines.¹¹⁻¹⁴ Cependant, leur instabilité à température ambiante est un frein pour leur stockage à l'échelle industrielle. Une autre stratégie consiste en l'insertion d'un groupement à effet inductif négatif en α ou β du carbonate cyclique à 5 chaînons permettant de le rendre plus réactif vis-à-vis des amines.¹⁵⁻¹⁸ Cette stratégie représente un des objectifs majeurs de cette thèse. D'autre part, la catalyse de la voie carbonate/amine est une voie envisageable pour l'amélioration de la cinétique de polymérisation.

Dans le contexte d'une chimie plus durable, la préparation de précurseurs bio-sourcés pour la synthèse de polymères est de plus en plus étudiée. Plusieurs groupes de recherche ont conçu des carbonates cycliques à partir de ressources renouvelables pour la synthèse de PHUs.¹⁹⁻²⁴ Cependant, la synthèse de ces derniers est freinée par le manque d'amines aliphatiques bio-sourcées commerciales. Seulement quelques industriels comme CRODA, Evonik ou BASF commercialisent des amines issues de la biomasse. En outre, des efforts sont nécessaires pour étendre cette plateforme de molécules présentant un large spectre d'applications.

Cette thèse se déroule dans le cadre du projet NIPU (WP3P8) financé par la SAS PIVERT,²⁵ impliquant le *Laboratoire de Chimie des Polymères Organiques* (LCPO) et le *Centre Technique Industriel des Huiles et Corps Gras* (ITERG, Pessac, France). Le partenariat entre l'ITERG et la SAS PIVERT a permis l'accès à des ressources renouvelables telles que les acides gras et leurs dérivés, dans le but de synthétiser des PHUs plus respectueux de l'environnement.

Cette thèse porte sur la conception de précurseurs oléo-sourcés pour la synthèse de polyuréthanes thermoplastiques sans phosgène ni isocyanate. Une plateforme d'amines bio-sourcées a tout d'abord été développée. La synthèse de carbonates cycliques substitués à 5 chaînons à partir d'acides gras a également été entreprise afin d'améliorer la cinétique de polyaddition entre carbonate et amine et d'obtenir une polymérisation compétitive en comparaison à la voie alcool/isocyanate.

Ce manuscrit est divisé en cinq chapitres. Le premier chapitre illustre l'état de l'art concernant les polyuréthanes sans isocyanate ni phosgène et se focalise plus particulièrement sur la polyaddition carbonate cyclique/amine. Dans un premier temps, les différentes voies d'accès aux amines sont exposées. Une attention particulière est portée à l'oxydation des alcools primaires en nitriles, permettant l'accès à des amines *via* une unique étape supplémentaire d'hydrogénation. Cette voie de synthèse représente un intérêt particulier du fait des conditions douces et des composés chimiques utilisés. D'autres voies telles que la métathèse croisée entre l'acrylonitrile et des dérivés d'acides gras ou la chimie thiol-ène de la cystéamine et de dérivés insaturés bio-sourcés sont aussi décrites. Dans une deuxième partie, la synthèse de différents types de carbonates cycliques ainsi que leur réactivité vis-à-vis des amines sont rapportées. L'influence des conditions de réaction et de la structure des monomères sur la réaction modèle carbonate/amine est exposée et permet de mieux comprendre les objectifs de cette thèse. La sélectivité et la catalyse de cette réaction sont également détaillées. Enfin, les travaux traitant de la synthèse de poly(hydroxyuréthanes)s et de leurs propriétés (masses molaires, propriétés thermomécaniques et autres) sont rapportés et permettent de dégager les points-clés nécessaires aux progrès de la chimie des PHUs. La dernière partie de l'état de l'art couvre les travaux de recherche concernant les PHUs synthétisés à partir de ressources renouvelables telles que le glycérol, la vanilline ou encore les huiles végétales.

Fort de cet état de l'art, cette thèse a été développée suivant trois grands axes : (i) la synthèse d'amines issues de ressources renouvelables, à partir de procédés respectueux de

l'environnement, (ii) la conception de carbonates cycliques substitués à 5 chaînons à partir d'huiles végétales et (iii) la synthèse et caractérisation de PHUs entièrement bio-sourcés.

Le Chapitre 2 de ce manuscrit couvre les accomplissements associés à la synthèse d'amines aliphatiques bio-sourcées à partir d'huiles de ricin et de colza (Schéma 3).

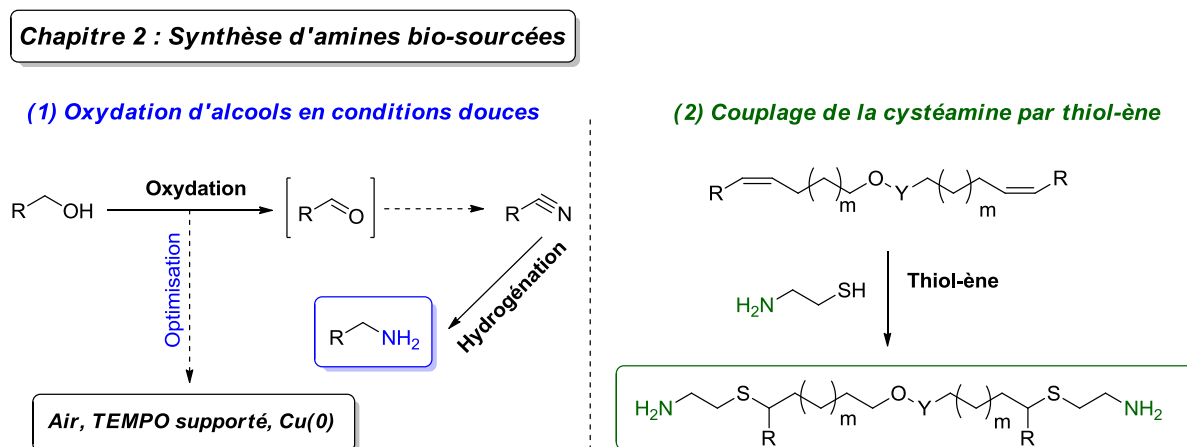


Schéma 3- Synthèses d'amines bio-sourcées par oxydation d'alcools et par chimie thiol-ène.

Dans un premier temps, la préparation de (di)amines a été conduite *via* l'oxydation sous oxygène des alcools correspondants en (di)nitriles, catalysée par le système TEMPO/cuivre, suivie d'une étape d'hydrogénation. L'étape d'oxydation a été optimisée de façon à rendre la synthèse plus verte et transposable à l'échelle industrielle. Pour ce faire, de l'air sous pression a été employé comme oxydant et l'hétérogénéisation du catalyseur *via* l'utilisation d'un TEMPO supporté sur silice ou l'addition de Cu(0) a été réalisée. Dans un deuxième temps, la synthèse d'amines primaires aliphatiques dérivées d'acide gras a été entreprise. Des diènes synthétisés par la dimérisation de deux dérivés d'acides gras ont été couplés par chimie thiol-ène à la cystéamine, elle-même issue de bio-ressources. Des monomères de structures très différentes ont donc été synthétisés par des voies respectueuses de l'environnement. Lorsque ces deux voies d'accès sont comparées en utilisant les 12 principes de la « Chimie Verte », l'oxydation des alcools en nitriles pour l'obtention d'amines renouvelables apparaît être la voie la plus durable et transposable à de nombreux alcools bio-sourcés.

Les chapitres 3, 4 et 5 exposent les résultats expérimentaux concernant la conception de carbonates cycliques plus réactifs à partir de dérivés oléagineux, pour la synthèse de PHUs (Schéma 4). Pour ce faire, plusieurs voies de synthèse ont été envisagées afin d'accéder à des

carbonates cycliques substitués par différentes fonctionnalités. Dans chaque cas, la chimie mise en œuvre implique les fonctions présentes sur les dérivés d'acides gras tels que les insaturations, les alcools, les esters, les acides et d'autres (composés bromés, tosylés, ...) ainsi que différents composés dérivés du glycérol (épichlorohydrine, carbonate de glycérol, diglycérol, thioglycérol, acrylate de méthyle).

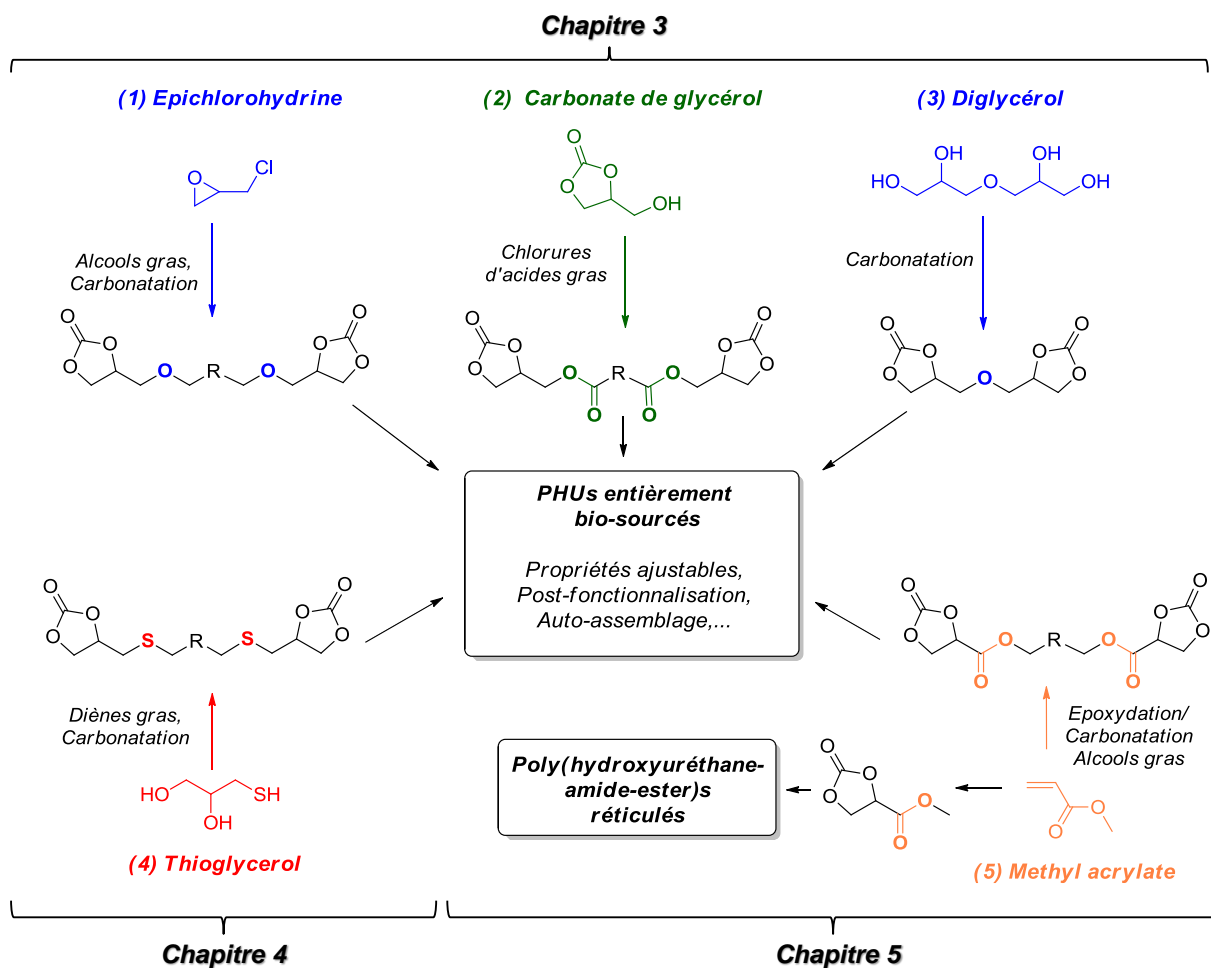


Schéma 4- Synthèses de carbonates cycliques substitués à 5 chaînons à partir de dérivés d'acides gras et de glycérol.

Une première plateforme de carbonates cycliques substitués en β par une fonction éther ou ester a été développée à partir de dérivés d'acides gras et de glycérol. Plus précisément, la fonction éther a été apportée au squelette lipidique *via* la substitution nucléophile de l'épichlorohydrine et d'un alcool gras, suivie d'une carbonatation sous CO_2 pressurisé. Concernant les carbonates substitués par une fonction ester, ils ont été conçus à partir de chlorure d'acides gras et du carbonate de glycérol. L'augmentation de la réactivité de ces carbonates cycliques vis-à-vis des amines a été mesurée par RMN et comparée à celle de carbonates réactifs (carbonates à 6 chaînons) et de carbonates cycliques gras non-substitués.

La fonction ester apporte une réelle amélioration dans la cinétique d'addition, à la fois dans le cas des réactions modèles et des polymérisations. Une attention particulière a été portée à l'étude des réactions secondaires comme l'uréthanisation, la formation d'oxazolidinones ou d'amides. Par exemple, les carbonates cycliques activés par une fonction ester sont sujets à des réactions secondaires d'amidation qui occasionnent une baisse des masses molaires des PHUs. D'une façon plus générale, la polymérisation de ces carbonates cycliques bio-sourcés avec diverses diamines a permis d'obtenir des PHUs de masses molaires allant jusqu'à 33200 g.mol⁻¹ avec des dispersités comprises entre 1.5 and 3.7.

Un monomère particulier issu de la carbonatation du diglycérol a également été synthétisé dans ce chapitre. Le DGDC, bis-carbonate cyclique substitué par une fonction éther, a permis l'obtention de PHUs montrant des propriétés physico-chimiques variables selon le comonomère utilisé. Des PHUs hydrosolubles ou pouvant s'auto-assembler dans l'eau ont été caractérisés et ouvrent des perspectives intéressantes dans le domaine des polyuréthanes sans isocyanate.

Dans la continuité du chapitre précédent, le Chapitre 4 détaille la synthèse de bis-carbonates cycliques à 5 chaînons possédant une fonction thio-éther en position β . Pour ce faire, les diènes dérivés d'acides gras utilisés dans le Chapitre 2 pour la synthèse d'amines primaires bio-sourcées ont été couplés par chimie thiol-ène au thioglycérol. Les tétraols résultant ont ensuite été carbonatés puis utilisés en polymérisation avec des diamines. A l'instar des effets de la fonction éther, la fonction thio-éther en β d'un carbonate cyclique rend ce dernier plus réactif vis-à-vis des amines. En tirant profit de la présence d'atomes de soufre dans les monomères synthétisés, la post-fonctionnalisation des PHUs résultants a été entreprise *via* la sulfonation et la synthèse de sels de sulfonium par la réaction d'époxydes avec les fonctions thio-éther du squelette polymère. Ces travaux préliminaires ont montré la possibilité d'ajuster les propriétés des PHUs par l'insertion de différents groupements sulfoniums, en utilisant des époxydes fonctionnalisés.

Dans un dernier temps, des recherches préliminaires concernant les solutions potentielles au manque de compétitivité de la voie carbonate/amine ont été menées. La catalyse de la réaction d'aminolyse des carbonates cycliques substitués à 5 chaînons a été considérée et l'effet de plusieurs types de catalyseurs incluant des bases et des acides de Lewis a été analysé. Les catalyseurs les plus efficaces se sont avérés être les bases de Lewis et ont été testés sur la

polymérisation des carbonates cycliques substitués dérivés d'acides gras. Les résultats obtenus montrent l'intolérance des fonctions ester « activantes » aux bases de Lewis, favorisant la réaction secondaire de transamidation et diminuant de façon conséquente la masse molaire des PHUs.

Comme dans les chapitres précédents, une deuxième stratégie visant à la modification de la structure du carbonate cyclique dans le but d'abaisser sa stabilité et d'augmenter sa réactivité vis-à-vis des amines a été adoptée. En effet, en procédant à l'époxydation/carbonatation de l'acrylate de méthyle, il est possible d'insérer un groupement ester en position α du carbonate cyclique. L'acrylate de méthyle carbonaté a été greffé à des alcools issus d'acides gras *via* une transesterification enzymatique. Ces carbonates cycliques ont montré une réactivité exacerbée vis-à-vis des amines. Cependant, la réaction de transamidation sur la fonction ester présente en α est favorisée et ne permet pas l'accès à des PHUs de hautes masses molaires. Cette réaction secondaire a ensuite été utilisée en polymérisant l'acrylate de méthyle carbonaté, monomère de type AA*, avec des diamines ou des amino-alcools en présence de TBD. Des polymères de type poly(hydroxyuréthane-amide-ester)s ont été obtenus et ont montré des propriétés variables selon le comonomère utilisé. Des réseaux tridimensionnels présentant des températures de transitions vitreuses allant jusqu'à 74°C et des taux de gonflement dans le DMF compris entre 90 et 764% ont pu être synthétisés lorsque les diamines les plus réactives ont été polymérisées avec l'acrylate de méthyle carbonaté.

En conclusion, ces travaux de thèse ont permis l'accès à une plateforme d'amines dérivées d'acides gras *via* deux types de synthèse, toutes deux respectueuses de l'environnement. Différents types de carbonates cycliques substitués par des fonctions éther, ester ou thio-éthers en β ou en α , ont également été conçus afin d'exacerber leur réactivité vis-à-vis des amines. L'analyse de la cinétique et des réactions secondaires pouvant avoir lieu durant la formation d'hydroxyuréthanes a été menée pour les différents carbonates synthétisés. Ces derniers ont été polymérisés avec des diamines, certaines provenant de la plateforme développée dans cette thèse, pour l'obtention de polyuréthanes bio-sourcés sans isocyanate ni phosgène possédant des propriétés modulables.

Afin d'assurer le transfert de la voie carbonate/amine à l'échelle industrielle et d'égaliser la voie alcool/isocyanate, il est nécessaire de poursuivre les recherches. La conception de catalyseurs sélectifs à l'ouverture de cycle des carbonates par des amines reste encore un sujet majeur. L'impact des procédés de polymérisation sur les matériaux obtenus, ainsi que l'analyse détaillée de leurs propriétés thermo-mécaniques sont de futures orientations à

considérer afin de valider le fort potentiel économique des polyuréthanes sans isocyanate (NIPU).

References

- (1) PlasticsEurope. *PlasticsEurope* **2015**, 1–34.
- (2) Mülhaupt, R. *Macromol. Chem. Phys.* **2013**, *214* (2), 159–174.
- (3) Okkerse, C.; van Bekkum, H. *Green Chem.* **1999**, *1* (2), 107–114.
- (4) Wang, C.; Kelley, S. S.; Venditti, R. A. *ChemSusChem* **2016**, 1–15.
- (5) Delidovich, I.; Hausoul, P. J. C.; Deng, L.; Pfützenreuter, R.; Rose, M.; Palkovits, R. *Chem. Rev.* **2016**, *116* (3), 1540–1599.
- (6) Wilbon, P. A.; Chu, F.; Tang, C. *Macromol. Rapid Commun.* **2013**, *34* (1), 8–37.
- (7) Maisonneuve, L.; Lebarbe, T.; Grau, E.; Cramail, H. *Polym. Chem.* **2013**, *4* (22), 5472–5517.
- (8) Engels, H. W.; Pirkl, H. G.; Albers, R.; Albach, R. W.; Krause, J.; Hoffmann, A.; Casselmann, H.; Dormish, J. *Angew. Chemie* **2013**, *52* (36), 9422–9441.
- (9) Maisonneuve, L.; Lamarzelle, O.; Rix, E.; Grau, E.; Cramail, H. *Chem. Rev.* **2015**, *115* (22), 12407–12439.
- (10) Maisonneuve, L.; More, A. S.; Foltran, S.; Alfoss, C.; Robert, F.; Landais, Y.; Tassaing, T.; Grau, E.; Cramail, H. *RSC Adv.* **2014**, *4* (49), 25795–25803.
- (11) Maisonneuve, L.; Wirotius, A.-L.; Alfoss, C.; Grau, E.; Cramail, H. *Polym. Chem.* **2014**, *5*, 6142–6147.
- (12) Tomita, H.; Sanda, F.; Endo, T. *J. Polym. Sci. Part A Polym. Chem.* **2001**, *39* (6), 860–867.
- (13) Tomita, H.; Sanda, F.; Endo, T. *J. Polym. Sci. Part A Polym. Chem.* **2001**, *39* (23), 4091–4100.
- (14) Yuen, A.; Bossion, A.; Gómez-Bengoña, E.; Ruipérez, F.; Isik, M.; Hedrick, J. L.; Mecerreyes, D.; Yang, Y. Y.; Sardon, H. *Polym. Chem.* **2016**, *7* (11), 2105–2111.
- (15) Tomita, H.; Sanda, F.; Endo, T. *J. Polym. Sci. Part A Polym. Chem.* **2001**, *39* (21), 3678–3685.
- (16) Garipov, R. M.; Sysoev, V. A.; Mikheev, V. V.; Zagidullin, A. I.; Deberdeev, R. Y.; Irzhak, V. I.; Berlin, A. Al. *Dokl. Phys. Chem.* **2003**, *393* (1–3), 289–292.
- (17) Lamarzelle, O.; Durand, P.-L.; Wirotius, A.-L.; Chollet, G.; Grau, E.; Cramail, H. *Polym. Chem.* **2016**, *7*, 1439–1451.
- (18) He, Y.; Goel, V.; Keul, H.; Möller, M. *Macromol. Chem. Phys.* **2010**, *211* (22), 2366–2381.
- (19) Foltran, S.; Maisonneuve, L.; Cloutet, E.; Gadenne, B.; Alfoss, C.; Tassaing, T.; Cramail, H. *Polym. Chem.* **2012**, *3* (2), 525–532.
- (20) van Velthoven, J. L. J.; Gootjes, L.; van Es, D. S.; Noordover, B. A. J.; Meuldijk, J. *Eur. Polym. J.* **2015**, *70*, 125–135.
- (21) Carré, C.; Zoccheddu, H.; Delalande, S.; Pichon, P.; Avérous, L. *Eur. Polym. J.* **2016**.
- (22) Besse, V.; Auvergne, R.; Carlotti, S.; Boutevin, G.; Otazaghine, B.; Caillol, S.; Pascault, J.-P.; Boutevin, B. *React. Funct. Polym.* **2013**, *73* (3), 588–594.
- (23) Proempers, G.; Keul, H.; Hoecker, H. *Des. Monomers Polym.* **2005**, *8* (6), 547–569.
- (24) Chen, Q.; Gao, K.; Peng, C.; Xie, H.; Zhao, Z. K.; Bao, M. *Green Chem.* **2015**, *17*, 4546–4551.
- (25) Institut PIVERT-<http://www.institut-pivert.com/>.

General Introduction

Polymers represent a huge class of materials employed in many domains such as packaging, automotive, construction, textile industry, etc. According to *PlasticsEurope*, the worldwide production reached 311 million tons in 2014¹ with 39.5% devoted to the packaging. Besides, the production of ‘plastics’ consumes 7% of the global oil resources annually produced.² However, the scarcity of fossil resources and the fluctuation of the barrel price represent issues to the synthetic plastic production durability. In the current context of sustainable chemistry together with the obligation to limit green house gas emissions, an effort is currently made to replace oil-based resources by renewable ones.

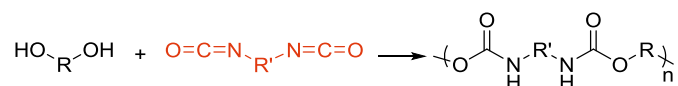
In this framework, biomass appears to be the only available resource of renewable carbon on Earth. Its regeneration time is evaluated in decades contrarily to the one of fossil resources that can reach several million years.³

In the last decades, numerous research teams achieved the synthesis of green and bio-based plastics⁴ to tackle the future needs, in agreement with a sustainable development. The use of biomass for the synthesis of polymers has been investigated following two main strategies: (i) the modification of available biopolymers such as cellulose, lignin or starch,⁵ (ii) the synthesis of polymers from building-blocks derived from biomass deconstruction or extraction.⁶⁻⁸

In the midst of the available bio-resources, vegetable oils appear as an interesting platform for the development of new building blocks for the design of polymers. Indeed, the triglyceride transesterification leads to the production of glycerol and fatty esters. These latter display a high content of functionalities such as unsaturation, ester or alcohol functions that can be directly used or derivatized for the preparation of monomers.

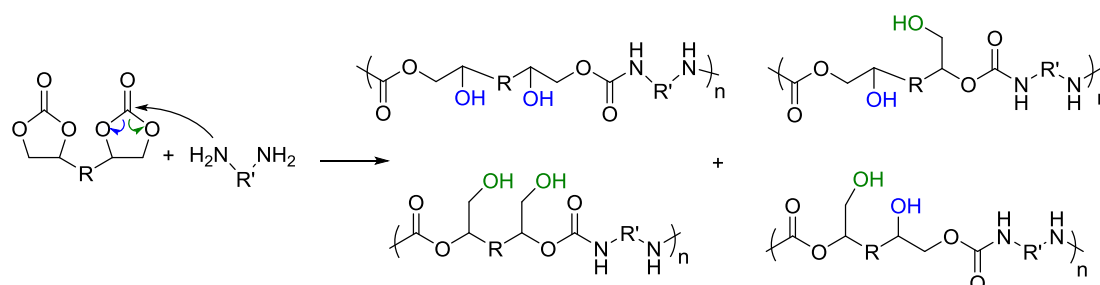
Among the different available plastics, Polyurethanes (PUs) represent an important class of specialty polymers principally produced as flexible or rigid foams and adhesives. They represented 5% of the global plastic market in 2014. PUs are classically prepared by the polyaddition between (poly)alcohols and (poly)isocyanates (see Scheme 1). This route is very competitive at the industrial scale as the precursors are largely available and the selectivity of the reaction is very efficient.⁹ For instance, several selective catalysts to the reaction between alcohol and isocyanate such as dibutyltin dilaurate (DBTL) or mercury-based compounds are currently used in PU preparation. Since the new REACH regulation was edited few years ago, research groups and industries need to replace hazardous chemicals and harsh reaction

conditions by greener intermediates and processes. Therefore, the harmful isocyanates that are themselves produced from the toxic phosgene, have to be circumvented. In this purpose, an increasing number of research groups investigate different routes to prepare PUs without employing isocyanate or phosgene. Non Isocyanate PolyUrethanes (NIPUs) have been synthesized by transurethanization using carbamates and alcohols as precursors or by copolymerization of aziridines with carbon dioxide, for instance.



Scheme 1- Polyurethane synthesis *via* the polyaddition of diols and diisocyanates.

Polyaddition of (poly) 5-membered ring cyclic carbonates and (poly)amines (see Scheme 2) is one of the most studied and promising pathways to synthesize sustainable polyurethanes.¹⁰ The aminolysis of cyclic carbonate leads to the formation of hydroxyurethanes, resulting in the presence of dangling primary or secondary hydroxyl groups on the polymer backbone. The inherent PHU structure can provide new properties such as hydrophilicity and enables the potential post-functionalization to bring original properties to these materials.



Scheme 2- Poly(hydroxyurethane) synthesis *via* the polyaddition of diamines and bis-cyclic carbonates.

The major drawback of the cyclic carbonate/amine route is the poor reactivity of 5-membered ring cyclic carbonates towards amines, resulting in material with lessened properties and preventing the preparation of high molar mass PHUs. Indeed, the polymerization rate is not competitive enough in comparison to the reaction time required for many industrial processes. Moreover, the conversions are generally incomplete, leading to residual monomers within the materials. This pattern is due to the low reactivity of cyclic carbonates towards amines, coming from the high stability of such compounds. For instance, fatty acid-based cyclic carbonates synthesized from an epoxidation/carbonation of unsaturations displayed high stability, as the electron-releasing effect conferred by the aliphatic chain nearby the cycle increases their stability.¹¹ Several solutions have been found to improve this feature. First, the

syntheses of 6-, 7- and 8-membered ring cyclic carbonates, displaying a higher ring strain and a lower stability, were achieved and demonstrated a significant impact on the polymerization rate when the polyadditions with diamines were performed.¹²⁻¹⁵ Unfortunately, most of the cyclic carbonates with larger ring size were not easy to handle at the industrial level due to their instability at room temperature. In order to decrease the cyclic carbonate stability and subsequently to favor the amine attack, an alternative strategy, consisting in the insertion of electron-withdrawing groups nearby the 5-membered cyclic carbonate, was implemented by several research groups.¹⁶⁻¹⁹ Such a strategy represents one of the major challenges of this thesis. Another solution is the use of metal or organocatalysts (ex: Lewis acids, TBD, DBU, thioureas, etc.) in order to increase the carbonyl electrophilicity of the cyclic carbonate and/or the nucleophilicity of the amine.

In the context of sustainability, another key point is the preparation of fully bio-based PHUs. Several research groups carried out the preparation of bio-based cyclic carbonates as precursors for further PHU syntheses.^{11,20-24} However, the preparation of fully bio-based PHUs is hindered by the obvious needs of commercially available aliphatic bio-based diamines, preferentially synthesized by eco-friendly processes. Only few bio-based diamines such as *Priamine*[®] from CRODA or 1,10-decanediamine from Evonik, have been reported to be commercial. Therefore, an important effort needs to be done to provide bio-based (di)amines for PHUs synthesis.

This thesis takes place in the frame of the NIPU project (WP3P8) implying the *Laboratoire de Chimie des Polymères Organiques* (LCPO) and the *Centre Technique Industriel des Huiles et Corps Gras* (ITERG, Pessac, France) and has been financially supported by the SAS PIVERT.²⁵ The partnership between ITERG and the SAS PIVERT enabled the convenient access to fatty acids from renewable resources in order to prepare new bio-based PHUs.

The purpose of this thesis was to synthesize vegetable oils-based precursors for thermoplastic PUs preparation, using a phosgene- and isocyanate-free route. More precisely, the cyclic carbonate/amine polyaddition was investigated and attempts were made to tackle the low reactivity of the 5-membered cyclic carbonates from fatty-acids. A platform of bio-sourced amines as precursor for PHU synthesis was also developed. The final goal of this work was to

make the polymerization process more competitive and attractive in comparison with the alcohol/isocyanate polyaddition.

This manuscript is divided in five chapters. The first chapter illustrates the state of the art about isocyanate- and phosgene-free PUs focusing on the amine/cyclic carbonate polyaddition, in order to provide the reader the basics to better understand the objectives and the achievements of this thesis. In this respect, the different routes to synthesize amines are first depicted, centralizing the development on the mild aerobic alcohol oxidation into nitrile intermediates for a subsequent amine production. New trends for the synthesis of bio-based amines are also described. The second part of this chapter covers the different works dealing with the cyclic carbonate/amine route, underlining the different synthetic approaches to prepare 5- to 8-membered ring cyclic carbonate precursors. In the purpose of understanding the challenges of this isocyanate-free route to PU, the mechanism and the catalysis of the cyclic carbonate aminolysis are then discussed, taking into account the selectivity of this route. The syntheses of various PHUs are reported as well as their related properties. An extra focus is finally made on bio-based poly(hydroxyurethane)s to introduce the context of this thesis.

The second Chapter of this manuscript covers the achievements related to the synthesis of more sustainable aliphatic amines using aerobic alcohol oxidation. Aliphatic bio-based alcohols were converted to the corresponding amine through an optimized aerobic oxidation in the presence of ammonia (in nitrile intermediates), followed by a hydrogenation step. A second route using thiol-ene “click” chemistry of cysteamine hydrochloride on dimerized fatty-acid derivatives was investigated for the obtention of long aliphatic diamines.

The Chapters 3 and 4 of this thesis deal with the synthesis of reactive 5-membered cyclic carbonates *via* the insertion of a heteroatom in beta position, using glycerol derivatives (epichlorohydrin, glycerol carbonate, diglycerol and thioglycerol) as well as different chemistries (nucleophilic substitution, carbonation, thiol-ene). Ether, ester (Chapter 3) and sulfur (Chapter 4) moieties were used as electron withdrawing groups placed in β position nearby the fatty acid-based cyclic carbonates for the enhancement of their reactivity towards aminolysis. The differences in reactivity between cyclic carbonates of different chemical structures have been quantified. These monomers were then successfully used as building

blocks for the synthesis of relatively high molar mass poly(hydroxyurethane)s, and the structure-property relationships of the so-formed PHUs were further investigated. On the one hand, the Chapter 3 exposes the synthesis of diglycerol dicarbonate from diglycerol and dimethyl carbonate. When copolymerized with hydrophilic diamines, this bis-cyclic carbonate conferred water solubility or self-assembly properties to the resulting PHUs. On the other hand, Chapter 4 presents our preliminary investigations about the post-functionalization of the sulfur-containing PHUs.

Lastly, investigations to further enhance the vegetable oil-based cyclic carbonate reactivity towards amines were implemented, using ‘ultra-activated’ monomers from the carbonated methyl acrylate, enabling the cyclic carbonate activation thanks to the presence of an ester moiety in α position nearby the cycle. Another study was conducted on the catalysis of the aminolysis using commercially available catalysts. The combined effect of catalysts and monomer activations was finally analyzed.

Chapter 1

State of the art: Towards isocyanate- and phosgene-free Poly(hydroxyurethane)s

Publication: L. Maisonneuve, O. Lamarzelle, E. Rix, E. Grau, H. Cramail, Isocyanate-Free Routes to Polyurethanes and Poly(hydroxyurethane)s, *Chemical Reviews*, **2015**, 115 (22),12407–12439

Keywords: Cyclic carbonate, amine, nitrile, alcohol oxidation, non-isocyanate polyurethane, poly(hydroxyurethane), thermoplastic, bio-based.

Mots-clés: Carbonate cyclique, amine, nitrile, oxidation des alcools, polyuréthane sans isocyanate, poly(hydroxyuréthane), thermoplastique, bio-sourcé.

Table of contents

Introduction	31
1. Routes towards bio-based amines	32
1.1. Synthesis of amines: generalities	33
1.2. Aerobic alcohol oxidation for the amine production.....	35
1.2.1. Alcohol oxidation into aldehyde intermediates	36
1.2.2. One-pot alcohol oxidation into nitrile intermediates	39
1.3. Amines from renewable resources	42
2. Cyclic carbonate syntheses	44
2.1. Synthesis of 5-membered cyclic carbonates (5CC).....	44
2.2. Synthesis of 6- to 8-membered cyclic carbonates (6CC- 8CC).....	47
2.3. Synthesis of bis-cyclic carbonates (bCC).....	49
3. Studies on the model cyclic carbonate/amine reaction	52
3.1. Mechanism of cyclic carbonate aminolysis.....	52
3.2. Kinetic and reaction conditions	53
3.3. Effect of the chemical structure of the amine.....	54
3.4. Effect of the substituent and size of the cyclic carbonate.....	55
3.5. Selectivity and by-products	57
3.6. Additives and catalysts for the cyclic carbonate/amine reaction.....	59
4. Thermoplastic Poly(hydroxyurethane)s (TPHUs)	61
4.1. Syntheses of PHUs and related molar masses	68
4.2. Selectivity and side reactions	70
4.3. Different reactivity for specific monomers	72
4.4. Thermo-mechanical properties and thermal stability of TPHUS	75
4.5. Towards bio-based PHUs.....	77
4.5.1. Vegetable oil-based cyclic carbonates to PHUs	77
4.5.2. Other bio-based cyclic carbonates to PHUs	81
Conclusions	83
References	84

Introduction

In the current context of sustainable chemistry development and new regulations, research groups and industries have to replace hazardous chemicals and harsh reaction conditions by greener intermediates and processes. In the past few years, the plastic market has grown interest for polyurethane materials. According to *PlasticsEurope*, the worldwide production reached 21 million tons in 2012.¹ These specialty performance polymers combine numerous properties required in aeronautic, medical applications, adhesives or even textile industries. Classically, polyurethanes (PUs) result from the polyaddition of a diol (or polyol) onto a diisocyanate (or poly-isocyanate). The latter is produced from the corresponding amine and phosgene which is highly toxic.

Therefore, alternative pathways for PU synthesis become more and more attractive for industry and academic research. Meier and coll.² reviewed modern and more sustainable routes to PUs precursors and particularly focused on the synthesis of bio-based isocyanates for greener polymerizations. Figure 1 presents an overview of the main synthetic routes to polyurethanes according to their dependence in phosgene and isocyanate.

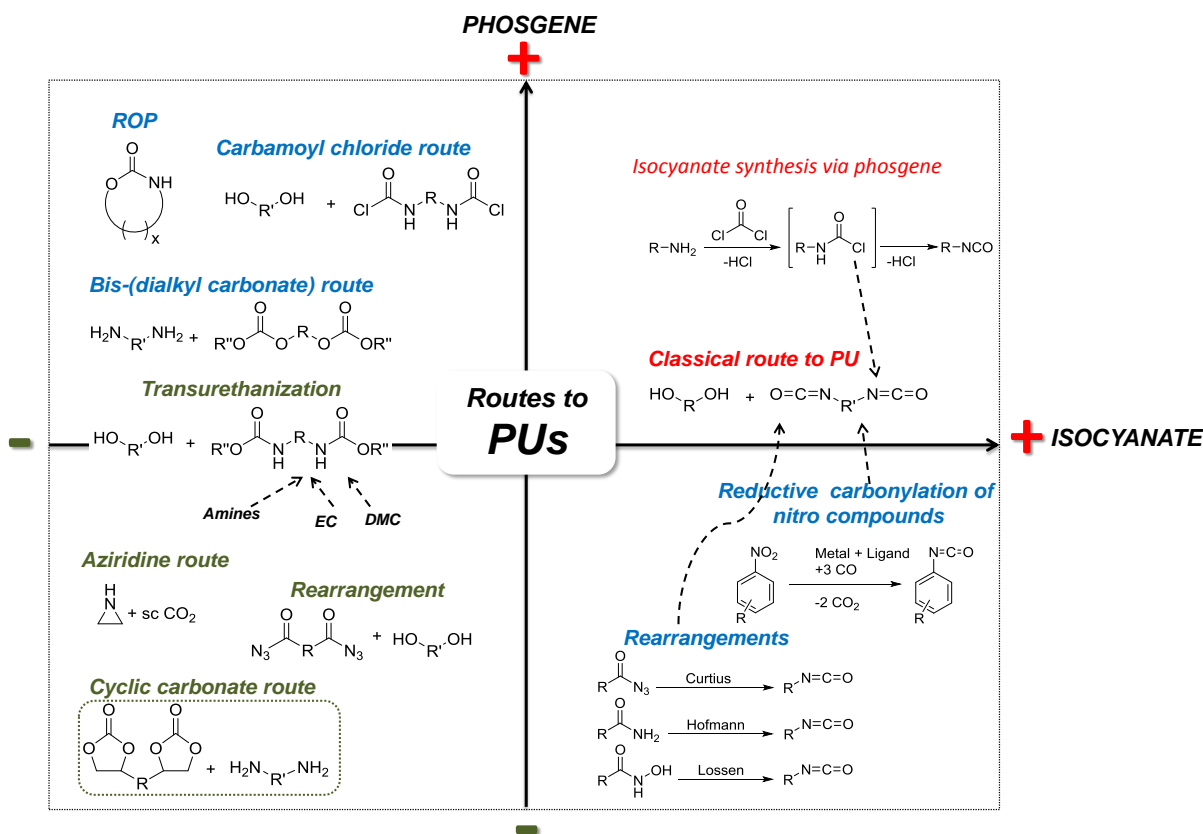


Figure 1 - Overview of synthetic routes to polyurethanes.

Among those methods, the copolymerization of aziridines with carbon dioxide is one of the less dependent in terms of phosgene and isocyanate content. But a green access to aziridines and their toxicity remains an issue.³ The rearrangement of acyl azide followed by its polycondensation with alcohol functions represents another route to access polyurethane, through an *in situ* isocyanate formation during polymerization.^{4,5} These pathways cannot replace the isocyanate route as some precursors or reagents used are not safe to handle. In this concern, the most studied and promising routes to PUs and PHUs are the transurethanization polycondensation between a bis-carbamate and a diol⁶⁻⁹ and the polyaddition between cyclic carbonates (CC) and amines.¹⁰⁻¹⁴ The present state of the art will only focus on the second mentioned pathway, which has been the most studied in the last decade.

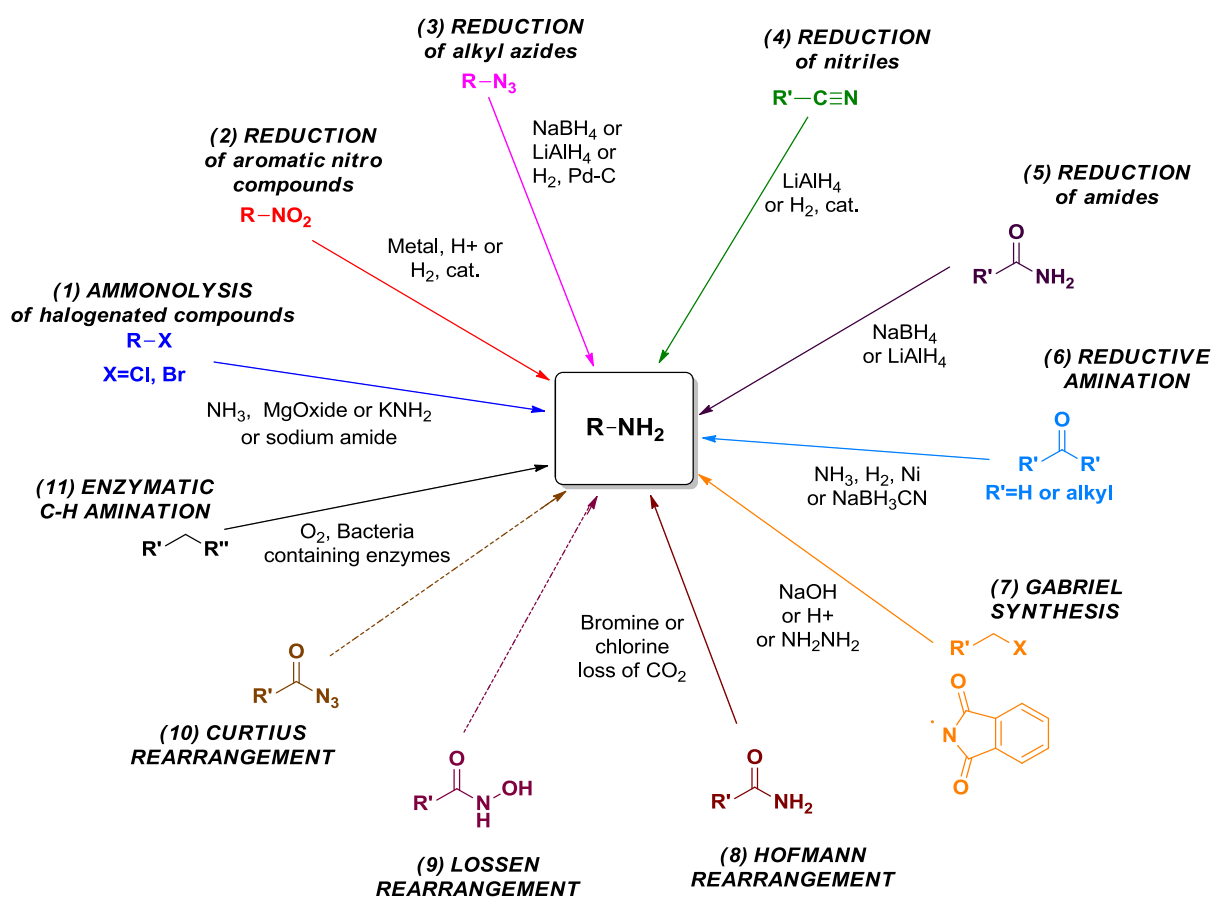
Thus, the first part of this chapter will be devoted to the synthesis of amines required for PHU production. The main routes to amines will be reviewed and specifically the green aerobic oxidation of alcohols in nitriles which represents one of the most attractive accesses to amines through nitrile hydrogenation. Available methods for bio-based amine synthesis will also be discussed. In a second part, CC synthesis as well as the corresponding model reactions and mechanisms of their aminolysis will be detailed. Finally, syntheses, properties and catalysis of thermoplastic poly(hydroxyurethane)s (PHUs) will be studied with an extra focus on PHUs from renewable resources.

1. Routes towards bio-based amines

In the plastic industry, amines and more specifically primary amines are broadly employed in the preparation of polymers such as epoxy resins, polyamides or even poly(hydroxyurethane)s (PHUs). Despite the ongoing interest for bio-based polymers, the cyclic carbonate/amine route suffers from a lack of bio-based amines and more specifically vegetable oil-based amines, restraining the access to fully bio-based polymers such as PHUs. Thus, the development of ‘greener’ methods to amines and diamines proves to be crucial and needs to be developed. Among the proposed routes to amines, the aerobic oxidation of alcohols has been extensively studied for aldehydes synthesis and was recently transferred to nitrile synthesis, enabling the obtention of amines *via* a nitrile hydrogenation step. New trends show that this process tends to be applied to raw materials from renewable resources. Cysteamine thiol-ene “click” chemistry on alkene-based renewable materials also appears as a green alternative to primary bio-based amines.

1.1. Synthesis of amines: generalities

Primary amines can be prepared by classical routes already described in organic chemistry and summarized in Scheme 1.¹⁵ The ammonolysis of halogenated compounds (1) is one of the most employed routes in industry. Primary amines can be either prepared by the reduction of nitro compounds (2), alkyl azides (3), nitriles (4) and amides (5) as well as by the reductive amination of ketones or aldehydes (6). Besides, they can be obtained by Gabriel synthesis (7) and through several sigmatropic rearrangements. Among them, Hofmann rearrangement (8) has been used for primary amine production and Lossen and Curtius (9-10) rearrangements can also indirectly lead to amines in the presence of water. Finally, an alkyl amination using an enzymatic process has been reported (11).

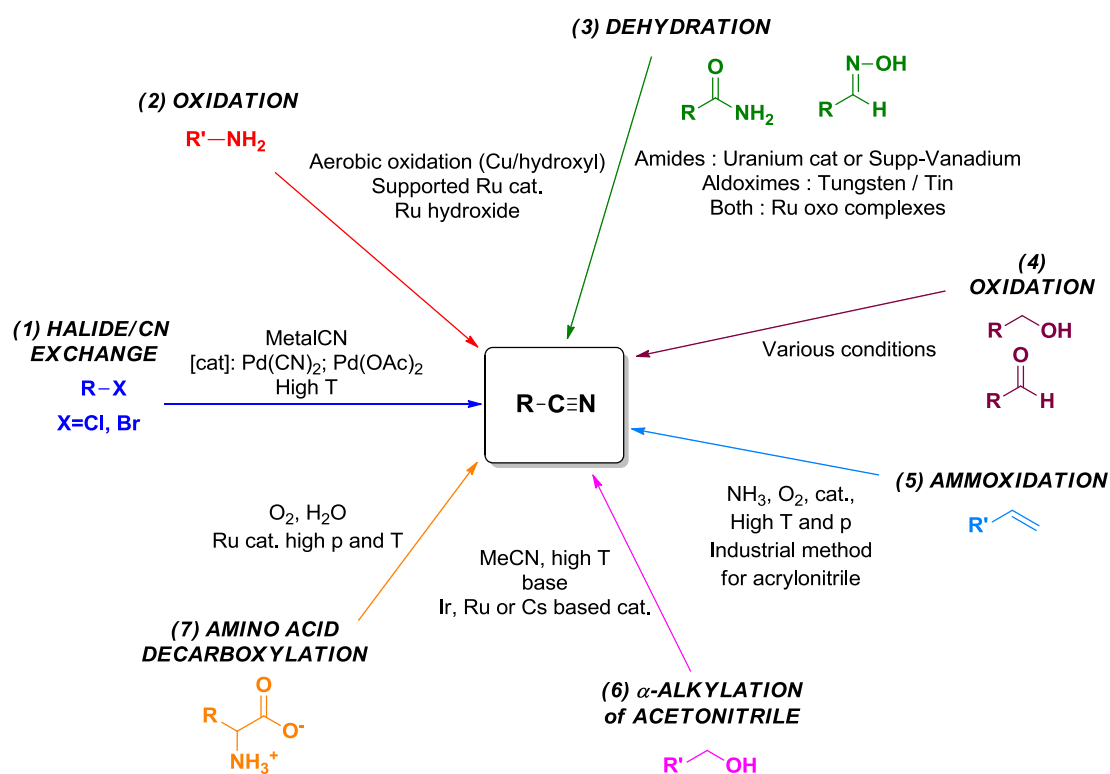


Scheme 1- Main approaches for the synthesis of amines.

Several drawbacks from these classical methods can be identified. First of all, the use of gaseous ammonia in the ammonolysis (1) and reductive amination (6) represents a major drawback at the industrial scale since this hazardous gas is commonly used under harsh conditions in terms of temperature. The latter can be lowered using good leaving groups but such a strategy reduces significantly the atom economy. Nonetheless, the main issue with the

alkylation of ammonia (1) is the multiple alkylation reactions that lead to a mixture of primary, secondary and tertiary amines with quaternary ammonium salts, usually difficult to separate. Among the principal routes employed, the reduction of alkyl azide intermediates (3) involves a nucleophilic addition with azide compounds such as NaN_3 , which are explosive and toxic. Moreover, a large number of steps are required to obtain the final amine. Regarding the reduction of amides (5), toxic acyl chloride precursors need to be prepared. Finally, Gabriel procedure (7) suffers from non-acceptable atom efficiency due to the generation of phthalimide derivatives. A recent pathway has emerged for benzylic compounds C-H amination (11), using a multi-enzyme cascade generated in a single bacterial whole-cell system.¹⁶ However, such procedure remains expensive and highly specific to benzylic compounds to be industrialized.

Among the methods described above, the reduction of nitriles (4) using dihydrogen appears as an attractive approach to prepare bio-based amines in mild conditions.



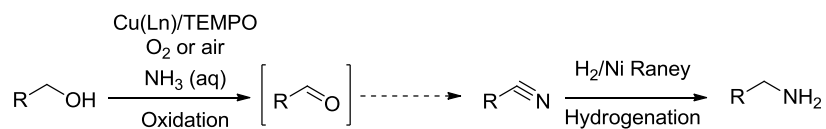
Scheme 2 - Major strategies toward the synthesis of nitriles.

Nitriles are one of the most versatile compounds employed in organic chemistry for the preparation of amines, amides and other molecules. Typically, aromatic nitriles are used for a large number of pharmaceutical applications, or in industrial processes. The main routes to

nitriles are summarized in Scheme 2 and comprise halide / CN exchange (1),^{17,18} dehydration of amide and aldoximes (3),^{19–22} oxidation of amine (2),^{23–25} ammoxidation of alkenes (5),^{26–28} decarboxylation of amino-acids (7),²⁹ α -alkylation of acetonitrile (6)³⁰ and, finally, the oxidation of alcohols or aldehydes (4). Nonetheless, most of the syntheses mentioned above imply harsh conditions of pressure and temperature, wastes and laborious work up. Moreover, high price of the chemicals involved and their toxicity represent barriers that have hindered the industrial development of nitrile production.

The aerobic one-pot oxidation of alcohols in the presence of aqueous ammonia is at this time one of the greenest way for nitrile derivatives production since most of the other procedures to access them need toxic reagents or produce wastes.

The strategy adopted in this manuscript to synthesize amines from alcohols oxidation is presented in Scheme 3 and requires to understand the alcohol oxidation into aldehyde intermediates. The latter will be presented in the next section before discussing the synthesis of nitriles by adding aqueous ammonia in the mixture composition.



Scheme 3 - Strategy for aliphatic primary amines through aerobic oxidation of alcohols.

1.2. Aerobic alcohol oxidation for the amine production

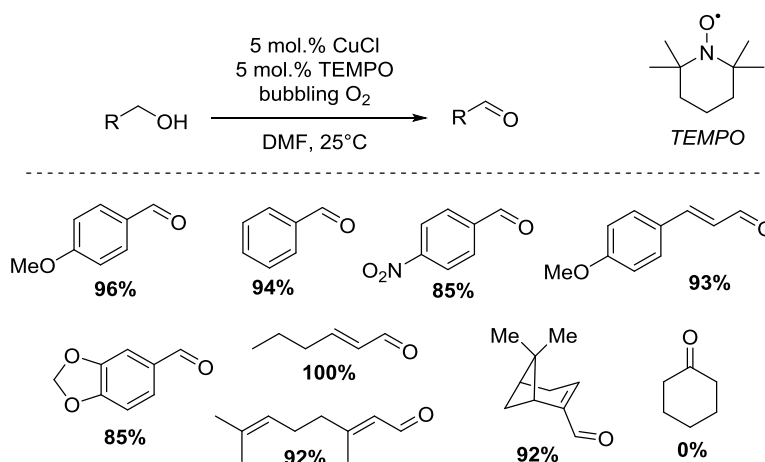
Alcohol oxidation in corresponding aldehydes has been extensively studied in the last decades. The copper/TEMPO catalyzed aerobic oxidation is one of the greenest and safest methods for this synthesis. Thus, the technology has been extended to one-pot synthesis of nitriles from alcohols in presence of ammonia. The main challenges for both aldehyde and nitrile syntheses are the development of even milder experimental conditions (room temperature, air as an oxidant), the improvement of the conversions for less reactive alcohols such as aliphatic primary alcohols, and finally the scalability of these syntheses at the industrial level.

In the next sections, the state of the art regarding the aerobic alcohol oxidation will be detailed for both aldehydes and nitrile preparations.

1.2.1. Alcohol oxidation into aldehyde intermediates

TEMPO (2,2,6,6-tetramethyl-1-piperidiny-N-oxyl) which is the most known and studied stable radical has been largely used for the oxidation of alcohols into aldehydes in combination with several metals as co-catalysts (Pd, Pt, Ru, ...). However, the present scope, based on published reviews,^{31,32} will focus only on Cu/TEMPO mediated systems for the oxidation of alcohols, as copper tends to be cheaper, less toxic and more tolerant to other functional groups than other metals.

The first aerobic alcohol oxidation using a Cu/nitroxyl catalytic system was proposed in the 80's by Semmelhack *et al.*³³ CuCl and TEMPO in DMF could lead to the oxidation of numerous activated primary alcohols. However, as aliphatic alcohols are known to be much less reactive than allylic or benzylic ones (Scheme 4), stoichiometric amounts of copper and TEMPO were required to oxidize these substrates under the reported conditions. The alcohol activation is in fact a key-parameter for alcohol oxidation pushing many research groups to investigate several parameters such as copper sources, ligands, nitroxyl group hindrance and/or reaction conditions to convert the less reactive alcohols.

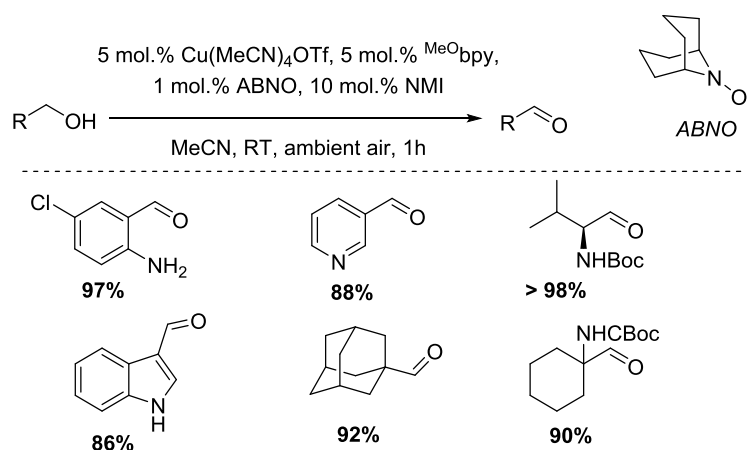


Scheme 4 - Aerobic oxidation of activated alcohols by CuCl/TEMPO in DMF with related aldehyde yields, reported by Semmelhack.³³

In 2004, Sheldon and co-workers³⁴ developed a system including Cu(II) salts, 2,2'-bipyridine (bpy) as a ligand and t-BuOK as a base in a CH₃CN/H₂O (2:1) solvent mixture. This catalyst system was able to oxidize activated alcohols in 2 to 5 hours, using 5 mol.% catalyst at 25°C with air as the oxidant. However, stronger conditions (heating at 40°C for 24 hours with 7.5 mol.% of TEMPO) were needed to convert unactivated primary alcohols such as 1-octanol. Koskinen *et al.*³⁵ also improved the catalytic system by bringing to their Cu(OTf)₂/TEMPO

system a base such as 1,8-diazabicyclo[5.4.0]undec-7-ene (DBU) and N-methylimidazole (NMI) in pure acetonitrile under O₂. Under the mentioned conditions, 1-decanol was almost completely converted in 5h.

In 2011, Stahl and co-workers³⁶ also reported an enhanced catalytic system Cu(I)/TEMPO/base in acetonitrile, proving the efficiency of Cu(I) rather than Cu(II) in the presence of a base. They also highlighted the enhanced reactivity of Cu(I) salts with a non-coordinating counter-anion such as OTf. However, the improved reactivity of Cu(I) was not maintained in aqueous solvent mixture. The authors demonstrated in the same work the higher tolerance of Cu/TEMPO catalytic systems to a wide range of functional groups in comparison with catalytic systems such as Pd(OAc)₂/pyridine and RuCl₂(PPh₃)₃/TEMPO. The same research group improved few years later the alcohol oxidation process with the objective to get a scalable process. They used a continuous flow reactor with 35 bars of 9 % O₂ in N₂, able to obtain high yields of aliphatic aldehydes with residence times from 30 to 45 min.³⁷ In another study from Stahl and co-workers,³⁸ an optimized catalytic system involving 1 mol.% of an unhindered TEMPO analogue (ABNO: 9-azabicyclo[3,3,1]nonane N-oxyl), 1 mol.% of Cu(MeCN)₄OTf, 5 mol.% of p-(Me)bpy and 10 mol.% of NMI could convert equivalently most of alcohols (benzylic, aliphatic, primary and secondary ones) under ambient air at room temperature in 1h (Scheme 5). This optimized system is among the most efficient methods for alcohol oxidation into aldehydes under air and proved to be stable over 1 year of storage at 5°C under air.³⁹

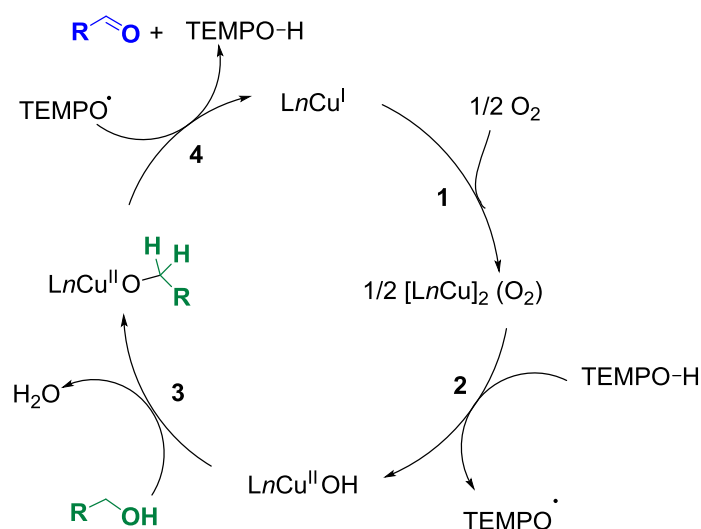


Scheme 5 – Aerobic Cu/ABNO catalyst system effective with diverse primary alcohols under ambient conditions with corresponding aldehyde yields, reported by Stahl.³⁸

These studies demonstrate that the intrinsic hindrance of nitroxyl mediators is a key-parameter to control the alcohol conversion, as the less hindered ABNO could transform almost all types of alcohols in comparison with the more hindered TEMPO. Iwabuchi and co-workers⁴⁰ also

correlated the inefficiency for TEMPO to convert less reactive alcohols (secondary and primary aliphatic ones) to the steric hindrance imparted by methyl groups nearby its stable radical.

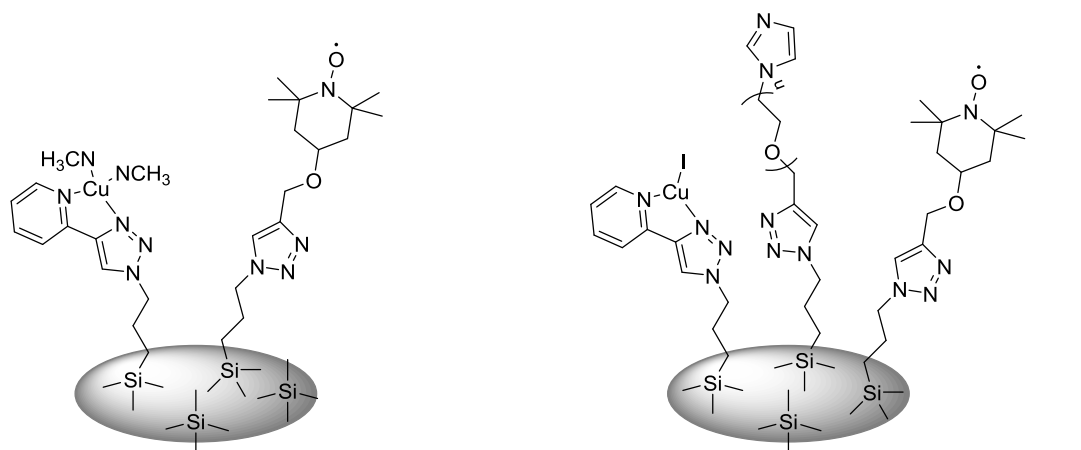
Regarding Cu/TEMPO oxidation, several mechanisms have been proposed throughout the years and authors did not agree on a single-one mechanism. However, Stahl and coll.^{38,41} proposed a mechanism that has been deeply investigated, involving analyses such as gas chromatography, *in situ* IR, EPR, cyclic voltammetry or UV-visible spectroscopy. The simplified catalytic cycle they suggested is illustrated in Scheme 6. The oxidation of CuI and TEMPO-H under oxygen provides Cu(II)-OH species and TEMPO (steps 1 and 2) as well as the corresponding base (LnCu(II)-OH). Afterwards, the oxidation of the alcohol continues through the formation of a Cu(II)-alkoxide species (step 3) followed by hydrogen atom transfer to the stable radical TEMPO and the aldehyde formation (step 4).



Scheme 6 - Mechanism of (bpy)Cu(I)/TEMPO-catalyzed alcohol oxidation deduced by Stahl and co-workers.⁴¹

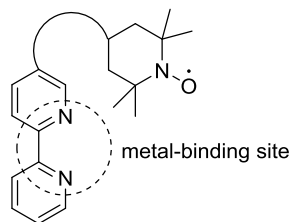
A new trend in the alcohol oxidation with Cu/TEMPO system is on the rise. Indeed, several research groups have synthesized supported catalytic systems to obtain a greener and scalable process. In the past few years, several research groups supported the TEMPO on silica gel or polymers such as poly(ethylene glycol) but catalytic systems did not include copper.^{42,43} However, Fernandes *et al.*⁴⁴ designed a bi-functional heterogeneous catalyst by grafting bipyridine and TEMPO derivatives by alkyne-azide “click” reaction onto silica (Scheme 7- (1)). The functionalized silica exhibited good catalytic properties for benzylic alcohol conversion under O_2 at 80°C at 5 mol.% Cu loading. The same authors further developed a trifunctional supported catalyst on silica by grafting in one single step, CuI, pyridyltriazol,

TEMPO and NMI sites (Scheme 7-(2)).⁴⁵ The major advantages conferred by such systems are the possible recycling and the synergetic effects obtained by concentrating all the catalytic entities close to the silica support. In the same purpose, Gao and co-workers⁴⁶ developed a bio-inspired bi-functional ligand binding bipyridine to TEMPO (Scheme 7-(3)). 5 mol.% of the so-formed system combined with 5 mol.% of copper salts and 10 mol.% of NMI in acetonitrile could convert selectively aliphatic alcohols at RT under air after 6 to 12h.



(1) *Fernandes et al.* - bifunctional supported catalyst

(2) *Fernandes et al.* - trifunctional supported catalyst



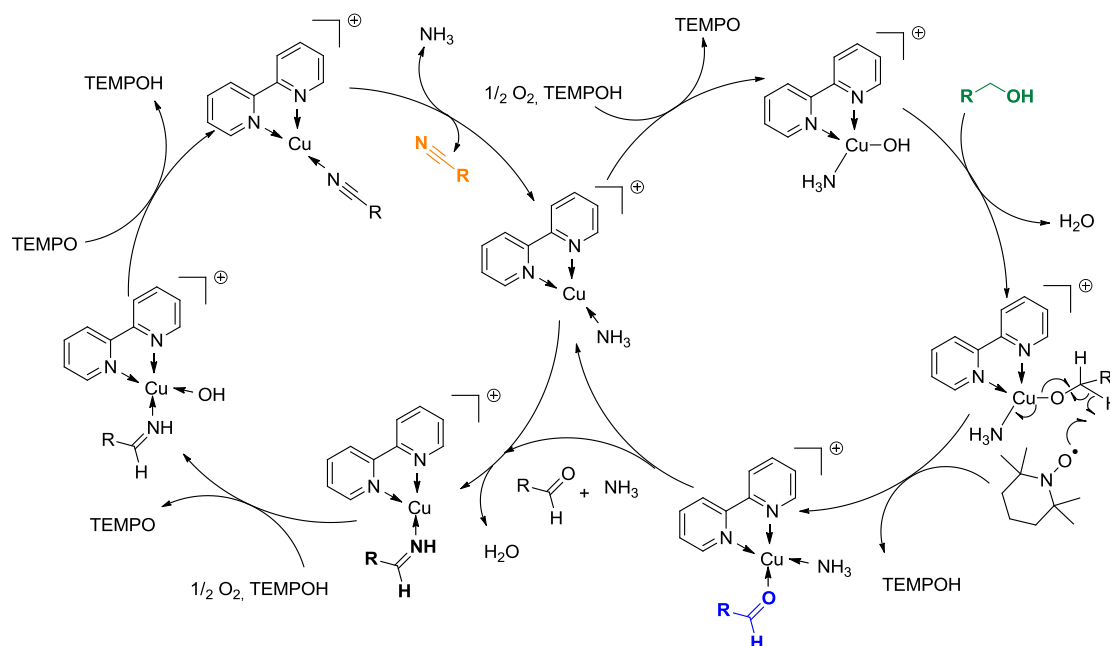
(3) *Gao and coll.* - bioinspired bi-functional ligand

Scheme 7 - Different supported catalytic systems for aerobic alcohol oxidation.

1.2.2. One-pot alcohol oxidation into nitrile intermediates

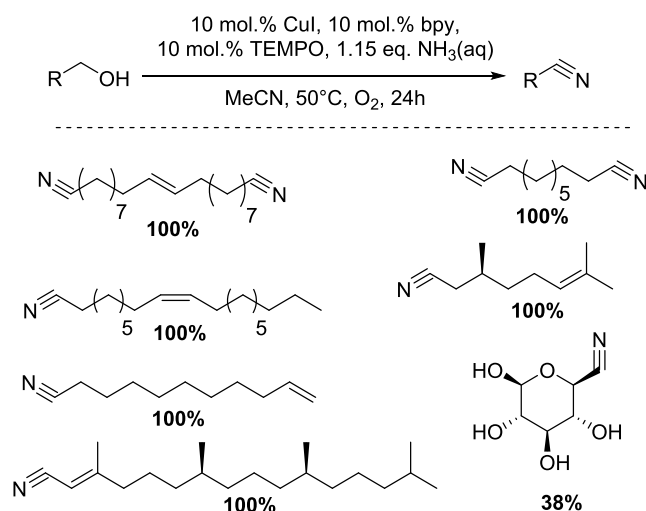
As discussed before, the catalytic aerobic oxidation of alcohols into aldehydes represents one of the greenest oxidation methods and has been recently transferred to the synthesis of nitriles in the presence of ammonia as source of nitrogen. Here, are reported the different alcohol oxidations in nitrile performed under oxygen or air with different catalytic systems. Besides, the use of cheap, available and low toxicity copper catalysts makes this strategy attractive for industrial applications. The optimizations carried out by the different research teams were directly inspired from the works performed on the alcohol oxidation into aldehydes (see part 1.2.1).

In 1989, Capdevielle and coll.⁴⁷ first reported the aerobic oxidation of aromatic alcohols into nitrile catalyzed with copper but in the absence of a nitroxyl co-catalyst. In 2013, Haruta *et al.*⁴⁸ described a procedure using MnO_2 under pressurized oxygen (0.85 MPa) and NH_3 gas at 100°C . Such approach was efficient but carried out at high temperature in autoclave. Based on the work of Sheldon's group⁴⁹, Tao *et al.*⁵⁰ have developed a procedure to oxidize benzylic alcohols into nitrile in the presence of $\text{Cu}(\text{NO}_3)_3/\text{TEMPO}$ as a catalytic system and aqueous ammonia under 1 atm. of oxygen at 80°C . Aryl nitriles were synthesized in high yield but the catalytic system was not suitable for aliphatic alcohol conversion in these conditions. In the meantime, Yin *et al.*⁵¹ described a double aerobic dehydrogenation of aromatic alcohols under mild conditions using a more reactive $\text{Cu}/\text{TEMPO}/\text{bipyridine}$ catalytic system and an excess of aqueous ammonia under oxygen at room temperature. However, aliphatic nitriles were presented in a lesser extent and were obtained under specific conditions, increasing temperature to 50°C under oxygen. A speculated mechanism inspired from the one suggested by Stahl and coll.⁴¹ has been proposed by this research group and is described in Scheme 8. In this cascade-based catalytic process, the first cycle of oxidation follows the one described by Stahl and coll. The next step is the quick conversion of aldehyde into nitrile. The authors demonstrated that the second oxidation is driven by the favored $\text{Cu}(\text{I})$ -imine complex and can afford nitriles. Additionally, they showed that TEMPO was essential for the two reaction steps (alcohol to aldehyde and aldehyde to nitrile) and that the first oxidation cycle was the limiting step of this one-pot synthesis.



Scheme 8 - Reaction mechanism for aerobic alcohol oxidation proposed by Yin *et al.*⁵¹

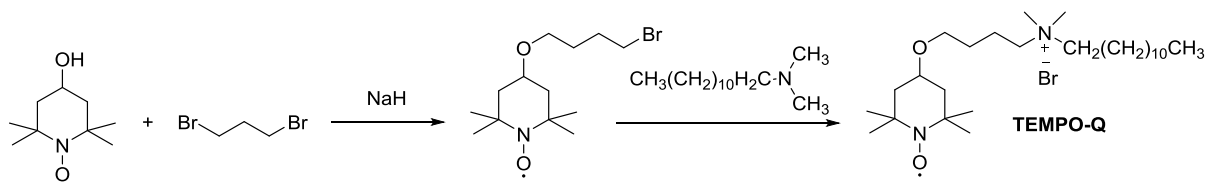
The approach of Yin *et al.*⁵¹ employing CuI/TEMPO/bipyridine under O₂ appears to be a desirable and one of the most versatile methods to convert alcohols into nitriles; still copper catalyst is cheap, available and presents a low toxicity. Nevertheless, benzylic alcohols were mainly used as substrates and the developed methods need further optimization for converting less reactive alcohols under ambient air. We recently carried out an optimization of the above-mentioned catalytic system, enabling a full conversion of bio-based aliphatic alcohols and diols such as 1,10-decanediol, 10-undecen-1-ol or citronellol in their corresponding nitrile forms (Scheme 9).⁵²



Scheme 9 - Aerobic oxidation of activated alcohols into nitriles by (bpy)CuI/TEMPO in MeCN with related nitrile conversions, reported by Cramail and coll.⁵²

In order to make the oxidation process greener, the use of air instead of pure O₂ as an oxidant is also reported. Mizuno and coll.⁵³ reported first the direct oxidation of alcohol into nitrile using a heterogeneous Ru(OH)_x/Al₂O₃ catalyst and an excess of aqueous ammonia under air pressure (6 atm.) at 120°C. Yadav *et al.*⁵⁴ described an oxidation under air at 135°C of primary alcohols using CuCl₂·2H₂O as a catalyst, in the presence of K₂CO₃ and ammonium formate as nitrogen source. Unfortunately, this procedure does not permit the conversion of aliphatic alcohols that would require working at high temperature. To avoid the use of O₂ as oxidant, Dornan *et al.*⁵⁵ utilized another procedure under air at 25-50°C with Cu(OTf)₂/TEMPO/bipyridine and aqueous ammonia to oxidize aldehydes or alcohols into nitriles. Aliphatic alcohols could not be converted into nitriles with this method but the authors could convert them by replacing the catalytic system by [Cu(MeCN)₄][OTf]/TEMPO/bipyridine at 50°C. This last catalytic system was applied on a petroleum-based aliphatic alcohol but was not fully optimized on bio-based alcohols.

A recent study published by Zaho and co-workers⁵⁶ demonstrated the conversion of various benzylic and allylic alcohols to the corresponding nitriles in solvent-free conditions using a N,N-dimethyl-(4-(2,2,6,6-tetramethyl-1-oxyl-4-piperidoxyl)butyl)dodecylammonium bromide (TEMPO-Q)/CuI/bpy as catalytic system. The synthesis and the structure of TEMPO-Q are schematized in Scheme 10. The use of such functionalized ionic liquid represents a greener pathway for such synthesis as a solvent is not required and TEMPO-Q can be recycled. Nonetheless, the tested aliphatic substrates could not be converted in the corresponding nitriles.



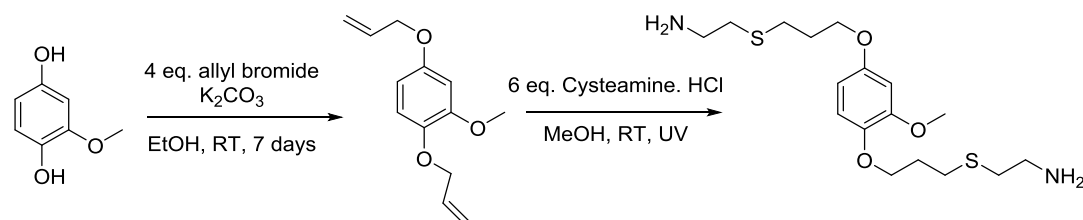
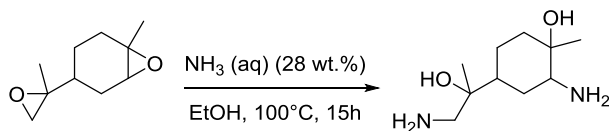
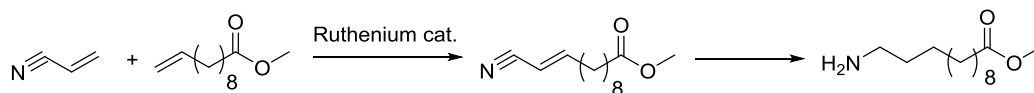
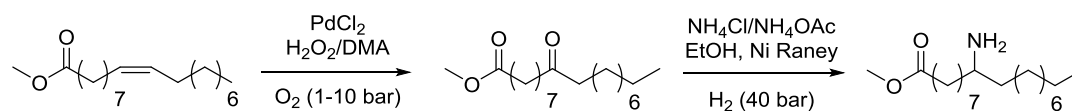
Scheme 10 - Synthesis of TEMPO-Q.⁵⁶

1.3. Amines from renewable resources

Although the synthesis of renewable amines has not widely been developed, vegetable oil-based amines have already been prepared employing different strategies. The first one consists in bringing the amine moiety *via* thiol-ene reaction⁵⁷⁻⁵⁹ on triglycerides or fatty acid double bonds with cysteamine, which is also bio-sourced. This approach has been applied on vanillin⁶⁰ (Scheme 11-(1)) or cardanol⁶¹ derivatives for further epoxy resin synthesis. Another route was the ring-opening of triglycerides epoxy intermediates with an excess of diamines.⁶² Similarly, Mulhaupt and Blattmann⁶³ access to limonene- and vegetable oil-based hydroxyl amines by reacting epoxy- or glycidylether moieties with aqueous ammonia at 100°C for 15h in a steel autoclave. (Scheme 11-(2)) Besides, Bruneau and co-workers⁶⁴⁻⁶⁶ deeply studied the cross-metathesis reaction of fatty acids with acrylonitrile (Scheme 11-(3)) in the purpose of obtaining long aliphatic diamines for further polymerizations.

Other routes dealing with the direct grafting of amine function onto the vegetable oil derivatives have been promoted. Few years ago, Biermann *et al.*⁶⁷ reviewed different methods for functionalizing unsaturated fatty acids with amine groups. Among them, the syntheses of nitrile,⁶⁶ amide,⁶⁸ acyl azide⁶⁹ or bromo- intermediates were described.

More recently, Meier and coll.⁷⁰ developed the oxofunctionalization of unsaturated fatty acid esters (Wacker process), leading to the formation of ketone on the aliphatic backbone that was subsequently reduced in primary amine under pressurized hydrogen, as depicted on Scheme 11-(4).

(1) *Caillol*(2) *Mulhaupt*(3) *Bruneau*(4) *Meier***Scheme 11 - Emerging strategies for the production of bio-based amines.**

Concerning industrial amine-based compounds from fatty acid derivatives, the most prominent example is the AB-type fatty amino acid precursor of PA-11, which is produced from castor oil for nearly fifty years from ricinoleic acid by Arkema under the trade mark Rilsan[®].^{71,72} The double bond of undecenoic acid is converted by HBr into the subsequent bromo-based derivative, which is then transformed in ω -amino-undecanoic acid by reaction with ammonia.⁷³ Another chemical company, Evonik, produces fully bio-based PA from the renewable decane-1,10-diamine (VESTAMID[®] Terra, fully bio-based PA-10,10 and PA-10,12). Besides, BASF and BAYER respectively produce commercial 1,4-butanediamine and 1,5-pentanediamine from renewable resources.

2. Cyclic carbonate syntheses

During the last decades, various cyclic carbonates have been prepared considering the growing interest for non-isocyanate polyurethanes. Here are reported the different approaches for their synthesis.

2.1. Synthesis of 5-membered cyclic carbonates (5CC)

The synthesis of 5-membered cyclic carbonates-based compounds (5CC, or 1,3-dioxolan-2-one) has been extensively studied along the years, through various methods. It is noteworthy that ethylene carbonate and propylene carbonate have been commercially available since over 45 years. Recently, the commercially available glycerol carbonate generated global interest in the community.⁷⁴⁻⁷⁶ Generally speaking, the 5CC can be achieved from linear oligo-carbonates, diols, halohydrins, olefins, substituted propargyl alcohols, halogenated carbonates and, in a larger proportion, from epoxy compounds and CO₂.⁷⁷⁻⁸⁰ The main approaches are summarized in the Scheme 12.

The group of Carothers⁸¹⁻⁸⁴ was the first to report the synthesis of CC with various sizes in the early 30's. CC were obtained by depolymerization of the respective linear oligo-carbonates using high temperatures and reduced pressure as well as various catalysts such as Sn(II), Mn(II), Fe(II), and Mg(II) chlorides, carbonates or oxides (Scheme 12-(13)).

Diols and polyols are ones of the main precursors, with epoxy compounds, for the synthesis of 5CC. The first route from diols is the phosgenation approach using phosgene or its derivatives such as the triphosgene (Scheme 12-(1)). For the first time in 1883, Nemirovsky synthesized ethylene carbonate directly by using phosgene and ethylene glycol.⁸⁵ As another example, Burk and Roof⁸⁶ synthesized 5CC from 1,2-diols and triphosgene using pyridine in CH₂Cl₂ at 50°C with yields in the range 87% to 99%. Endo and coll.^{87,88} also used triphosgene for the synthesis of CC. The high toxicity and hazards of phosgene make this way not suitable even if high yields of CC could be reached.

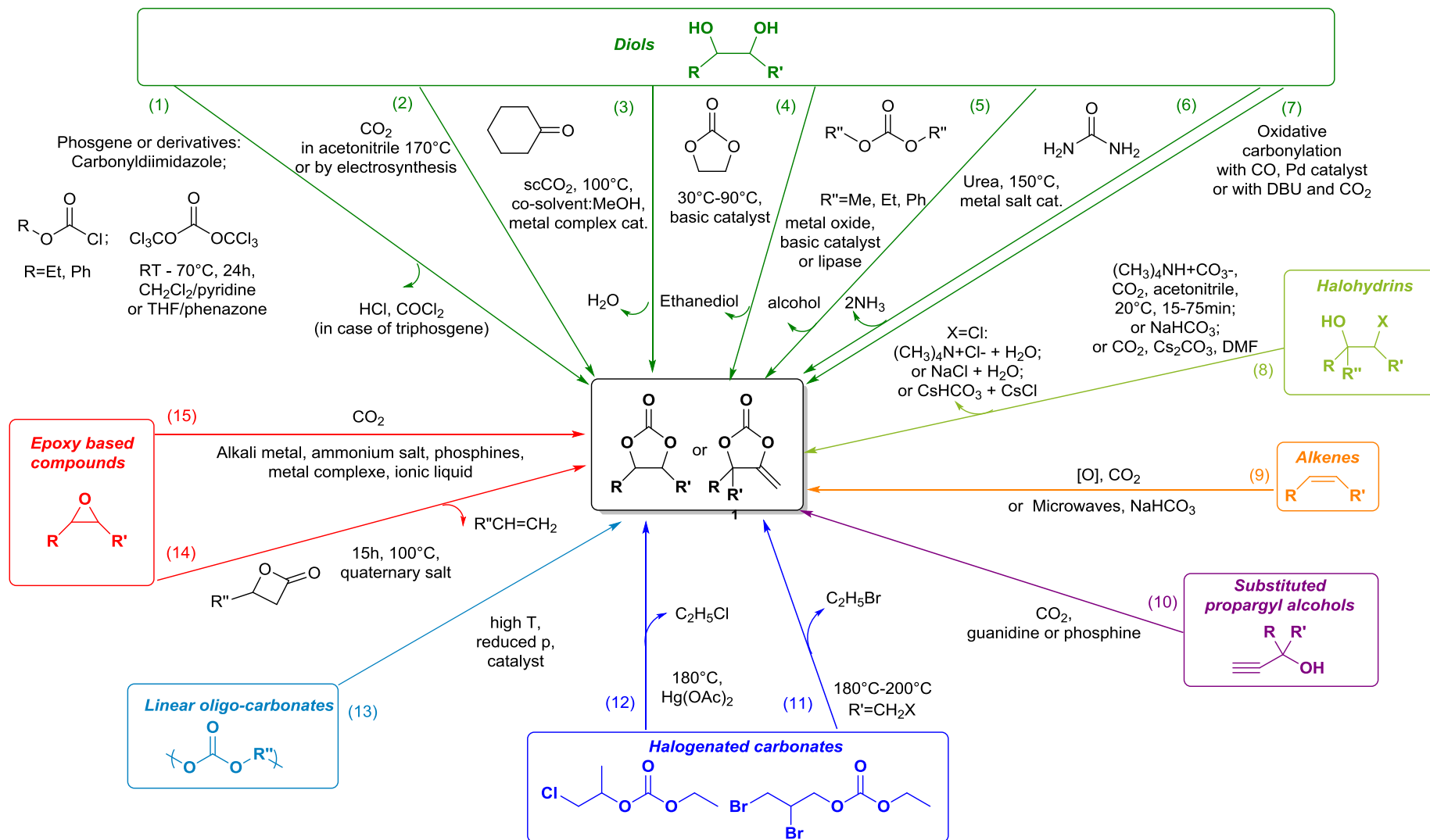
Other methods are the reactions of 1,2-diols with carbon dioxide using metallic acetates in acetonitrile⁸⁹ or by electrosynthesis^{90,91} (Scheme 12-(2)), and the oxidative carbonylation with carbon monoxide using, for instance, palladium-based catalysts (Scheme 12-(7)).^{92,93} The approach involving the formation of a ketal from ethylene glycol and cyclohexanone, which then reacts in the presence of supercritical CO₂ is also a route to CC (Scheme 12-(3)).⁹⁴ In another way, the carbonate interchange reaction between 1,2-diols and ethylene carbonate⁹⁵ (Scheme 12-(4)) or dialkyl carbonates (dimethyl carbonate, diethyl carbonate or diphenyl

carbonate) (Scheme 12-(5)), leads to CC with good yields (40-80%) in the presence of catalysts such as organic bases, metal oxide (MgO, CaO, La₂O₃) catalysts, hydrotalcite or enzymes.^{10,78,96-99} The reaction with urea in the presence of catalysts is another possibility for the synthesis of CC from 1,2-diol (Scheme 12-(6)).^{100,101} Lim *et al.*¹⁰² achieved the synthesis of cyclic and linear carbonates from diols and alcohols by using a transition metal free synthesis. The cyclization process was carried out with DBU (1,8-Diazabicyclo[5.4.0]undec-7-ene) in dibromomethane under 5 to 10 bars of CO₂, leading to good yields (47-86%).

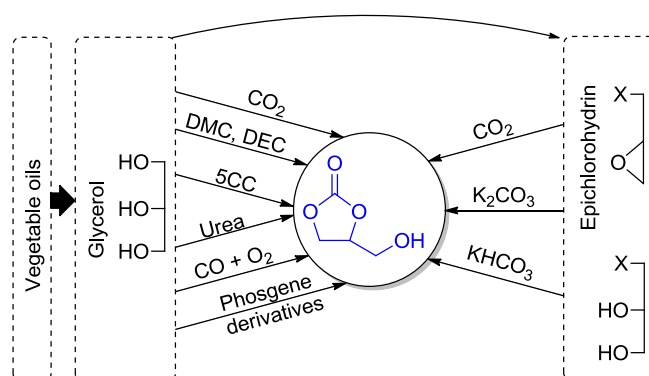
Cyclic carbonates can also be prepared from halohydrins using sodium bicarbonate (Scheme 12-(8))¹⁰³ or cesium carbonate in DMF¹⁰⁴ under mild conditions, or directly from olefins by oxidative carboxylation (Scheme 12-(9)).^{105,106} Furthermore, the reaction of substituted propargyl alcohols with CO₂ (Scheme 12-(10)) in the presence of guanidine catalyst can produce CC with yields up to 82%.¹⁰⁷ The phosphine-catalyzed transformation of propargyl alcohol (Scheme 12-(10)) gives also access to CC.¹⁰⁸ Taking another example, halogenated carbonates can be converted into CC at a temperature between 180°C and 200°C (Scheme 12-(11)-(12)).^{109,110}

In addition, epoxy compounds can be converted into CC by the reaction with β-butyrolactone (Scheme 12-(14))¹¹¹ or, in a much more common approach, by the chemical insertion of CO₂ (Scheme 12-(15)). The latter strategy has been extensively studied throughout different reaction conditions and catalyst optimizations. This method presents various advantages compared to the previous presented routes. Indeed, first the recapture of the CO₂ is a benefit regarding both the economical and environmental points of view.¹¹² Second, even if this reaction is usually performed at high pressure, in presence of a suitable catalyst, very high yields can be reached and it is a 100% atom economical reaction. The carbon dioxide both acts as an aprotic solvent and as a reagent.¹¹³ A plethora of catalysts has been investigated including homogeneous or heterogeneous ionic liquids, ammonium or phosphonium salts, amines, metal oxides, metal halides and metal complexes leading to good conversions. The most commonly used catalysts are the tetraalkylammonium halides.^{80,114-116}

Starting from olefin moieties, Yang *et al.*¹¹⁷ showed a possible one-pot microwave assisted synthesis of CC, passing by an epoxide intermediate, using NaHCO₃ as co-reactant.

Scheme 12 - Main routes for the synthesis of 5-membered cyclic carbonates.^{7-9,118}

A particular case of 5CC, which is already commercially available and bio-based, is the glycerol carbonate.⁷⁴⁻⁷⁶ The latter can be synthesized either from glycerol (obtained from vegetable oils by saponification or methanolysis) following the methods developed above, or from activated glycerol (3-chloro-1,2-propanediol) or epichlorohydrin using CO₂ or alkaline carbonate as sketched in Scheme 13. From glycerol, one of the most interesting routes would be the use of CO₂ to reach glycerol carbonate; however this route suffers from low conversions and yields. The more suitable processes are up to date the use of ethylene carbonate or dialkyl carbonates.⁷⁶



Scheme 13 - Synthesis of glycerol carbonate. (DMC=dimethyl carbonate, DEC=diethyl carbonate, 5CC=ethylene carbonate).

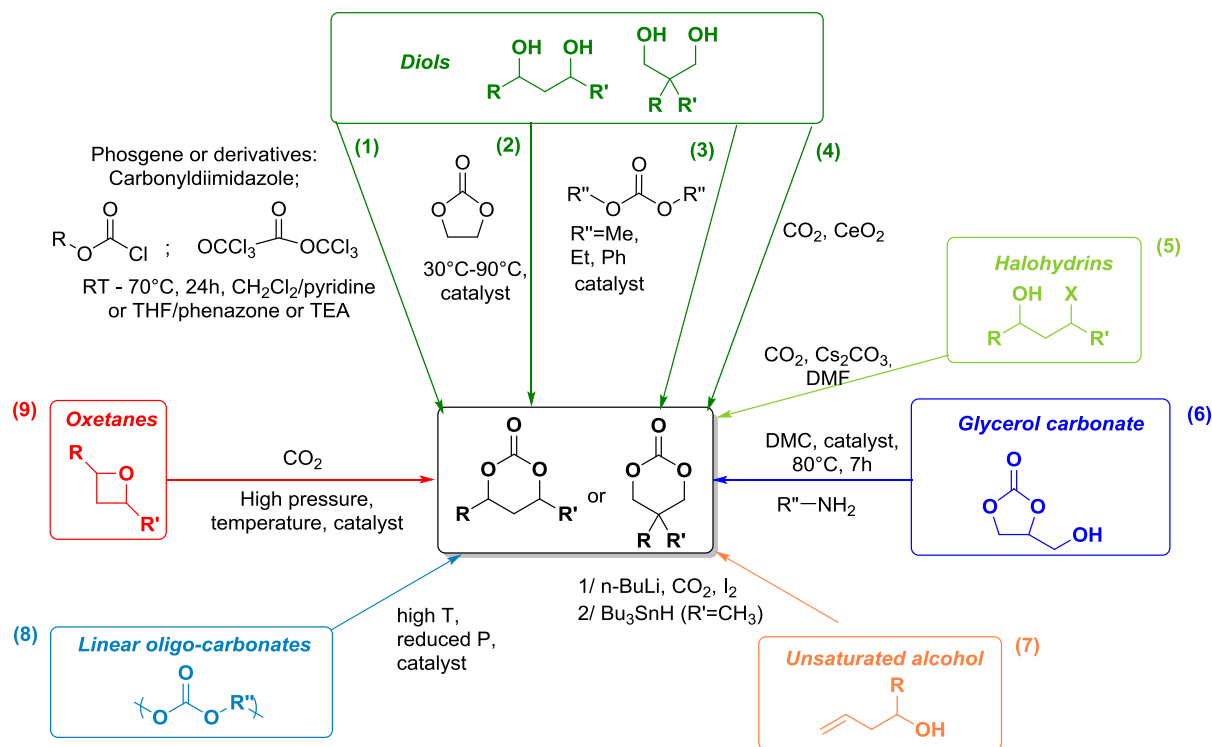
2.2. Synthesis of 6- to 8-membered cyclic carbonates (6CC- 8CC)

The 6-membered cyclic carbonates (6CC) can be prepared by similar methods as the ones used for the synthesis of 5CC.⁹ The latter can be achieved in a large proportion from 1,3-diols (also indirectly from glycerol carbonate) and, in a lower extent from 3,4-unsaturated alcohols, oxetanes using CO₂, or halohydrins. The main approaches are summarized in the Scheme 14.

The depolymerization process of linear oligo-carbonate presented in the previous part is still applied in the synthesis of 6- and 7-membered and of larger size aliphatic CC (Scheme 14-(8)). In another method, the 1,3-diols or 1,4-diols can be transformed into 6CC and 7CC respectively using phosgene derivatives such as triphosgene (Scheme 14-(1))^{88,119} or ethyl chloroformate.^{74,75} A closed method to afford 6CC from 1,3-diols is the use of dialkyl carbonates (Scheme 14-(3)). The presence of a catalyst is essential for this carbonate interchange.⁷⁹ Possible catalysts are alkaline metals,^{120,121} amines, basic ion-exchange resins,¹¹ oxides, alkoxides, or carboxylate salt of zinc, titanium, or tin,¹²²⁻¹²⁴ enzymatic catalysts,¹²⁵ etc. Pyo *et al.*^{125,126} reported that 6CC with functional groups could be

synthesized in the presence of lipase (Novozym 435), in a solvent-free medium by transcarbonation.

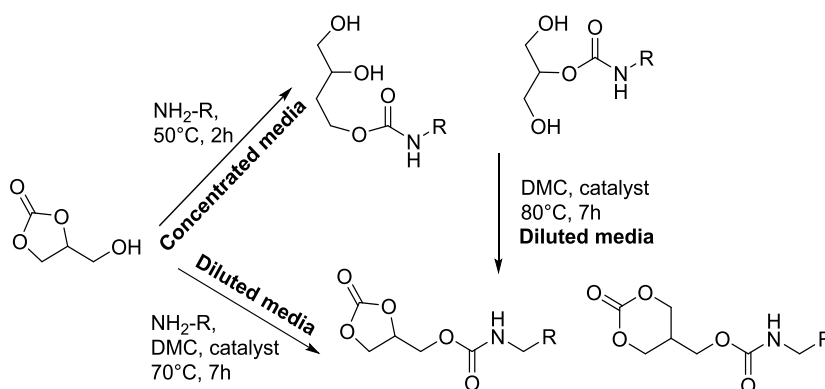
The possibility of synthesizing 5CC and 6CC with α -urethane group from glycerol carbonate and dimethyl carbonate (DMC) (Scheme 14-(6); Scheme 15) has been investigated in the presence of various catalysts, without solvents.¹²⁷



Scheme 14 - Main synthetic methods for the synthesis of 6-membered cyclic carbonates.

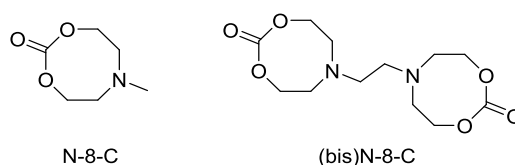
Another study exhibited the synthesis of 6CC from various diols with CO_2 (130-160°C, 5MPa) and CeO_2 as catalyst (Scheme 14-(4)).¹²⁸ The selectivity and the yields were particularly high (up to 99%). The reaction of oxetane with CO_2 (Scheme 14-(9)) can also be used to prepare 6CC. The addition of CO_2 is less efficient in the case of oxetane than for epoxides. Moreover, the efficiency of this reaction dramatically decreases with the number and the size of the substituents.^{129,130} The 6CC have also been synthesized from halohydrins with CO_2 using cesium carbonate in DMF (Scheme 14-(5)).¹⁰⁴

In the case of 7CC, the latter can be prepared by the same carbonation reaction pathways as those leading to 5CC and 6CC, or by reaction of an appropriate diol with phosgene (or its derivatives) in the presence of phenazone. Moreover, according to the depolymerization method, the corresponding cyclic dimers are formed almost exclusively when the expected monomer cycle size is from 7 to 12.⁷⁷



Scheme 15 - Synthesis of 5- and 6-membered cyclic carbonates with an α -urethane group.¹²⁷

More recently, Yuen *et al.*¹³¹ synthesized a 8CC from bio-based diethanolamine and dimethyl carbonate (Scheme 16, N-8-C). The mono-cyclic carbonate was dimerized for further polyaddition with diamines to achieve poly(hydroxyurethane)s.



Scheme 16 - Mono and bis 8-membered ring cyclic carbonates.¹³¹

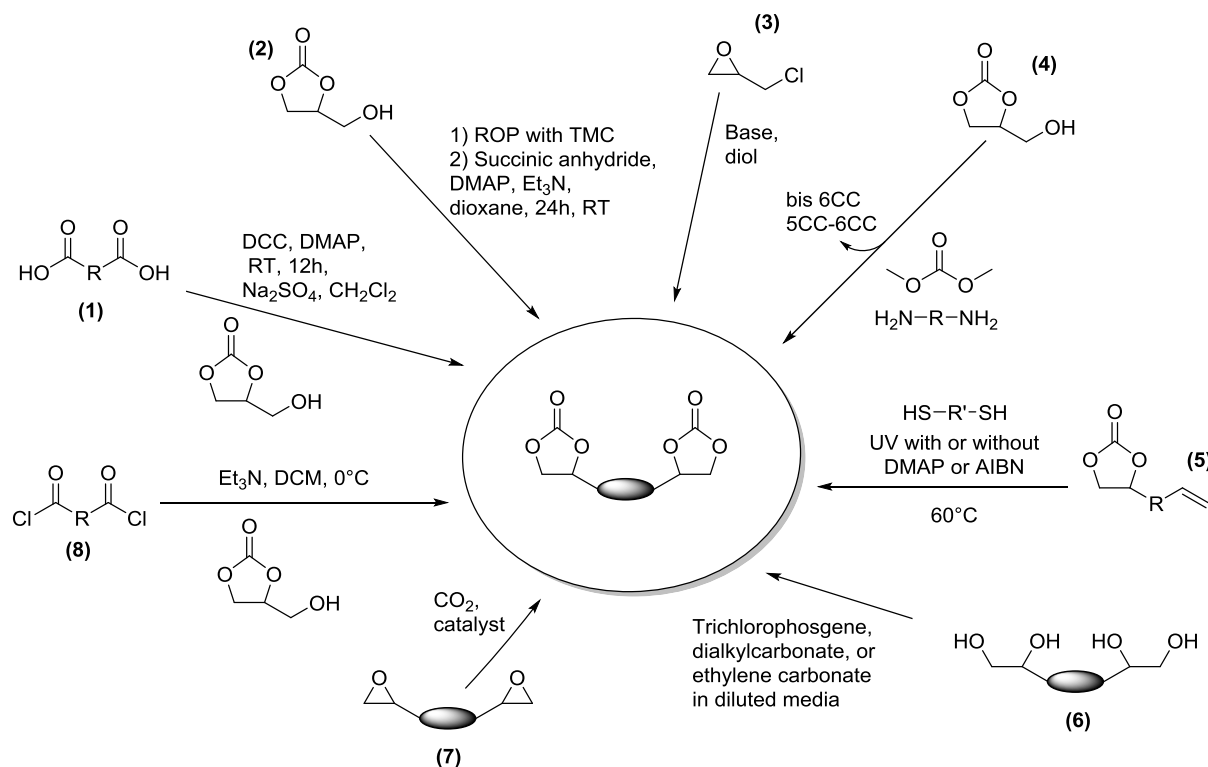
2.3. Synthesis of bis-cyclic carbonates (bCC)

In order to obtain poly(hydroxyurethane)s by polyaddition, various techniques have been developed to synthesize bis-cyclic carbonates (bCC). For the first presented methods, the b5CC are derived from already formed 5CC which present another reactive group such as in glycerol (hydroxyl) or in unsaturated-based cyclic carbonate (double bond). In order to keep the CC functions, mild reaction conditions are required for the coupling.

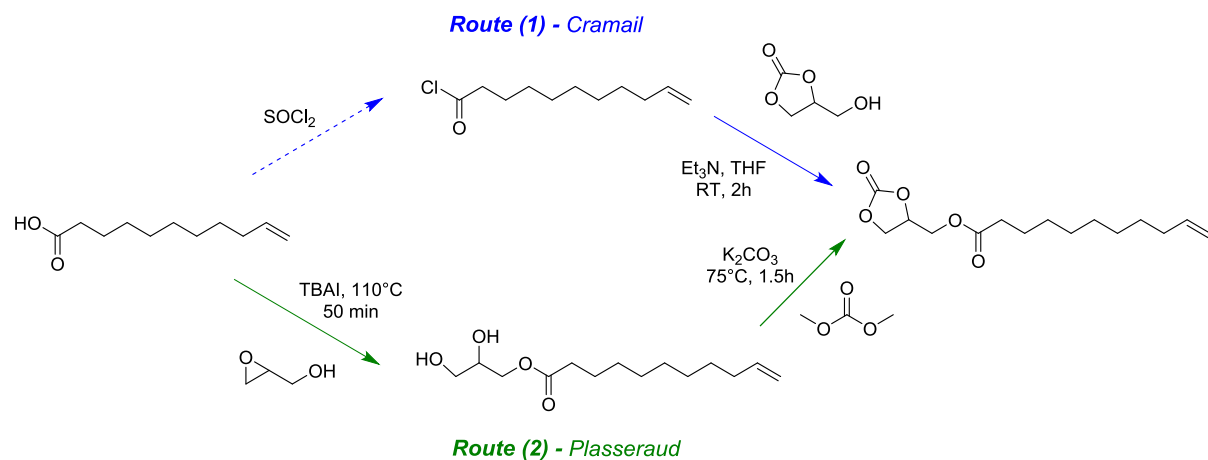
Scheme 17 illustrates the various routes to synthesize b5CC. Similar methods have been employed for the coupling to obtain b6CC.^{87,132}

From glycerol carbonate, a transesterification with a diacid using dicyclohexylcarbodiimide (DCC) and dimethylaminopyridine (DMAP) (Scheme 17-(1)) at room temperature enables the formation of a bCC.^{7,133} Besides, Carré *et al.* synthesized a bCC from sebacoyl chloride¹³⁴ or from terephthaloyl chloride¹³⁵ with glycerol carbonate (Scheme 17-(8)), using triethylamine in dry DCM to perform the reaction. The same strategy has been recently applied by Cramail

and coworkers¹³⁶ on undecenoyl chloride for the obtention of activated lipidic CC (Scheme 18-(1)). The same molecule has been synthesized by Passeraud and coll.¹³⁷ using an innovative route through glycidol addition on undecenoic acid in the presence of TBAI as catalyst, followed by the formation of the 5CC towards DMC substitution on diol (Scheme 18-(2)). A further metathesis reaction enabled the preparation of the corresponding b5CC.



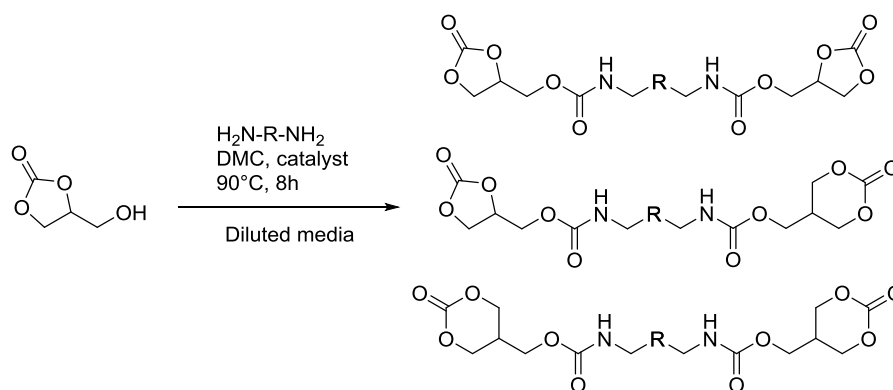
Scheme 17- Synthesis of 5-membered bis-cyclic carbonates.



Scheme 18 - Two strategies from (1) Cramail's and (2) Plasseraud's groups towards the synthesis of undecenoic acid-based cyclic carbonate.^{136,137}

The ring-opening polymerization of TMC has also been carried out using the hydroxyl of the glycerol carbonate as initiator. The bCC was then obtained by chemical transformation of the chain ends with succinic anhydride, followed by a transesterification with glycerol carbonate (Scheme 17-(2)).¹³⁸ Another option is the thiol-ene reaction on unsaturated CC by photochemical initiation (Scheme 17-(5))^{139,140} or *via* thermal means using azobisisobutyronitrile.^{87,132,139}

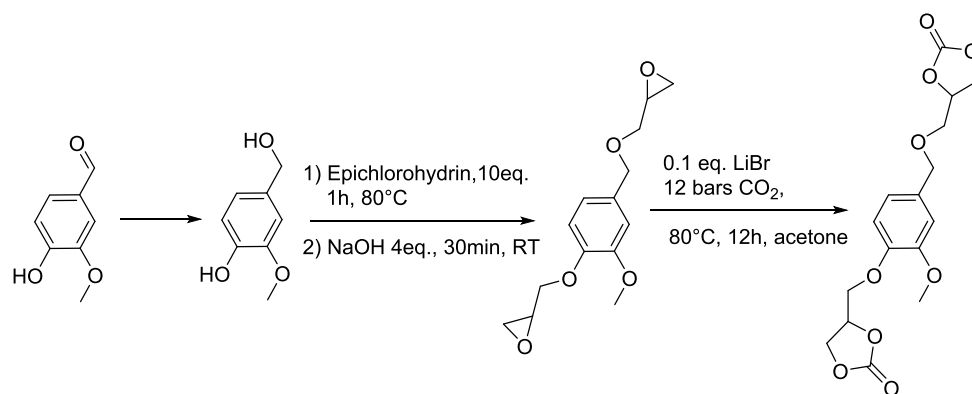
Mouloungui and coll.¹²⁷ prepared a mixture of 5CC and 6CC directly from glycerol carbonate, dimethyl carbonate and diamine (Scheme 17-(4), Scheme 19). The authors optimized the conditions by playing on the solubility properties of dimethyl carbonate and methanol and by using a strong basic liquid catalyst.



Scheme 19 - Synthesis of 5- and 6-membered bis-cyclic carbonates from glycerol carbonate, dimethyl carbonate and diamine.¹²⁷

Following another strategy, other bis or poly(5CC)s were synthesized either from bisepoxy^{141–143} or polyepoxides¹⁴⁴ by insertion of CO_2 (Scheme 17-(7)), or from tetraols or polyols using phosgene derivatives,¹⁴⁵ diethyl carbonate,^{146,147} imidazole carboxylic esters or ethylene carbonate⁹⁵ (Scheme 17-(6)) in adequate conditions.

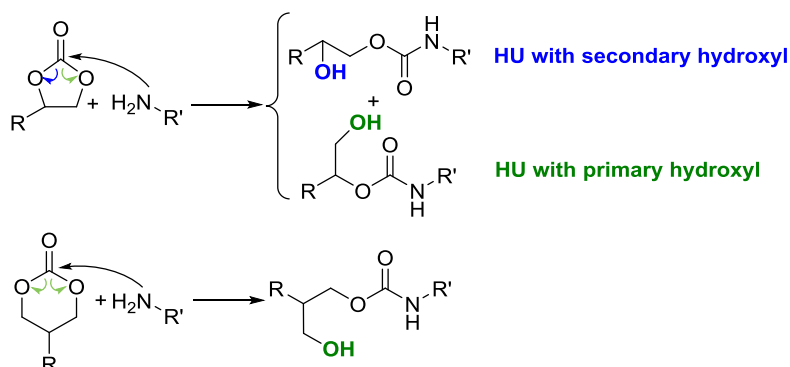
Caillol and coll.⁶⁰ synthesized several monomers based on vanillin as polymer precursor. The corresponding bis-carbonate was synthesized by reduction of vanillin, followed by the reaction with epichlorohydrin. The resulting bis-epoxide was carbonated under CO_2 pressure at 80°C (Scheme 17-(3), Scheme 20). The same strategy was proposed by Lamarzelle *et al.*¹³⁶ for the synthesis of monocyclic carbonate from 10-undecen-1-ol leading, *via* metathesis reaction, to bCC with an ether function in β position nearby the cycle.



Scheme 20 - Synthesis of bis-cyclic carbonate from vanillin moiety.⁶⁰

3. Studies on the model cyclic carbonate/amine reaction

Before performing the synthesis of PHUs, authors have studied the reactivity of CC with amines on model reactions to have a better understanding of the nucleophilic addition reaction between CC and amines, as illustrated in the Scheme 21.



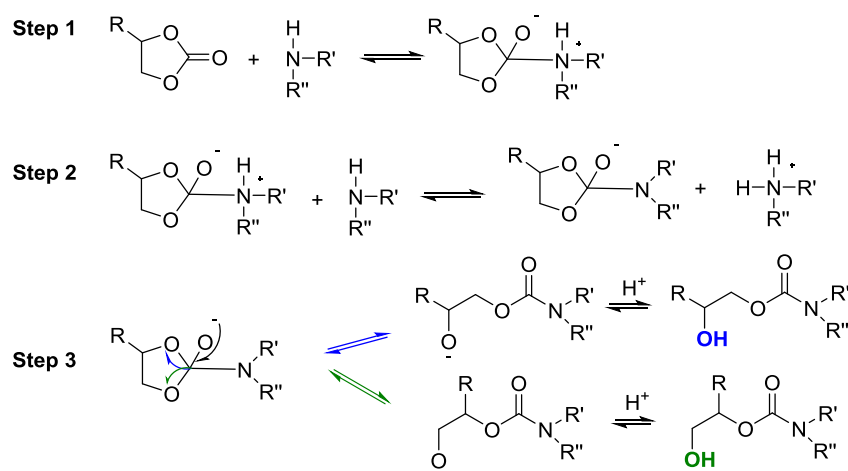
Scheme 21 - Model reaction on 5- and 6-membered cyclic carbonates leading to hydroxyurethanes.

3.1. Mechanism of cyclic carbonate aminolysis

Two reaction mechanisms have been proposed. First, Tomita *et al.*¹⁴⁸ suggested a mechanism through an amphoteric tetrahedral intermediate (Scheme 22). Garipov and coworkers^{149,150} proposed a similar mechanism proceeding in three steps and involving also a tetrahedral intermediate.

Zabalov *et al.*¹⁵¹ established by means of DFT calculations that hydroxyurethane formation may progress notably throughout a six centers ring intermediate based on the 5CC and two amine molecules, one playing a catalytic role.

Finally, the authors agree that the participation of a second amine molecule is necessary and substantially accelerates the process.



Scheme 22 - Mechanism through the formation of a tetrahedral intermediate for the reaction between 5-membered cyclic carbonates and amines.

3.2. Kinetic and reaction conditions

The kinetic of the reaction has been studied by different research groups. Moreover, various reaction conditions have been tested in the literature for the addition of amines on CC. Some authors pointed out the effect of the temperature, the initial concentration of the reactants and the solvent.

The increase of the reaction temperature leads to higher reaction rate. However, Burgel *et al.*¹⁵² proved that using a temperature higher than 100°C resulted in the formation of oxazolidinone as by-product. Besides, depending on the selected solvent, the reaction rates are variable. Most of the reactions are performed in DMSO or DMF. Tomita *et al.*^{148,153} demonstrated a slight increase of conversion and yields for reaction in toluene compared to DMSO.

Concerning the effect on the reaction of the presence of solvent and the initial concentration of the reactants, it has been shown in various studies that the reaction of CC and amines occurs faster in bulk than in solvent.¹⁵⁴ A decrease of the initial concentration of the reactants also affects the reaction rate as it has been shown by Tabushi *et al.* (review by Webster *et al.*)¹⁵⁵, Nemirovsky *et al.*¹⁵⁶ and Burgel *et al.*¹⁵⁷

The majority of the authors who studied the kinetic of the reaction of CC with amines in aprotic solvents agree on a kinetic of an overall second order.^{88,148,154,156,158–161} However, few

reports relate higher kinetic order with respect to the amine,¹⁴⁹ as well as the auto-catalytic effect of the hydroxyurethane formed.¹⁵⁵

The polyaddition of amines onto CC is governed by several parameters such as solubility, type of solvents, concentration and temperature. Besides, the chemical structure of both amines and CC has a significant impact on the polymerization rate.

3.3. Effect of the chemical structure of the amine

The chemical structure of the amine influences the reaction rate as proved by numerous studies. All authors agree that secondary amines are less reactive, even non-reactive, toward CC compared to primary ones. The nucleophilicity of the amine seems to govern its reactivity.^{88,149,152,155,157,162}

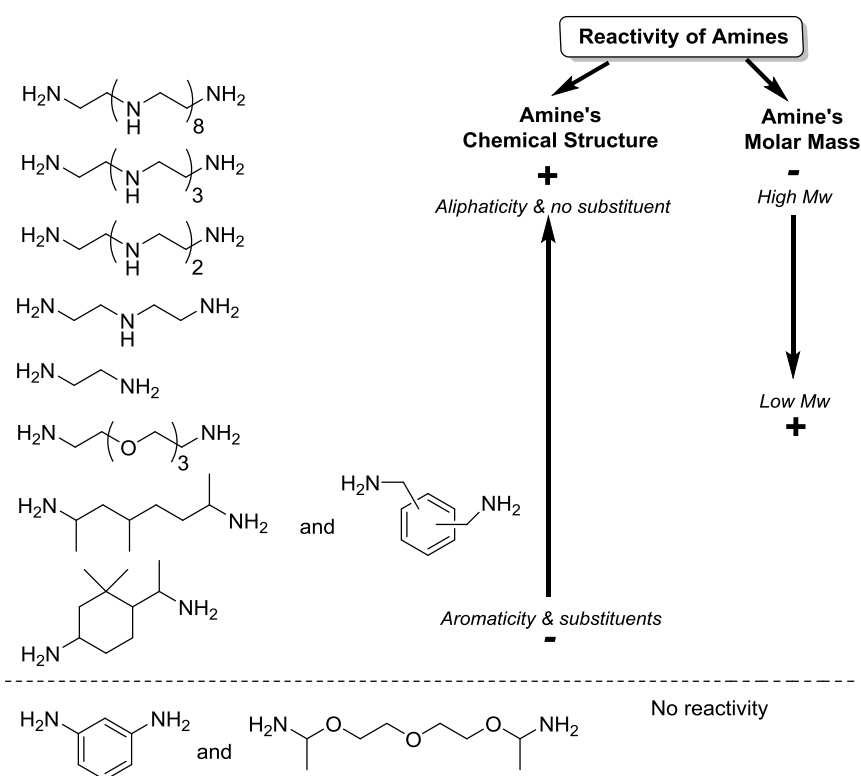


Figure 2 - Scale of reactivity of various amines toward a model cyclic carbonate (according to Diakoumakos *et al.*¹⁶⁴).

Lately, Camara *et al.*¹⁶³ also studied the lower reactivity of secondary amines towards CC. Nevertheless, according to their observation on a model reaction, the authors pointed out the possibility for polyhydroxyurethanes bearing secondary amine functions in their backbone to cross-link with the remaining CC from a certain temperature.

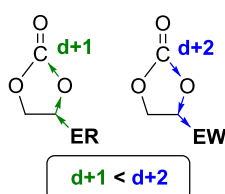
Besides, Diakoumakos *et al.*¹⁶⁴ demonstrated that amines with strong electron-withdrawing groups in α or β position with respect to the reactive amino group are less reactive. Besides, their research indicates that the molar mass of amines has a certain influence on their reactivity. Higher molar mass amines were less reactive than shorter ones. The scale of reactivity of the tested amines was illustrated in Figure 2. Demonstrating a same trend, Nohra *et al.*¹⁶⁵ found that as the alkyl chain of the amine increases, the carbonate yield slightly decreases.

The authors concluded that the reaction rate depends on the nucleophilicity, the chemical structure and the steric hindrance of the amine.^{88,164}

3.4. Effect of the substituent and size of the cyclic carbonate

Several studies relate the effect of the CC substituent on the reaction rate and the final isomer product. First papers reported either that electron withdrawing groups nearby the CC decreased the reaction rate (Mikheev *et al.* reviewed by Webster *et al.*¹⁵⁵), or that the CC substituent has a limited influence on the reaction rate (Couvret *et al.*¹⁵⁴). Those conclusions are not in accordance with more recently published literature.

Tomita *et al.*¹⁴⁸ studied a large series of mono-substituted 5CC and found that the aminolysis rate increased as the electron-withdrawing character of the substituent increased. Garipov *et al.*¹⁴⁹ proved that the presence of an electron releasing substituent (+I) in the CC results in a decrease of the partial positive charge on the carbonyl carbon. This results in a reactivity decrease of the CC towards amine. On the contrary, electron-withdrawing substituents (-I) increase the electrophilicity of the carbonyl carbon and thus favor higher reaction rate with amines (Scheme 23). This statement was supported by a recent study published by Cramail and co-workers¹³⁶ where several ‘activated’ monocyclic carbonates presenting ether or ester moieties in β position were found more reactive towards aminolysis than their aliphatic-substituted counterpart.



Scheme 23 - Effect of the electron releasing (ER) and electron withdrawing (EW) substituents.

In the same line, He *et al.*¹⁵⁹ examined the reactivity of various 5CC bearing either urethane with the oxygen atom near the CC in α or in β . The authors concluded that the more distant the electron-withdrawing group is from the CC, the less reactive it is.

Another method to increase CC reactivity towards aminolysis is the use of 6-, 7- and 8CC that have been reported to be much more reactive than 5-membered ones.

Ochiai *et al.*¹⁵⁸ found out that the difference in reactivity between 5CC and 6CC comes from the different ring-strain. In 2001, two chemically similar bCC were synthesized by another research group⁸⁷, one with two 5-membered rings (b5CC) and the second one with 6-membered rings (b6CC). The b6CC was converted quantitatively after 48 hours although the conversion of the b5CC was only 67% during this time period. Moreover, the b6CC enabled forming PHUs with a molar mass of 26000 g.mol⁻¹ after 48h, whereas the molar mass obtained in the case of b5CC was only of 15000 g.mol⁻¹ after 14 days. The calculated reaction rate constant enabled quantifying the higher reactivity of the 6CC toward the 5-membered one: $k_{b6CC-30^{\circ}C} = 0.70 \text{ L.mol}^{-1}.\text{h}^{-1}$; $k_{b6CC-50^{\circ}C} = 0.89 \text{ L.mol}^{-1}.\text{h}^{-1}$; $k_{b6CC-70^{\circ}C} = 1.07 \text{ L.mol}^{-1}.\text{h}^{-1}$ and $k_{b5CC-30^{\circ}C} = 0.03 \text{ L.mol}^{-1}.\text{h}^{-1}$; $k_{b5CC-50^{\circ}C} = 0.06 \text{ L.mol}^{-1}.\text{h}^{-1}$; $k_{b5CC-70^{\circ}C} = 0.10 \text{ L.mol}^{-1}.\text{h}^{-1}$. The reaction rate for the b6CC was lower than the one calculated for the 6CC, probably because of the lower mobility of the reactive sites of the bifunctional monomer and polymer ends. In contrast, they were almost equal in the case of bifunctional and monofunctional 5CC, certainly because of their low reactivity. Besse *et al.*¹³² in 2013 also observed higher molar mass for the PHU from b6CC compared to the ones from b5CC. He *et al.*¹⁶⁶ confirmed the difference in reactivity of the two different size rings, studying monomers bearing a 5CC and a 6CC.

Additionally, Tomita *et al.*⁸⁸ found that 6CC were more reactive than the 5-membered homologues, with reaction rate constants 29 to 62 times higher. Maisonneuve *et al.*¹⁶¹ confirmed their greater reactivity with a factor 30 between both reaction rate constants.

Going even further, the group of Endo¹¹⁹ prepared b7CC and observed higher reactivity and molar mass than with b5CC and b6CC. Molar masses up to 35700 g.mol⁻¹ were obtained after only 6 hours of reaction. Regarding 6CC and 7CC, the authors did not mention any side reaction generated by the attack of the primary hydroxyl group formed onto the carbonyl of the CC. However, due to the high reactivity of the 7CC, its reaction rate constant in DMSO at 50°C was not calculated.

Lately, Yuen *et al.*¹³¹ carried out the synthesis of an atypical 8CC (Scheme 16, N-8-C) that exhibited towards aminolysis a 20 times higher k_{app} than ethylene carbonate. The enthalpy of

hydroxyurethane formation was evaluated at $-12.2 \text{ kcal.mol}^{-1}$ and was highly superior to the ones exhibited by 5CC⁸⁸ ($\Delta H_{f5CC} = -1.14 \text{ kcal.mol}^{-1}$). The higher reactivity was also confirmed in polymerization with molar masses up to 47000 g.mol^{-1} when polyaddition between (bis)N-8-C carbonate (Scheme 16, (bis)N-8-C) and hexamethylenediamine was conducted for 24h in DMF at room temperature.

Although the higher ring-strain confers enhanced reactivities to 6-, 7- or even 8CC, the latest are hardly operable at the industrial scale due to their tremendous instability. The synthesis of 5CC bearing electron withdrawing substituents appears as one of the most promising methodology with catalysis to increase the CC reactivity towards amines.

3.5. Selectivity and by-products

Two isomers can be formed while reacting 5CC with amines: one with primary hydroxyl groups and one with secondary ones. In the case of the reaction between 6CC, only primary hydroxyl groups are obtained if the carbonate is substituted in β of the oxygen (Scheme 21).

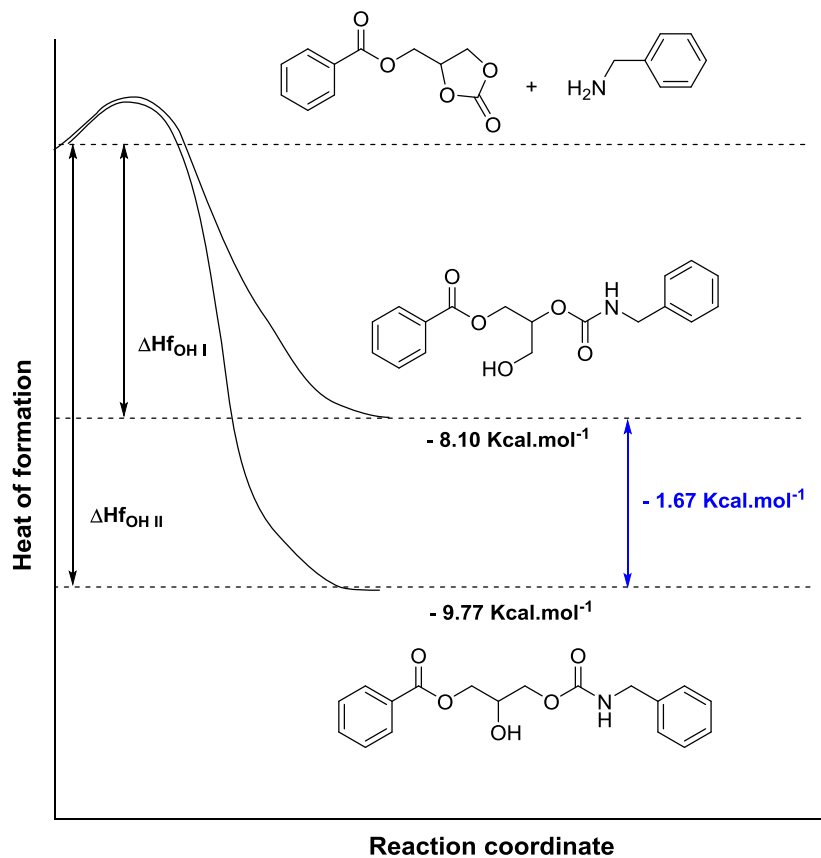


Figure 3 - Energy profile of ring-opening addition of 5-membered cyclic carbonate with benzylamine.¹⁴²

As a general trend, it was found that substituted 5CC react with amines to give preferentially secondary hydroxyl groups. Steblyanko *et al.*¹⁴² reacted glycerol carbonate benzoate with benzyl amine at room temperature. The secondary hydroxyl group product was predominant in a OH_I:OH_{II} ratio of 18:82. They carried out theoretical calculations and confirmed that the secondary hydroxyl product was enthalpically more stable than the primary hydroxyl group product by about 1.67 kcal.mol⁻¹: $\Delta H_{f(\text{OH I})} = -8.10 \text{ kcal.mol}^{-1}$ and $\Delta H_{f(\text{OH II})} = -9.77 \text{ kcal.mol}^{-1}$ (Figure 3).

Accordingly the bond orders in substituted 5CC calculated by the *ab initio* method, indicate that there should be more of the hydroxyurethane containing secondary hydroxyl moieties than hydroxyurethane containing primary hydroxyl groups (Figure 4).^{148,153}

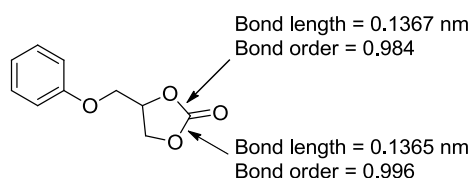


Figure 4 - Bond lengths and order calculated by the *ab initio* method using the STO-3G basis set.¹⁴⁸

Authors found an influence of the solvent and the chemical structure of amines and CC on the region-isomers ratio, although the selectivity of hydroxyurethane seems independent of the reaction temperature. Tomita¹⁵³ conducted a study of the effect of reaction conditions on the structure of the urethane formed. Their analysis indicated an isomer ratio slightly dependent on the solvent polarity and the amine structure. For instance, the isomer with secondary hydroxyl is less formed in DMSO than in toluene.^{148,153} The influence of the amine chemical structure was reported by different research groups^{167,168} One of them showed that a lower amount of hydroxyurethanes containing secondary hydroxyl groups was obtained when benzylamine was preferentially used to hexylamine.¹⁵³ Another research group concluded that as the alkyl chain of the amine increases, the yield increases and the ratio OH_I:OH_{II} increases.¹⁶⁵ With secondary amines, an equivalent proportion of OH_I and OH_{II} has been reported.¹⁶⁵

In addition, the effect of the CC substituents was clearly demonstrated and explained by the mechanism (Scheme 22).^{148,149,154} The selectivity of the reaction favored the formation of secondary hydroxyl-based hydroxyurethane as the electron withdrawing character of the substituent increased.¹⁴⁸ Indeed, the inductive effect increases the acidity of the negatively

charged oxygen and stabilizes the transition state. The reaction thus favors the formation of structures with secondary hydroxyl groups. Iwasaki *et al.*¹⁶⁹ also observed this trend with phenyl substituents having para-groups of different electron-withdrawing effect. As an extreme result, Ochiai¹⁷⁰ obtained only secondary hydroxyl group performing the reaction between diethyltriamine and carbonated epichlorohydrin.

3.6. Additives and catalysts for the cyclic carbonate/amine reaction

Theoretically, the ring-opening reaction of CC by amines may be accelerated through activation of the monomers. To this purpose, either weakly Lewis acidic or oxophilic additives may be added to increase the electrophilicity of the CC group, or basic additives can be used to increase the nucleophilicity of the amines and even to deprotonate the amines. Another possibility is to use a Lewis base to attack the carbon of the CC carbonyl. The Lewis base will be then a potential good leaving group that will favor the attack of the amine molecule.

Concerning the catalysis of this reaction, almost exclusively patents have been reported. There are only few papers that deal with this specific point, which are discussed in priority after a general overview. Most of the tested catalysts and additives used are summarized in Figure 5. Different classes of catalysts have been tested, among them organic catalysts, organometallic catalysts and salts.

Amongst organic catalysts, either strong bases (such as 4-pyrrolididino pyridine, guanidines (TBD, MTBD), 1,4-diazabicyclo[2.2.2]octane (DABCO), piperazine and triethylamine)¹⁷¹⁻¹⁷⁵ or strong or weak Brönsted acids (glacial acid acetic, methanesulfonic acid)¹⁷¹ have been used for the catalysis of the CC/amine reaction. Salts combining an alkali metal or ammonium salt cation, with an anion such as OH⁻, CO₃²⁻, Br⁻, Cl⁻,... or a strong base have also been tested.^{171-173,176} Interestingly, Detrembleur and coworkers¹⁷⁷ employed a bicomponent organocatalyst composed of an onium salt and a fluorinated alcohol for successive carbonation of epoxidized soybean oil and its polymerization with an amino-telechelic oligamide. Regarding Lewis acids, lithium based salts such as Li₂O, LiBr, LiCl, LiOH, LiF,... were investigated.^{174,178-180} For organometallic catalysts, zinc, tin and chrome-based compounds have been found to have some activity to catalyze the CC / amine reaction.^{167,171,180,181}

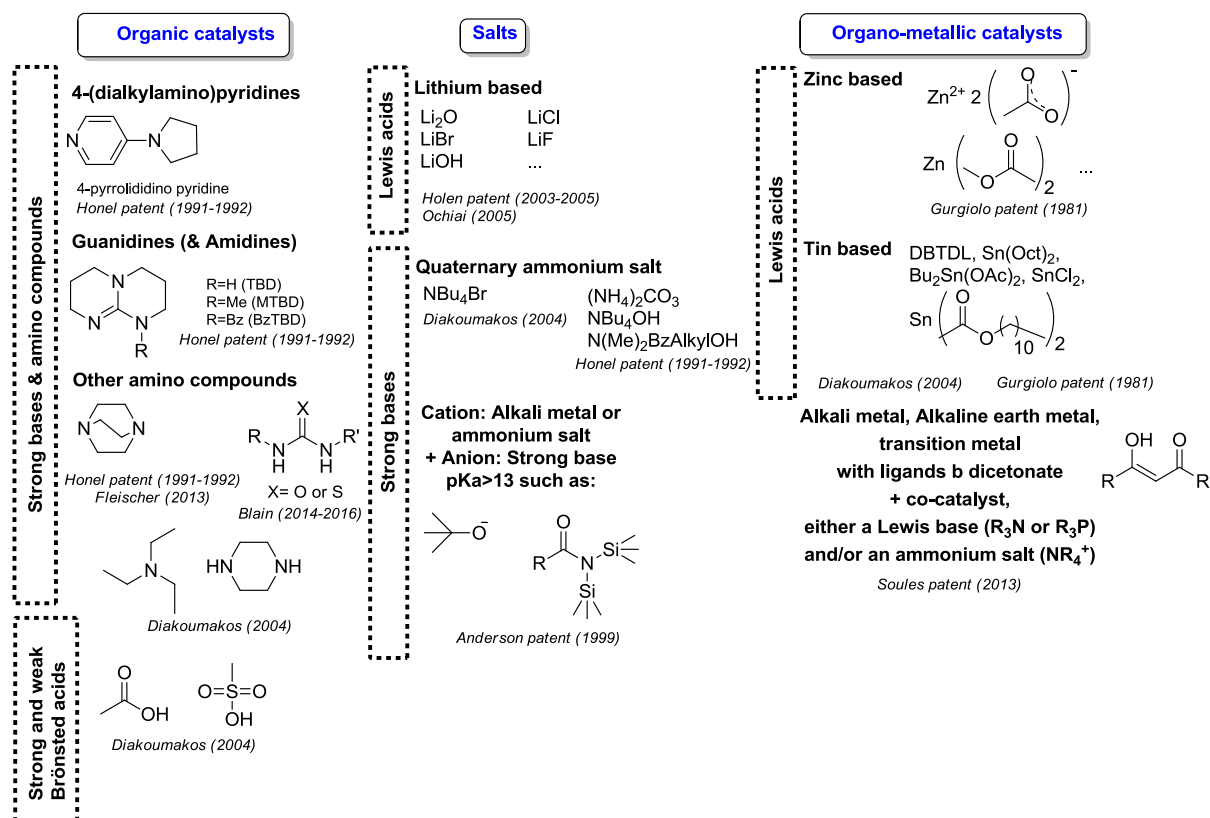
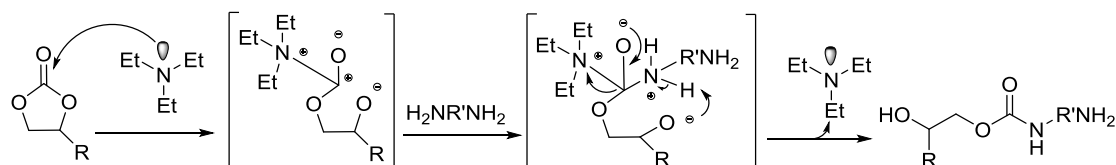


Figure 5 - Various tested catalysts for the cyclic carbonate/amine reaction.

Alkali metal-based Lewis acid such as LiCl, LiBr or LiF can be employed to increase the reaction rate.^{140,182} They activate the carbonyl group without the deactivation of the amine. Ochiai *et al.*¹⁸⁰ observed that the higher molar masses were obtained with LiCl, LiF and Bu₄Sn, which give molar masses of 36700 g.mol⁻¹ (\bar{M}_n , Đ=1.84), 31600 g.mol⁻¹ (\bar{M}_n , Đ=1.71) and 32700 g.mol⁻¹ (\bar{M}_n , Đ=1.70) respectively, compared to 19300 g.mol⁻¹ (\bar{M}_n , Đ=1.88) without catalysis in the same conditions.

The reaction can also be effectively catalyzed by the use of triethylamine which reduces the activation energy of the reaction by up to 17.5% compared to that of the non-catalyzed system.¹⁷¹ The authors proposed a mechanism for the catalysis with triethylamine as depicted in Scheme 24.



Scheme 24 - Proposed mechanism of the activation of cyclic carbonates with triethylamine.¹⁷¹

In the same study, various other catalysts, including acids (glacial acetic acid, methanesulfonic acid), bases (piperazine, TBABr, or tin-based catalysts (tin (II) octanoate, DBTL), etc. were also used effectively.

Fleischer *et al.*¹⁷⁴ performed the polyaddition between a b5CC and hexane-1,6-diamine in mold. The authors observed that 1 w.% of DABCO could increase the conversion from 60% to 90% at room temperature in 2 min.

In 2014, Andrioletti and coll.¹⁶⁰ carried out a complete screening of catalytic systems for the ring opening of CC by amines in solvent model reactions. Organocatalysts displayed a higher efficiency than inorganic Lewis acids. TBD and cyclohexylphenyl thiourea appeared as promising catalysts for production of poly(hydroxyurethane)s. The same team recently replaced expensive thioureas by the more available and cheaper ureas¹⁸³ in the aminolysis of CC. Interestingly, a correlation between catalytic efficiency and (thio)urea pKa was made, directing further developments towards the design of new catalysts. Therefore, less acidic and more soluble urea catalysts that are less likely to be deactivated through deprotonation would be an attractive approach for the catalysis of CC aminolysis.

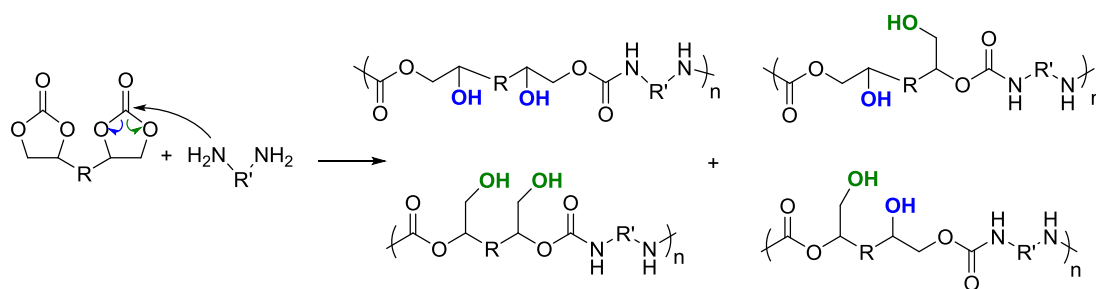
Maisonneuve *et al.*¹⁸⁴ performed a catalytic study in bulk using a model reaction between the propylene carbonate and the hexylamine. Schreiner catalyst, LiCl, DBU, ZnAc, MTBD or DMP were loaded at 5 mol.%. Catalysts were effective at the beginning of the reaction. However, after 1h, similar conversion to uncatalyzed system was observed. This could be explained by the high H-bonds density progressively formed with the conversion, due to the generated hydroxyl groups.

Besides, a cooperative catalysis has been developed by Scheidt and co-workers¹⁸⁵ who used TBD and LiOTf as co-catalyst for the ring-opening of CC by amines at room temperature. This new Lewis acid/Lewis base combination substantially decreased reaction times for tested model reactions and polymerizations.

4. Thermoplastic Poly(hydroxyurethane)s (TPHUs)

The polyaddition of b5CC and diamines, leading to the formation of linear PHUs (thermoplastic PHU, TPHU) with primary or secondary alcohols (Scheme 25), represents the most challenging route to NIPU. One of the pioneers in this field are Groszos *et al.*;¹⁸⁶ the authors patented in 1957 the preparation of oligo hydroxylurethanes by the reaction between

CC, amine compound and urea. Studies on CC^{77,155,187} and PHUs¹⁰⁻¹⁴ have been reviewed by several research groups.



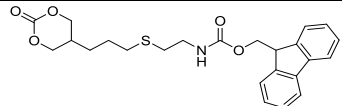
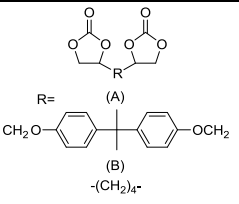
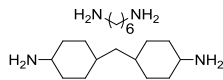
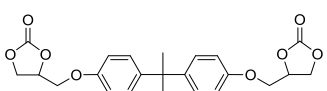
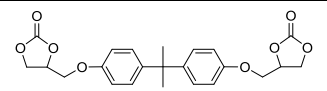
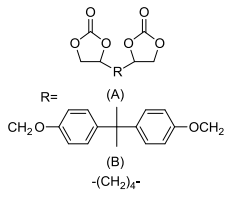
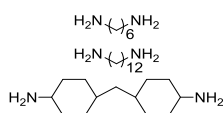
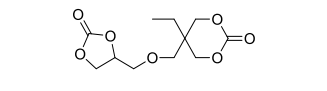
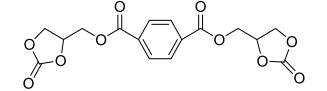
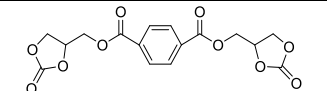
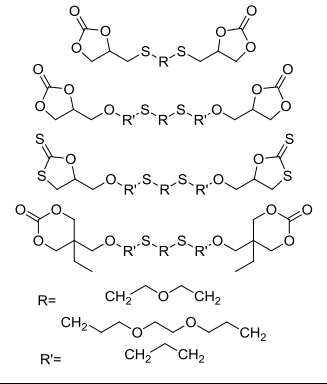
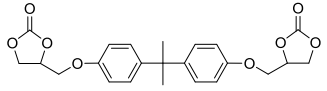
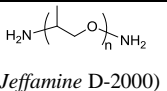
Scheme 25 - Synthesis of polyhydroxyurethanes from bis 5-membered cyclic carbonates and diamines.

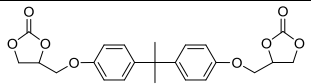
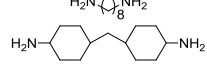
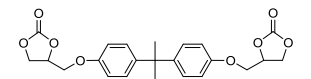
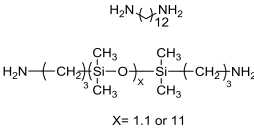
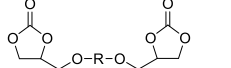
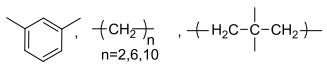
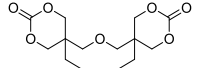
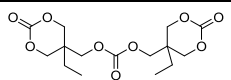
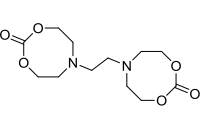
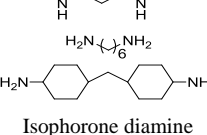
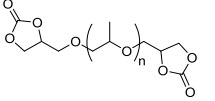
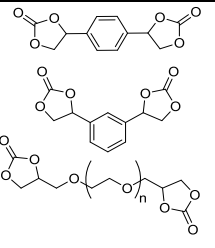
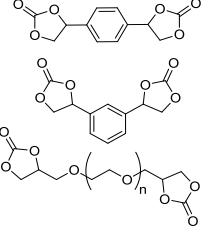
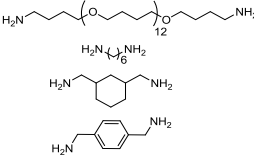
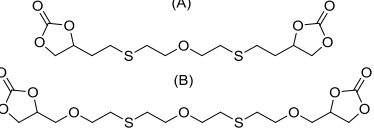
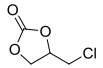
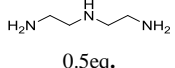
The PHUs obtained by this route exhibit various advantages such as the by-pass of isocyanate and phosgene making the process safer, and the capture of CO₂ in some cases. The hydrolytic stability is also an advantage of this pathway. Indeed, no particular caution during the storage processes is required and no formation of irreversible side products (urea and CO₂) like in the classical isocyanate/alcohol route is observed.⁹ Besides, the possibility to prepare materials with no release of volatile organic compounds promotes the use of this route for coating applications.⁷ The presence of hydroxyl groups in the structure gives specific properties to the polymer. The hydroxyl groups formed at the β-carbon atom of the urethane moiety can participate into intramolecular and intermolecular hydrogen bonds. Those hydrogen bonds combined with non-porous materials and the absence of thermally labile biuret and allophanate groups enable improved thermal stability and chemical resistance to non-polar solvents.^{9,188} The authors disagree on the water absorption effect of PHUs compared to classical PUs. Some claimed lower water absorption thanks to the hydrogen bonds,¹¹ but others presented higher water absorption due to the hydrophilicity of the polymer formed.⁸⁷ Moreover, the reactive pendant hydroxyl groups enable further post-functionalizations of the PHUs with chemical and biological functionalities.⁶

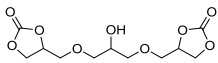
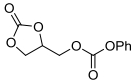
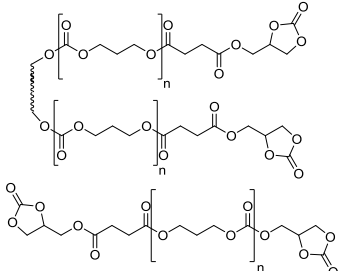
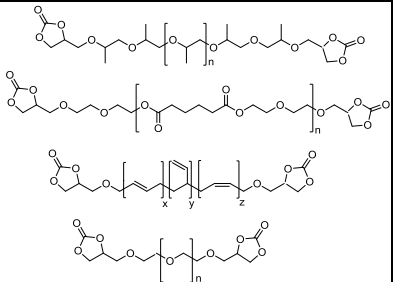
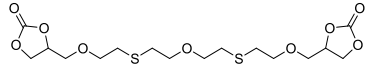
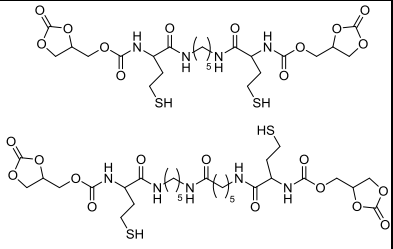
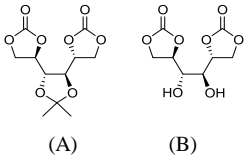
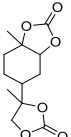
Many authors reported the preparation of PHUs from bis- or poly-cyclic carbonates and di- or poly-amines or from AB or AB_x monomers with a CC and an amino group. Due to the scope of this manuscript, only thermoplastic poly(hydroxyurethane)s will be discussed in this part. The Table 1 presents an overview of the poly(hydroxyurethane)s described in the literature.

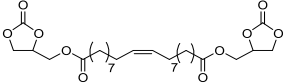
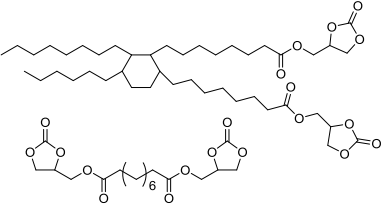
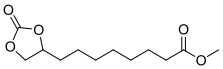
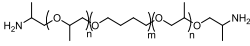
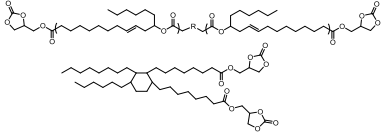
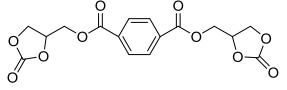
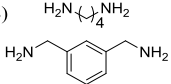
Table 1- Summarized literature about thermoplastic Poly(hydroxyurethane)s.

Bis-Cyclic carbonates	Diamines	Reaction conditions	\bar{M}_n (g/mol), [D]	Thermal properties (°C)	Ref
<i>Petroleum-based cyclic carbonates</i>					
	Primary aliphatic unhindered diamine C_2-C_{20}	EtOAc, DMSO, DMF, benzene, 0-140°C	Higher \bar{M}_n in solvent	-	103
	$H_2N-(CH_2)_x-NH_2$ $x=2,3,6,12$ 	DMSO, 24h, 70°C or 100°C (no reaction at RT)	13000-28000 [1.39-2.16] ^a	$T_g=34^f$ $T_d=310$	141
	1,6-diaminohexane, xylene diamine, 1,8-diamino-3,6-dioxaoctane and piperazine Many secondary diamines (N,N'-dibenzyl ethylene diamine)	DMSO, 75°C	3170-7700 [1.6-2.35] ^b	-	189
		DMAC, DBU(1eq.) or TEA(2eq.), 24h	13000-24000 [1.3-1.58] ^a	-	190
	$H_2N-(CH_2)_x-NH_2$ $x=2,3,5,6$ 	DMF, 10 mol.L ⁻¹ , RT, 72 h	6300-7700 [1.52-1.80] ^a	$T_g=3-29^f$ $T_{d10\%}=177-277$	142
		DMSO, 1 mol.L ⁻¹ , 100°C, 24h	4300-12900 [1.18-1.99] ^e	$T_g=50-102$ $T_d=339-388$	143
	$H_2N-(CH_2)_x-NH_2$ $x=2,3,5,6$ 	DMSO, 0.5 mol.L ⁻¹ , 70°C, 30d	-	-	153
		- DMAC, 1 mol.L ⁻¹ , 50°C, 24h - B6CC 100% conv. and 67% for B5CC in 48h - B5CC conv. did not reach 100% even after 14d	B6CC: 26000 (48h) ^a B5CC: 15000 (14d)	-	87
		DMSO, 0;5 mol.L ⁻¹ , 30-50-70°C, 6h	10900-35700 [1.3-2.8] ^a	-	119

 fluorenylmethoxycarbonyl (Fmoc)-protected amino groups		DMSO, 1 mol.L ⁻¹ , 30-50 or 70°C, 14d	3200-11000 [1.1-1.2] ^a	-	191
		Water, 0.5 mol.L ⁻¹ , organic solvent and surfactant free, 50- 100°C, 24h/48h	500-4400 [1.03-2.16] ^a	-	192
		DMSO, 1.7 mol.L ⁻¹ , 70°C, 6h + 5mol.% Additives such as lithium salts, NaCl, Bu ₄ NCl, CaCl ₂ , Bu ₄ Sn, Bu ₂ Sn(OAc) ₂ , K ₂ CO ₃ , CaH ₂	- without additive: 19300 [1.88] ^{a, *} - with additive: 14600-36700 [1.73-1.84] ^{a, *}	-	180
		DMSO, 1 mol.L ⁻¹ , LiCl, 70°C, 24h, Y=93%	26200 [1.71] ^{a, *}	T _g = 46 ^f	193
		1/ Ionic liquid, 0.2- 1 mol.L ⁻¹ , 70°C, 24h Y:88-92% 2/ water : N-n- butylimidazolium hexafluorophosphate (0.5:1), different T°C, 24h, Y:51-94%	1/ 4200-20800 [1.7-2.11] ^a 2/ 600-5100 [1.57-7.54] ^a	-	194
	1,6-diaminohexane, 4,9- dioxadodecane-1,12- diamine, triethylenetetramine and combination	Solvent, RT or T°C (60-90°C), in one or two step, 3d (°C) or 60d (RT), Y:85-96%	1340-8800 [1.45-2.11] ^a	-	166
		DMF, 1.3 mol.L ⁻¹ , 75-120°C, 48h	8000-20000 [1.9-2.5] ^c	T _g = 41-48 depend on the polymerization T°C	195
	Various diamines	DMF, 75°C, 48h	3800-18000 [≈2] ^c	T _g = 4-78	133
	Isophorone diamine, diethylenetriamine	(A) DMF, RT or 60°C, 90h (B) THF, 16h, hydroxyethylacrylate (C) DMF, RT or 60°C, 24h, 2 mol.% diisopropylethyl- amine	1800-20400 [1.4-3.1] ^c	T _g = -29-19 ^f T _{d20%} = 252- 296	132
	 (Jeffamine D-2000)	Solvent, microwave reactor (10-50 min, 50-250 W), 5% catalyst (LiBR or TBAC)	8600-13000 [1.05-1.24] ^e	T _d = 150-268	196

		DMSO, TBD, 20h + 4h quenching, RT- 80°C	5430-53400 [1.17-1.39] ^a	-	175
		PGMAC (propylene glycol monomethyl ether acetate), 80-100°C, 24h	12000-15500 [1.76-3.7] ^e	T _g = 1-40 T _{d5%} = 300	197
 R = 		Bulk, 60°C 20 min, 80°C 2h No catalyst	25400-30200 [1.18-1.22] ^a	T _g = -2-9 T _{d5%} = 206-266	198
		DMF, 0.5 mol.L ⁻¹ , 70°C, 24h	3800-6300 [2.11-2.61] ^a	-	199
		DMF, 0.27 mol.L ⁻¹ , -10°C, 48h	1500-2000 [2.08-2.76] ^b	-	200
	 Isophorone diamine	DMSO-d6 or D2O, 1 mol.L ⁻¹ , 25-80°C, 24h	19500-47000 [1.22-1.66] ^a	-	131
	Ethylenediamine	Bulk, 60°C, 4h	1000-3000 [1.6-3.6] ^e	T _g = -19 - 20 T _{d50%} = 287-290	201
		Bulk, 80°C	-	T _g = -67 – 27 (determined by DMA)	202
		DMF 0.6 mol.L ⁻¹ , 70°C, 24h	M _n : 3100-10000 M _w : 12200-48300 ^e	T _g = -70 - -60 (determined by DMA)	203
Semi bio-based cyclic carbonates					
 (A) (B)		DMF, 75°C, 24h	(A)7000 [1.5] ^c (B)9000 [3.2] ^c	(A) T _g = -14 ; T _{d5%} = 227 (B) T _g = -31 ; T _{d5%} = 227 ^g	139
	 0.5eq.	Polyaddition proceeded through nucleophilic addition of the primary amino group to the cyclic carbonate structure (THF, RT) and quaternization of the secondary amino group with the chloromethyl (in	940-3120 [1.18-1.81] ^e	-	170

		molten salts)			
	$\text{H}_2\text{N}(\text{CH}_2)_6\text{NH}_2$	25-50-70-100°C, 8h, in a mold $T < 70^\circ\text{C}$	-	$T_g = 20^f$	174
 AA* monomer	$\text{H}_2\text{N}(\text{CH}_2)_x\text{NH}_2$ $x=2,3,4,5,6$	DMAC, 2 mol.L ⁻¹ , RT, 20h	6400-8700 [1.46-1.57] ^d	$T_g = 22.6-52.8^f$ $T_d = 225$	204
	$\text{H}_2\text{N}(\text{CH}_2)_6\text{NH}_2$ 5eq.	DCM, 43 mmol.L ⁻¹ 70°C, 5d	68100 [1.2] ^a	-	138,205
	Jeffamines (230-2000 g.mol ⁻¹)	Bulk, 25-80°C, catalysts (LiBr, 'BuOK, ZnCl ₂ , LiOTf, ...), 16 h	1100-68000 [1.8- 2.6] ^{a,b}	-	206
	$\text{H}_2\text{N}(\text{CH}_2)_{10}\text{NH}_2$	DMF, 80°C, 6 days	10300 [2.2] ^c	-	207
Fully bio-based cyclic carbonates					
 Thiolactone couplers	Various diamines	DMF or THF, 0.35 mol.L ⁻¹ , 70°C, 13-43h	3100-6400 [1.99-3.33] ^c	-	208
 (A) (B)	$\text{H}_2\text{N}(\text{CH}_2)_6\text{NH}_2$	DMAC, diglyme, dioxane, THF, 0.1- 0.2 mol.L ⁻¹ , 25-80°C, 12-24h	\bar{M}_w : 20000- 87000 [1.4-1.6] ^d	(A) $T_g = 50-70^f$ (B) $T_g = 64-79$; $T_m = 160-190$ $T_d = 180-224$	209
	1,4-diaminobutane, 1,6- diaminohexane, isophorone diamine, 1,8-diaminooctane	Bulk, 60°C then gradually until 120°C	960-1840 [1.2-1.5] ^b	$T_g = 33-70$ Amorphous or $T_m = 80-100$	210

	$\text{H}_2\text{N}(\text{CH}_2)_6\text{NH}_2$ Isophorone diamine	Bulk, 100°C, 48h	6000 [2.8] ^b	$T_g = -9 - 11^f$ $T_{d5\%} = 251-274^g$	137
	$\text{H}_2\text{N}(\text{CH}_2)_8\text{NH}_2$ Priamine	1) Bulk, 75°C, 2h 2) Polymer spread on sheets, oven 75°C, 94h	6000 [3.1] ^b Mainly cross-linked	$T_g = -9 - 11^f$ $T_{d5\%} = 251-274^f$	216
	$\text{H}_2\text{N}(\text{CH}_2)_{12}\text{NH}_2$ 	1) TBD, 70-180°C, 24h or 3 days 2) 180°C vacuum, 2-3h	-	$T_g = -85 - 11^f$ $T_{d5\%} = 272-319^f$	217
	Priamine	Bulk, 20-130°C, 24h-14 days	\bar{M}_w : 9300-35500 [1.7-2.6] ^b	$T_g = -55 - -23^f$ $T_{d5\%} = 190-232^f$	218
	(A) Priamine 1075 or Jeffamine D2000 (B) $\text{H}_2\text{N}(\text{CH}_2)_4\text{NH}_2$ 	1) DMF, 75°C, 24h to 12 days 2) Chain extension with (B) 75°C, 24h to 7 days	4550-11850 [1.8-3.1] ^b	$T_g = -52 - 31^f$	135

bCC=bis-cyclic carbonate; nCC=n-membered cyclic carbonate; Y=Yield; conv=conversion; T=temperature; RT=room temperature; SEC conditions = ^a: (DMF/LiBr, PS St) * phosphoric acid; ^b: (THF, PS St); ^c: (DMF, PMMA St); ^d: (DMAC, LiCl, PS St), ^e: other conditions; DSC conditions = ^f: 10°C/min; ^g: 20°C/min

4.1. Syntheses of PHUs and related molar masses

The synthesis of thermoplastic poly(hydroxyurethane)s (PHUs) *via* the ring opening of bCC by diamines leads to polymer materials with pendant hydroxyl groups, differing from the classical PU structure. This inherent property consequently impacts the polymerization behaviors (conversions, kinetic profiles,...) as well as the polymer properties (molar masses, solubility, phase segregation...) due to the important hydrogen bonding imparted by the dangling functions.

Generally, the PHU reported in the literature suffer from low molar masses in the range 10000 g.mol⁻¹ to 20000 g.mol⁻¹ (\bar{M}_n), impacting the final PHUs thermo-mechanical properties. As discussed above, the inherent structure of the PHUs can be pointed out in the obtention of low molar mass materials. Besides, the lack of 5CC reactivity towards amine, leading to low conversions and consequently low molar masses has been recognized as the major issue for the achievement of high molar mass materials. To circumvent this issue, several polymerization parameters such as the solvent, the temperature,^{141,209} the monomer concentration,²⁰⁹ the chemical structure of the monomers or the use of catalysts were studied in order to improve the molar masses and the subsequent PHU properties.

The polyaddition of b5CC and diamines are mostly carried out in solvent with a high polarity such as DMSO, DMAC and DMF at a reactant concentration from 0.5 to 1 mol.L⁻¹ and from room temperature (reaction times in days) to 100 °C. Proempers *et al.*²⁰⁹ screened different solvents and demonstrated that higher yields and molar masses were obtained with aprotic less polar solvents such as dioxane and THF compared to high polar aprotic DMAC and diglyme.

Various studies have reported the solubility issues in common organic solvents displayed by PHUs. As a general trend, PHUs were found to be less soluble in organic solvents than their analogue PUs.¹⁴¹ Presumably due to the hydrophilicity given by the hydroxyl groups along the polymer backbone, the PHUs were in majority only soluble in aprotic solvents with high polarity such as DMSO, DMF and DMAC.^{142,143} Moreover, Steblyanko *et al.*¹⁴² observed that monomer solubility and concentration were strongly influencing the polymer yields.

Some papers also report the synthesis of PHUs in bulk, with the objectives to obtain high molar mass materials. Lately, Sheng *et al.*¹⁹⁸ synthesized PHUs with different bCC and diamines in bulk at 80°C. Molar masses up to 30200 g.mol⁻¹ could be reached. Similar results were obtained by Maisonneuve *et al.*¹⁸⁴; the authors obtained PHUs of 31100 g.mol⁻¹ performing their polymerizations in bulk (70-140°C, 1-13 days). More recently, Rix *et al.*²¹⁸ performed bulk polymerization of low melting point fatty acid based-CC and diamines at room temperature. Nonetheless, acceptable molar masses were reached after long polymerization times (14 days) with PHU of 35500 g.mol⁻¹ (\bar{M}_w , Đ=1.9).

The temperature of the reaction has also an influence on the polyaddition of b5CC and diamines. This expected behavior has been observed and quantified by the group of Endo.^{87,190} The authors observed that the yield increased with the temperature¹⁸⁶ and calculated the effect of the temperature on the reaction rate constant (from 0.03 L.mol⁻¹.h⁻¹ at 30°C to 0.10 L.mol⁻¹.h⁻¹ at 70°C). The activation energy (E_a) could be evaluated as 9.2 and 24.9 kJ.mol⁻¹ for the b6CC and b5CC, respectively.⁸⁷ The higher reaction rates at higher temperature were explained by the decrease of the viscosity of the mixture with temperature. Indeed, the viscosity increases along the polymerization with the formation of pendant hydroxyl groups onto the polymer chain, inducing an increase of hydrogen bonding.¹⁷⁴ In order to optimize the reaction temperature, Benyahya *et al.*¹⁹⁵ performed a complete rheological study on the polyaddition of a b5CC and decane-1,10-diamine in DMF. A temperature beyond 120°C was shown to be excessive for the polymerization, due to side reactions (see part 2.3.3).

Additionally, the chemical structure of the monomers can strongly influence the PHUs molar masses. For instance, less soluble diamines lead to lower molar masses.¹⁴² while aromatic diamines cause a decrease in molar masses due to a lowering of the structural flexibility.¹⁴³ With regard to the CC structure, the inductive effect of the substituent nearby the 5CC plays a role on its reactivity. Most of the polymerizations reported in the literature were performed with CC bearing an electron-withdrawing substituent on the α , β or γ position. In the latter study, Tomita *et al.*¹⁸⁶ polymerized an inactivated 5CC with 4,9-dioxadodecane-1,12-diamine. The authors managed to reach only a conversion of 95% and a molar mass of 15000 g.mol⁻¹ after 14 days. In the same trend, Maisonneuve *et al.*¹⁸⁴ performed polymerizations with various diamines and different bCC bearing aliphatic backbone next to the CC moiety. PHUs of molar masses in the range 11000-31110 g.mol⁻¹ were achieved

Another method to improve PHU molar masses consists in designing α,ω -end functionalized prepolymers. As an example, Guillaume and coll.²⁰⁶ synthesized poly(hydroxyurethane)s with molar masses up to 68000 g.mol⁻¹, obtained by processing the reaction between *Jeffamine* and pre-polymers from functionalized polyols with glycerol carbonate at the chain end.

Excluding CC-terminated prepolymers, the highest molar masses reported at the moment were achieved using the reactive 8CC synthesized by Yuen *et al.*¹³¹ (Scheme 16). Polyaddition were carried out in DMF at room temperature to afford PHUs with molar masses in the range 19500-47000 g.mol⁻¹ (\bar{D} :1.22-1.66).

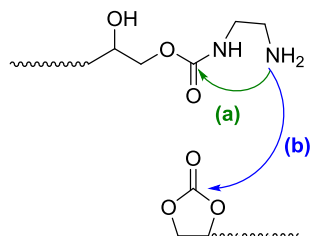
Lastly, the presence of a catalyst in the system can greatly influence the molar mass of the final poly(hydroxyurethane). Ochiai *et al.*¹⁸⁰ compared the polymerization between a bCC and the 1,12-diaminododecane with and without catalyst. PHUs molar mass could be doubled -from 19300 to 36700 g.mol⁻¹ using LiCl as a catalyst. As it is mentioned above, Annunziata *et al.*²⁰⁶ also reached high molar masses (\bar{M}_n up to 68000 g.mol⁻¹) using LiBr as catalyst.

4.2. Selectivity and side reactions

The polyaddition of b5CC and diamines lead to the formation of primary and secondary alcohols along the polymer backbone, with a majority of secondary alcohols. According to the monomers and experimental conditions, ratios between primary and secondary alcohols were found from 38:62 to 6:94.^{194,209,219}

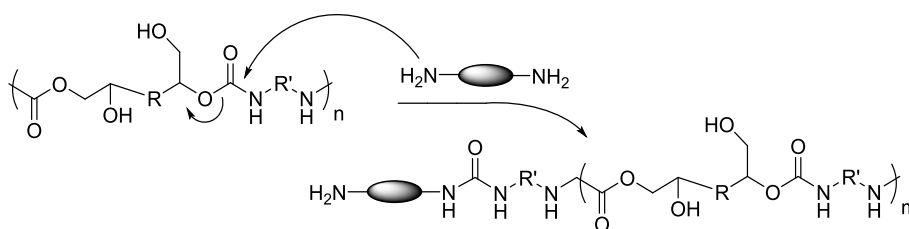
Very few studies reported the presence or the quantification of potential side products. Kihara *et al.*¹⁴¹ found lower molar masses while using ethylene and propylene diamines. Their hypothesis was that a cyclization with the neighboring urethane to afford cyclic urea (Scheme

26) was occurring. However, the authors were not able to confirm this hypothesis maybe due to the low quantity of the so-formed rings. Urea formation was also reported by Bürgel *et al.*¹⁸⁹ when performing the polyaddition in bulk at high temperature.



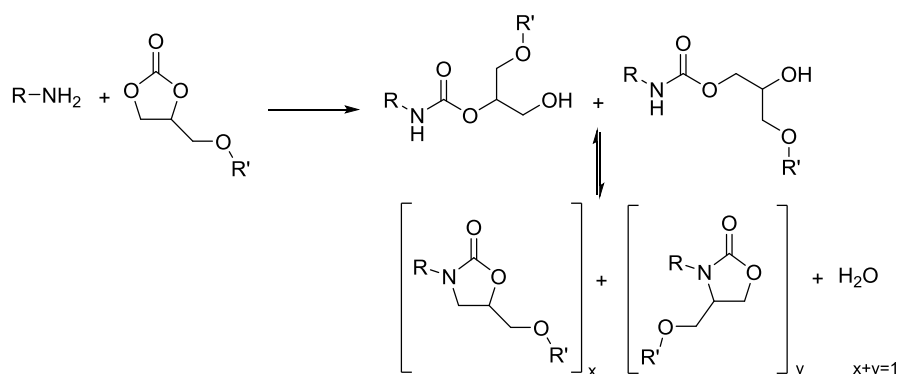
Scheme 26 - Reactions involved during poly(hydroxyurethane) synthesis – (a) cyclization process and (b) addition process.¹⁴¹

5CC bearing ester groups can be also subjected to amidation reaction in the presence of amines (Scheme 27). Indeed, Boyer *et al.*²¹² found that the formation of amide linkages was dependent on the type of diamine used. While no amide groups could be detected in the case of diamines as IPDA, some ester groups were converted into amide functions when ethylene diamine (EDA) was used as co-monomer. Amidation side reactions were likely observed by Lamarzelle *et al.*¹³⁶ in the synthesis of PHUs containing ester groups in their aliphatic backbone, thus leading to a reduction of the molar masses and an increase of dispersities. However, Endo and coll.¹⁴² polymerized a carbonated diglycidyl terephthalate presenting ester functions (in β position nearby the CC and in α position of the aromatic cycle) with aliphatic diamines. They demonstrated that with this monomer, no amidation of the ester function occurs during the polymer formation by IR analyses.



Scheme 27 - Amidation side reaction leading to urea formation in the PHU backbone.

Lately, Besse *et al.*²⁰⁷ published a complete study demonstrating the formation of ureas, oxazolidinones (Scheme 28) and some dehydration products during the reaction between CC and amines. The numerous by-products identified by HRMS and ¹³C DEPT NMR analysis explained the inability of PHUs to reach high molar masses.

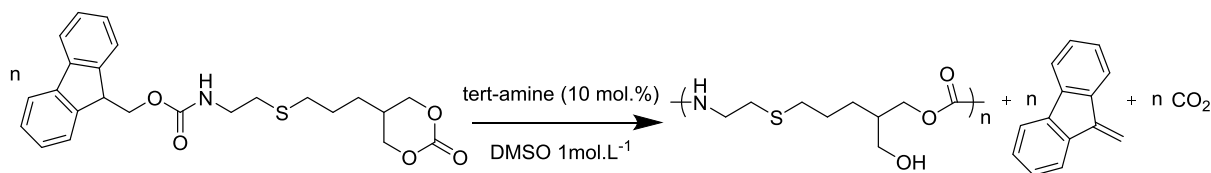


Scheme 28 - Dehydration reaction leading to oxazolidinone formation.²⁰⁷

For the higher ring-strain CC, a gelation was sometimes observed during polymerization with diamines. Maisonneuve *et al.*¹⁶¹ demonstrated the formation of a 3D network when a b6CC was polymerized with diamines. This result was attributed to the reaction between pendant hydroxyl groups present onto the PHU backbone and the residual 6CC. Yuen *et al.*¹³¹ also detected a partial gelation of PHU when 8CC was polymerized above room temperature.

4.3. Different reactivity for specific monomers

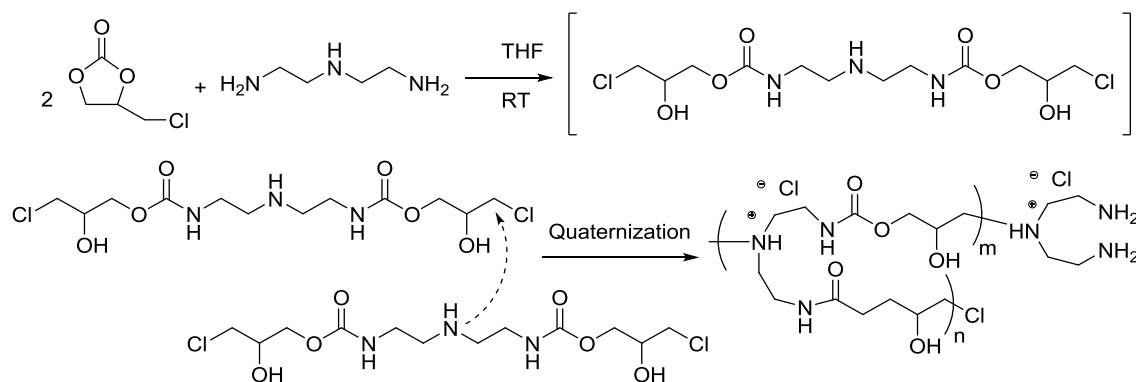
PHUs from particular monomers as well as their specificity and reactivity are developed in this part. One example of AB monomer has been reported in the literature by Tomita *et al.*¹⁹¹ in 2001. The authors synthesized a precursor bearing a protected amine group and a 6CC (Scheme 29). The polymerizations were performed at different temperatures in DMSO during 14 days. The use of 10 mol.% of tertiary amines such as N,N-diisopropylethylamine, 4-(dimethylamino)pyridine or triethylamine was necessary for the *in situ* deprotection of the amino group. However, the molar masses were low, in the range 3200-11000 g.mol⁻¹ with dispersities of 1.1-1.2.



Scheme 29 - Polyaddition of the protected AB type monomer synthesized by Tomita *et al.*¹⁹¹

Following another strategy, Kihara *et al.*¹⁸⁶ synthesized optically active PHUs from a 5CC and L-lysine hydrochloride. 2 eq. of triethylamine or 1 eq. of DBU were used. The higher molar mass obtained was 24000 g.mol⁻¹ with a dispersity of 1.58.

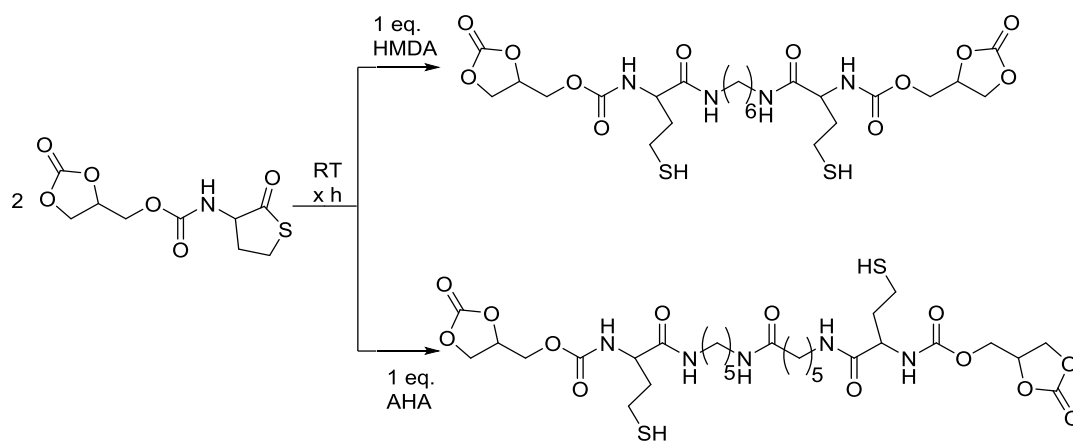
A particular case concerning the branched cationic PHUs prepared by Ochiai *et al.*¹⁷⁰ can also be mentioned (Scheme 30). The polyaddition proceeded through the nucleophilic addition of the primary amino group of diethylenetriamine (DETA) onto the carboxyl group of carbonated epichlorohydrin (Cl5CC), followed by the quaternization of the secondary amino group with the chloromethyl group in molten salts, resulting in hyperbranched polymers.



Scheme 30 - Synthesis of branched cationic PHU via polyaddition of Cl5CC with DETA.¹⁷⁰

Various AA* monomers (i.e. monomers bearing 2 different functions that can both react with the comonomer) with at least one 5CC have been reported in the literature. The first example of AA* monomers was reported by Ubaghs *et al.*²⁰⁴ The authors synthesized a precursor having both a 5CC and a linear carbonate with a phenol as leaving group. The polymerizations were carried out 20h in DMAC at room temperature in the presence of various aliphatic diamines. Molar masses in the range 6400-8700 g.mol⁻¹ were obtained with dispersities from 1.46 to 1.57. This polymerization involved the removal of phenol as by-product. Other leaving groups were also tested by the preparation of different bifunctional carbonate coupling agents from glycerol.²²⁰

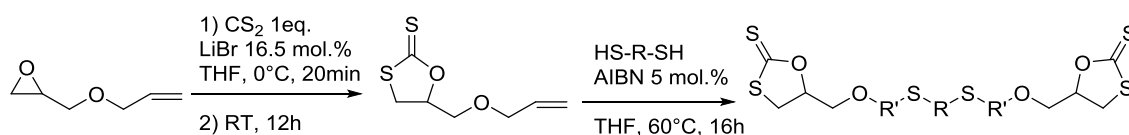
Besides, another AA* monomer bearing a 5CC and a 5-membered thio-lactone has been prepared by Keul *et al.*²⁰⁸ (Scheme 31). This AA* was reacted with HMDA or amines having urethane or ether linkages (AHA) in DMF or THF to produce poly(hydroxyurethaneamide)s. Molar masses in the range 3100-6400 g.mol⁻¹ were reached with dispersities in between 1.99-3.33. Such dispersity values higher than 2 have been explained by the presence of few disulfide bonds formed between thiol groups. Based on the higher reactivity of the thio-lactone group, the authors were able to prepare dimers having two 5CC.²⁰⁸



Scheme 31 - Reaction of thio-lactone-based 5CC with HMDA (hexamethylene diamine) and AHA (6-amino-N-(5-aminopentyl)hexanamide).²⁰⁸

Following a similar strategy, He *et al.*¹⁶⁶ synthesized AA* monomers with one 5CC and one 6CC. The interest of using such AA* monomers is to take advantage of the reactivity discrepancy between 5CC and 6CC. Indeed, by reacting only the 6CC moiety with amines for instance, the synthesis of a 5CC-terminated molecule can be achieved. The latter was used in further reactions (ex: post-functionalization). Besides, by reacting the AA* monomer with diamines, molar masses from 1340 to 8800 g.mol⁻¹ were obtained (\bar{D} =1.45-2.11).

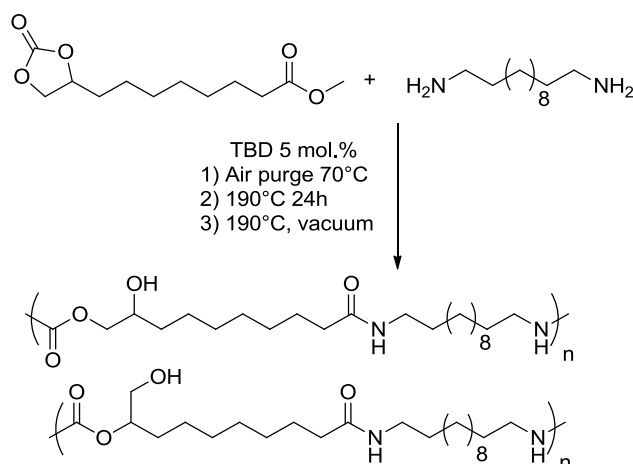
In 2013, Besse *et al.*¹³² compared the reactivity of various bis-1,3-oxathiolane-2-thiones (Scheme 32). Slightly lower molar masses (\bar{M}_n =7000 g.mol⁻¹ and \bar{D} =1.9) were obtained for the poly(thiourethane) prepared with diethylenetriamine, compared to the ones prepared with the b5CC (\bar{M}_n :10300-13000 g.mol⁻¹ and \bar{D} =2.1-2.2). Moriguchi *et al.*²²¹ also studied the polyaddition of bis-1,3-oxathiolane-2-thiones with diamines and obtained molar masses from 5000 to 12000 g.mol⁻¹.



Scheme 32 - Synthesis of bis-1,3-oxathiolane-2-thione.¹³²

A last interesting example has been recently developed by Zhang *et al.*²¹⁷ who carried the epoxidation/carbonation of the terminal unsaturation of methyl undecenoate. The resulting AA*-monomer was polymerized with an equimolar amount of diamine, first in presence of TBD at 70°C, followed by an increase in temperature at 190°C for 24h and additional 2h under vacuum (Scheme 33). The resulting semi-crystalline poly(amide-hydroxyurethane)s was insoluble in common solvents, prohibiting a SEC analysis. However, its chemical

structure as well as the ratio between primary and secondary hydroxyl groups (22:88) could be determined by ^1H NMR, using deuterated-HFIP as solvent.



Scheme 33 - Synthesis of poly(amide-hydroxyurethane)s from cyclic carbonate methyl undecenoate and 1,12-diaminodecane.²¹⁷

4.4. Thermo-mechanical properties and thermal stability of TPHUS

Various studies have been reported on the thermo-mechanical properties as well as the thermal stability of the synthesized PHUs.

The results clearly showed the expected influence of the chemical structure of the monomers onto the glass transition temperature, the presence or not of a melting point and the degradation temperature as exposed below. The glass transition temperatures range between -85°C ²¹⁷ and 102°C ¹⁴³, depending on the chemical structure of the monomers. Semi-crystalline PHUs were also achieved with melting temperatures in the range 80°C ²¹⁰ to 190°C ²⁰⁹. With aliphatic diamines, different studies demonstrated that the glass transition temperature decreases with longer aliphatic diamines due to lower urethane linkage density along the polymer backbone.^{133,142,204} In the case of aromatic diamines, Kim *et al.*¹⁴³ logically observed higher glass transition temperatures than with aliphatic ones.

Concerning the degradation temperatures, only general trends can be given due to the disparity of the analyses. The highest thermal degradation at 5 w.% loss was reported by Kim *et al.*¹⁴³ to be up to 388°C for PHUs with a large part of aromatic structures. In contrary, Proempers *et al.*²⁰⁹ reported one of the lowest starting thermal decomposition (180°C) displayed by a PHU synthesized from a D-mannitol-based CC.

Moreover, Fleischer *et al.*¹⁷⁴ were the first to study some mechanical properties for linear PHUs. Young modulus of 7 ± 1 MPa, tensile strength of 9 ± 2 MPa and elongation at break of $280\pm 50\%$ were obtained for a PHU from a 5CC and hexane-1,6-diamine. More recently, other research groups published a detailed mechanical characterization of PHUs. Torkelson and coll.²⁰² synthesized PHU elastomers from divinylbenzene bCC hard segment and PEG-, PPG- or PTMO-based diamines as soft segment, using other diamines as chain extender. The resulting materials displayed elastomeric response and tunable tensile properties with Young's modulus ranging from 27 to 200 MPa, tensile strength from 0.3 to 9.7 MPa and elongation at break up to 2000%. Averous and coll.¹³⁵ described PHUs materials also synthesized from a chain extension method between hard-segmented diamines (1,4-butanediamine, m-xylene diamine) and soft-segmented prepolymers from terephthaloyl chloride-based bCC and long chain diamines (*Jeffamine* or *Priamine*). By varying the nature and the ratio between hard and soft-segmented diamines, thermo-mechanical properties were tuned with Young's modulus ranging from 8 to 25 MPa, tensile strength from 0.7 to 3.6 MPa and elongation at break in between 330 and 700%. The previous studies enabled to elucidate linear PHU thermo-mechanical properties, even if further investigations are required in this field.

The CC/amine polyaddition confers new properties to polyurethane materials since hydroxyl groups are generated. However, their presence along the polyurethane backbone dramatically changes material properties and subsequent applications.

Only few studies investigated the differences between thermoplastic PU and PHUs properties. Carré *et al.*²¹⁶ prepared TPUs and TPHUs with equivalent architectures in order to compare their respective properties. Evidently, PHU presented lower molar masses than PU because of the limited reactivity of CC towards amines. The authors also underlined the restrained solubility of PHU in common solvents caused by the presence of hydroxyl groups within the material. Besides, a higher thermal stability was displayed by PHUs respectively to their PU homologues.

Furthermore, Leitsch *et al.*²⁰² demonstrated the critical role of H-bonding conferred by the pendant hydroxyl groups in nanophase separation of elastomeric PHUs. They showed that phase mixing was induced by H-bonding between hydroxyl and ether moieties (from PEG segments), preventing the segregation of urethane linkages into hard-segment domains. Along these lines, Long and coll.²¹⁷ demonstrated a higher moisture uptake with PHU than with traditional PU. Very recently, Cornille *et al.*²²² achieved the synthesis of comparable PU and

PHU thermosets, with the purpose to study the difference in thermo-mechanical and adhesive properties between both polymers. PHUs showed similar storage modulus but enhanced adhesion properties on wood, glass and painted aluminium support, compared to classical PUs.

Other trends suggest cross-linking or further post-functionalization to tune properties such as hydrophobicity or thermo-mechanical behaviors.^{182,193,209} For instance, the group of Endo²⁰⁰ recently carried out the post-functionalization of PHU dangling hydroxyl groups with succinic anhydride, enabling the polymer solubilization in water.

4.5. Towards bio-based PHUs

As presented previously in this manuscript, numerous studies have been developed to prepare 5CC for PHUs synthesis. However, due to the depletion of fossil resources, chemistry knows today a growing interest for bio-based precursors. Indeed, biomass including vegetable oils, lignin or polysaccharides represents an attractive resource for producing polymers. From this perspective, different research groups worked on the synthesis of bio-based (or semi-bio-based) CC in order to replace petroleum-based PHUs, using fatty acids and glycerol from transesterification of vegetable oils or other interesting natural molecules such as limonene or D-mannitol.

4.5.1. Vegetable oil-based cyclic carbonates to PHUs

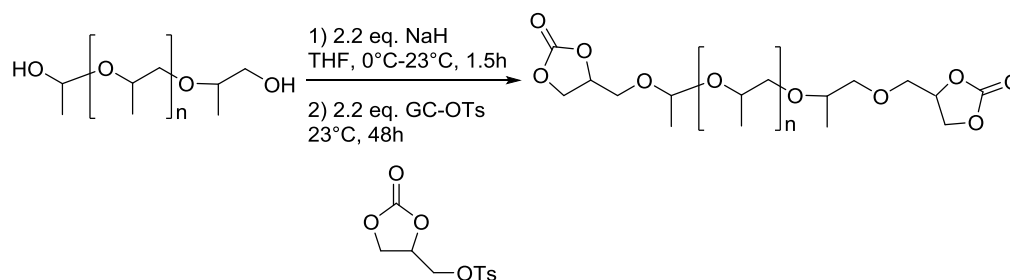
As far as vegetable oils are concerned, the 5CC monomers have been mainly synthesized from glycerol carbonate or by epoxidation followed by carbonation of the fatty acid chain unsaturations.

For instance, Carpentier and coll.²⁰⁶ used prepolymers such as poly(propylene glycol), poly(ethylene glycol) and polybutadiene bearing terminal hydroxyl groups (Scheme 34). A nucleophilic substitution was performed with tosylated-glycerol carbonate in alkaline condition to obtain bCC prepolymers. The authors achieved one of the highest molar masses ever reported in the literature (\bar{M}_n : 68000 g.mol⁻¹, DMF/LiBr, PS Std) while polymerizing the prepolymers with various *Jeffamines*.

The glycerol platform was also used by Ochiai *et al.*¹⁷⁰ The authors first synthesized cyclic (chloromethyl)ethylene carbonate from the carbonation of epichlorohydrin, that can be easily obtained by chlorination of glycerol²²³ instead of using allyl chloride as starting material. An atypical polymerization was then performed in two steps, comprising the polyaddition of a

diamine on the bCC, followed by the quaternization of the secondary amino groups (Scheme 30).

Using another strategy, Fleischer *et al.*¹⁷⁴ carbonated glycidyl ether of glycerol to end up with an activated bCC with a pendant hydroxyl group. The PHU molar mass was not reported but a complete conversion in 4h at 70°C was mentioned.



Scheme 34 - Synthesis of the glycerol carbonate-functionalized prepolymers.²⁰⁶

Vegetable oils can be used as raw material for the production of carbonated oils. However, the uncontrolled functionality of the triglycerides (Figure 6) restrains the control of PHUs structure and properties. The use of such poly(cyclic carbonate)s leads to thermosets that are not described in this manuscript. However, when carbonated triglycerides were polymerized with amino-telechelic biobased oligoamide, a thermoplastic behavior was observed due to the limited reactivity of such diamines.²²⁴

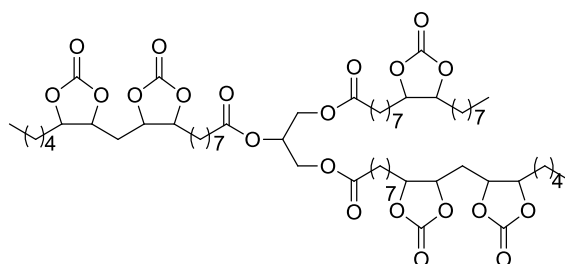
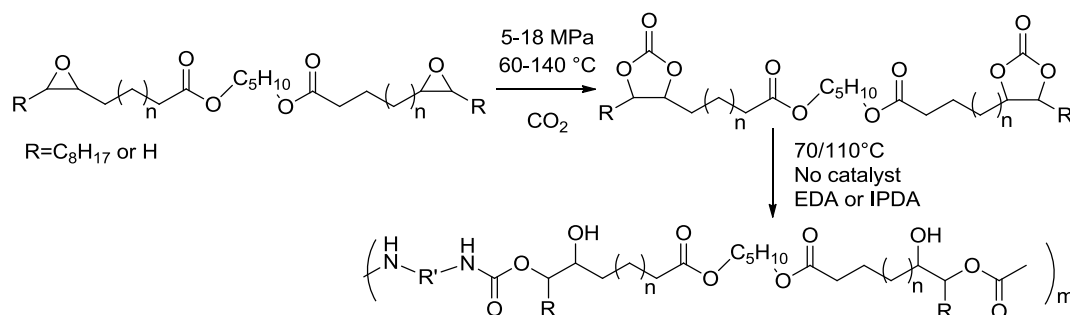


Figure 6 - Structure of carbonated soybean oil.

The first example relating the synthesis of thermoplastic PHUs from fatty acid derivatives was reported by Boyer *et al.*²¹² in 2010. The fatty acid-based b5CC were synthesized by a three-step process composed of (1) a transesterification of fatty acid methyl esters, (2) an epoxidation of the double bonds and (3) a carbonation of the resulting epoxides. The solubility of the fatty acid or triglyceride-based mono-, bis- and poly-epoxides in supercritical CO₂ has been studied.²²⁵ Two b5CC, internal carbonated fatty acid diester and terminal carbonated fatty acid diester, prepared from methyl oleate and methyl undecenoate

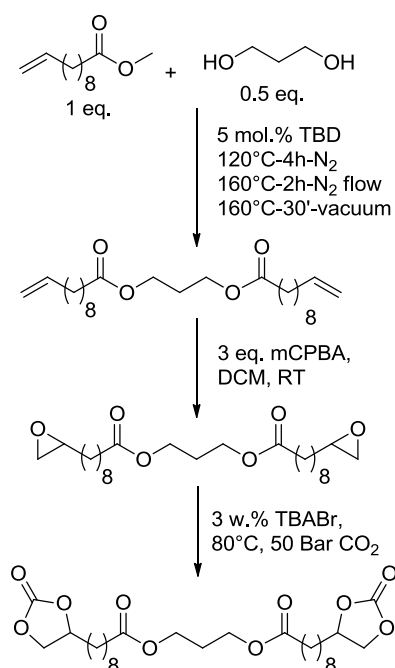
respectively, were polymerized with ethane-1,2-diamine (EDA) and isophorone diamine (IPDA) to form PHUs containing hydroxyl moieties (Scheme 35).^{212,226} The PHUs exhibited molar masses up to 13500 g.mol⁻¹ (\bar{M}_w) and relatively low glass transition temperatures ranging from -25°C to -13°C. Nevertheless, an amidation side reaction occurred between EDA and the ester linkages of the diester bCC, giving amide groups, which can partly explain the low molar masses.^{212,226}



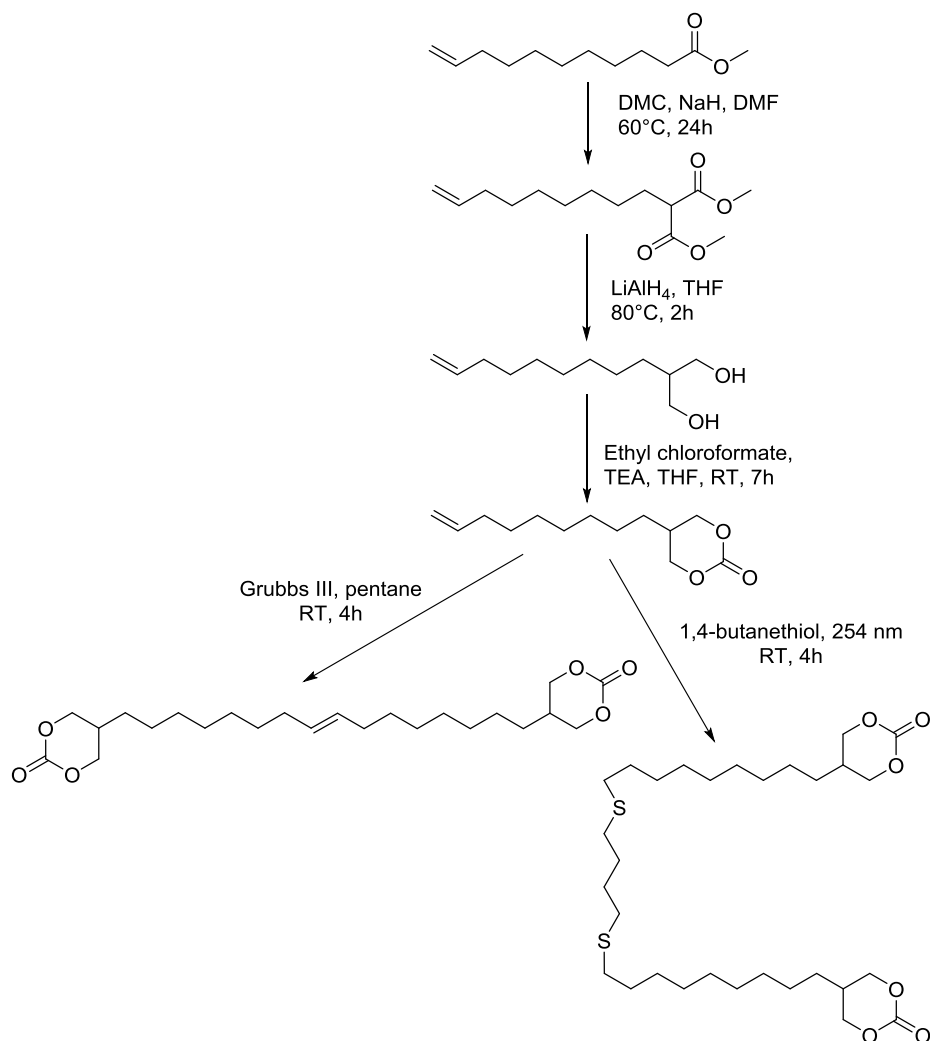
Scheme 35 - Bis-cyclic carbonates and poly(hydroxyurethane)s from fatty acid or fatty acid methyl ester.²¹²

Few years ago, Cramail *et al.*¹⁸⁴ reported the synthesis of several fatty acid based bCC using the epoxidation/carbonation strategy. Two fatty acid chains were first dimerized by amidation or transesterification reactions with 1,4-butanediamine, piperazine, N,N'-dimethylpropane-1,3-diamine, N,N'-dihexyldecane-1,10-diamine and 1,3-propanediol. The produced aliphatic bis-unsaturated was epoxidized and carbonated following the procedure indicated in Scheme 36. The polymerization of these dimers presenting different central blocks with various diamines (such as *Jeffamine*, isophorone diamine or 1,4-diaminobutane) led to a broad range of T_g from -29°C to 55°C.

Another study carried out by Maisonneuve *et al.*¹⁶¹ exhibited the synthesis of more reactive b6CC from methyl undecenoate by malonization, reduction and carbonation of the resulting diol. The mono-cyclic carbonate obtained was dimerized either by thiol-ene or metathesis reaction (Scheme 37). The synthesized b6CC were effectively used as building blocks for thermoplastic isocyanate-free PHUs in combination with 1,12-dodecanediamine as comonomer. Molar masses up to 23000 g.mol⁻¹ ($\bar{D}=1.7$) were obtained after only one day in DMF at 50°C. At higher conversion, a chemical gel was obtained, probably due to CC ring opening by the formed hydroxyl function. However, the formation of such a gel was not completely elucidated.



Scheme 36 - Strategy for the synthesis of 5-membered bis-cyclic carbonates from fatty acid derivatives.¹⁸⁴



Scheme 37 - General procedure for bis 6-membered cyclic carbonate synthesis from methyl undecenoate.¹⁶¹

More recent studies have been undertaken by Averous's and Cramail's groups for the synthesis of fully bio-based PHUs from long chain fatty-acids^{216,218} or undecenoic acid derivatives.¹³⁶ (Table 1).

Hence, fatty acid derivatives represent a platform of bio-based building blocks for poly(hydroxyurethane)s synthesis. Caillol and coll.¹⁹⁵ highlighted the large possibilities offered by this platform for both linear and cross-linked polymers.

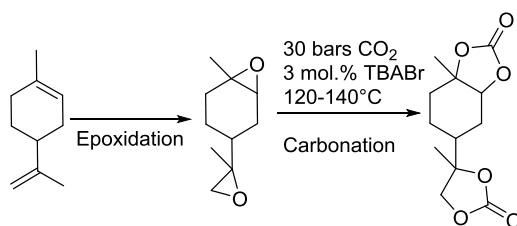
In two different studies,^{214,215} diglycerol dicarbonate was synthesized from diglycerol and dimethyl carbonate. The short dimer was subsequently reacted with several diamines to obtain PHUs with molar masses ranging from 4100 to 9400 g.mol⁻¹. The abundance of reactive hydroxyl functionalities present along the PHU backbone could enable further curing process and post-functionalization.

Nohra *et al.*¹¹ mentioned in their critical review the alternative use of vegetable oils as starting material. Besides, other bio-based molecules can be chemically modified to meet the needs of PHUs production as it is detailed in the next part.

4.5.2. Other bio-based cyclic carbonates to PHUs

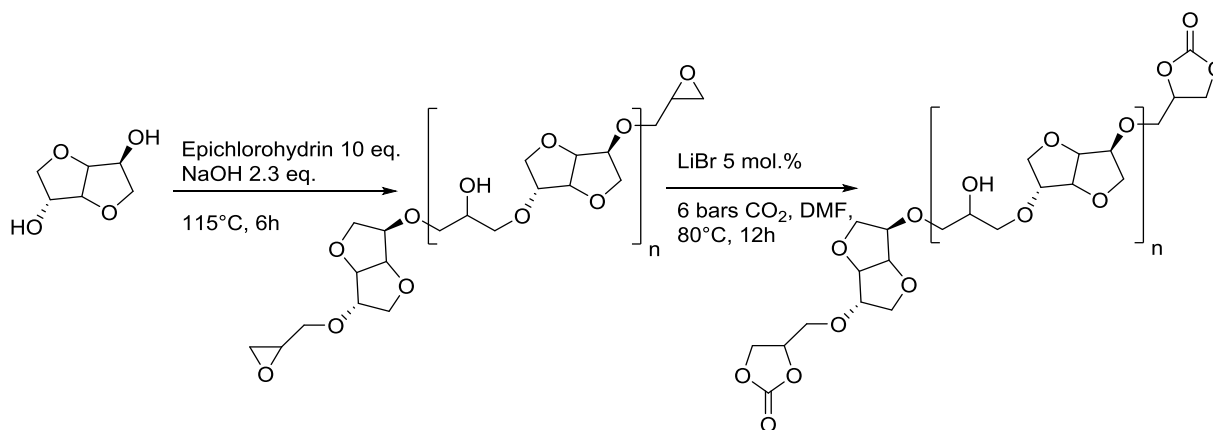
Few years ago, Proempers *et al.*²⁰⁹ modified the D-mannitol by carbonation to obtain the bis(ethylene carbonate) monomers 3,4-*O*-isopropylidene-D-mannitol-1,2:5,6-dicarbonate and the D-mannitol-1,2:5,6-dicarbonate. PHUs molar masses were in the range of 20000 to 87000 g.mol⁻¹ with dispersity of 1.6.

Another research team²¹⁰ converted the limonene in a bCC by the epoxidation/carbonation strategy (Scheme 38). In contrast to conventional plant-oil-based CC, such terpene-based CC afford much higher CO₂ fixation and do not contain ester groups. Novel linear PHUs and prepolymers were obtained with diamines such as 1,4-butanediamine, 1,6-hexamethylene diamine, 1,12-dodecanediamine and isophorone diamine. The highest T_g (70°C) was observed when the two polymerized monomers were cyclo-aliphatic.



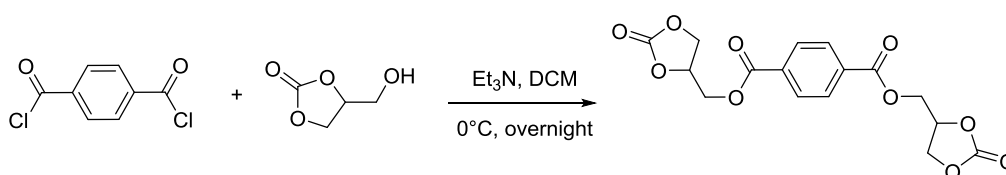
Scheme 38 -Limonene-based bis-cyclic carbonate synthesis.²¹⁰

In 2013, Besse *et al.*²¹¹ synthesized isosorbide diglycidyl ether oligomers by reaction of epichlorohydrin on the hydroxyl functions of the bio-based diol. The carbonation of the resulting molecule was performed to obtain an isosorbide-based bCC (Scheme 39) that was then polymerized with four commercial diamines. The polymerizations were completed within 12h and showed PHUs with T_g values from -8°C to 59°C .



Scheme 39 - Isosorbide-based bis-cyclic carbonate synthesis.²¹¹

Lately, new bCC were designed from lignin-derived bisphenols, by glycidylation and subsequent carbonation.²¹³ Rigid PHUs with T_g from 44 to 90°C and molar masses up to $\bar{M}_w=46000 \text{ g}\cdot\text{mol}^{-1}$ were obtained after polymerization between the produced dimers and various diamines. In the same lines, Carré *et al.*¹³⁵ polymerized a rigid aromatic bCC obtained from terephthaloyl chloride and glycerol carbonate (Scheme 40) with soft- and hard-segmented diamines with the aim to tune PHUs thermo-mechanical properties.



Scheme 40 - Terephthaloyl chloride-based bis-cyclic carbonate synthesis.²¹¹

Conclusions

This chapter reviewed the literature towards more sustainable polyurethanes, focusing on the CC/amine polyaddition leading to poly(hydroxyurethane)s. First, the main different routes for amine synthesis have been mentioned. Among them, the mild aerobic oxidation of alcohol precursors using copper/nitroxyl catalysts appeared as the greenest route towards nitriles and amines. In a second part, the synthesis of CC and their model reaction with amines have been developed in detail. Finally, an extensive report on the synthesis of PHUs has been realized and details the monomer reactivities, kinetic data, selectivity of the reaction, molar masses and thermal properties of the resulting PHUs.

Nonetheless, side reactions during the polyaddition have been observed by formation of urea or oxazolidinones for instance. This route needs further investigations to avoid side reactions in order to improve the polymer molar masses, usually below 30000 g.mol^{-1} . But the main issue of the CC/amine route remains its non-competitive reactivity compared to the classical isocyanate/alcohol one. Academic research has developed 6- to 8CC with the purpose to increase the ring opening kinetic of CC by amines, but the pot life of these monomers is too short (due to hydrolysis of the CC) and their syntheses too tedious for industrial applications. New research trends suggest the synthesis of more reactive 5CC or the use of catalysts to make this route more attractive for the PU industry.

Furthermore, in view of the fossil fuel depletion, more and more raw materials such as lignin, fatty acid derivatives or glycerol are used to produce green monomers, bringing different properties to the final polymers depending on their structure. In this context, we worked both on the preparation of diamines and reactive 5CC from glycerol and fatty acid derivatives in order to achieve fully bio-based thermoplastic PHUs.

Chapter 2

Bio-based amine synthesis through alcohol oxidation or thiol-ene “click” chemistry

Publication : Hibert, G.; Lamarzelle, O.; Maisonneuve, L.; Grau, E.; Cramail, H. *Eur. Polym. J.* **2016**, *82*, 114–121.

Keywords: Amine, nitrile, alcohol oxidation, copper-TEMPO, hydrogenation, thiol-ene, fatty-acids

Mots-clés : Amine, nitrile, oxidation des alcools, cuivre-TEMPO, thiol-ene, hydrogénation, dérivés d'acides gras

Table of contents

Introduction	93
1. Bio-based amine synthesis via alcohol oxidation into nitrile	94
1.1. Bio-based alcohol oxidation into nitrile under oxygen	95
1.2. Optimized oxidation of bio-based alcohols into nitrile under air	96
1.2.1. Copper catalyst screening	96
1.2.2. Copper ligand screening	98
1.2.3. Effect of temperature and pressure	99
1.2.4. Optimized system applied to other substrates	101
1.3. Heterogeneization of the catalysis: supported-TEMPO and Cu(0)	102
1.3.1. Supported catalysis using TEMPO-Si	102
1.3.2. Cu(0) additive	106
1.4. Bio-based diamines synthesis	108
2. Fatty acid-based amine via thiol-ene “click” chemistry	110
2.1. Synthesis of fatty acid-based dienes	110
2.2. Thiol-ene coupling of fatty acid-based dienes with cysteamine.HCl	111
3. Comparison of the two routes	114
Conclusions	117
References	118
Experimental and Supporting Information	119

Introduction

In the context of bio-based poly(hydroxyurethane)s, development, this chapter is dedicated to the design of bio-based and more specifically fatty acid-based amines which is one of the two monomers required in PHUs synthesis. Indeed, there is a lack of green and facile routes to bring amine functions onto fatty acid substrates. Therefore, two approaches have been considered in this work with respect to the amination of vegetable oil derivatives: (i) the oxidation of alcohol into nitrile followed by a hydrogenation step and (ii) the thiol-ene coupling of cysteamine hydrochloride on fatty acid-based dienes.

The first part of this chapter is devoted to the aerobic alcohol oxidation route. A preliminary study based on the work of Yin *et al.*¹ has been recently achieved by us and has showed an optimized copper/ligand/TEMPO catalytic system under oxygen for the formation of an aliphatic nitrile platform². This work is summarized in the part 1.1 of this chapter. Afterwards, in order to achieve a greener process, different Cu/ligand/mediator/temperature/pressure systems have been tested under air to get optimized conditions for the aliphatic dinitrile synthesis. Various bio-based alcohols such as 10-undecen-1-ol, oleyl alcohol or citronellol were converted into the corresponding nitriles using the optimized conditions under air, showing the versatility of this optimization. Besides, supported-TEMPO was used under oxygen as an interesting mediator for industrial oxidation scale-up in order to recover the catalyst and to overcome the use of TEMPO, the latter being toxic. In a last point, copper (0) was inserted in the catalytic system to decrease the amount of expensive copper catalysts. Diamines were readily obtained by hydrogenation of the synthesized dinitriles under pressurized dihydrogen.

Secondly, several fatty acid-based dienes were synthesized from oleic and undecenoic acid derivatives through transesterification or etherification reactions. Cysteamine hydrochloride was then coupled by thiol-ene “click” chemistry allowing us to prepare of fatty acid-based diamines.

Lastly, the two routes were compared according to the 12 principles of the ‘Green Chemistry’. The strategy adopted for the synthesis of fatty acid-based diamines is summarized in Figure 1.

Strategy adopted in Chapter 2

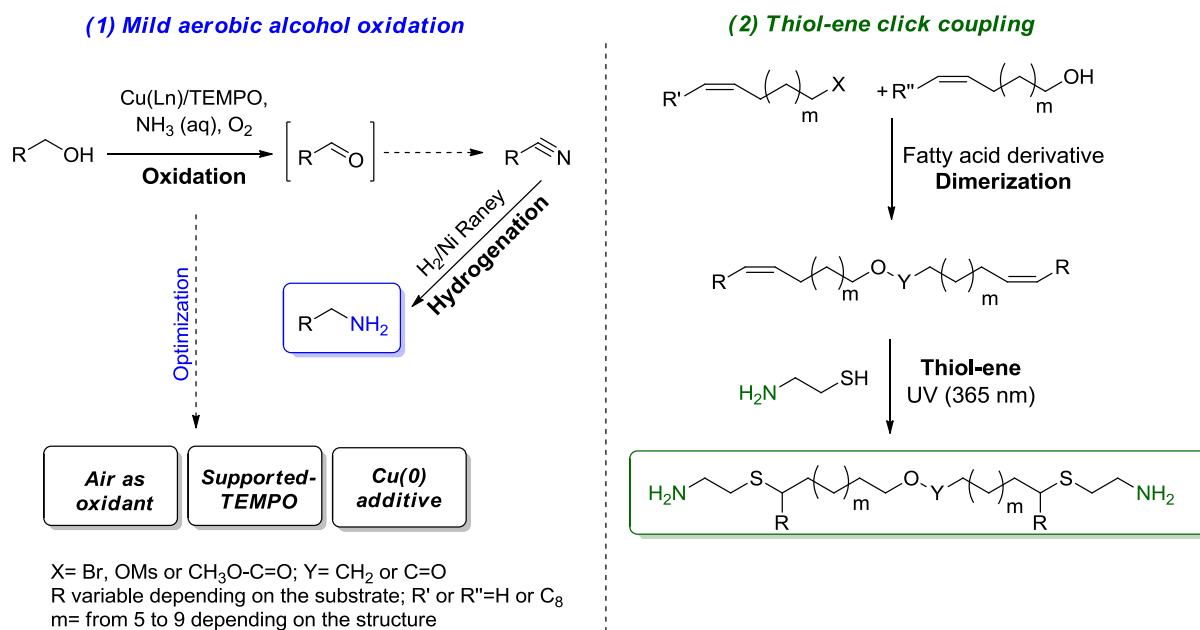


Figure 1 – Strategy adopted in the Chapter 2 for the synthesis of fatty acid-based amines.

1. Bio-based amine synthesis *via* alcohol oxidation into nitrile

The first considered route involves the preparation of nitrile intermediates from bio-based alcohols followed by a reduction step into the corresponding amines. As described in Chapter 1, aerobic alcohol oxidation in corresponding aldehydes has been extensively studied in the last decades.^{3,4} More recently, the technology has been extended to a one-pot synthesis of nitriles from alcohols in presence of aqueous ammonia. Yin *et al.*¹ were the first to report an efficient catalytic system (bpy)CuI/TEMPO for nitrile synthesis under oxygen in which Cu(I) is the central species of both oxidation cycles (see Chapter 1, Scheme 6). However, the process was not optimized for aliphatic primary alcohols and plurifunctional substrates.

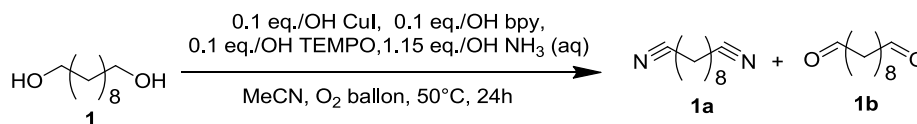
First, the mild aerobic oxidation of primary aliphatic alcohols was optimized under oxygen. Then, a full study was carried out in order to transfer the process under air. Finally, solutions for the scalability of the process such as supported catalysis or copper (0) addition were investigated.

1.1. Bio-based alcohol oxidation into nitrile under oxygen

Based on the strategy developed by Yin *et al.*¹, our research group has optimized the nitrile synthesis through alcohol oxidation in aerobic conditions (under O₂), especially with the purpose of converting aliphatic alcohols.

In this study, the optimization was performed on 1,10-decanediol and the optimized system was applied to several bio-based alcohols. The effect of the temperature on the conversion of 1,10-decanediol into **1,10-decanedinitrile (1a)**, see Scheme 1) was studied showing an optimal temperature of 50°C. Indeed, above this temperature, ammonia turned to gas and was less efficient with respect to the nitrile formation as it has already been mentioned by Dorman *et al.*⁵

The influence of the catalyst loading (CuI, bpy, TEMPO) on the nitrile conversion was then investigated at 50°C. As expected, no oxidation occurred in absence of any catalytic system. The conversion of alcohol into nitrile increased when the quantity of catalyst was increased. Full conversion of alcohol was obtained with 7.5 mol.% of catalyst per mole of hydroxyl function. The formation of **1,10-decanedinitrile** was confirmed by the appearance of the protons at 2.3 ppm in α -position of the nitrile function (see Figure 2).

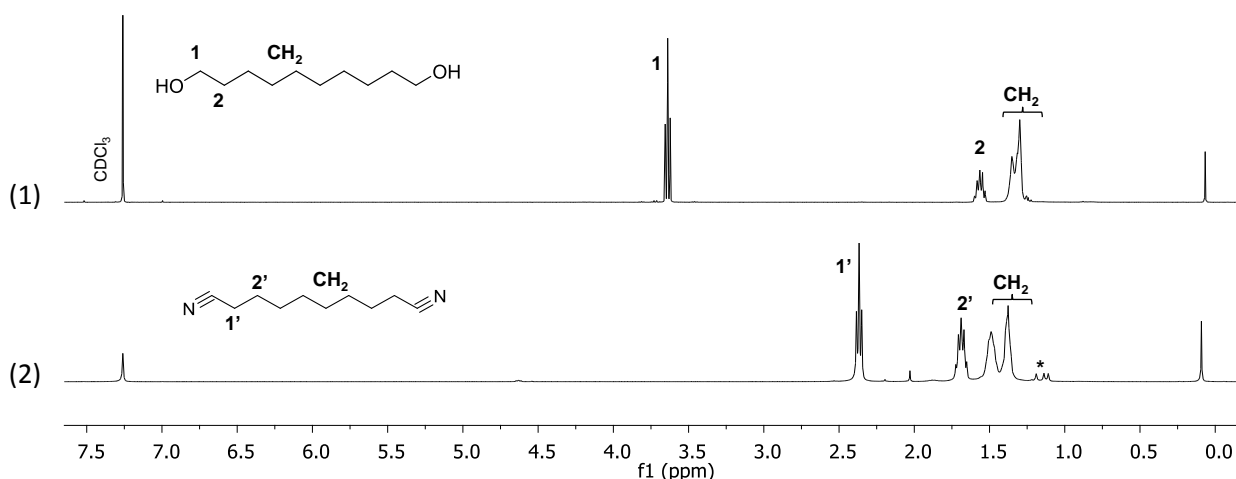


Scheme 1 - Optimized reaction conditions for the oxidation of 1,10-decanediol into 1,10-decanedinitrile under oxygen at 50°C, in acetonitrile, during 24h.

The optimized system (see Scheme 1) was then extended to other bio-based primary alcohols such as 10-undecen-1ol, oleyl alcohol or terpenes (citronellol and phytol), leading to full conversions in most cases. Only dinitriles were purified for a further hydrogenation step; the conversions and yields are reported in Table 1. This oxidation reaction allowed the one-pot synthesis of various nitrile compounds from primary aliphatic alcohols and appears to be green (high atom efficient, catalyzed process, easy catalyst removal) but also highly efficient and versatile to produce bio-based nitrile compounds.

Table 1 - Dinitrile conversions determined by ^1H NMR spectroscopy and yields after purification by flash column chromatography (eluent: cyclohexane-ethyl acetate (100:0 to 70:30)).

Dinitriles	Conversions in nitrile (%)	Yield (%)
<i>1,10-decanenitrile</i>	100	90
<i>Und-C20-dinitrile</i>	100	53

**Figure 2 - Stacked ^1H NMR spectrum of (1) 1,10-decanediol and (2) 1,10-decanenitrile in CDCl_3 (^(*)Impurities).**

1.2. Optimized oxidation of bio-based alcohols into nitrile under air

The same investigations were performed on the oxidation of 1,10-decanediol under air instead of oxygen.

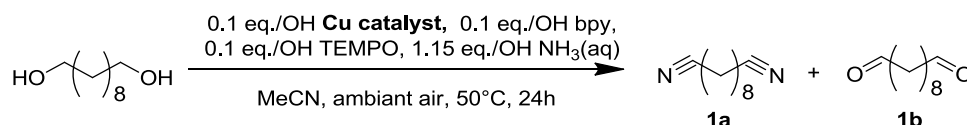
For all the optimization experiments, 1,10-decanediol, copper catalyst, copper ligand, TEMPO and aqueous ammonia were reacted in acetonitrile for 24h under air (see ESI† for detailed protocols). The crude reaction mixture obtained was analyzed by ^1H NMR without purification and the conversion was calculated thanks to the disappearance of the protons in alpha of the alcohol (triplet at 3.6 ppm) and the appearance of the characteristic protons in alpha of the nitrile (triplet at 2.3 ppm) or the proton of the aldehyde function (singlet at 9.75 ppm).

1.2.1. Copper catalyst screening

Different copper catalysts were first screened using bipyridine as ligand under air at 50°C. All results are summarized in Table 2. Indeed, CuI was not enough efficient under air (27% nitrile formation) while a full conversion was reached using oxygen as it was shown in the previous

part. The highest conversion in nitrile (**1a**) was obtained with Cu(OAc) (entry **4**), reaching 38%. However, when Cu(OAc)₂ was used (entry **8**), 70% of alcohols were converted but only 25% of nitriles were obtained (45% of aldehyde intermediates **1b**). The second oxidation cycle of the imine into nitrile appeared to be not completed.¹

Table 2 - Copper catalyst screening for the optimization of the Cu/TEMPO catalyzed oxidation of 1,10-decanediol under air.^a



Entry	Copper catalysts	Conversions (%) ^b	
		1a	1b
1	CuI	27	0
2	CuBr	22	2
3	CuCl	15	8
4	CuOAc	38	10
5	Cu(MeCN) ₄ OTf	30	0
6	CuBr ₂	22	2
7	CuCl ₂	15	0
8	Cu(OAc) ₂	25	45
9	Cu(OTf) ₂	25	0

^a: Reaction conditions : 1 eq. (2.9 mmol) of 1,10-decanediol, 0.2 eq. of copper catalyst, 0.2 eq. of bipyridine, 0.2 eq. of TEMPO, 2.3 eq. (6.8 mmol) of NH₃(aq), 5 mL of acetonitrile, air balloon, 24h, 50°C; ^b: Determined by ¹H NMR in CDCl₃

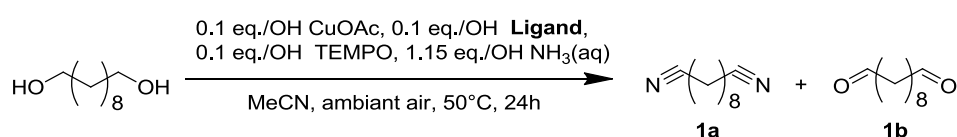
Additionally, the conversion into nitrile using copper (I) and (II) chloride was lower than with copper (I) and (II) bromide, itself lower than with copper iodide. Stahl *et al.*⁶ showed that in the cases of Cu(I) salts with non-coordinating anions such as TfO⁻ or I⁻, the conversion of alcohols into aldehydes was higher under air. This feature could be linked to the soft electronic density of iodide that enables a higher reactivity of the copper. Broadly speaking, the conversion of alcohols into nitriles was more efficient using copper (I) catalysts instead of copper (II) ones (entries 1, 4, 5). This behavior has been noticed by Stahl *et al.*⁶ in the first aerobic oxidation cycle of alcohols into aldehydes. The catalytic efficiency of the different copper catalysts could have been correlated to their redox potentials but the measurements of the latter were not realized in our conditions.

Finally, CuOAc was chosen as copper catalysts for the further optimization of the catalytic system under air.

1.2.2. Copper ligand screening

CuOAc enabled a relatively good conversion of alcohol into nitrile and was selected to perform the ligands screening. The electron-rich bipyridine is the classical ligand employed with Cu catalysts in the literature for alcohol oxidation.^{1,3,7} Several bi-dentate nitrogen ligands derived from bipyridine were evaluated in combination with CuOAc/TEMPO and the influence of functional groups grafted on the two pyridine cycles was thus studied. The conversions of alcohols into nitriles and aldehydes are reported in Table 3.

Table 3 - Ligand screening for optimization of the CuOAc/TEMPO catalyzed oxidation of 1,10-decanediol under air.^a



Entry	Ligands	Conversions (%) ^b	
		1a	1b
1		4	0
2		38	10
3		53	12
4		17	8
5		30	0
6		4	2
7		17	0
8		34	0

^a: Reaction conditions : 1 eq. (2.9 mmol) of 1,10-decanediol, 0.2 eq. of Cu(OAc), 0.2 eq. of ligand, 0.2 eq. of TEMPO, 2.3 eq. (6.8 mmol) of NH₃(aq), 5 mL of acetonitrile, air balloon, 24h, 50°C. ^b: Determined by ¹H NMR in CDCl₃.

Para-methyl groups on bipyridine ligand (p-Me(bpy)) improved the conversion of alcohols into nitriles (entry 3). However, longer aliphatic chains grafted on both cycles do not enhance the conversion (entry 4), presumably due to solubility issues in a polar solvent like acetonitrile. Bipyridine ligands bearing withdrawing functional groups such as methoxy group

leads to lower but acceptable conversion (entry **5**) in comparison to bipyridine ligand, while the catalytic system using bipyridine grafted with bromo groups exhibited really low nitrile conversion (entry **6**). As a general trend, bipyridine ligand efficiency was decreased while the electron density of the bipyridine center was depleted by electron withdrawing groups. Aliphatic amine ligands were also tested and showed lower activity than bipyridine. Finally, the copper(ligand) couple CuOAc(p-(Me)bpy) exhibited the best alcohol conversion under ambient air with 53% of alcohols converted into nitriles.

1.2.3. Effect of temperature and pressure

The influence of temperature and pressure was investigated on CuOAc (p-(Me)bpy)/TEMPO system under air as an oxidant.

In the range 30°C to 50°C, the conversion of alcohols into nitriles remained stable (around 60%) and only the formation of aldehyde was temperature dependant. The first oxidation cycle can be considered as the limiting step of the one-pot aerobic oxidation. The optimal temperature for this catalytic system was 40°C with 82% of global conversion of 1,10-decanediol in **1,10-decanedinitrile (1a)** and 1,10-decanedialdehyde (**1b**) (see Figure 3). However, at 60°C, the conversion drops to 20%. Indeed, from a certain temperature, a fraction of the aqueous ammonia turns to gas and is not able to convert alcohols into nitriles anymore. Indeed, the mechanism proposed by Yin *et al.*¹ (see Chapter 1, Scheme 6) highlights the important role of ammonia in the first aerobic oxidation cycle leading to aldehyde formation. Besides, it is noteworthy to mention that each catalytic system has probably its own optimal temperature.

Pressurized air was then applied on the CuOAc(p-(Me)bpy)/TEMPO system at 40°C. A pressure increase enabled significant higher alcohol conversions (see Figure 4). Indeed, the oxygen contained in the pressurized air is inclined to be consumed to reach an equilibrium governed by Le Châtelier principle, driving the formation of **1,10-decanedinitrile 1a**. The maximum conversion (98%) was reached using 30 bars of pressurized air leading to 92% of **1,10-decanedinitrile 1a**. This optimized catalytic system is summarized in Figure 5 and would be interesting for an industrial scale-up. One could note that higher pressure should give complete conversion with the help of specific equipments.

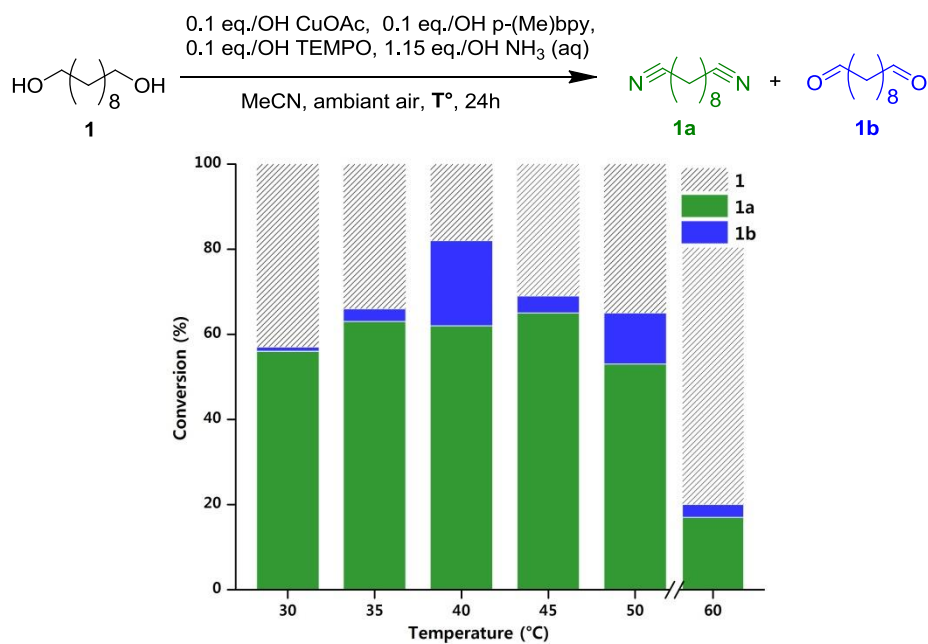


Figure 3 - Influence of the temperature on the oxidation of 1,10-decanediol, under air (atmospheric pressure).

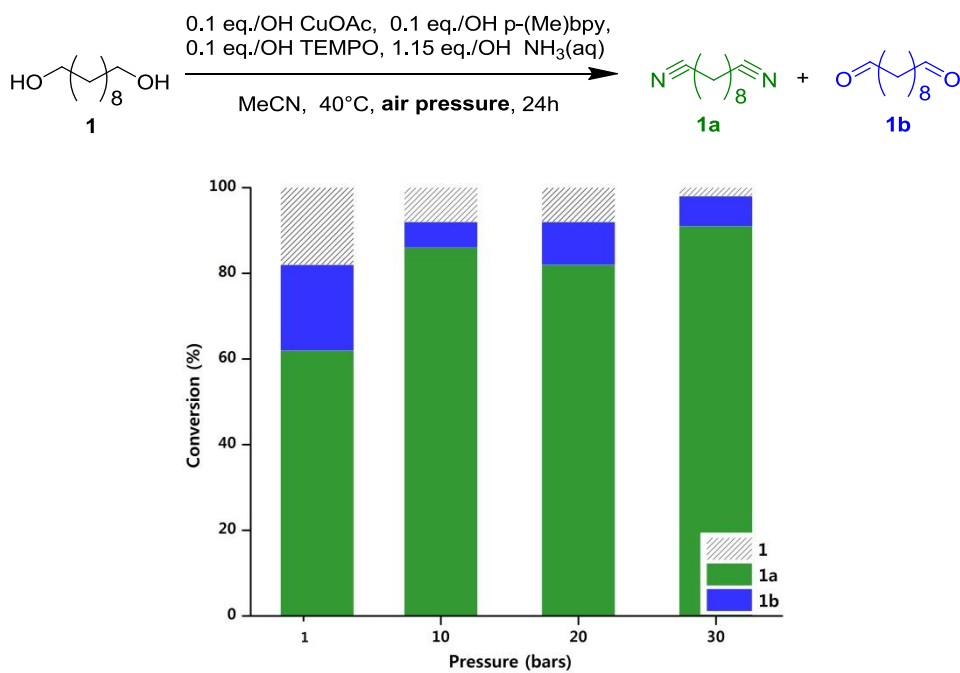


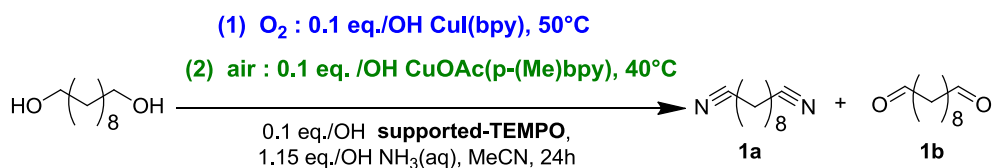
Figure 4 - Influence of the air pressure on the oxidation of 1,10-decanediol at 40°C.

to their lower solubility in the polar acetonitrile. Interestingly, the amounts of aldehydes obtained were generally very low enabling an easy recovery of the nitrile compounds. An optimization for each alcohol substrate would be necessary in these aerobic oxidation conditions. However, to the best of our knowledge, this is the first time that several bio-based aliphatic alcohols were converted into nitrile compounds using air as an oxidant.

1.3. Heterogeneization of the catalysis: supported-TEMPO and Cu(0)

1.3.1. Supported catalysis using TEMPO-Si

In order to transfer the oxidation process at the industrial scale and to encounter the toxicity of TEMPO, a supported catalytic system was investigated. Such heterogeneous catalyst could also be of interest for industrial continuous batches, enabling several uses and recycling, with a constant TEMPO efficiency. Some studies using heterogeneous supported catalysts have already been carried out but mostly for benzylic alcohols oxidation into their corresponding aldehydes.^{8,9}



Scheme 2 - Optimized reaction conditions for the oxidation of 1,10-decanediol (1) under O₂ and (2) under air, with supported-TEMPO as nitroxy mediator.

Reactions with supported-TEMPO were performed in a round bottom flask containing a fritted glass filter to recycle the heterogeneous catalyst (see ESI). 1,10-decanediol, supported-TEMPO, copper catalyst, copper ligand and aqueous NH₃ were reacted in acetonitrile for 24h under air or oxygen. At the end of the reaction, a washing procedure was applied and the supported-TEMPO was kept in the balloon for being reused.

Preliminary tests were carried out to select the most efficient conditions for heterogeneous catalysis (see Table ESI† 1). Oxidations were performed on 1,10-decanediol using two types of supported-TEMPO and the two different optimized catalytic systems, CuOAc(p-(Me)bpy) and CuI(bpy), respectively investigated under air and oxygen (see Scheme 2). TEMPO supported on silica (TEMPO-Si) and on polystyrene (TEMPO-PS) were both tested. All the results demonstrated that the first catalytic cycle efficiency was below 10% of alcohol conversion regardless the reaction conditions.

It is noteworthy to mention that a complete conversion of aldehyde into nitrile was reached either with TEMPO-Si or TEMPO-PS under oxygen. In these conditions, the aldehyde formation cycle is thus the limiting step. TEMPO-Si was more efficient than TEMPO-PS in converting alcohols into nitriles, with respectively 7 and 2% of conversions. However, none of the supported-catalysts was able to convert alcohols using air as an oxidant.

Afterwards, a recycling study was carried out under O₂ using the corresponding catalytic system CuI(bpy) (see Scheme 2-(a)) , to evaluate the TEMPO-Si efficiency over several cycles (see Figure 6). TEMPO-Si was inserted in a round bottom flask containing a fritted glass filter (see ESI) to recycle the heterogeneous catalyst. CuI, bipyridine and 1,10-decanediol were refill at the beginning of each cycle after a complete washing of the TEMPO-Si with DCM and acetone.

The two first cycles leads to a low conversion (5%) as it has been noticed in preliminary tests, whereas the next cycles allowed higher conversions up to 25%. During the first cycle, the TEMPO-Si turned from orange to green, even after having applied the washing procedure. The notable increase of the catalytic efficiency after the second cycle could be correlated to a CuI(bpy) accumulation onto the silica surface, forming a heterogeneous and unique catalytic system (that could not be completely removed by the washing procedure). Therefore, CuI(bpy) concentration increased in the mixture reaction while supported-TEMPO and 1,10-decanediol remained at the constant loading, leading to higher alcohol conversions. This hypothesis was confirmed by a copper elementary analysis of the support showing an adsorption of 14.2 w.% of copper at the silica interface, corresponding to 0.65 eq. of CuI/mol of 1,10-decanediol adsorbed after 9 cycles. Following the hypothetical mechanism proposed by Yin *et al.*¹ (see Chapter 1, Scheme 6), the dehydrogenation of the alcohol and of the aldehyde would be eased when the TEMPO and the CuI(bpy) are closer to each other. Gao and co-workers¹⁰ also demonstrated that a bio-inspired bi-functional ligand binding bipyridine to TEMPO could convert aliphatic alcohols to aldehydes in good yields thanks to the proximity of the two catalytic components. From the 3rd cycle, the conversion was maintained, demonstrating that the maximum of CuI absorption into the TEMPO-Si was probably reached. However, a decrease of the catalyst efficiency was observed from the 10th cycle of recycling and was related to the TEMPO leaching and to irreversible mediator oxidation, leading to inactive species.

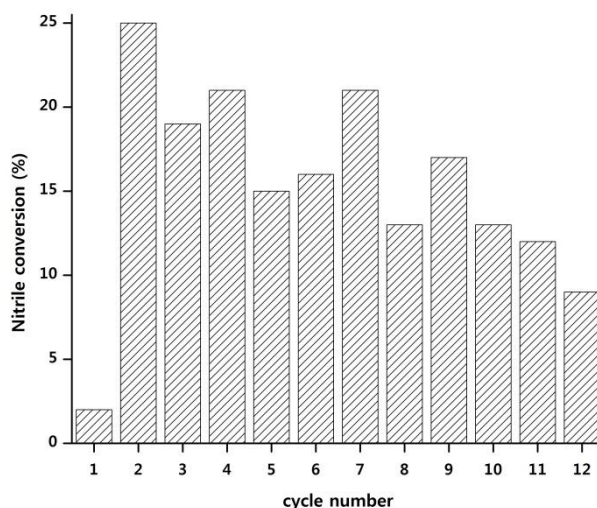


Figure 6 - Recycling study of the TEMPO-Si over 12 cycles of 1,10-decanediol oxidation into 1,10-decanedinitrile.

In order to test the reproducibility of the procedure, two similar recycling studies were performed during 12 cycles of 24h (see Figure 7). All reagents were inserted in the recycling flask at the beginning of the 1st cycle. TEMPO-Si was washed between each cycle and further reused. At the beginning of cycles 2, 3 and 4, CuI(bpy), 1,10-decanediol, aqueous ammonia and acetonitrile were refilled. In order to determine the influence of the adsorbed remaining CuI(bpy) on the conversion of the alcohol, CuI(bpy) catalyst was not refilled for cycles 5, 6 and 7. The flask was restocked with the catalytic system afterwards (from cycle 8 to 12). The estimated heterogeneous catalyst colour is indicated for each cycle by the colour of the bar (see Figure 7).

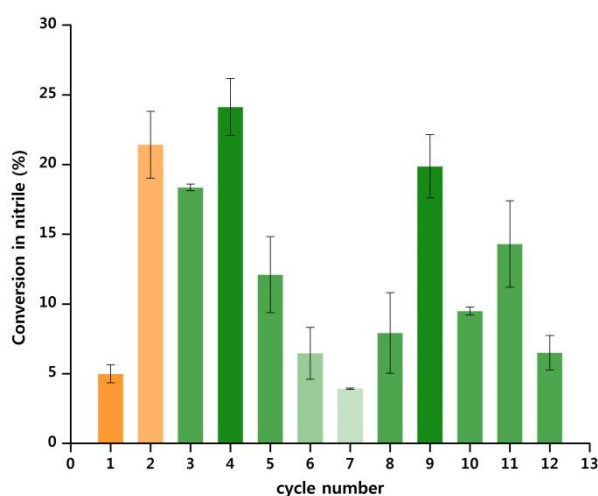


Figure 7 - Full recycling study of the TEMPO-Si. Bar colors are representative of the support colors during the aerobic oxidation. Error bars are given over 2 recycling studies.

The first cycle enabled a low conversion of 1,10-decanediol (5%) as it has been observed in the first recycling study. As already discussed, the green colour of the TEMPO-Si appeared at the 3rd cycle confirming the copper adsorption at the interface. Even if the conversion decreased after the 5th cycle because CuI and bipyridine were not refilled anymore, the catalytic system remained active due to the adsorption of CuI(bpy) on the supported-catalyst interface (the catalyst colour remained green). Logically, the conversions of alcohols into nitriles were in correlation with the catalyst colour: low amount of nitriles were obtained when the catalyst green colour became less intense. These observations confirmed that a fraction of the catalyst system was adsorbed onto the TEMPO-Si and was still converting alcohols into nitriles. When the system was refilled with CuI and bipyridine (from cycles 8 to 12), the alcohol conversion increased to reach 20% (cycle 9). Nonetheless, TEMPO-Si exhibited a loss of efficiency from the 10th cycle as it has been observed in the first recycling study (see Figure 6).

This experiment has proved the ability of adsorption/desorption of CuI(bpy) on TEMPO-Si and has provided a better understanding of this heterogeneous catalytic system. The vicinity of TEMPO and CuI(bpy) thanks to the adsorption of the latter onto silica probably increased the efficiency of the catalytic system as it has been noticed by Gao and coll.¹⁰

A last study was carried out to analyse the respective adsorption of CuI and bipyridine onto the TEMPO-Si. CuI, bipyridine and 1,10-decanediol were introduced for each cycle (1st to 4th). From the 5th cycle, CuI and/or bipyridine were not refilled anymore. The efficiency of each catalytic system was evaluated considering the loss percentage of conversion, in comparison to the conversion reached at the 4th cycle. The results are depicted in Figure 8.

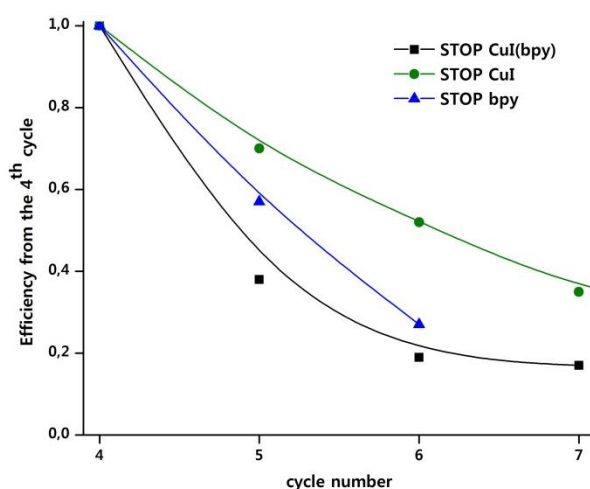


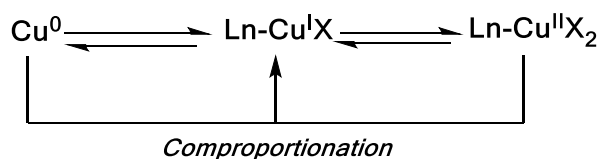
Figure 8- Efficiency of the catalytic system after stopping the refill in (■) CuI(bpy), (●) CuI, (▲) bipyridine.

When both CuI and bipyridine were no longer introduced in the reaction mixture, the catalytic efficiency showed a sharp decrease from the next cycle and was reduced by 2.5.

However, while copper iodide was not refilled, the efficiency decreased slower confirming the efficient adsorption of CuI on the TEMPO-Si surface. Contrarily, when the bipyridine refill was stopped, the efficiency of the catalytic system decreased faster, showing the crucial need of CuI chelation by ligands and the less important adsorption of bpy on the silica support.

1.3.2. Cu(0) additive

Cu(0) is well-known as a Cu(I) ion regenerating agent in the Atom Transfer Radical Polymerization (ATRP).¹¹ As explained in the Scheme 3, the addition of Cu(0) in the reaction medium induces comproportionation of Cu(II) and Cu(0) species thus generating Cu(I). In the one-pot double aerobic alcohol oxidation, Cu(I) represents the central active species of both cycles.



Scheme 3- Comproportionation mechanism for copper catalysts observed in ATRP-SARA.¹¹

Herein, Cu(0) was introduced in the catalytic system to favour copper oxidation state regeneration, reducing also the amounts of expensive copper catalysts used. The copper was washed with a concentrated HCl solution before being used, to increase its active surface by removing copper oxides. The study is summarized in Table 5. The Cu(0) addition was first carried out on the optimized system under oxygen (0.2 eq. of CuI(bpy)-TEMPO). Such catalytic system could not fully convert the alcohols into nitriles and dropped to 18% of conversion (entry 1). Indeed, the lack of Cu(II) species in the initial medium inhibited the comproportionation with Cu(0), leading to poor Cu(I) concentration and consequently low conversions.

Additionally, 41% of alcohols were converted into nitriles just after adding 0.2 eq. of bipyridine and an excess of Cu(0) without any copper catalyst. This experiment attested the chelation of Cu(0) by bipyridine, enabling its solubilisation in acetonitrile (entry 2).

Afterwards, Cu(0) was introduced in excess without any copper catalysts and ligands leading to a conversion of 10% in nitrile (entry **3**). This phenomenon could be due to the inherent solubilization of copper by the water present in aqueous ammonia.

Table 5- Experiments on different copper(ligand)/TEMPO systems under oxygen with additional Cu(0) in the reaction mixture.^a

Entry	Cu(L)	Cu(L) eq.	Cu(0) eq.	Conversions (%) ^b	
				1a	1b
1	CuI(bpy)	0.2	excess	16	2
2	(bpy)	0.2	excess	41	0
3	-	-	excess	10	8
4	Cu(OAc) ₂ (bpy)	0.2	0	45	1
5	Cu(OAc) ₂ (bpy)	0.2	1	96	0
6	Cu(OAc) ₂ (bpy)	0.1	1	98	1
7	Cu(OAc) ₂ (bpy)	0.05	1	65	26

^a: Reaction conditions : 1 eq. (2.9 mmol) of 1,10-decanediol, 0.2 to 0 eq. of copper catalyst, 0.2 to 0 eq. of ligand, 0.2 eq. of TEMPO, 1 eq. or an excess of Cu(0), 2.3 eq. (6.8 mmol) of NH₃ (aq), 5 mL of acetonitrile, O₂ balloon, 24h, 50°C.

^b: Determined by ¹H NMR in CDCl₃.

Besides, Cu(0) improved the conversion when a Cu(II) catalyst such as Cu(OAc)₂ was used under oxygen with bipyridine as ligand. Indeed, 45% of alcohol was converted into nitriles without Cu(0) addition (entry **4**). However, when 1 eq. of Cu(0) was introduced in the catalytic system, the conversion significantly increased from 45% to 96% (entry **5**). The use of a Cu(II) catalyst permitted the efficient comproportionation with Cu(0) for Cu(I) generation and subsequent conversion of alcohol in nitrile. The Cu(OAc)₂(bpy) loading was then reduced to 0.1 eq. (entry **6**) and 0.05 eq. (entry **7**) in order to decrease the amount of copper catalyst and to see the influence on the alcohol conversions. The conversions were up to 100% with 0.1 eq. of copper(ligand) loading and 1 eq. of Cu(0) per mol of 1,10-decanediol. Nonetheless, an additional decrease of Cu(OAc)₂-bpy equivalent at 0.05 eq. led to 65% of nitrile formation.

In conclusion, bio-based aliphatic nitriles were obtained from mild aerobic oxidation of alcohols for a suitable hydrogenation step leading to aliphatic primary amines (see part 1.4.). In agreement with the ‘Green Chemistry’ principles, the copper/TEMPO-mediated alcohol oxidation was first optimized under air. Additional experiments were performed to unravel the Cu(0) role in the nitrile intermediate preparation.

1.4. Bio-based diamines synthesis

The synthesized dinitriles previously obtained were first purified through alumina/celite column to remove the copper catalyst with dichloromethane as an eluent. The solvent was evaporated under vacuum and the resulting viscous orange transparent liquid was then purified by flash chromatography (eluent: cyclohexane-ethyl acetate from 100:0 to 70:30).

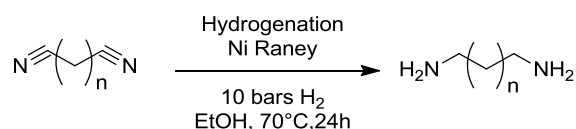


Figure 9 - General procedure for the hydrogenation of dinitrile derivatives under pressurized dihydrogen.

The purified derivatives were reduced into diamines as monomers for further PHU syntheses (see Chapter 3). *1,10-decanedinitrile* and *Und-C20-dinitrile* were thus completely reduced into amines in ethanol under 10 bars of H₂ at 70°C for 24h, using Raney Nickel as hydrogenation catalyst (see Figure 9). 93% of *1,10-decanedinitrile* was converted in *1,10-diaminodecane* that was purified by precipitation in acetone with a yield of 43%. Nonetheless, the *Und-C20-dinitrile* was fully converted in its corresponding diamine, thus, the crude product did not necessitate further purification.

The 1,10-diaminodecane was partially soluble in chloroform. In addition, the *Und-C20-diamine* was insoluble in most of the common organic solvents, except from methanol and ethanol. Their purity could not be analyzed by GC or HPLC. However, the *1,10-decanediamine* synthesized through the Cu/TEMPO-mediated alcohol oxidation exhibited a similar ¹H NMR spectrum than the commercial one, attesting its high purity grade.

The formation of the two corresponding diamines has been demonstrated by FTIR and ¹H NMR spectroscopy. In FTIR, the stretching band of nitrile functions at 2243 cm⁻¹ disappeared and the stretching band of amine functions appeared in the range 3000-3500 cm⁻¹ (see Figure 10). On the ¹H NMR spectrum, the triplet at 2.4 ppm corresponding to the proton nearby the nitrile function disappeared and a triplet at 2.6 ppm corresponding to the protons nearby the amine function appeared (see Figure ESI† 7 and Figure 11). Thus, these two diamines *1,10-decanediamine* (10DA) and *Und-C20-diamine* (20DA) have been successfully synthesized by reduction of the corresponding dinitriles. Such a procedure could be easily applied to the platform of other synthesized nitrile compounds.

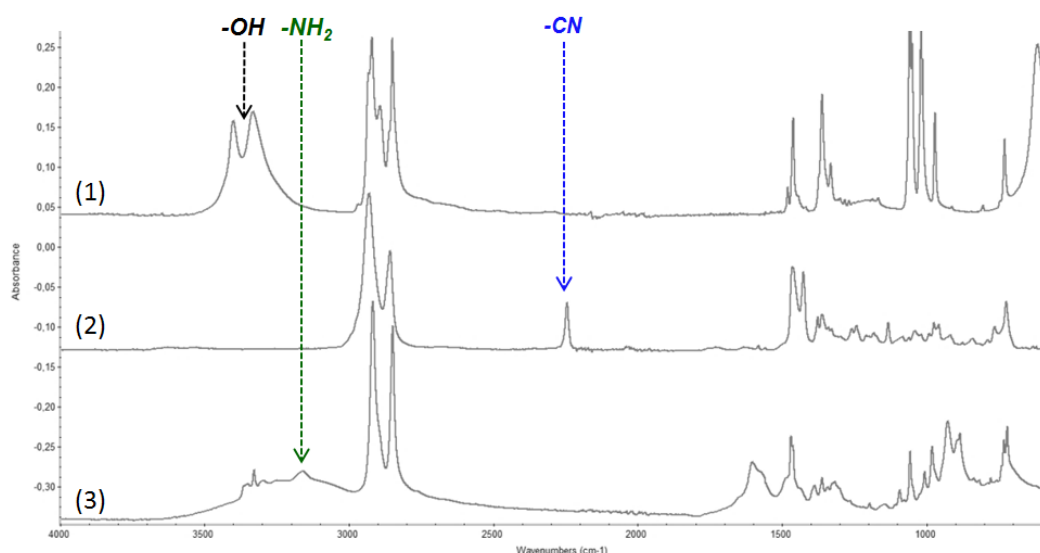


Figure 10 - Stacked FTIR of (1) 1,10-decanediol (2) 1,10-decanedinitrile and (3) 1,10-diaminodecane.

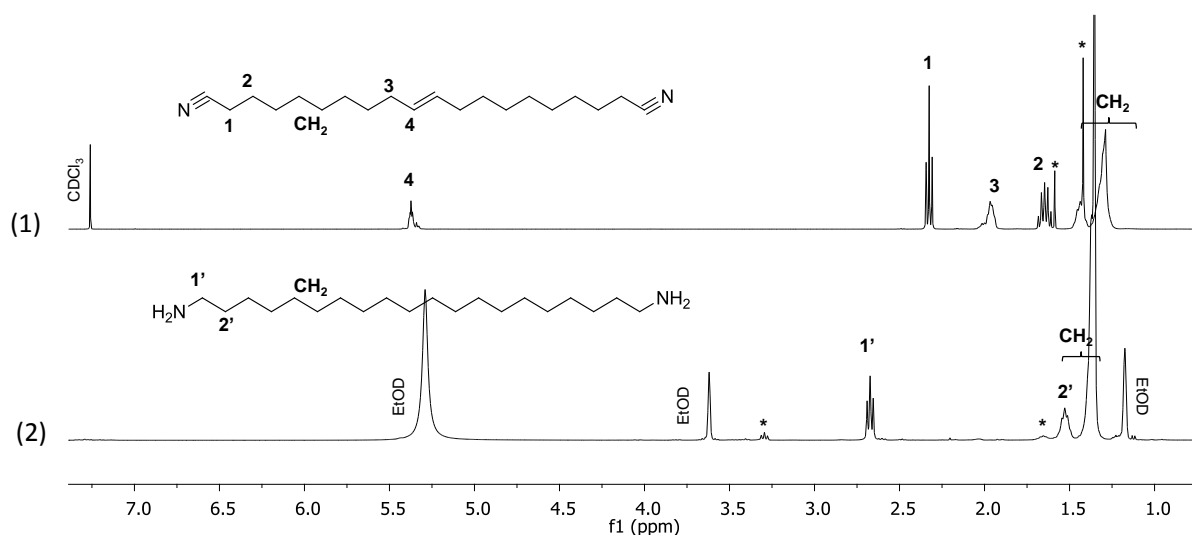


Figure 11 - Stacked ^1H NMR spectra of (1) Und-C20-dinitrile in EtOD and (2) Und-C20-diamine in CDCl_3 (* impurities).

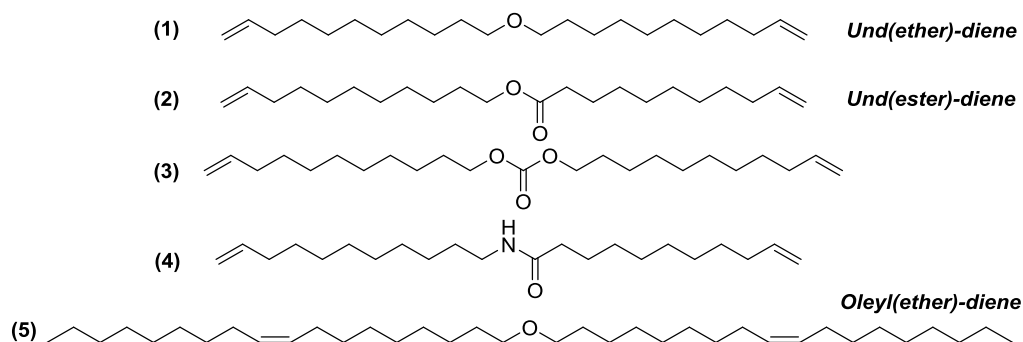
Therefore, two diamines were obtained from the optimized alcohol oxidation process. As a general trend, aliphatic diamines are difficult to purify either by chromatography due to their high polarity or by recrystallization due to their high insolubility in main organic solvents. However, relatively pure diamines (^1H NMR analysis) for further poly(hydroxyurethane)s synthesis could be obtained through an optimized alcohol oxidation process using air as an oxidant or supported-TEMPO as mediator.

2. Fatty acid-based amine *via* thiol-ene “click” chemistry

A second route to access fatty acid bio-based diamines was developed using thiol-ene coupling on dimerized unsaturated fatty-acid derivatives. The synthesis of di(poly)amines from unsaturated fatty-acids was already reported by thiol-ene “click” chemistry with cysteamine hydrochloride (Cys.HCl).¹²

2.1. Synthesis of fatty acid-based dienes

A large platform of fatty acid-based dienes was developed by Lebarbé *et al.*¹³ to perform ADMET polymerization (see Scheme 4). This last work demonstrated the poor solubility in common organic solvents of the fatty acid-based substrate containing an amide linkage. In the present study, only the fatty acid-based dienes *Und(ether)-diene*, *Und(ester)-diene* and *Oleyl(ether)-diene* represented in Scheme 4 (see (1), (2) and (5)), were synthesized by dimerization of fatty acid derivatives from castor, canola or olive oils. Indeed, only ether and ester linkages were targeted for this study in order to increase the solubility of the so-formed dienes in usual organic solvents.



Scheme 4 - Fatty acid-based dienes synthesized by (1), (5) etherification, (2) transesterification, (4)transamidation and (3)transcarbonation.¹³

Und(ester)-diene (2) was synthesized by transesterification between methyl-10-undecenoate and 10-undecen-1-ol with TBD as catalyst. Besides, *Und(ether)-diene* (1) and *Oleyl(ether)-diene* (5) were synthesized by etherification of respectively 1-bromo-10-undecene with 10-undecen-1-ol and oleyl methanesulfonate with oleyl alcohol. The detailed syntheses are given in Supporting Information. The conversions were followed by ¹H NMR with the disappearance of the protons nearby the alcohol as well as the bromo or mesyl functions. As

an example, the stacked ^1H NMR spectra depicted in Figure 12 show the disappearance of the protons in alpha of the alcohol and in alpha of the bromo function, and the appearance of the protons nearby the ether rotula of the *Und(ether)-diene*. All the synthesized dienes were purified by flash chromatography and exhibited purity up to 100% by GC.

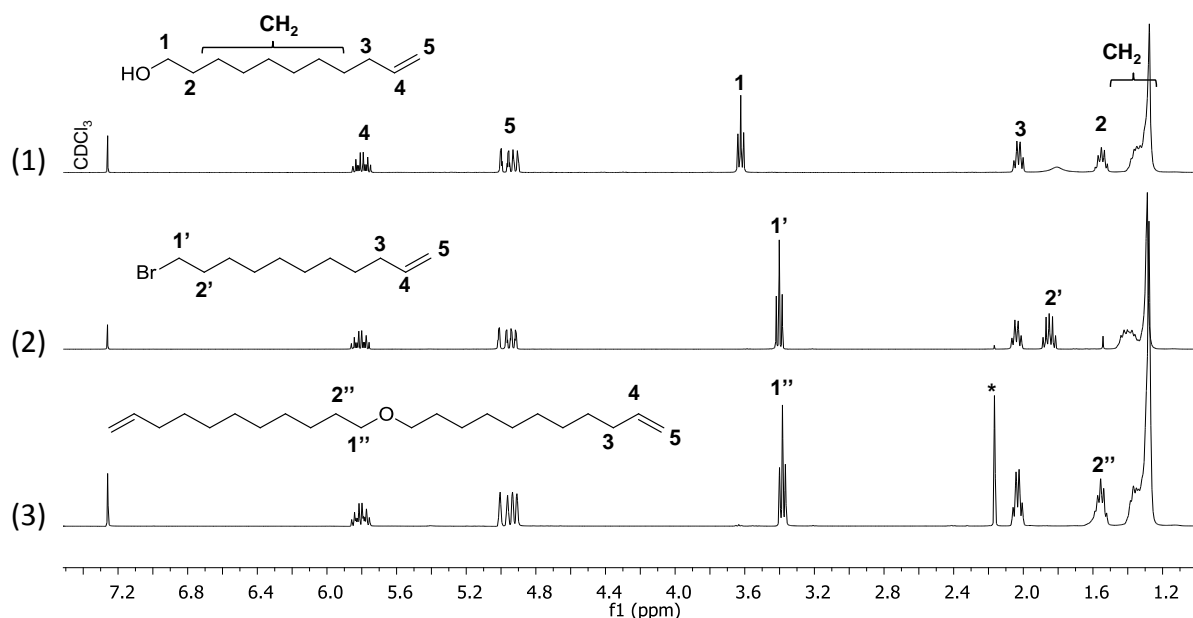


Figure 12 - Stacked ^1H NMR spectra of (1) 10-undecen-1-ol, (2) 1-bromo-10-undecene and (3) Und(ether)-diene in CDCl_3 . (* impurities).

2.2. Thiol-ene coupling of fatty acid-based dienes with cysteamine.HCl

In order to obtain diamines from the dimerized bis-unsaturated fatty acids, the latter were coupled by thiol-ene “click” chemistry with Cys.HCl. The reaction proceeds by addition of a functional thiol onto a double bond, most often *via* a free radical mechanism that can be thermally or photo-initiated (see Figure 13). The mechanism involves the formation of a thiol radical from the abstraction of a hydrogen atom initiated by applying UV-light (with or without photoinitiator) or by heating the reaction medium. The so-formed thiol radical attacks the alkene, forming a C-S bond and a carbon centered radical. This latter abstracts a proton from another thiol resulting in an anti-Markovnikov thiol ether product. The other species can in turn propagates the radical.¹⁴ This “click” chemistry has gained attention in the last decades as green methodology and enables the production of amine in one step by grafting Cys.HCl onto the unsaturations of fatty acids. This strategy has already been adopted by several research groups to synthesize bio-based di- or polyamines from vanillin, cardanol or vegetable oil derivatives.^{15,16,17}

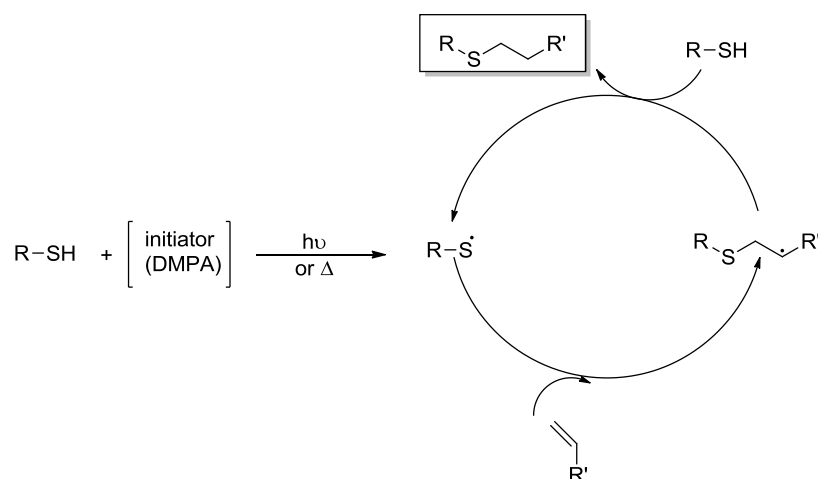
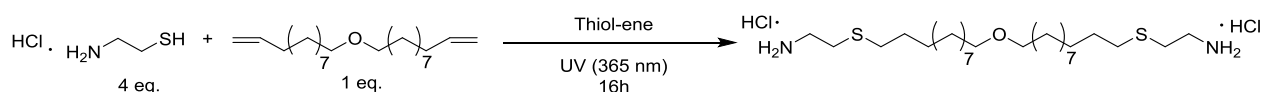


Figure 13 - Mechanism of thiol-ene addition on terminal alkenes.¹⁴

The dienes synthesized in the previous part were therefore reacted with Cys.HCl, in a mixture of methanol:DCM (1:1) in order to dissolve the two reagents. For the *Und(ether)-diamine* and *Und(ester)-diamine*, the reaction was carried out with 2 equivalents of Cys.HCl per double bond, in a UV reactor (365 nm) at room temperature, for 16h without photoinitiator. The standard reaction conditions are reported in Scheme 5. In these conditions, the fatty acid derivatives presenting external double bonds, that are known to be much more reactive than the corresponding internal ones, were easily converted in diamines. However, the synthesis of *Oleyl(ether)-diamine*, derived from an internal unsaturated fatty acid diene, required the use of DMPA as photoinitiator and UV irradiations through an optical fiber (350-400 nm) that can improve the conversions and decrease the reaction time. Additionally, the equivalent of Cys.HCl per double bond was increased to 10 eq. for the same reasons. These reaction conditions were not optimized further but led to higher conversions than with a simple UV lamp.



Scheme 5 - Standard conditions for thiol-ene coupling of fatty acid-based dienes (here *Und(ether)-diene*) with Cys.HCl under UV irradiation (365 nm).

During the reaction, *Und(ether)-diamine* and *Und(ester)-diamine* precipitated in the solvent mixture. At the end of the reaction, the latter were filtered, washed abundantly with a saturated NaHCO₃ solution to recover the diamine form and to remove the excess of Cys.HCl. Finally, the obtained white powders were rinsed with ethyl acetate. As it was the case for the

diamines synthesized *via* the alcohol oxidation in the first part of this chapter, the purity could not be analyzed either by HPLC or GC because of insolubility issues. Concerning the *Oleyl(ether)-diamine*, the crude product was dissolved in chloroform and the organic phase was washed until neutrality before drying and solvent reconcentration. The *Oleyl(ether)-diamine* was obtained as a yellow viscous liquid after purification by flash chromatography (eluent: DCM:methanol).

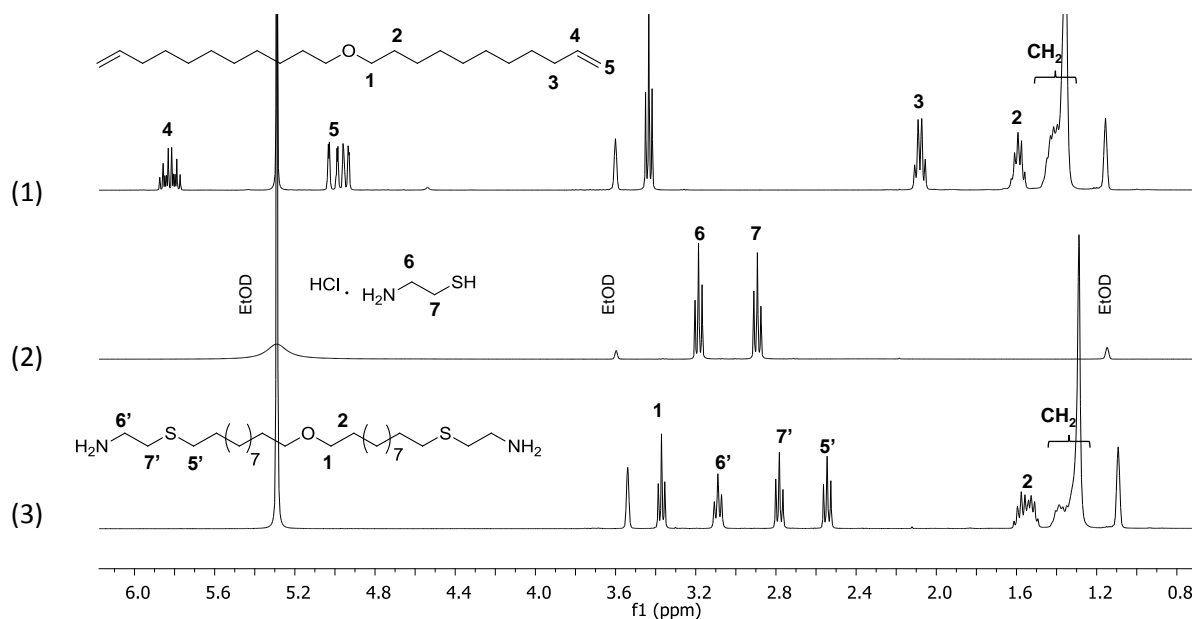


Figure 14 - Stacked ^1H NMR spectra of (1) Und(ether)-diene (2) Cysteamine hydrochloride and (3) Und(ether)-diamine in EtOD.

The reaction was confirmed by ^1H NMR with the disappearance of the characteristic protons of the terminal unsaturations (5.8 and 5 ppm) for *Und(ether)-diene* and *Und(ester)-diene* (see Figure 14 and Figure 15), that exhibited respectively 100% and 90% conversion after 16h of irradiation under UV (365 nm). Markovnikov product was not observed by ^1H NMR as the characteristic CH_3 shift below 1 ppm was not detected. The NMR analyses were done on MeOD or EtOD adding few drops of trifluoroacetic acid (TFA) to help the dissolution of the two solid diamines. For *Oleyl(ether)-diene* synthesis, the reaction was followed thanks to the disappearance of the internal unsaturation signal at 5.33 ppm that showed a conversion of 70% in 2h under UV irradiation using an optical fiber (350-400 nm). Due to the equal probability for the attack of Cys.HCl on the carbons 9 or 10 of the unsaturation, the ratio between the two regioisomers was assumed to be 50:50.

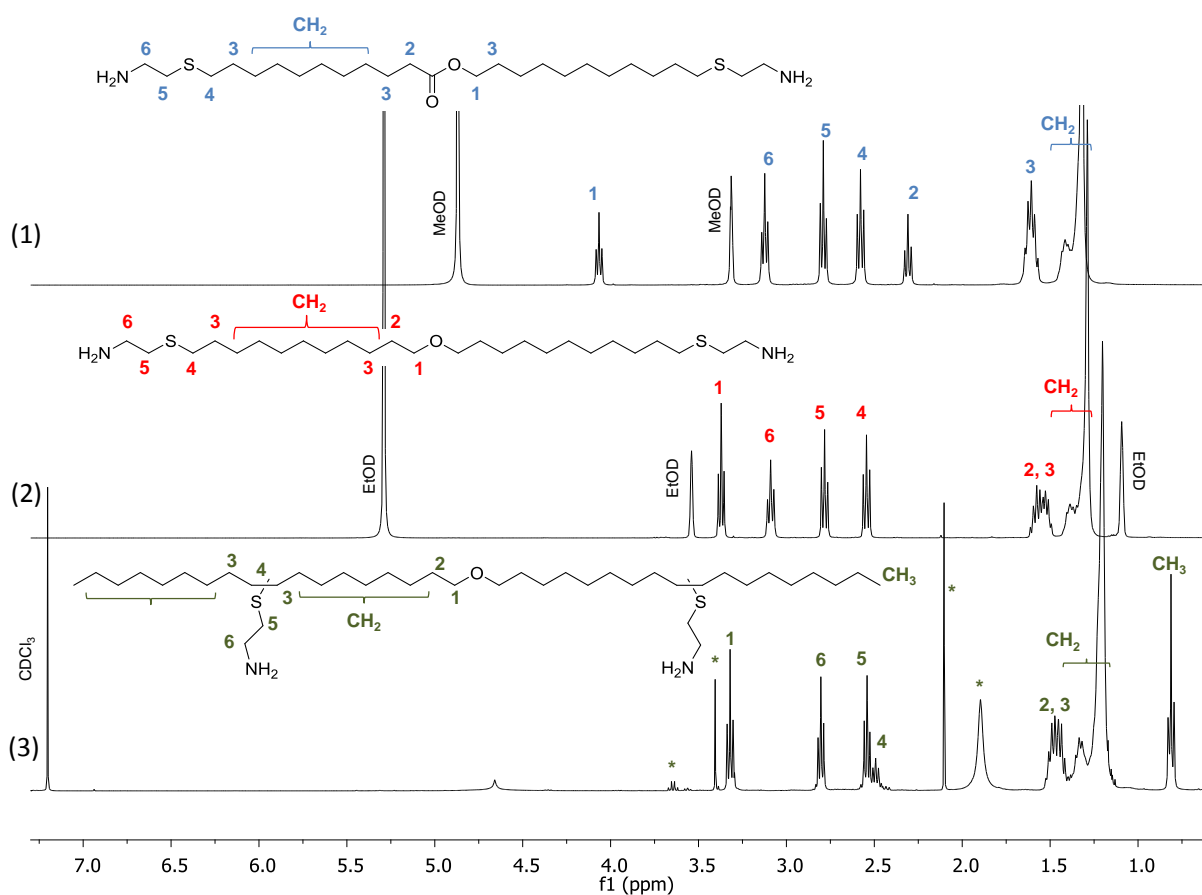


Figure 15 - Stacked ^1H NMR spectra of (1) Und(ester)-diamine in MeOD with TFA (2) Und(ether)-diamine in EtOD with TFA and (3) Oleyl(ether)-diamine in CDCl₃. (* impurities).

3. Comparison of the two routes

The two routes investigated to synthesize (di)amines from usual vegetable oil derivatives need to be compared, taking into account the 12 principles of the ‘Green Chemistry’ listed in Table 6. Particularly, the number of steps, the by-products and wastes, the catalysis or even the toxicity of chemicals were considered. Conversions and yields, valorization and purification of the intermediates and amines were also taken into account.

The method involving nitriles appears to be more attractive: cheap available catalysts, high atom efficiency, low toxicity of the reactants, mild reaction conditions, water as by product, high conversions and decent yields (53-90%). This route finds its limitation in the use of ammonia at the industrial scale-up, requiring special anti-corrosive autoclaves. Also, high quantities of solvents were required for nitrile intermediate purification. Concerning the *Und-C20-diamine*, an important optimization on the initial diol formation needs to be done in

order to limit the isomerization during 10-undecen-1-ol metathesis and thus to control the chain length of the aliphatic diamines (see ESI† for GC).

Table 6 – Comparison of the two routes towards diamine synthesis, according to the 12 principles of the ‘Green Chemistry’.

Green chemistry principles	Alcohol oxidation/Hydrogenation route	Thiol-ene route
Prevent waste	✓ Water as by product, need to be purified	✓ No by-product, no waste
Atom economy	✓ Aerobic oxidation	✓ Thiol-ene “click” chemistry ✗ 2eq. of thiol at least
Less hazardous synthesis	✓ Mild conditions ✗ Harmfull and corrosive ammonia	✓ Mild conditions
Design safe chemicals	✓ Long aliphatic diamines	✓ Longer aliphatic diamines ✗ Sulfur-containing monomers
Safe solvent and auxiliaries	✗ Solvent (acetonitrile) / high amount for purification (cyclohexane)	✗ Solvent for syntheses (DMSO, DCM, MeOH) ✗ Solvent for diene purification (cyclohexane)
Design for energy efficiency	✓ Low temperature ✗ Pressurized reactors	✗ High temperature for fatty-acids dimerization ✗ UV reactors
Use of renewable feedstock	✓ Accessible bio-based alcohols	✓ Cysteamine from decarboxylation of bio-based lysine ✓ Accessible fatty-acid derivatives
Reduce derivatives / Number of steps	✓ 2 steps ✓ One-pot synthesis from alcohol to nitrile	✓ 2 steps
Catalysis (vs. stoichiometric)	✓ Cu/TEMPO catalysis	✗ High equivalents of cysteamine ✗ No catalyst
Design for degradation	✗ No degradable function	✓ Ester moieties integrated in diamine backbone enable degradation
Real time analysis or pollution prevention	-	-
Inherent safe chemistry for accident prevention	✗ Pressurized reactors for hydrogenation	✓ Optic fiber instead of UV reactors

On the other hand, the thiol-ene “click” chemistry has gained attention from the scientific community in the past few years since no by-products were formed and mild conditions were used. Therefore, this route appears as an easy and green methodology for the synthesis of bio-based amines in good yields, especially from vegetable oils that present a high content of alkene functions. The process is reliable and efficient when terminal dienes are used as starting material, which is not the case with internal unsaturations which require harsh conditions and higher equivalents of cysteamine that needs to be recovered and recycled. However, one of the major drawbacks of this route is the use of sulfur-containing reagents that could restrain the industrial scale up.

Regarding the number of steps and the purification, the two routes are hardly comparable as they mainly depend on the chemical structure of the substrates. It is noteworthy to underline that the two approaches lead to diamines with completely different structures and heteroatom contents. Concerning the reactive intermediate valorization, dienes could be used for polymer synthesis by ADMET¹³ and nitrile compounds from aerobic oxidation of alcohols could find other applications in pharmaceuticals, agricultural or even in fine chemicals synthesis.

Conclusions

In conclusion, a platform of aliphatic diamines has been synthesized from castor and canola oil derivatives such as methyl undecenoate or methyl oleate. Two routes have been investigated to answer the high demand in aliphatic diamines as monomer for thermosets and thermoplastics syntheses (epoxy resins, polyamides, PHUs).

The first one was the preparation of (di)nitriles from the corresponding alcohols using mild conditions with a copper catalytic system, oxygen as an oxidant and aqueous ammonia as a nitrogen source. This route has been optimized in order to get a greener process, using air as an oxidant or TEMPO supported on silica as heterogeneous and recyclable mediator. The optimized process under air was successfully applied to different types of alcohol derived from renewable resources. Reductions of the formed primary dinitriles led to fatty acid-based diamines. This optimized ‘nitrile pathway’ appears to be highly efficient and green for the synthesis of bio-based amines from the corresponding primary alcohols.

The second approach was based on the thiol-ene coupling between bio-based cysteamine hydrochloride and several dimerized fatty acid-based derivatives. The sus-mentioned synthesis finds its limitation in the thiol-ene coupling on internal unsaturation, which implies 10 eq. of cysteamine per double bound and the use of a photoinitiator. Moreover, the so-formed diamines present at least 26 carbons in their aliphatic backbone that could reduce their reactivity towards the aminolysis of cyclic carbonates¹⁸ and consequently lower the polymerization rate during PHU production. Besides, this strategy could have been applied to mono fatty-acid derivatives comprising one or more unsaturations to access di- or polyamines, increasing the amine index.

Some of the fatty acid-based diamines presented in this chapter were used as comonomers for fully bio-based thermoplastic poly(hydroxyurethane)s synthesis, as discussed in the Chapter 3.

References

- (1) Yin, W.; Wang, C.; Huang, Y. *Org. Lett.* **2013**, *15* (8), 1850–1853.
- (2) Hibert, G.; Lamarzelle, O.; Maisonneuve, L.; Grau, E.; Cramail, H. *Eur. Polym. J.* **2016**, *82*, 114–121.
- (3) Ryland, B. L.; Stahl, S. S. *Angew. Chemi.* **2014**, *53* (34), 8824–8838.
- (4) Cao, Q.; Dornan, L. M.; Rogan, L.; Hughes, N. L.; Muldoon, M. J. *Chem. Commun.* **2014**, *50* (35), 4524–4543.
- (5) Dornan, L. M.; Cao, Q.; Flanagan, J. C. A.; Crawford, J. J.; Cook, M. J.; Muldoon, M. J. *Chem. Commun.* **2013**, *49*, 6030–6032.
- (6) Hoover, J. M.; Stahl, S. S. *J. Am. Chem. Soc.* **2011**, *133*, 16901–16910.
- (7) Steves, J. E.; Stahl, S. S. *J. Am. Chem. Soc.* **2013**, *135* (42), 15742–15745.
- (8) Fernandes, A. E.; Riant, O.; Jonas, A. M.; Jensen, K. F. *RSC Adv.* **2016**, *6*, 36602–36605.
- (9) Prebil, R.; Stavber, G.; Stavber, S. *European J. Org. Chem.* **2014**, *2014* (2), 395–402.
- (10) Wang, L.; Bie, Z.; Shang, S.; Lv, Y.; Li, G. *RSC Adv.* **2016**, *6*, 35008–35013.
- (11) Konkolewicz, D.; Wang, Y.; Krys, P.; Zhong, M.; Isse, A. A.; Gennaro, A.; Matyjaszewski, K. *Polym. Chem.* **2014**, *5* (15), 4409–4417.
- (12) Stemmelen, M.; Lapinte, V.; Habas, J.; Robin, J. **2015**, *68*, 536–545.
- (13) Lebarbé, T.; More, A. S.; Sane, P. S.; Grau, E.; Alfos, C.; Cramail, H. *Macromol. Rapid Commun.* **2014**, *35* (4), 479–483.
- (14) Claudino, M. Thiol – ene Coupling of Renewable Monomers : at the forefront of bio-based polymeric materials, Thesis, University of Stockholm, **2011**.
- (15) Darroman, E.; Auvergne, R.; Boutevin, B.; Caillol, S. *Eur. J. Lipid Sci. Technol.* **2014**, *116* (2), 178–189.
- (16) Cornille, A.; Froidevaux, V.; Negrell, C.; Caillol, S.; Boutevin, B. *Polymer.* **2014**, *55* (22), 5561–5570.
- (17) Fache, M.; Darroman, E.; Besse, V.; Auvergne, R.; Caillol, S.; Boutevin, B. *Green Chem.* **2014**, *16* (4), 1987–1998.
- (18) Diakoumakos, C. D.; Kotzev, D. L. *Macromol. Symp.* **2004**, *216* (1), 37–46.

Experimental and Supporting Information

Experimental Methods

Synthesis of diamines via alcohol oxidation

• ***Und-C20-diol synthesis:*** In an oven-dried Schlenk tube, 10-undecen-1-ol (20 g, 117 mmol) was dissolved in pentane dried on CaH₂. Afterwards, Grubbs 2nd generation metathesis catalyst (1 mol.%, 0.99 g, 1.17 mmol) was added. The reaction was performed under inert atmosphere at room temperature for 72h. As the reaction was running, the product got precipitated, which allows the shift of the equilibrium toward the formation of the diol. The product was purified by two recrystallizations in toluene. ***Und-C20-diol*** was obtained as a white powder with a purity of 60% (determined by GC, due to isomers). Yield: 43%. ¹H NMR (CDCl₃, 25°C, 400 MHz), δ (ppm): 5.37 (m, 2H), 3.64 (t, 4H), 1.94 (m, 4H), 1.56 (m, 4H), 1.28 (m, 24H).

• **General procedure for 1,10-decanedinitrile synthesis :** In a 50 mL one-neck round bottomed flask, 1 eq. of 1,10-decanediol (2.9 mmol, 0.5 g), 0.2 eq. of copper precursor, 0.2 eq. of TEMPO, 0.2 eq. of copper ligand were added. 5 mL (0.58 mol.L⁻¹) of acetonitrile was introduced and the flask was capped with a rubber septum. The solution was stirred with a magnetic stirrer and heated to the desired temperature (30 to 60°C) in an oil bath. Two balloons were filled with O₂ or air and attached to a syringe that was inserted through the septum. When the desired temperature was reached, 0.45 mL (6.8 mmol of NH₃) of aqueous ammonia solution at 28 w.% was added to the solution *via* a syringe. The resulting orange-brown solution was stirred over 24h. As the reaction is running, the reaction mixture turned blue or green depending on the copper precursor used. The solvent was then removed using a rotary evaporator. Aliquot was dissolved in CDCl₃ and analysed by ¹H NMR spectroscopy. When purification was needed, the residue was eluted with DCM through an alumina/celite column to remove the copper precursor. The solvent was evaporated under vacuum and the resulting viscous orange transparent liquid was purified by flash chromatography (eluent: cyclohexane-ethyl acetate, 80:20).

1,10-decanedinitrile synthesis with CuOAc and p-(Me)bpy at 40°C : In a round-bottom flask 1 eq. (2.9 mmol, 0.5 g) of 1,10-decanediol, 0.2 eq. of CuOAc (0.58 mmol, 71 mg), 0.2 eq. (0.58 mmol, 92 mg) of TEMPO, 0.2 eq. (0.58 mmol, 11 mg) of p-(Me)bpy and 5 mL (0.58 mol.L⁻¹) of acetonitrile were added. Two balloons filled with air were attached to the flask.

When 40°C was reached, 0.45 mL (6.8 mmol) of aqueous ammonia solution at 28 w.% was added to the solution *via* a syringe and the mixture was stirred over 24h.

• **General procedure for nitrile synthesis under pressure:** As in the general procedure, 1,10-decanediol, copper precursor, copper ligand, TEMPO, acetonitrile and aqueous ammonia were added in a jacketed pressure reactor. The mixture was then mechanically stirred at 255 rpm and heated to 40°C by a water circulation for 30 min. Compressed air was slowly introduced to reach the desired pressure (5 to 30 bars). The reaction mixture was left over 24h. The reactor was slowly depressurized and the solvent was removed using a rotary evaporator.

1,10-decanedinitrile: The dinitrile was obtained as a transparent liquid after flash column chromatography (cyclohexane:ethyl acetate 90:10 to 50:50). Yield: 90%. ¹H NMR (CDCl₃, 25°C, 400 MHz), δ (ppm): 2.34 (t, 4H), 1.66 (m, 4H), 1.46 (m, 4H), 1.35 (m, 4H). ¹³C NMR (CDCl₃, 25°C, 100 MHz), δ (ppm): 119.82 (CN), 28.60 (CH₂), 25.40 (CH₂-CH₂-CN), 17.23 (CH₂-CN). IR (cm⁻¹): 2932, 2859, 2244, 1464, 1427.

Und-C20-dinitrile: *Und-C20-dinitrile* was obtained as a viscous transparent liquid after flash column chromatography (eluent: cyclohexane-ethyl acetate 100:0 to 70:30). Yield: 53%. ¹H NMR (CDCl₃, 25°C, 400 MHz), δ (ppm): 5.37 (m, 2H), 2.31 (t, 4H), 1.96 (m, 4H), 1.63 (m, 4H), 1.44 (m, 4H), 1.30 (m, 16H). ¹³C NMR (CDCl₃, 25°C, 100 MHz), δ (ppm): 130.42 (CH=CH), 119.94 (CN), 32.62 (CH₂-CH=CH), 29.63-28.74 (CH₂), 25.41 (CH₂-CH₂-CN), 17.22 (CH₂-CN). IR (cm⁻¹): 2924, 2855, 2244.

• **General procedure for nitrile synthesis with recyclable supported-TEMPO:** The reaction was performed in a round bottom flask containing a fritted glass filter to recycle the supported-TEMPO (see Figure ESI† 6). The reaction was performed with 0.15 g (0.9 mmol, 1 eq.) of 1,10-decanediol, 0.23 g (0.16 mmol, 0.2 eq.) of TEMPO-Si or 0.17 g (0.17 mmol, 0.2 eq.) of TEMPO-polymer bound, 0.2 eq. of copper precursor, 0.2 eq. of copper ligand, 2.3 eq. of NH₃ and 1.5 mL of acetonitrile. Two balloons filled with air or oxygen were attached to the flask. At the end of the reaction, the mixture was dissolved in additional acetonitrile and filtered through the fritted-glass. The supported-TEMPO remaining in the flask was successively washed with acetonitrile and dichloromethane. The solvent filtrate was removed and the supported-TEMPO was placed under vacuum before being reused.

• **General procedure for diamine synthesis via hydrogenation of dinitrile:** Purified dinitrile, ethanol (0.1 g/mL) and Raney nickel (0.5 mL Raney nickel 50 w.% slurry in water per g of product) were added in a jacketed pressure reactor. Dihydrogen was loaded to a pressure of 10 bars. The reactor was then heated to 70°C by a water circulation and the reaction mixture was left 24h. Raney nickel was removed by filtration on a paper filter and ethanol was removed using a rotary evaporator. A washing procedure was applied when necessary.

1,10-decanediamine: *1,10-decanediamine* was obtained as a white powder after being precipitated in acetone to remove the remaining dinitrile. Conversion: 93%. Yield: 43%. ¹H NMR (CDCl₃, 25°C, 400 MHz), δ (ppm): 2.64 (t, 4H), 1.40 (m, 4H), 1.25 (m, 12H), 1.14 (m, 2.NH₂). ¹³C NMR (CDCl₃, 25°C, 100 MHz), δ (ppm): 42.30 (CH₂-NH₂), 29.7-27 (CH₂). IR (cm⁻¹): 3330, 3257, 3163, 2919, 2848.

UndC-20-diamine: *Und-C20-diamine* was obtained after filtration and evaporation as a white/yellow powder. Conversion: 100%. Yield: 51%. ¹H NMR (EtOD, 25°C, 400 MHz), δ (ppm): 2.67 (t, 4H), 1.51 (m, 4H), 1.37 (m, 32H). ¹³C NMR (EtOD, 25°C, 100 MHz), δ (ppm): 42.5 (CH₂-NH₂), 33.9-27.9 (CH₂). IR (cm⁻¹): 3299, 2916, 2850.

Synthesis of diamines via thiol-ene coupling

Und(ether)-diene synthesis: Into a round bottom flask, 2 eq. of sodium hydride (0.55 g, 22.8 mmol) were stirred with 70 mL of DMSO under inert atmosphere. 1 eq. of 10-undecen-1-ol (1.94 g, 11.4 mmol) was slowly added. The reaction mixture was then stirred at room temperature for 10 min. To this, 1-bromo-10-undecene (2.66 g, 11.4 mmol) was added dropwise. After 16h, DMSO was removed under reduced pressure and excess sodium hydride was deactivated by aqueous solution of ammonium chloride. DCM (50 mL) was added and the organic layer was washed with saturated NaHCO₃ 3 times and with water. The organic layer was dried over anhydrous magnesium sulphate, filtered and reconcentrated. Conversion: 100%. The crude product was purified by flash column chromatography using a mixture of cyclohexane-ethyl acetate (100:0 to 80:20) as eluent and obtained as a white powder. Yield: 36%. Purity by GC: 100%. ¹H NMR (CDCl₃, 25°C, 400 MHz), δ (ppm): 5.73 (m, 2H), 4.96 (m, 4H), 3.36 (t, 4H), 1.94 (q, 4H), 1.49 (m, 4H), 1.20-1.27 (m, 24H). ¹³C NMR (CDCl₃, 25°C, 100 MHz) δ (ppm): 138.8 (CH₂=CH-), 113.7 (CH₂=CH-), 70.3 (CH₂-O-CH₂-), 32.3-25.4 (-CH₂-). IR (cm⁻¹): 3077, 2923, 2852, 1116.

Oleyl(ether)-diene synthesis: Into a round bottom flask, 2 eq. of sodium hydride (0.89 g, 37.2 mmol) were stirred with 70 mL of DMSO under inert atmosphere. 1 eq. of oleyl alcohol (5 g, 18.6 mmol) was slowly added. The reaction mixture was then stirred at room temperature for 10 min. To this, oleyl methanesulfonate (6.45 g, 18.6 mmol) was added drop-wise. After 16h, DMSO was removed under reduced pressure and excess sodium hydride was deactivated by aqueous solution of ammonium chloride. DCM (50 mL) was added and the organic layer was washed with saturated NaHCO₃ 3 times and with water. The organic layer was dried over anhydrous magnesium sulphate, filtered and reconcentrated. Conversion: 100%. The crude product was purified by flash column chromatography using a mixture of cyclohexane-ethyl acetate (100:0 to 70:30) as eluent and obtained as viscous transparent oil. Yield: 37%. Purity by GC: 100%. ¹H NMR (CDCl₃, 25°C, 400 MHz), δ (ppm): 5.33 (m, 4H), 3.39 (t, 4H), 1.99 (m, 8H), 1.54 (m, 4H), 1.30 (m, 44H), 0.86 (t, 6H). ¹³C NMR (CDCl₃, 25°C, 100 MHz), δ (ppm): 129.7 (-CH₂=CH₂-), 70.9 (CH₂-O-CH₂-), 31.9-23.1 (-CH₂-), 13.9 (-CH₃). IR (cm⁻¹): 3005, 2921, 2852, 1464, 1117.

Und(ester)-diene synthesis: 1 eq. of methyl 10-undecenoate (17.47 g, 88 mmol), 1 eq. of 10-undecen-1-ol (15 g, 88 mmol) and 0.05 eq. of TBD were stirred under nitrogen flow 4h at 120°C, 2h at 160°C then 1h under vacuum at 160°C. Conversion: 90%. The product was purified using flash column chromatography (eluent: cyclohexane-ethyl acetate, 80:20) and obtained as a white powder. Yield: 83%. Purity by GC: 100%. ¹H NMR (CDCl₃, 25°C, 400 MHz), δ (ppm): 5.81 (m, 2H), 4.97 (m, 4H), 4.07 (t, 2H), 2.28 (t, 2H), 2.03 (q, 4H), 1.64 (m, 4H), 1.38-1.29 (m, 24H). ¹³C NMR (CDCl₃, 25°C, 100 MHz), δ (ppm): 173.9 (-C=O), 139.2 (CH₂=CH-), 114.3 (CH₂=CH-), 64.5 (-CH₂-C=O-O-CH₂-), 34.3 (-CH₂-C=O-O-CH₂-), 33.5 (CH₂=CH-CH₂), 29.5-25 (-CH₂-). IR (cm⁻¹): 3077, 2924, 2854, 1736.

- **General procedure for thiol-ene coupling:** Dimerized bis-unsaturated fatty acids were reacted with cysteamine hydrochloride in a mixture of methanol:DCM (1:1) using DMPA as photoinitiator when needed. The reaction was carried out in a UV reactor (365 nm) for 16h, or 2h under UV irradiation using an optical fiber (350-400 nm) in the case of the *Oleyl(ether)-diamine* synthesis.

Und(ether)-diamine synthesis: *Und(ether)-diene* (1 eq., 0.5 g, 1.55 mmol), cysteamine hydrochloride (4 eq., 0.7 g, 6.2 mmol) were reacted in the UV reactor. Conversion: 94%. The heterogeneous mixture obtained was filtered and the resulting white powder was abundantly washed with a saturated NaHCO₃ solution and then with methanol. Yield: 72%. ¹H NMR (EtOD+TFA, 25°C, 400 MHz), δ (ppm): 3.35 (t, 4H), 3.11 (t, 4H), 2.77 (t, 4H), 2.56 (t, 4H),

1.58 (m, 8H), 1.45-1.30 (m, 28H). ^{13}C NMR (EtOD+TFA, 25°C, 100 MHz), δ (ppm): 70.8 ($\underline{\text{C}}\text{H}_2\text{-O-CH}_2$), 38.9 ($-\underline{\text{C}}\text{H}_2\text{-NH}_2$), 31.6 ($-\text{S-}\underline{\text{C}}\text{H}_2\text{-CH}_2$), 29.7-29.3 (CH_2), 28.8 ($-\text{S-}\underline{\text{C}}\text{H}_2\text{-CH}_2\text{-NH}_2$). IR (cm^{-1}): 3332, 2917, 2851, 2488, 1121.

Oleyl(ether)-diamine synthesis: *Oleyl(ether)-diene* (1 eq., 0.44 g, 0.84 mmol), cysteamine hydrochloride (20 eq., 1.91 g, 16.8 mmol) were reacted using the UV optic fiber (350-400 nm) using DMPA (10 w.%, 44 mg) as photoinitiator. Conversion: 70%. The solvent was evaporated and the crude product was dissolved in chloroform and then washed 3 times with NaHCO_3 until pH 7 and 3 times with water. The organic phase was dried with MgSO_4 , filtered and reconcentrated. The crude product was purified by flash column chromatography (eluent: DCM-methanol, 100:0 to 50:50) to obtain a yellow viscous liquid. Yield: nd. ^1H NMR (CDCl_3 , 25°C, 400 MHz), δ (ppm): 3.38 (t, 4H), 2.85 (t, 4H), 2.58 (t, 4H), 2.55 (t, 2H), 1.51 (m, 12H), 1.38-1.26 (m, 48H), 0.85 (t, 6H). ^{13}C NMR (CDCl_3 , 25°C, 100 MHz), δ (ppm): 70.9 ($\underline{\text{C}}\text{H}_2\text{-O-CH}_2$), 45.9 ($-\text{S-}\underline{\text{C}}\text{H}(\text{CH}_2)_2-$), 41.7 ($-\underline{\text{C}}\text{H}_2\text{-NH}_2$), 35.2 ($-\text{S-}\underline{\text{C}}\text{H}(\underline{\text{C}}\text{H}_2)_2-$), 34.1 ($-\text{S-}\underline{\text{C}}\text{H}_2\text{-CH}_2\text{-NH}_2$), 32.1-22.7 (CH_2), 14.1 (CH_3). IR (cm^{-1}): 3355, 2921, 2851, 1572, 1463, 1115.

Und(ester)-diamine synthesis: *Und(ester)-diene* (1 eq., 0.5 g, 1.49 mmol), cysteamine hydrochloride (4 eq., 0.67 g, 5.9 mmol) were reacted in a mixture of methanol:DCM (5mL) without DMPA in the UV reactor. Conversion: 100%. The heterogeneous mixture obtained was filtered and the resulting white powder was abundantly washed with a saturated NaHCO_3 solution. The amine was recrystallized in EtOH. Yield: 45%. ^1H NMR (MeOD+TFA, 25°C, 400 MHz), δ (ppm): 4.07 (t, 2H), 3.12 (t, 4H), 2.79 (t, 4H), 2.58 (t, 4H), 2.29 (t, 2H), 1.61 (m, 8H), 1.42-1.32 (m, 28H). ^{13}C NMR (MeOD+TFA, 25°C, 100 MHz), δ (ppm): 175.3 ($-\text{O}=\underline{\text{C}}\text{-O-}$), 65.29 ($-\text{O}=\text{C-}\underline{\text{O-CH}}_2$), 39.9 ($-\underline{\text{C}}\text{H}_2\text{-NH}_2$), 32.4 ($\underline{\text{C}}\text{H}_2\text{-O}=\text{C-}\underline{\text{O-CH}}_2$), 30.6 ($-\text{S-}\underline{\text{C}}\text{H}_2\text{-CH}_2$), 30.5-26.1 (CH_2), 30.3 ($-\text{S-}\underline{\text{C}}\text{H}_2\text{-CH}_2\text{-NH}_2$). IR (cm^{-1}): 3316, 2916, 2848, 2511, 1724.

Supporting Information

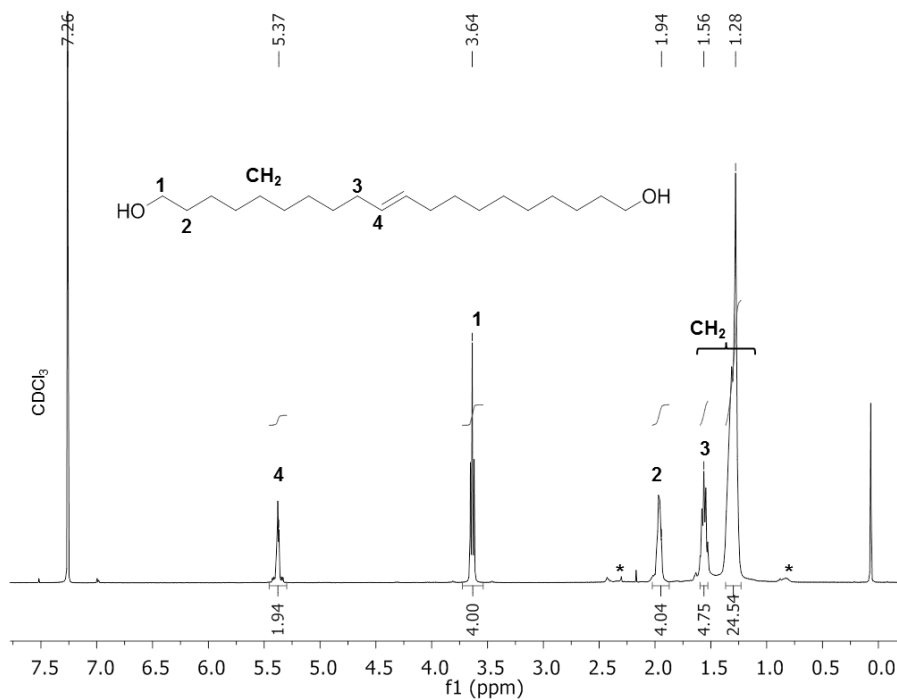


Figure ESI 1- ^1H NMR spectrum of Und-C20-diol in CDCl_3 (*Impurities).

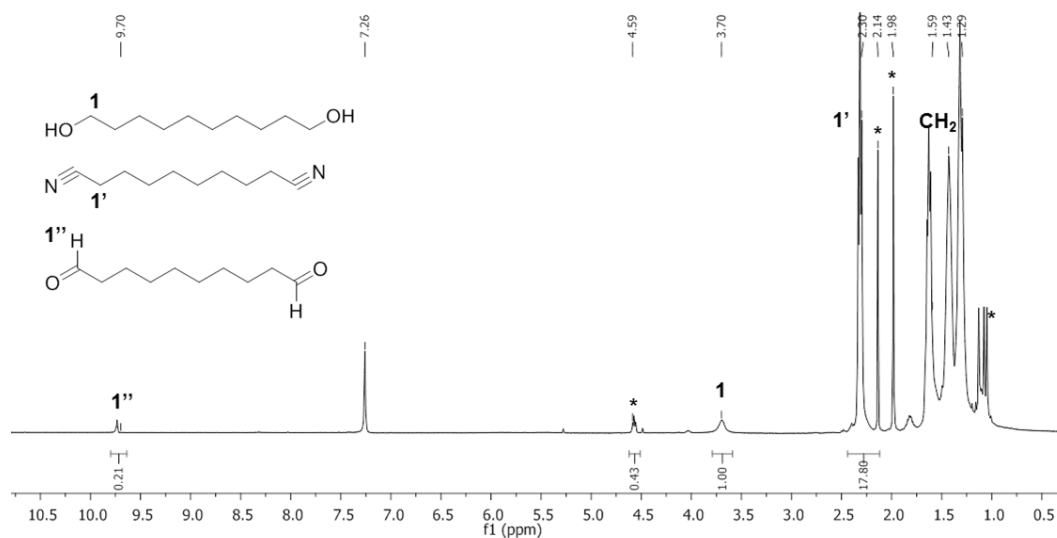


Figure ESI 2 - ^1H NMR spectrum of the oxidized products from 1,10-decanediol under the optimized reaction conditions (0.2 eq. of $\text{Cu}(\text{OAc})/\text{p}(\text{Me})\text{bpy}/\text{TEMPO}$, 40°C , 30 bars of air) in CDCl_3 (*Impurities).

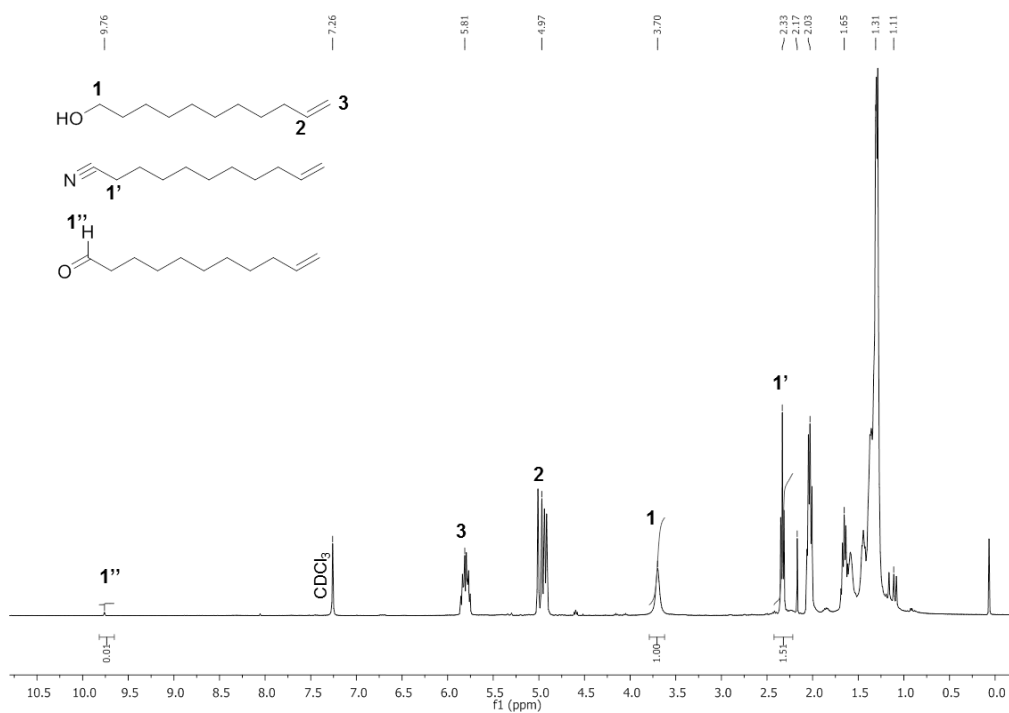


Figure ESI 3 - ^1H NMR spectrum of the oxidized products from 10-undecene-1-ol under the optimized reaction conditions (0.1 eq. of Cu(OAc)/p-(Me)bpy/TEMPO, 40°C, 30 bars of air) in CDCl₃.

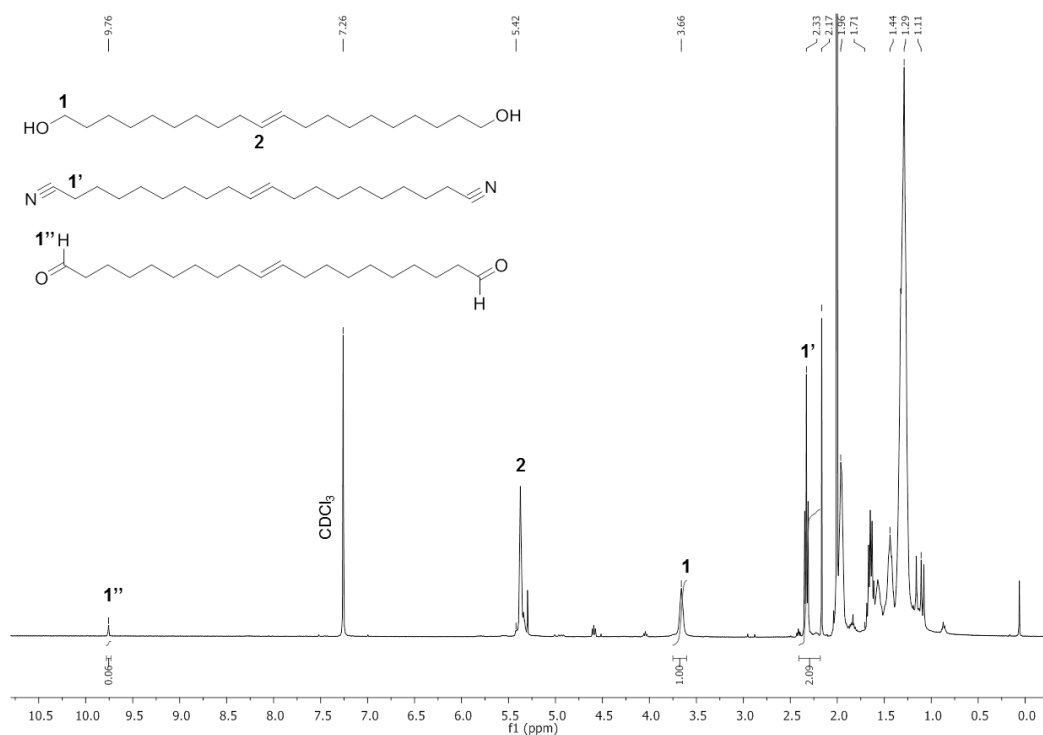


Figure ESI 4 - ^1H NMR spectrum of the oxidized products from Und-C20-diol under the optimized reaction conditions (0.2 eq. of Cu(OAc)/p-(Me)bpy/TEMPO, 40°C, 30 bars of air) in CDCl₃.

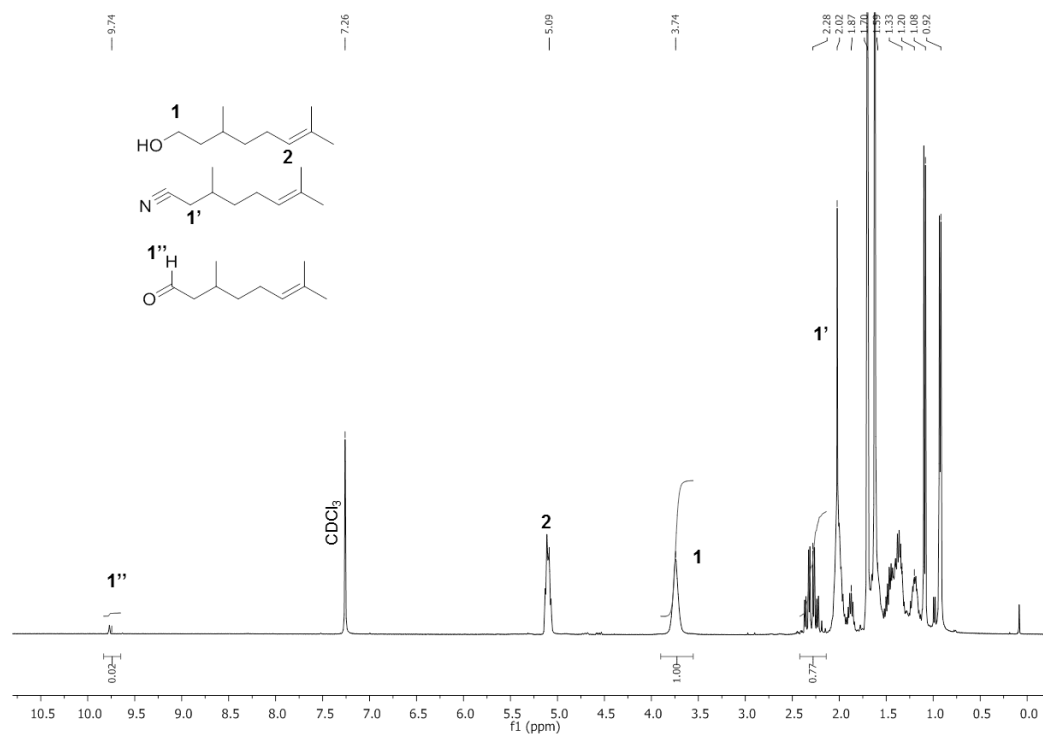


Figure ESI 5 - ^1H NMR spectrum of the oxidized products from citronelol under the optimized reaction conditions (0.1 eq. of $\text{Cu}(\text{OAc})/\text{p}(\text{Me})\text{bpy}/\text{TEMPO}$, 40°C , 30 bars of air) in CDCl_3 .

Table ESI 1 - Alcohol oxidation using supported-TEMPO under the optimized systems under air or oxygen.^a

Entry	Substrate	Cu/L	atm	Mediator	Conversion in nitrile (%) ^b
1	1,10-decanediol	CuI/bpy	O_2	TEMPO-Si	7
2	1,10-decanediol	CuI/bpy	O_2	TEMPO-PS	2
3	1,10-decanediol	CuI/bpy	O_2	50% TEMPO-Si	4
4	1,10-decanediol	$\text{CuOAc}/\text{p}(\text{Me})\text{bpy}$	air	TEMPO-Si	0
5	1,10-decanediol	$\text{CuOAc}/\text{p}(\text{Me})\text{bpy}$	air	TEMPO-PS	0
6	1,10-decanediol	$\text{CuOAc}/\text{p}(\text{Me})\text{bpy}$	10 bars air	TEMPO-Si	0

^a: Reaction conditions : 1 eq. of alcohol, 0.1 eq. of copper precursor, 0.1 eq. of ligand, 0.1 eq. of supported-TEMPO/
OH function, 1.15 eq. of $\text{NH}_3(\text{aq})/\text{OH}$ function, in acetonitrile, air or O_2 balloon, 24h, 40 or 50°C .

^b: Determined by ^1H NMR in CDCl_3 .



Figure ESI 6 - Round bottom flask containing a fritted glass filter to recycle the supported-TEMPO, with a system to attach the balloons containing oxygen or air.

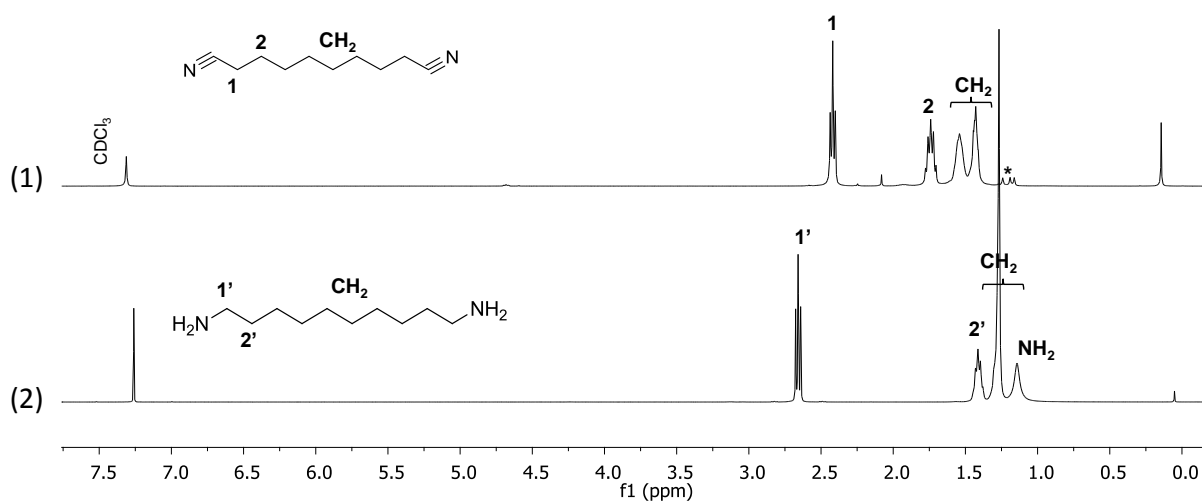


Figure ESI 7 - Stacked ¹H NMR spectra of (1) 1,10-decanedinitrile and (2) 1,10-diaminodecane in CDCl₃ (* Impurities).

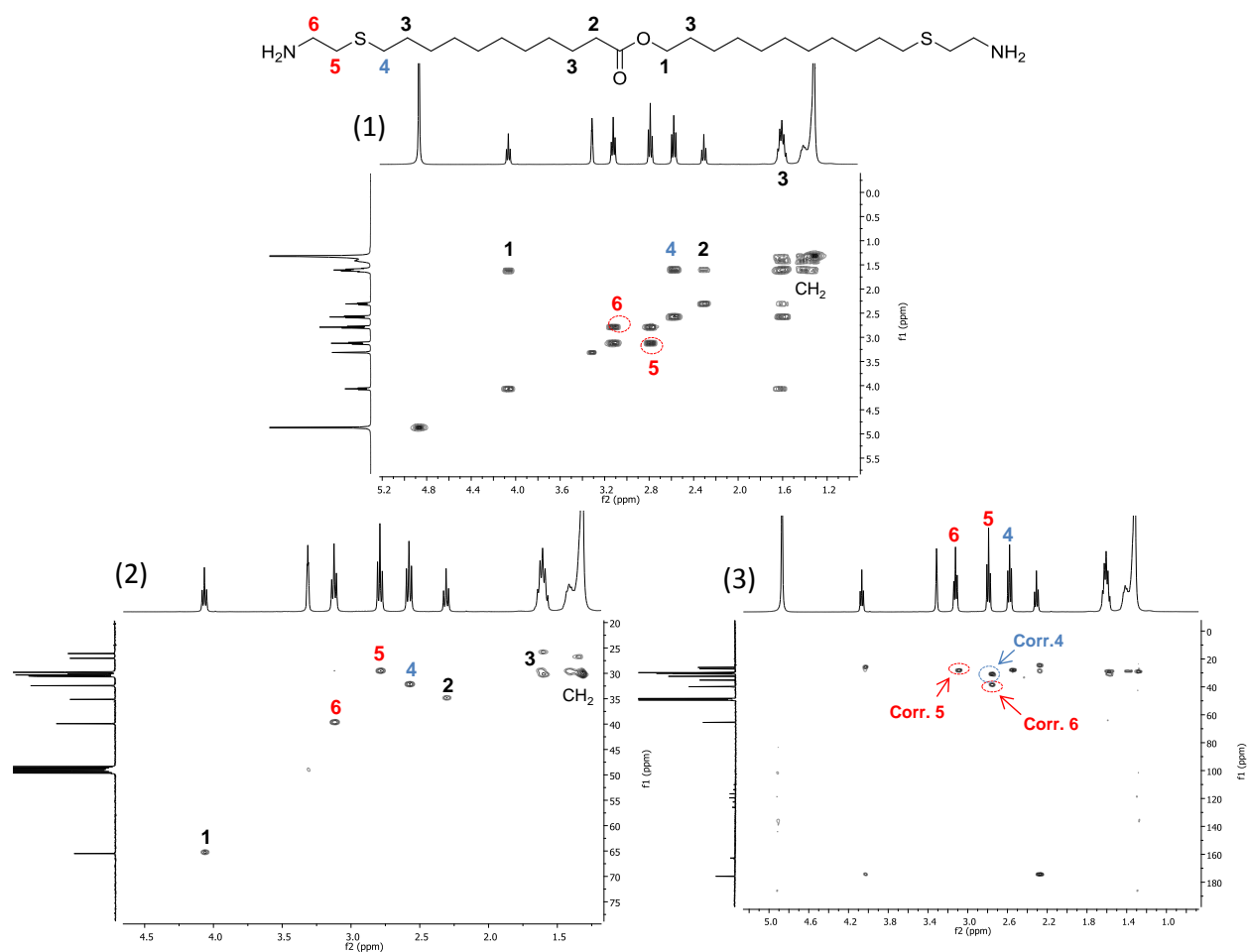


Figure ESI 8 - (1) ^1H - ^1H COSY NMR, (2) ^1H - ^{13}C HSQC NMR and (3) ^1H - ^{13}C HMBC NMR of Und(ester)-diamine in MeOD with TFA, in order to determine the position of protons 4, 5 and 6.

Chapter 3

Activated fatty acid- and glycerol-based cyclic carbonates towards Poly(hydroxyurethane)s synthesis

Publication: O. Lamarzelle *et al.*, Polymer Chemistry, **2016**, 7, 1439-1451

Keywords: Cyclic carbonate, fatty-acids, glycerol, non-isocyanate polyurethane, poly(hydroxyurethane), thermoplastics.

Mots-clés: Carbonate cyclique, acides gras, glycerol, polyurethane sans isocyanate, poly(hydroxyuréthane), thermoplastiques.

Table of contents

Introduction	131
1. Activated fatty acid-based cyclic carbonates towards PHUs	132
1.1. Synthesis of activated lipidic cyclic carbonates.	132
1.1.1. Ether-activated monomers from epichlorohydrin	133
1.1.2. Ester-activated monomers from glycerol carbonate	135
1.1.3. Comparison between the two routes.....	136
1.2. Kinetic measurements and reactivity comparison	137
1.2.1. Comparison between activations.....	138
1.2.2. Impact of different parameters influencing the kinetics	140
1.2.3. Side reactions, by-products and selectivity	143
1.3. Poly(hydroxyurethane)s synthesis.....	146
2. Diglycerol dicarbonate as an activated monomer for PHUs.....	153
2.1. Monomer synthesis and characterization	154
2.1.1. Diglycerol carbonation toward DGDC.....	154
2.1.2. Characterization and properties	155
2.2. Poly(hydroxyurethane) synthesis and applications	158
2.2.1. DGDC-based PHUs with tunable properties varying diamine nature.....	158
2.2.2. PHUs from DGDC with different purity grade	162
2.2.3. DGDC-based copolymers.....	164
Conclusions	168
References	170
Experimental and Supporting Information	172

Introduction

Thermoplastic poly(hydroxyurethane)s (TPHUs) raised industrial and academic research curiosity¹⁻⁷, since their synthesis is achieved *via* the ring opening of bis-cyclic carbonates with diamines, enabling the replacement of phosgene and isocyanates employed in the classical polyurethane (PU) manufacture. In view of the fossil fuel depletion, the use of building-blocks from renewable resources such as vegetable oils is on the rise.⁸ Combining PHUs synthesis and bio-based compounds, a large platform of fatty acid-based cyclic carbonates as poly(hydroxyurethane) precursors has already been synthesized by epoxidation/carbonation routes.^{3,9-11} However, such monomers exhibited a slow polymerization rate towards amines, due to the electron-releasing alkyl chains which deactivate the cyclic carbonates. To tackle this issue, academic research has developed larger sized-ring cyclic carbonates in order to increase their ring strain and so their reactivity towards aminolysis.¹²⁻¹⁷ Our research group has already investigated the preparation of vegetable oil-based 6-membered cyclic carbonates from bio-sourced methyl undecenoate.¹⁸ The major issue with these monomers is their instability when stored at room temperature. An alternative route consists in inserting a heteroatom nearby the 5-membered cyclic carbonate to improve its reactivity,^{12,13,19-31} preserving its stability. Herein, the first part of this chapter covers the synthesis of new activated lipidic cyclic carbonates from glycerol carbonate and epichlorohydrin, bringing respectively an ester or an ether linkage in β position of the carbonate. After kinetic investigations of the cyclic carbonate aminolysis on model compounds, the corresponding activated bis-cyclic carbonates were polymerized with several diamines and exhibited enhanced reactivities. A specific spotlight on the side reactions that could occur in both model reaction and polymerization is also discussed.

In a second part, a focus is made on diglycerol dicarbonate (DGDC), a short glycerol-based cyclic carbonate presenting an oxygen atom in beta position nearby the cycle. Its inherent structure could confer to this b5CC a high reactivity towards aminolysis. The DGDC was synthesized and fully characterized by NMR, X-ray and kinetic measurement before being polymerized with various diamines as comonomers. Taking advantage of the polar feature of the DGDC-based PHUs, their self-assembly in water was investigated, opening the route to potential applications in the fields of biomedicine and pharmacy.

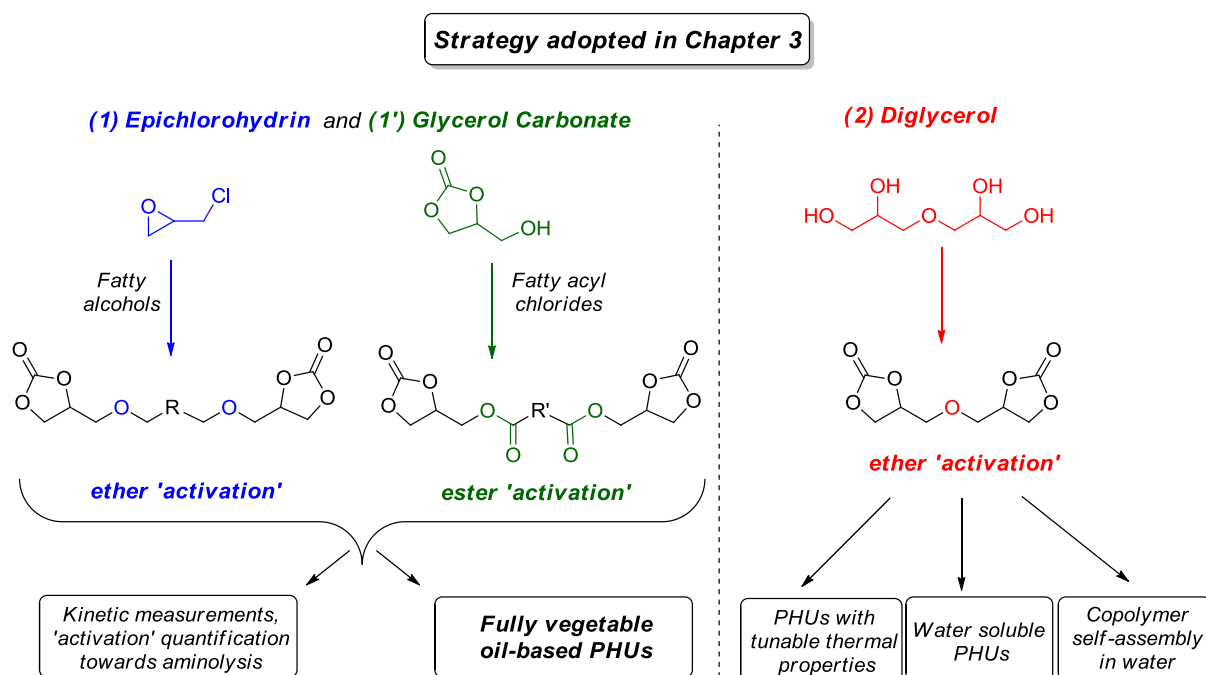
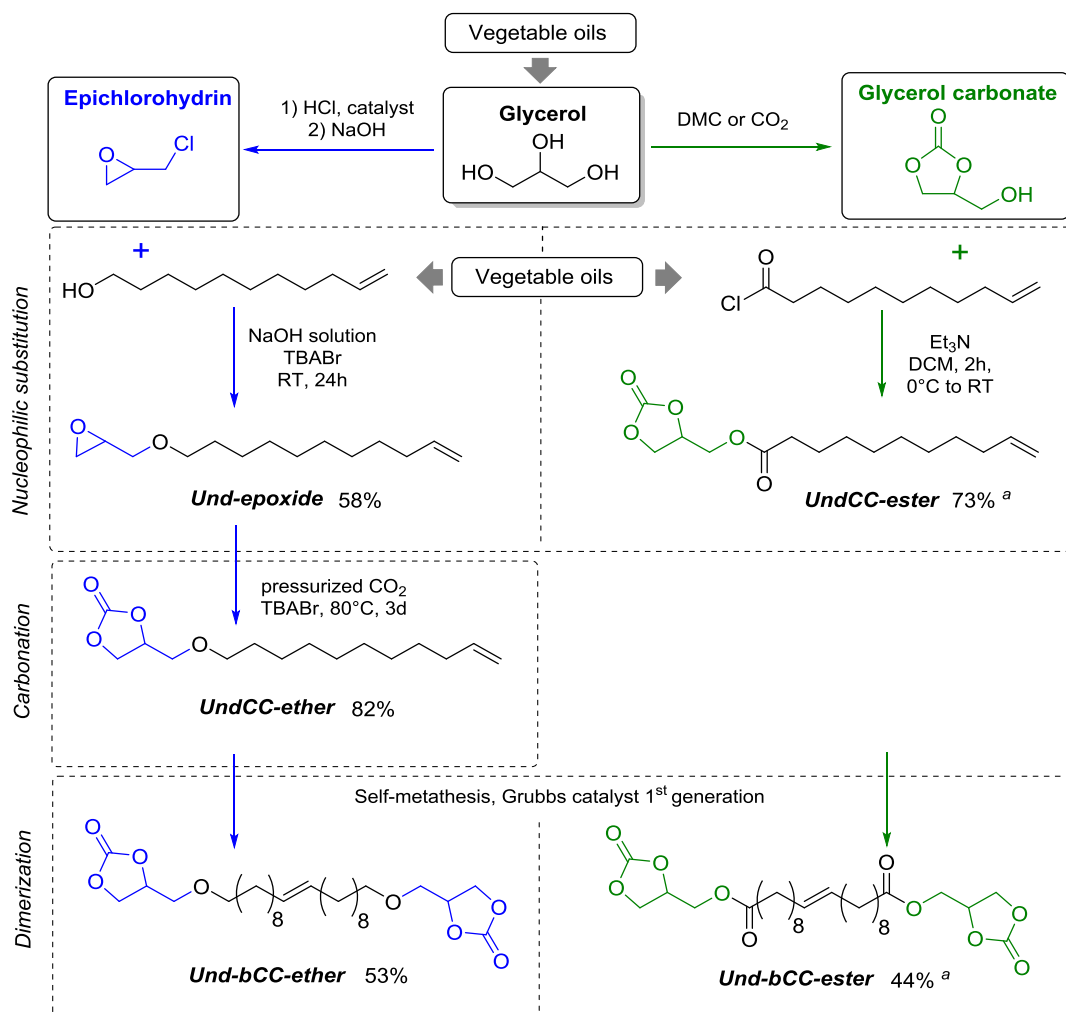


Figure 1 – Strategy adopted in the Chapter 3 for the synthesis of ether- and ester-activated cyclic carbonates from fatty acids and glycerol derivatives.

1. Activated fatty acid-based cyclic carbonates towards PHUs

1.1. Synthesis of activated lipidic cyclic carbonates.

Activated 5-membered cyclic carbonates were prepared from glycerol and fatty acid derivatives. Ester and ether moieties were introduced in β position to the cyclic carbonate, in order to enhance its reactivity towards amines. As illustrated in Scheme 1, ether- and ester-activated lipidic bis-cyclic carbonates were synthesized using respectively a three-step and a two-step procedure starting respectively from epichlorohydrin and glycerol carbonate. Their detailed syntheses are described in the next parts.



Scheme 1- Synthetic routes to activated lipidic bis-cyclic carbonates Und-bCC-ether (left) and Und-bCC-ester (right) with isolated yields. ^a The yield can be dramatically increased by subsequent reconcentration of the recrystallisation filtrate and further recrystallization.

1.1.1. Ether-activated monomers from epichlorohydrin

Lipidic cyclic carbonates with an ether moiety in β position of the carbonate ring could be easily obtained using epichlorohydrin as reagent, which can be produced by chlorination of glycerol.³² This “epichlorohydrin strategy” has already been adopted by several research groups for the synthesis of cyclic carbonates.^{26,27,29,33,34} As illustrated in Scheme 1, the synthesis of **Und-bCC-ether** from epichlorohydrin involved three steps (i) the nucleophilic substitution of the epichlorohydrin with 10-undecen-1-ol (ii) the carbonation of the resulting epoxide and finally (iii) the dimerization by metathesis reaction. The chemical structure of the resulting bis-cyclic carbonate as well as the different intermediates, were assessed by NMR spectroscopy and FTIR (see Figure 2). The **Und-epoxide** was synthesized for 24h at room temperature from 1eq. of 10-undecen-1-ol, using 10 eq. of epichlorohydrin, 15 eq. of NaOH via a 50 w.% solution and 0.1 eq. of TBABr as transfer agent. The conversion reached 72%

and no side reactions were observed in these conditions. After extraction with ethyl acetate, the product was purified by flash chromatography (58% yield). The carbonation of the *Und-epoxide* was performed in an autoclave during 3 days at 80°C, at 40 bars of pressurized CO₂ using 3 w.% TBABr as catalyst to reach full conversion. *UndCC-ether* was obtained as viscous transparent oil after flash chromatography (82% yield).

The monofunctional *UndCC-ether* was then “dimerized” *via* metathesis reaction of the terminal double bond. The reaction was processed at room temperature in dichloromethane under inert atmosphere using 0.5 mol.% of 1st generation Grubbs metathesis catalyst for the coupling. A conversion of 99% was achieved after 3 days as estimated by NMR spectroscopy. The *Und-bCC-ether* was obtained as a clear grey powder with a yield of 53% after flash chromatography (eluent: cyclohexane/ethyl acetate).

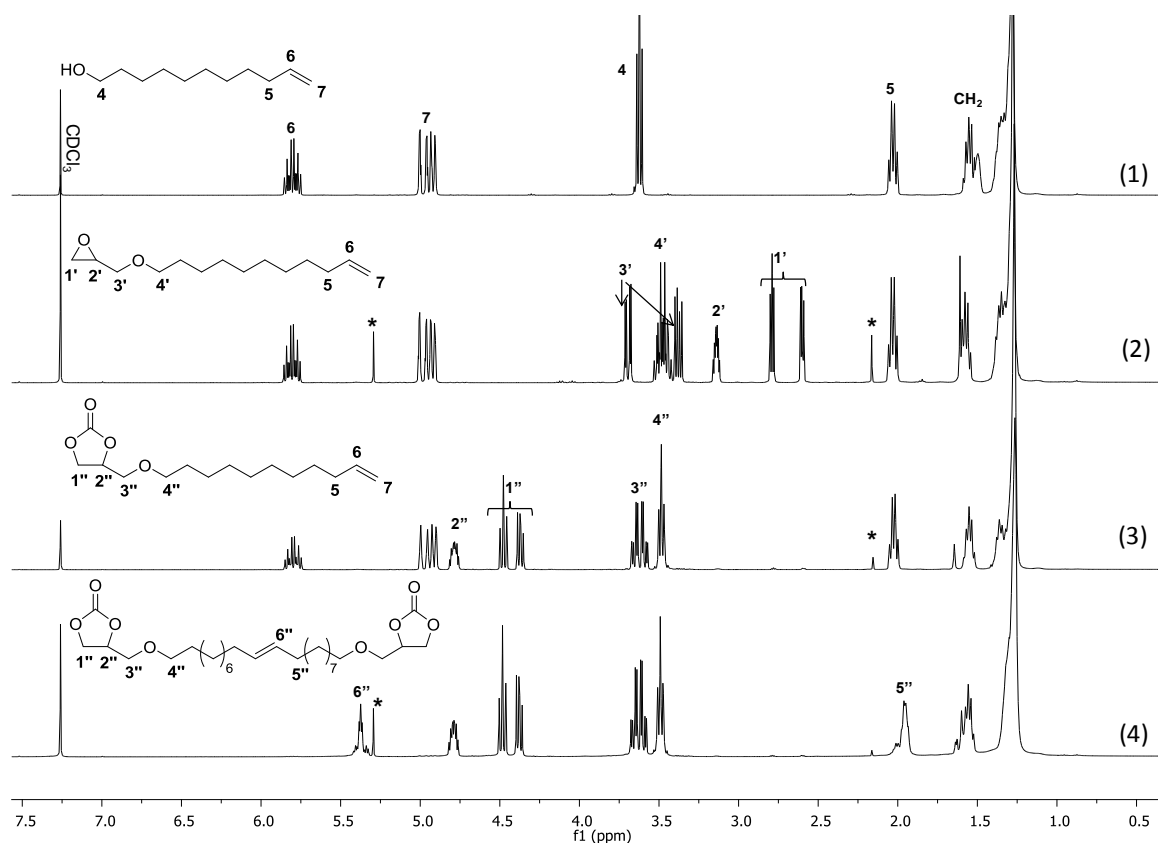


Figure 2 - Stacked ¹H NMR spectra of (1) 10-undecen-1-ol, (2) Und-epoxide, (3) UndCC-ether and (4) Und-bCC-ether (All analyses were performed in CDCl₃,) (*: residual solvents)

The shorter bCC, *Seb-epoxide*, was synthesized using harsher conditions (see ESI) for which side reactions, like oligomerization, were detected by ¹H NMR. Thus, the optimized conditions were the ones used for the synthesis of *Und-epoxide*. The carbonation conditions were similar and enabled the preparation of *Seb-bCC-ether* (see ESI). In this case, no

dimerization reaction was necessary as the starting material 1,10-decanediol was already bifunctional. *Seb-bCC-ether* was purified by flash chromatography and obtained as a pure white solid (99% purity by GC) with 47% yield.

1.1.2. Ester-activated monomers from glycerol carbonate

A second route to activated cyclic carbonates is based on the glycerol carbonate as building block that has been frequently employed to introduce the cyclic carbonate functionality onto different structures.^{17, 35–38} In this case, bis-cyclic carbonates activated by an ester moiety in β position of the cycle were obtained by esterification between fatty acid chloride from undecenoic acid and glycerol carbonate (see Scheme 1). The synthesis was scalable and ITERG could provide us 20 g-batches of *UndCC-ester* for a further dimerization by metathesis. *UndCC-ester* was first purified by recrystallization in heptane and obtained in 73% yield. The dimerization was successfully achieved with the same reaction conditions than for *Und-bCC-ether* synthesis. *Und-bCC-ester* was recrystallized in cold DCM (-20°C) and obtained as a grey powder with a yield of 44%. The ¹H NMR spectrum of the purified activated bCC is presented in Figure 3.

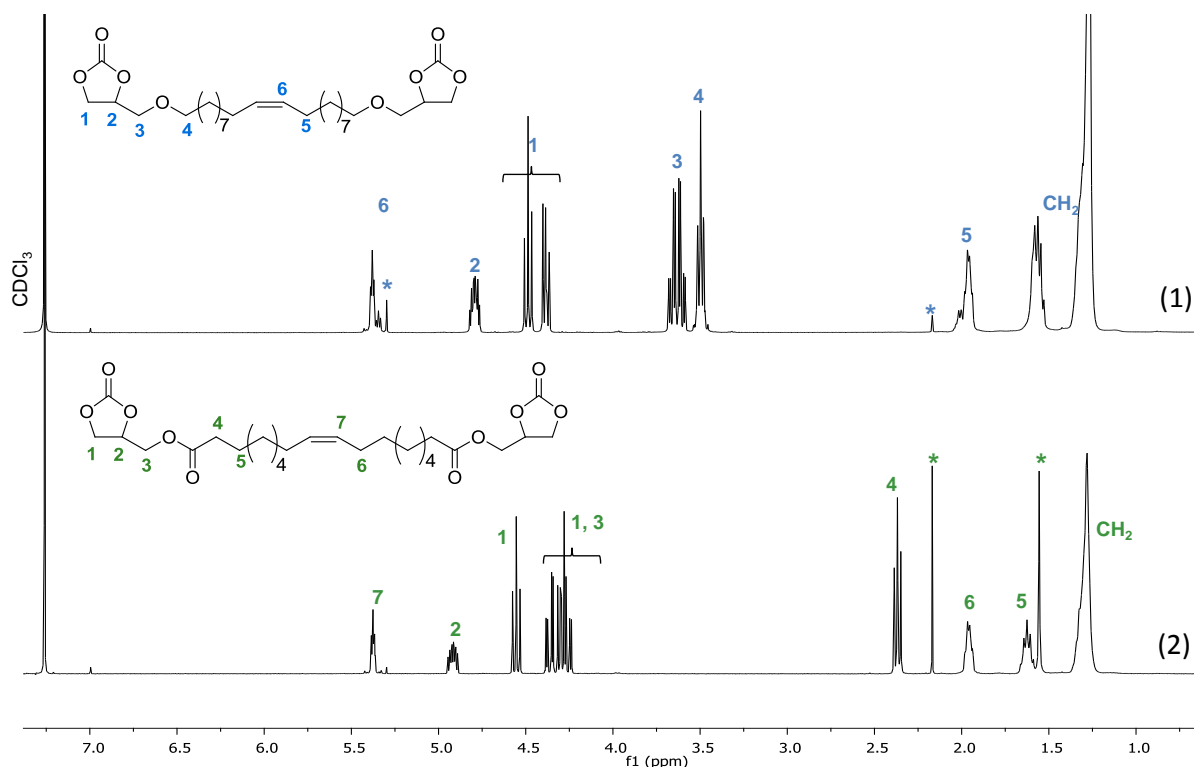


Figure 3 – Stacked ¹H NMR spectra of (1) Und-bCC-ether and (2) Und-bCC-ester in CDCl₃. (*: residual solvents)

It should be mentioned that this molecule was synthesized by Bigot *et al.*³⁹ who used glycidol and undecenoic acid as starting materials.

Similar synthesis was performed on sebacoyl chloride to achieve in one step, the corresponding activated C₁₀-bCC *Seb-bCC-ester* that was obtained as a white powder with 47% yield after flash chromatography (see ESI).

1.1.3. Comparison between the two routes

Both pathways lead to interesting cyclic carbonate structures but require to be compared in terms of starting materials, chemical transformations and properties.

Both starting materials are derived from the saponification of triglycerides. The “ester route” utilizes straightly the acid moiety present on fatty acids to perform the acyl chloride synthesis. However, the “ether route” requires the use of fatty acid-based alcohols obtained after fatty acid reduction, leading to an additional step on the raw material.

Regarding the cyclic carbonate synthesis from the above-mentioned starting materials, the two routes imply both 3 steps if the synthesis of acid chloride is taken into account for the “ester route”. From a “Green Chemistry” point of view, the atom economy is identical from one route to another, as HCl and ethylene were produced from the two syntheses. Nonetheless, the syntheses of *Seb-bCC-ester* and *Seb-bCC-ether* were conducted in two steps from the bifunctional sebacic acid and sebacoyl chloride respectively and don't require the dimerization by metathesis contrarily to *Und-bCC-ester* and *Und-bCC-ether*.

Besides, the monomers result from green processes such as the carbonation of epoxides and glycerol with CO₂ or the metathesis reaction which are performed in mild and catalytic conditions.⁴⁰

Focusing now on the ‘epichlorohydrin route’, the inherent toxicity of this compound stands in contradiction with the production of isocyanate-free polyurethanes, which avoids the use of toxic phosgene. Nevertheless, the nucleophilic substitution between alcohols and epichlorohydrin has been extensively studied for bringing an ether moiety nearby the cyclic carbonate in mild conditions.^{26,27,29,33,34} On the other hand, the glycerol carbonate route finds its limitation in the use of the reactive and corrosive thionyl chloride, especially in industrial processes.

With regard to the use of solvent, the “ether route” displays the advantage of employing epichlorohydrin as a reactive solvent whereas the “ester route” uses the hazardous DCM for

Und-CC-ester synthesis. Contrarily, the cyclic carbonates from the “ester route” can be purified by recrystallization that is less solvent-consuming than the flash chromatography employed in the “ether route”.

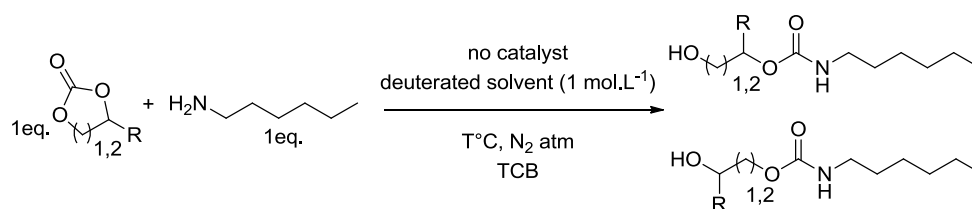
Focusing now on the monomer properties, all of the synthesized bCC were solid powders with melting temperatures ranging from 54 to 111°C. Ester-containing carbonates exhibited the highest melting temperatures due to the less flexible architecture imparted by the ester function. Considering that, the bulk-polymerization of the above-mentioned monomers cannot be performed at moderate temperatures. Besides, the monomers obtained from a metathesis reaction displays a slight grey coloration conveyed by the residue of Grubbs catalyst used in such synthesis.

1.2. Kinetic measurements and reactivity comparison

In order to quantify the difference in reactivity between classical 5-membered cyclic carbonates and the synthesized activated cyclic carbonates, kinetic experiments were monitored *in situ* by ¹H NMR spectroscopy. Several monocyclic carbonates such as TMC (trimethylene carbonate), *UndCC-ester*, *UndCC-ether*, *Und-6CC* (5-(non-8-en-1-yl)-1,3-dioxan-2-one), *OleylCC-ester*, *OleylCC-ether*, *Oleyl-6CC* and *Dec-5CC* (carbonated 1-decene) were reacted with hexylamine at 50°C in DMSO-d₆ at 1 mol.L⁻¹, with trichlorobenzene (TCB) as internal reference (see Scheme 2). Some experiments were performed at various temperatures (25-70°C) and in different solvents (benzene-d₆, chloroform-d and ethanol-d₆) to examine their influence on the kinetic of the model reaction. The cyclic carbonate conversion was followed *in situ* by ¹H NMR for 24h thanks to the disappearance of the CC protons between 4.2 and 5.1 ppm and the appearance of the protons in alpha of the urethane function at 2.9 ppm (see Figure 4). The syntheses of mono-cyclic carbonates are reported in ESI.

Using a similar procedure, the catalyst-free model reaction between 10-undecen-1-ol and hexyl isocyanate was conducted in order to compare the kinetic of the addition between alcohols and isocyanates with the aminolysis of cyclic carbonates.

It is noteworthy to mention that the model reactions were performed in a NMR tube where the diffusion of active species is limited in comparison to the classical reactions under stirring. The kinetic profiles were consequently not completely representative of the reality.



Scheme 2- Model reaction of various cyclic carbonates with hexylamine in different conditions.

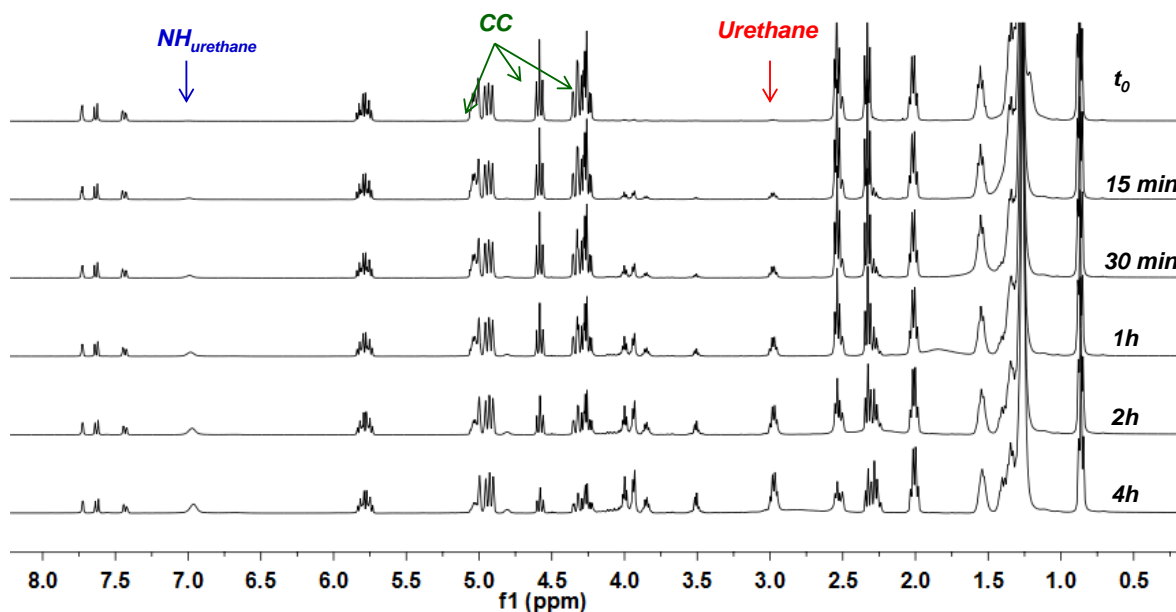


Figure 4 - Stacked ^1H NMR spectra of the reaction between UndCC-ester and hexylamine with a ratio 1:1, at 50°C in DMSO-d_6 at 1 mol.L^{-1} .

1.2.1. Comparison between activations

According to the literature, conversions of cyclic carbonates followed a second order kinetic law until 50-60% of conversion. Then, the kinetics of the reaction slowed down and the conversion ultimately reached a plateau. This feature can be attributed to several parameters such as the limited diffusion occurring in the NMR tube, the hydroxyurethane solubility or the high amount of hydrogen-bonding due to the produced hydroxyl groups, hindering the reaction.

As the reaction between cyclic carbonate and amine follows a second order kinetic law, the apparent reaction rate constants (k_{app}) were calculated upon the 6 first hours of reaction with the formula described in Equation 1. All the results are summarized in Table 2.

$$\frac{x}{1-x} = k_{app} C_0 \Delta t$$

Equation 1 - 2nd order kinetic law formula: Time-(x/(1-x))

The *UndCC-ester* and *UndCC-ether* were compared to the reactive 6-membered ring cyclic carbonates TMC and *Und-6CC* from methyl undecenoate. A purely aliphatic 5-membered ring cyclic carbonate (*Dec-5CC*) was also synthesized from 1,2-epoxydodecane and CO₂ in order to obtain a low benchmark and to see the effect of an hetero-atom insertion within the aliphatic chain, on the reactivity of a 5CC. *Dec-5CC* exhibited the lowest reactivity in terms of aminolysis with hexylamine, as it is depicted in Figure 5.

The enhancement of 5CC reactivity has already been described in the literature^{12,13,19–30} and was attributed to the negative inductive effect of the ester and ether groups in β position of the cycle moiety, explaining the highest conversions obtained for *UndCC-ether* and *UndCC-ester*. The latest displayed a similar reactivity to the lipidic *Und-6CC* and followed the same kinetic tendency as TMC (see Figure 5). Upon the six first hours at 50°C, k_{app} (*UndCC-ester*) was equal to 0.44 L.mol⁻¹.h⁻¹ and comparable to k_{app} (TMC) = 0.55 L.mol⁻¹.h⁻¹. On the other hand, *UndCC-ether* kinetic profile clearly demonstrates a lower reactivity than *UndCC-ester*. This feature could be assigned to the lower negative inductive effect and the higher positive mesomeric effect of the oxygen atom, stabilizing the cycle and decreasing its subsequent reactivity. From a kinetic point of view, DFT calculations in Table 1 highlight the longer bond length and the ensuing enhanced reactivity towards ring-opening, when an ester moiety is placed nearby the cycle (see entry **3**, Table 1). The increase of the bond length correlates with the minimized mesomeric effect in the case of the ester activation. Thermodynamically speaking, the ester moiety exhibits a higher enthalpy of urethane formation, confirming the better carbonate activation.

Meanwhile, the kinetic of the model reaction between 10-undecen-1-ol and hexyl isocyanate was plotted (see Figure 5, orange dotted curve) and compared to the activated 5CC and hexylamine one. Surprisingly, the kinetic of the alcohol/isocyanate addition was slower than the ones obtained during aminolysis of activated cyclic carbonates. Nonetheless, the alcohol/isocyanate addition remains the most viable route to PUs in terms of kinetic, as selective catalysts were found and used to increase dramatically the reaction rate of the urethane formation. Moreover, aromatic isocyanates are known to exhibit high activity and are commonly used for room temperature ‘Do-It-Yourself’ applications.

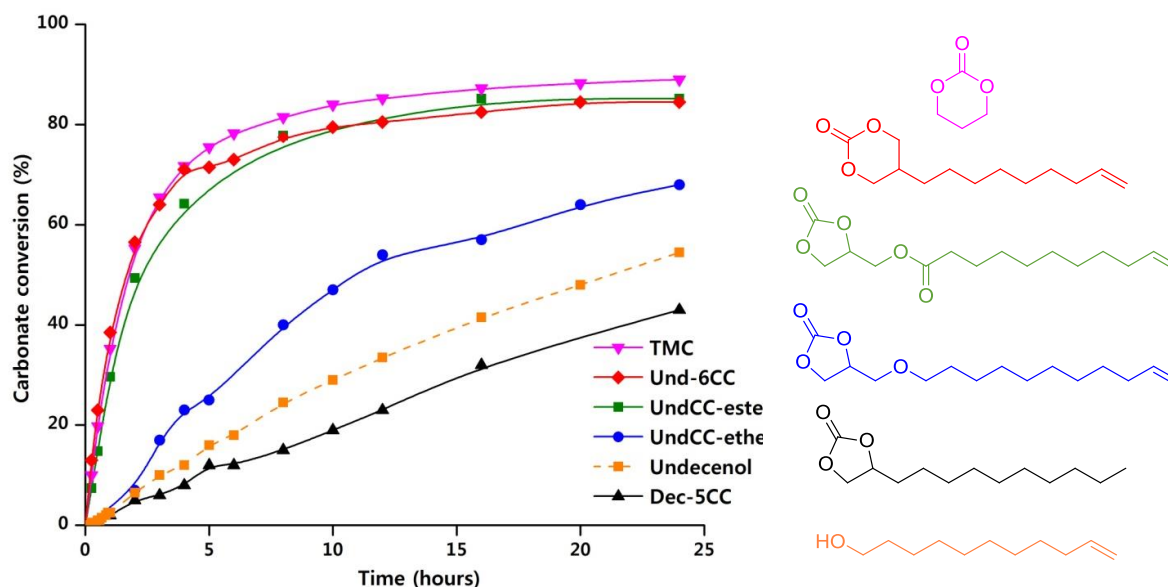


Figure 5 - Effect of various cyclic carbonates activations on the kinetic of the reactions with hexylamine followed by ^1H NMR over 24h (50°C , 1 mol.L^{-1} in DMSO-d_6 , ratio 1:1); and comparison with the alcohol/isocyanate addition.

Table 1- Length of cyclic carbonate bonds and urethane formation enthalpies for different cyclic carbonate substituents $-\text{X}$ calculated by DFT (see Materials and Methods).

Entry	$-\text{X}$	Bond length (\AA)	Bond length (\AA)	ΔH_f (kJ.mol^{-1})	ΔH_f (kJ.mol^{-1})
1	$-\text{CH}_3$	1.358	1.361	-14.91	-36.33
2	$-\text{OMe}$	1.358	1.363	-27.36	-55.90
3	$-\text{OC(O)Me}$	1.361	1.363	-57.96	-62.83

1.2.2. Impact of different parameters influencing the kinetics

Several parameters impacting the kinetics such as the chain length, the solvent or the temperature have been studied for a better understanding of the model reaction between cyclic carbonates and amines.

Firstly, the chain length effect has been investigated in model reaction. For that purpose, *OleylCC-ester*, *OleylCC-ether* and *Oleyl-6CC* were synthesized from methyl oleate derivatives. No significant influence of the chain length was observed on *Und-6CC* and *Oleyl-6CC* when kinetic experiments were carried out. Nevertheless, activated 5CC were impacted by the number of carbons of the aliphatic chain. As an example, *OleylCC-ether*

exhibited 51% conversion after 24h instead of 68% for the corresponding C₁₁-synthon *UndCC-ether* (see Figure 6). These results could be due to the lower solubility and of C₁₈-compounds in DMSO-d₆, imparted by their longer aliphatic chain. The concentration in active species was subsequently reduced and the reaction kinetic was consequently slower. Corresponding k_{app} were calculated upon the six first hours of reaction (Table 2) and confirmed the observed tendency.

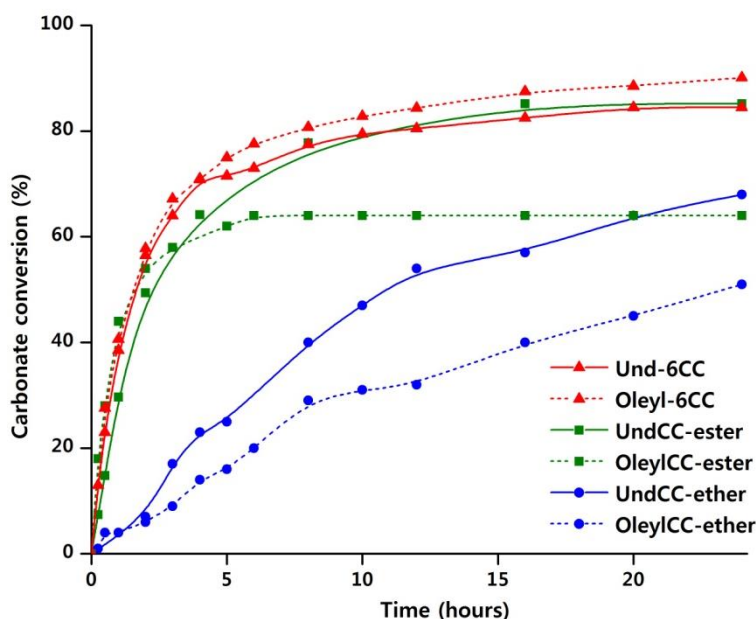


Figure 6 - Chain length effect on the kinetic of the reactions between reactive cyclic carbonates and hexylamine (1 mol.L⁻¹ in DMSO-d₆, ratio 1:1, 50°C)

Model reactions on *UndCC-ester* were then monitored at 25°C and 70°C with regard to see the impact of the temperature on the ring opening kinetic of the cyclic carbonate. In order to estimate the reaction rate constants (k_{app}), $x/(1-x)$ was plotted as a function of time (see Figure 7). The second order kinetic law was verified upon the 6 first hours and the reaction rate constants were 0.15, 0.44 and 0.80 L.mol⁻¹.h⁻¹ at 25, 50 and 70°C respectively (see Table 2).

From the Arrhenius plot, the activation energy of this monocyclic carbonate could be estimated at 27 kJ.mol⁻¹ (see ESI). In the literature, Endo and coll.¹³ reported activation energies of 10.1 and 24.6 kJ.mol⁻¹ for 5CC and 6CC respectively. Additionally, Maisonneuve *et al.*¹⁸ calculated from the Arrhenius plot an activation energy of 21 kJ.mol⁻¹ for *Und-6CC*, which supports its similar reactivity with *UndCC-ester*.

Table 2 - Reaction rate constants obtained for the different model reactions between cyclic carbonates and hexylamine (ratio 1:1) in DMSO-d6 (1mol.L⁻¹)

Cyclic carbonate (CC)	Temperature (°C)	k _{app} (L.mol ⁻¹ .h ⁻¹) ^a
<i>TMC</i>	50	0.58
<i>Und-6CC</i>	50	0.44
<i>UndCC-ester</i>	25	0.15
	50	0.44
	70	0.80
<i>UndCC-ether</i>	50	0.09
<i>Dec-5CC</i>	50	0.03
<i>Oleyl-6CC</i>	50	0.58
<i>OleylCC-ester</i>	50	0.65 [0-1]h
		0.15 [1-6]h
<i>OleylCC-ether</i>	50	0.04

^a: Calculated upon the 6 first hours of the kinetics performed in NMR, from a second order kinetic law. (Equation 1)

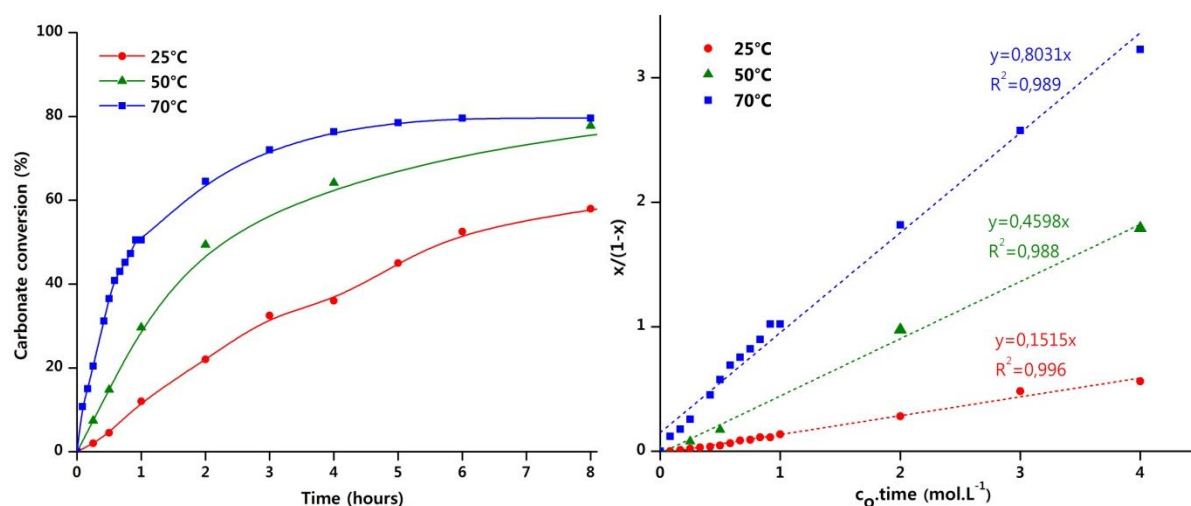


Figure 7- Effect of the temperature on the kinetic of the reactions between UndCC-ester and hexylamine (1 mol.L⁻¹ in DMSO-d6, ratio 1:1).

Finally, the impact of four different deuterated solvents on conversions and kinetic behaviours was investigated on the model reaction between *UndCC-ester* and hexylamine at 25°C, to prevent solvent evaporation inside the NMR apparatus. Benzene-d6, chloroform-d, DMSO-d6 and ethanol-d6 were chosen to represent a range of non-polar, polar, aprotic and protic solvents. DMSO-d6 was used in the previous kinetic experiments, as DMF was the selected solvent for polymerization (see part 1.3) and exhibited close properties to DMSO. Chloroform-d gave interesting results in terms of conversion but could not be used in polymerization as the lipidic cyclic carbonates were not always soluble in this polar solvent. Concerning benzene-d6, the curve presented in Figure 8 demonstrated a higher reactivity at

the beginning of the reaction than with DMSO-d₆. However, the conversion did not reach 60% after 8h of reaction. This statement could be related to the inability of benzene-d₆ to solubilize the produced hydroxyurethanes. In contrast, ethanol-d₆ pushed the conversion up to 100% in 5h instead of 55% in DMSO-d₆ and the k_{app} in ethanol-d₆ (2.89 L.mol⁻¹.h⁻¹) was 20 times higher than in DMSO-d₆ (0.1754 L.mol⁻¹.h⁻¹) (see the plot $x/(1-x)=f(t)$ in Figure 8). The latest behaviour was attributed to the shielding of hydrogen bonding between hydroxyurethanes that could be provided by such polar and protic solvent. Indeed, it has been shown by Garipov *et al.*⁴¹ that a protic solvent could increase the electrophilicity of the cyclic carbonate, by hydrogen bonding between the carbonyl and the solvent, favoring the amine attack. Webster *et al.*⁴² also reviewed that the reaction rates were higher in protic solvents than in aprotic ones.

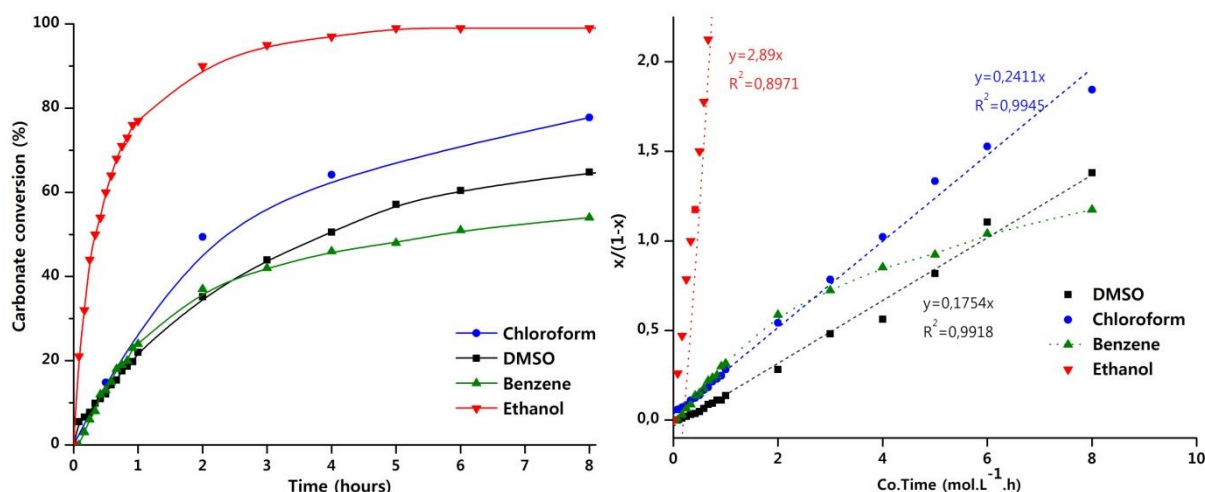
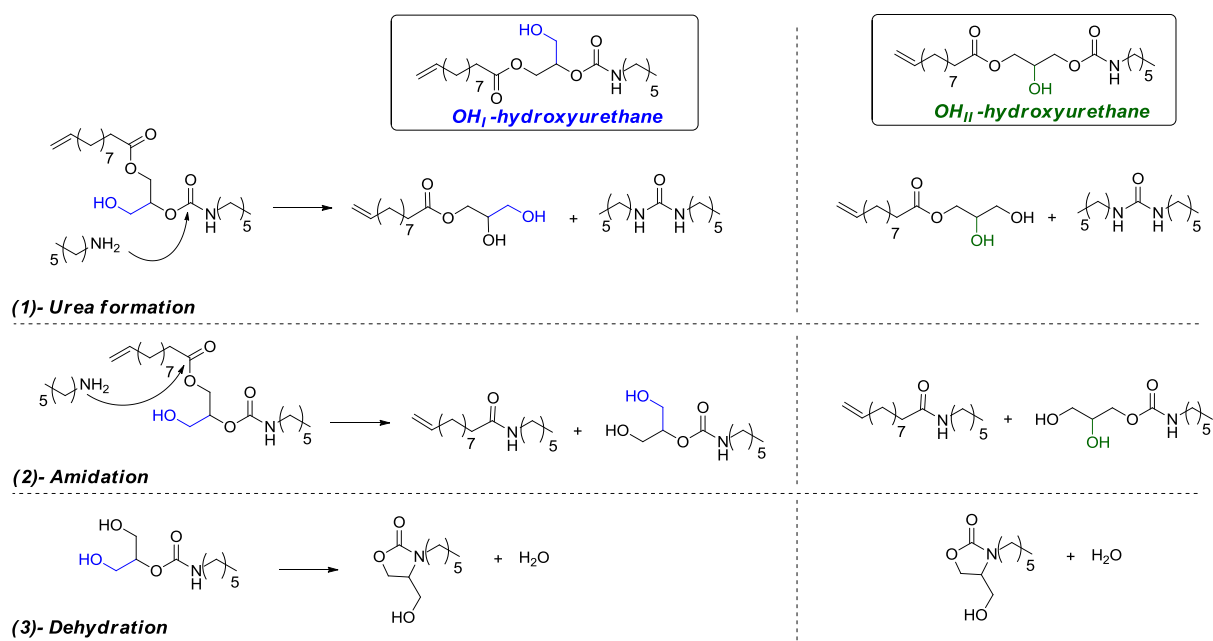


Figure 8 - Effect of the solvent on the kinetic of the reaction between UndCC-ester and hexylamine (1 mol.L⁻¹ in deuterated solvents, 25°C, ratio 1:1)

1.2.3. Side reactions, by-products and selectivity

In addition to the analysis of carbonate consumption, these kinetics experiments allow us to investigate the side reactions during the aminolysis of cyclic carbonate (see Scheme 3). The ¹H NMR proton of the *UndCC-ester* reaction with hexylamine is presented in Figure 3. The urethane signals appearance at 2.98 ppm as well as the progressive disappearance of protons characterizing the cyclic carbonate (5.06, 4.63 and 4.32 ppm) confirmed the hydroxyurethane formation. The major products from the model reaction were fully characterized using 1D and 2D NMR spectroscopy (see Figure 9 and ESI) and the ratio between primary and secondary alcohols could easily be calculated by integration of protons **2'** and **2''** respectively (see Figure 9). Nevertheless, by-products were also obtained during the model reaction between

hexylamine and *UndCC-ester*. As it has already been described in prior studies, primary amines can react with urethane functions to form ureas.^{9,43,44} HSQC, HMBC and TOCSY NMR analyses proved the presence of urea functions in the mixture, thanks to the attribution of correlated CH-OH (4.9 ppm) and CH₂-OH (4.05-4.15 ppm), characterizing the diol obtained during the formation of urea (Scheme 3-(1)). Its existence was also confirmed by ESI analysis (see ESI†), as Caillol and coll.⁴⁴ have recently done in a complete study about side reactions occurring during PHUs synthesis. A slight amount of oxazolidinones (Scheme 3-(3)) resulting from the dehydration of hydroxyurethanes was also detected by ESI analysis. Besides, it is also known that an ester function is prone to side reactions with primary amines (see Scheme 3-(2)).⁹ In our case, a few percentage of amidation was highlighted using ¹H NMR analysis, thanks to the distinctive labile proton of the amide at 7.6 ppm. Moreover, ¹³C NMR analysis (see ESI) could confirm the presence of the typical O=C-NH carbon at 171.7 ppm. Percentages of major side reactions were calculated using specific labile H of urea (6.7 ppm), urethane (6.9 ppm) and amide (7.6 ppm) functions (see ESI). The results are shown in the Table 3 for *UndCC-ester* and *UndCC-ether* at 50% of conversion in cyclic carbonates.



Scheme 3 – Proposed side reactions on UndCC-ester-based primary and secondary hydroxyurethanes: (1) urea formation, (2) amidation and (3) dehydration.

Urea and amides were formed in relatively low proportions, as by-product percentages were not above 5% when 50% conversion in cyclic carbonates were reached, for all tested conditions. In the case of *UndCC-ester*, amidation reaction could be prevented by decreasing the temperature to 25°C. Still at 65% conversion after 24h at 25°C, amide functions were not

produced. However, urea formation appeared to be independent of the temperature and exhibited the same proportions at 25°C and 50°C.

Table 3 - Proportions of products and by-products during the model reaction of UndCC-ester and UndCC-ether with hexylamine at 50% conversion in cyclic carbonates.

Proportions (%)	UndCC-ester			UndCC-ether	Dec-5CC
	25°C	50°C	70°C	50°C	50°C
Urea ¹	2,8	2,7	nd*	2.9	4
Amide ¹	0	2,1	nd*	0	0
Urethane ¹	97.2	95.2	nd*	97.1	96
Ratio OH _I :OH _{II}	18 : 82	23 : 77	23:77	28 : 72	60:40

*Calculation of proportions impossible due to overlapping of chemical shifts; ¹:Proportions calculated with the Equations in ESI.

For the two activated mono-cyclic carbonates, the isomer ratio OH_I:OH_{II} was found to be in accordance with the DFT calculations (see Table 1) and with the literature, which has reported a clear trend for the formation of secondary hydroxyl groups during the ring-opening of cyclic carbonates by amines.²¹ However, the pure aliphatic 5CC exhibited 60% of primary alcohols and this trend has already been observed by Maisonneuve *et al.*¹¹ in a prior study (50%:50%). Additionally, lowering the temperature from 50°C to 25°C could lead to the slight increase of produced secondary hydroxyl groups.

Unfortunately, the impact of the solvent on by-products could not be evaluated. Indeed, the labile proton NMR shifts were not identified because of proton exchange between the molecules and the solvent in the case of EtOH-d₆. In chloroform-d and benzene-d₆, labile protons were not visible. Unfortunately, the impact of the solvent on the selectivity could not be determined because of ¹H NMR signal overlaps in the selected deuterated solvents.

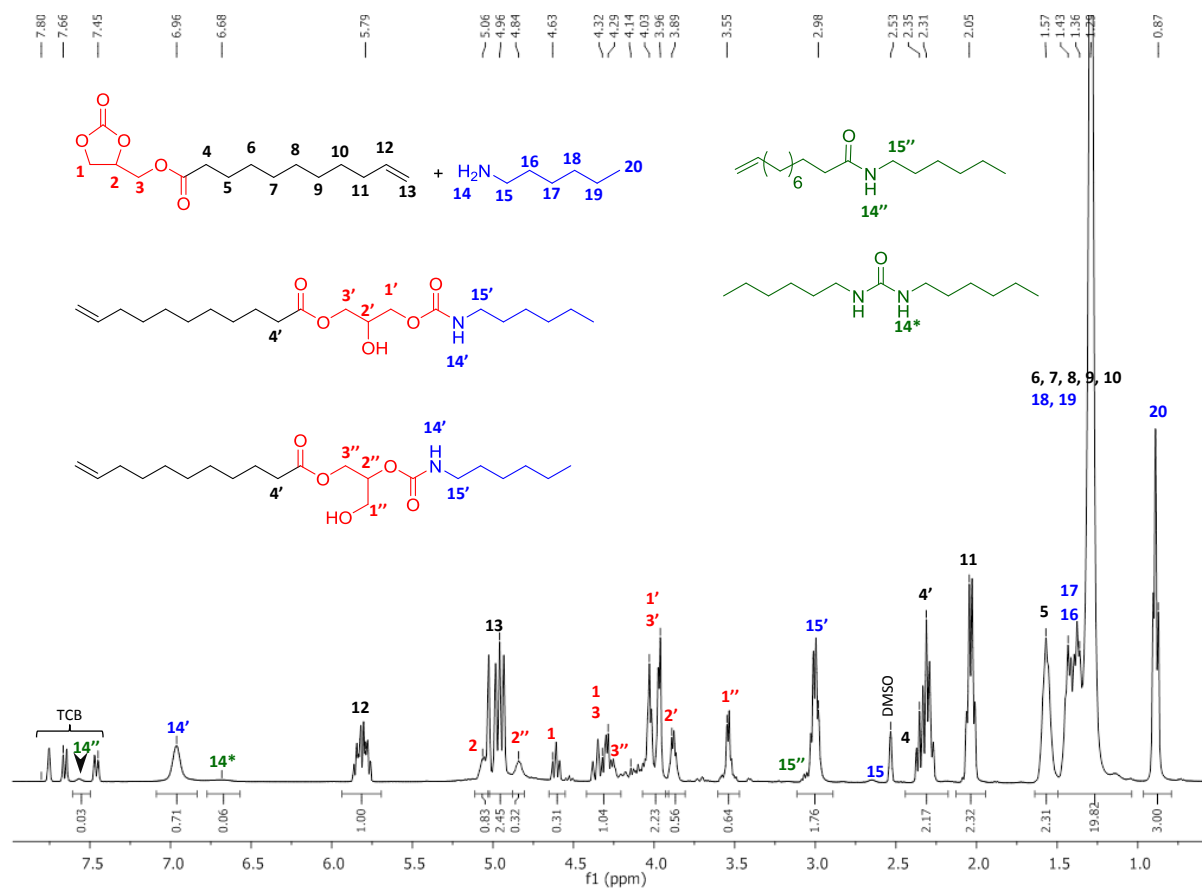


Figure 9 - ^1H NMR of the model reaction between UndCC-ester and hexylamine in DMSO- d_6 at 1 mol.L^{-1} at 50°C after 2 days.

1.3. Poly(hydroxyurethane)s synthesis

After the kinetic experiments, ether- and ester- activated 5-membered cyclic carbonates were tested in polymerization. PHUs were synthesized from *Und-bCC-ether*, *Und-bCC-ester*, *Seb-bCC-ether*, *Seb-bCC-ester* and *b5CC* with 1,6-diaminohexane (6DA), 1,10-diaminododecane (10DA), *Und-C20-diamine* (20DA, see chapter 2 for the synthesis), N,N'-methylhexylamine (m-6DA) and 1,3-cyclohexanebis(methylamine) (6cDA) as comonomers, in order to study the impact of the monomer structures on PHU properties. The polymerizations were performed in DMF at 1 mol.L^{-1} at 70°C under nitrogen atmosphere without any catalyst. In agreement with previous NMR kinetic experiments, one polymerization was completed in EtOH (1 mol.L^{-1}) at 70°C under ambient atmosphere in order to evaluate the impact of a protic and polar solvent on PHU conversion and molar mass.

Bulk polymerizations could not be achieved due to the high melting point of monomers. Besides, the temperature used was explained by the monomer solubility issues in DMF at room temperature. Afterwards, the polymers were characterized without prior quenching and precipitation after 7 days. PHUs formation was followed by ^1H NMR with the disappearance

of the signals in α -position nearby the cycle in the ranges 4.2-4.6 ppm and the presence of the characteristic protons $\text{CH}_2\text{-NHC(O)O}$ at 2.98 ppm. The PHU formation was confirmed by FTIR (see Figure 10) thanks to the appearance of bands at $1663\text{-}1684\text{ cm}^{-1}$ and $1505\text{-}1545\text{ cm}^{-1}$, attributed to the urethane function. The formation of -NH and -OH groups was verified by the presence of a wide signal between $3600\text{ and }3100\text{ cm}^{-1}$. Table 4 gives the polymerization results in terms of conversion, by-product proportions, ratios between primary and secondary hydroxyl groups, molar masses and thermal properties.

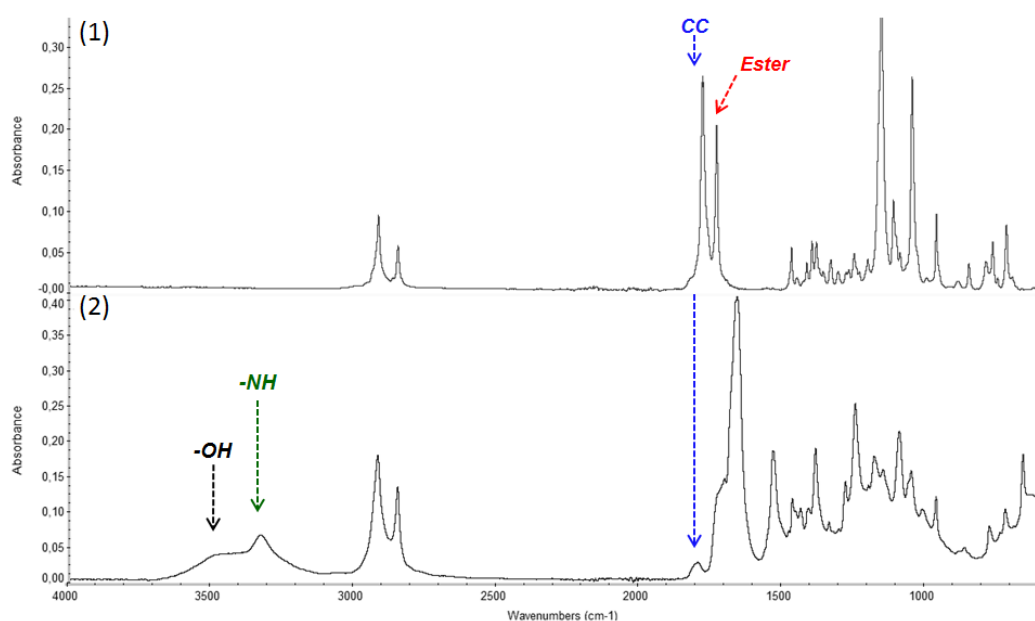


Figure 10 – Stacked FTIR spectra of (1) Und-bCC-ester and (2) PHU 4.

The chemical structures of **PHU 1**, **PHU 2** and **PHU 4** were elucidated thanks to ^1H , ^{13}C and 2D (COSY, HSQC) NMR spectroscopies as illustrated in Figure 11. SEC data given in Table 4 presents molar masses in the range $2500\text{ to }33200\text{ g}\cdot\text{mol}^{-1}$ with dispersities ranging between 1.5 and 3.7, depending on the conditions used. In all cases, more secondary hydroxyl groups were formed during PHU synthesis as it has already been noticed in previous works.^{25,44,45}

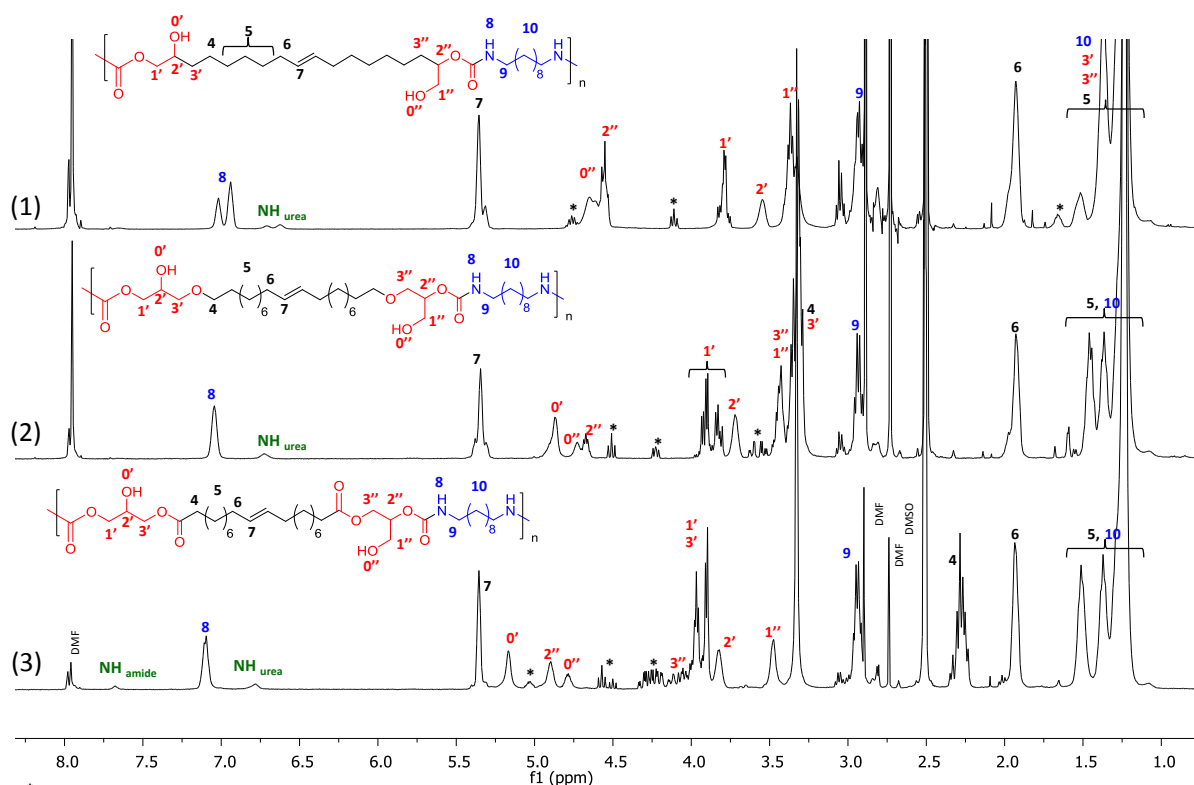


Figure 11 - Stacked ^1H NMR spectra of (1) PHU 1, (2) PHU 2 and (3) PHU 4 in DMSO-d_6 at the end of the polymerizations. (*: residual monomers/chain ends)

As expected, the SEC trace depicted in Figure 12 and the data given in Table 4 highlight the relatively high molar masses obtained for **PHU 2** ($\bar{M}_n=7500 \text{ g}\cdot\text{mol}^{-1}$) and **PHU 4** ($\bar{M}_n=12000 \text{ g}\cdot\text{mol}^{-1}$), using respectively *Und-bCC-ether* and *Und-bCC-ester* as bis-cyclic carbonates, contrarily to **PHU 1** which exhibits a molar mass of $6000 \text{ g}\cdot\text{mol}^{-1}$ when polymerized with 10DA. The latter results corroborate the prior kinetic measurements, i.e. the enhancement of the carbonate reactivity by adding ether or an ester moiety nearby the cyclic carbonate. The **PHU 2** SEC profile located at higher retention time in comparison with **PHU 3** one confirmed the lower reactivity of the ether-activated dimer *Und-bCC-ether*. Additionally, the **PHU 6** resulting from the polymerization between *Und-bCC-ester* and 6DA exhibited a high molar mass of $33500 \text{ g}\cdot\text{mol}^{-1}$ with a dispersity of 2.3. Indeed, as it was discussed in the Chapter 1, 6DA presents a higher reactivity than 10DA towards cyclic carbonates, thanks to its short carbon chain. To the best of our knowledge, here is reported one of the highest PHU molar masses obtained from lipidic-based cyclic carbonates.

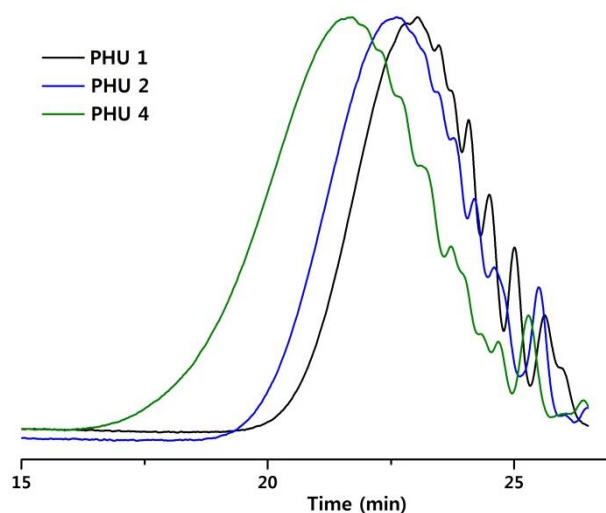


Figure 12 - Size exclusion chromatography of PHU 1, PHU 2 and PHU 4 at the end of the polymerization of respectively b5CC, Und-bCC-ether and Und-bCC-ester with 10DA (DMF, LiBr, PS standards).

However, the formation of urea was observed for all PHUs (see Table 4) and demonstrated the unavoidable side reaction highlighted in the kinetic section. MALDI-TOF analyses support the formation of urea at the chain ends and inside the **PHU 4** backbone (see ESI). Moreover, the amidation reaction, taking place during *Und-bCC-ester* polymerization, was detected with the characteristic labile proton of the amide (7.6 ppm) and by mean of MALDI-TOF analysis. *Und-bCC-ester* showed in polymerization a similar proportion of amide functions than *UndCC-ester* in model reaction. Nonetheless, the more reactive the amine, the higher the presence of amide function: **PHU 6** derived from 6DA contained a relative proportion of 6% of amide groups instead of 2.6% for **PHU 4** from 10DA as comonomer.

The effect of the cyclic-carbonate backbone length on PHU properties was investigated through **PHU 4** and **PHU 11** obtained respectively from a C₂₀ and a C₁₀-ester activated dimer. **PHU 11** synthesized from the shorter *Seb-CC-ester* displayed a molar mass of 13700 g.mol⁻¹ with a dispersity of 3.7 in agreement with its high reactivity. Nonetheless, **PHU 11** demonstrated a higher proportion of 5.9% of amide functions, probably due to the higher density of ester linkages along the polymer backbone. The amidation tended to decrease the molar masses and to increase the dispersity, explained by the cleavage of the polymer chains. The same comparison was made with **PHU 2** and **PHU 10** that were respectively obtained from *Und-bCC-ether* and *Seb-bCC-ether*. In this case, the PHU molar mass was doubled (15000 g.mol⁻¹, Đ=1.68) with the shorter bCC, highlighting its higher reactivity and the advantage of an ether-activation that prevents the amidation side reaction.

Furthermore, when ethanol was used as a solvent for PHU synthesis (**PHU 5**), a complete conversion was reached in 24h as it has already been noticed in the kinetic monitoring part (see part 1.2.2). This statement has not been observed with DMF and could be attributed to

the ability of ethanol to prevent intra- and inter-chain hydrogen bonding, enabling chain-ends to react further. However, the low molar mass obtained ($2500 \text{ g}\cdot\text{mol}^{-1}$) was in contradiction with the full cyclic carbonate conversion. MALDI-TOF analysis of **PHU 5** (see ESI) provided the evidence of the transesterification side reaction occurring between the nucleophilic ethanol and ester functions, resulting in a cleavage of the polymer chains and to a subsequent low molar mass. Nonetheless, when the same experiment was conducted in tertbutanol which is a non-nucleophilic solvent, cyclic carbonate conversion reached 96% in 24h and the resulting PHU exhibited a molar mass of $60000 \text{ g}\cdot\text{mol}^{-1}$ ($\bar{M}_n=1.4$, see ESI). This interesting result highlights the importance of setting the reaction conditions according to the monomer structures.

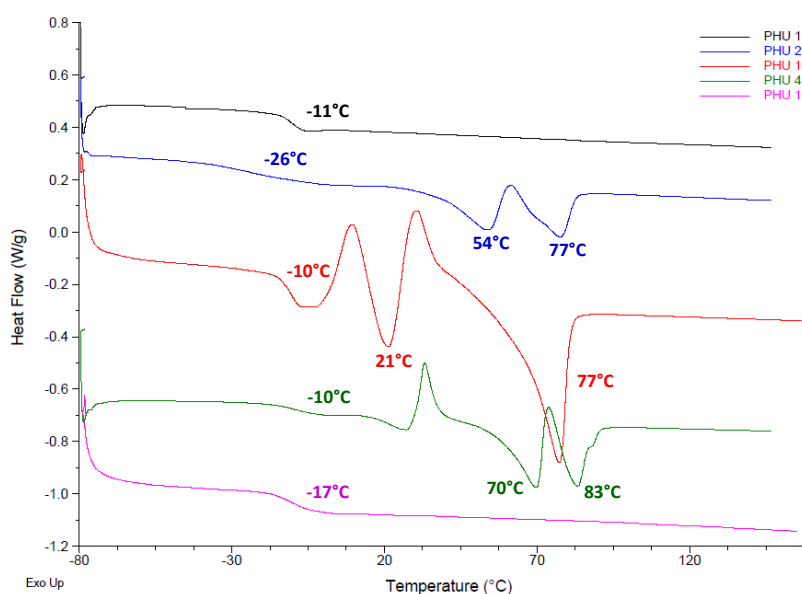


Figure 13 - DSC second heating cycle ($10^\circ\text{C}/\text{min}$) of the synthesized PHU (PHU 1, 2, 4, 10 and 11) to study the influence of the bCC monomer size on thermal properties.

The thermal properties of the prepared PHUs were examined by DSC and TGA, using a prior isothermal procedure at 160°C for 15 min in order to remove DMF traces from the samples. The PHUs were semi-crystalline or amorphous depending on the monomer used. Relatively low T_g in the ranges -32 to 10°C conferred by the aliphatic monomer backbones were obtained. Semi-crystalline **PHU 2**, **PHU 4** and **PHU 10** showed two melting peaks that could reveal two types of crystalline clusters or segregation between soft and hard segments (see Figure 13). Moreover, a cold recrystallization is observed at 33°C for the **PHU 4** and **PHU 10** due to the possible reorganization of the polymer chains above the T_g .

The thermal properties of the synthesized PHUs can be correlated with their chemical structure. For instance, the ether-rotula structure of *Und-bCC-ether* conferred to **PHU 2** a T_g

of -26°C , whereas **PHU 4** displayed a higher T_g imparted with a harder segmented monomer (see Figure 13). In addition, **PHU 11** reached a T_g of -17°C , showing that the T_g was not higher when the number of carbons between the two cyclic carbonate decreased (in comparison to **PHU 4**).

Likewise, the effect of the chemical structures of the amine could be analyzed. It is noteworthy to mention the plastification effect brought by the methyl group of the secondary diamine (m-6DA) on **PHU 7**. This amorphous PHU showed a T_g of -32°C whereas the semi-crystalline **PHU 6** synthesized with the corresponding primary diamine, 6DA, exhibited a T_g of -26°C (see Table 4). Moreover, against all expectations, no enhancement of thermal properties was detected when the cyclic diamine 6cDA⁴⁶ was used as comonomer with *Und-bCC-ester*. This observation has been attributed to the low molar mass obtained for **PHU 8**.

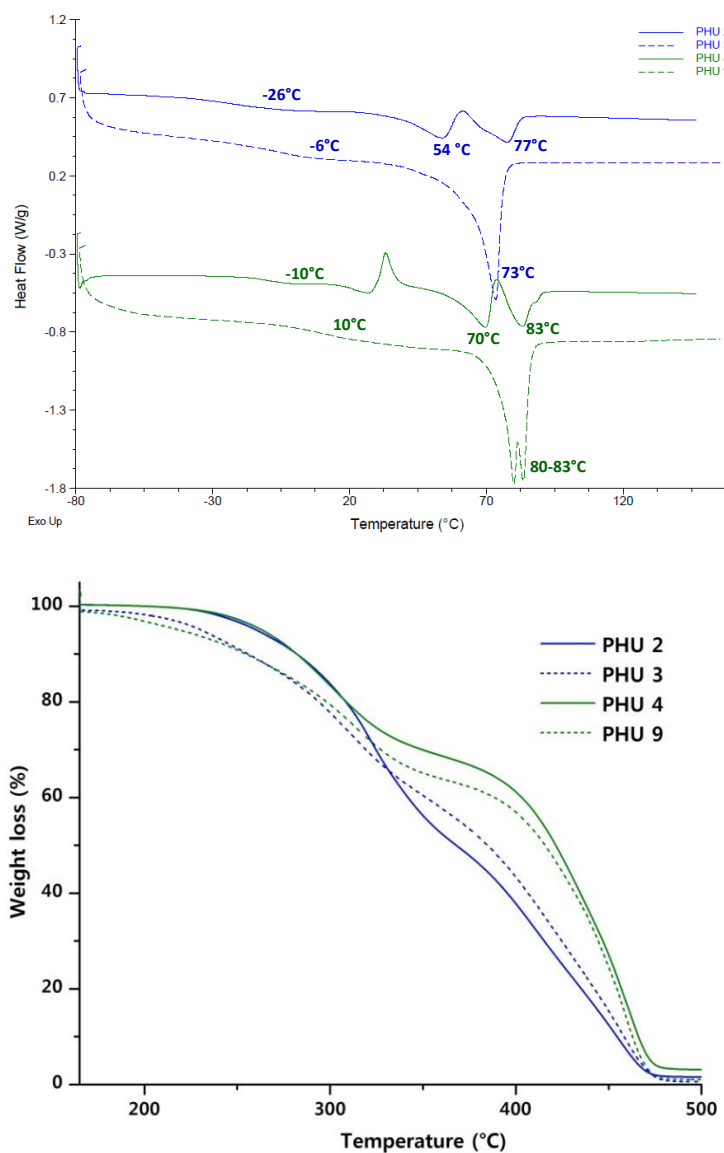


Figure 14 – Second heating cycle ($10^{\circ}\text{C}/\text{min}$) of PHU 2, 3, 4 and 9 and corresponding TGA traces from 160°C (after DMF removal) to 500°C .

Lastly, the effect of the diamine chain length on PHU properties was investigated. Figure 14 illustrates large melting peaks for 20DA-based **PHU 3** and **PHU 9**, demonstrating the important crystallinity provided by 20DA. Indeed, it has been already reported that a crystallinity increase in PE-like polymers leads to a T_g increase.⁴⁷ This statement could justify the T_g value of 20°C, above the ones obtained for 10DA-based **PHU 2** and **PHU 4**. Indeed, lower T_g were obtained for 10DA-based PHU ($T_g = -10^\circ\text{C}$) and for 6D-based PHU ($T_g = -32^\circ\text{C}$).

As a general trend, the thermal degradations at 5 w.% loss were in the range 250-280°C for all PHUs, except for 20DA-based PHUs that showed $T_{d5\%}$ around 230°C.

To conclude this part, reactive cyclic carbonates were synthesized from epichlorohydrin and glycerol carbonates both derived from glycerol. These carbonates displayed higher reactivities in model and polymerization reactions in comparison to the non-activated aliphatic 5CC. However, amidation side reactions were observed when ester-activated cyclic carbonates were polymerized.

2. Diglycerol dicarbonate as an activated monomer for PHUs.

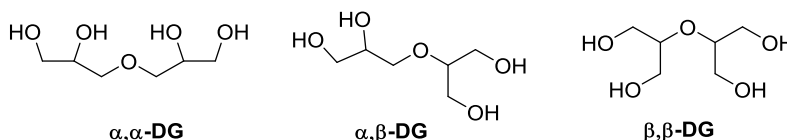
Another strategy to prepare activated cyclic carbonate is based on diglycerol as starting material; the latter is a bio-based and cheap intermediate derived from the etherification of glycerol. A one-step procedure to synthesize the ether-activated diglycerol dicarbonate (DGDC) from diglycerol has been performed with dimethyl carbonate and La_2O_3 as specific catalyst. DGDC was easily purified by recrystallization and characterized by NMR, X-ray and kinetic measurement. When polymerized with diamines, this reactive synthon was not subjected to amidation side reactions as for ester-activated cyclic carbonates depicted in the previous chapter.

DGDC was first polymerized with several classical diamines resulting in relatively high molar mass PHUs. Also, PHU properties could be tuned according to different purity grade of DGDC. In a last part, DGDC was (co)-polymerized with water-soluble and lipidic diamines, leading to the formation of self-assemblies in water.

2.1. Monomer synthesis and characterization

2.1.1. Diglycerol carbonation toward DGDC

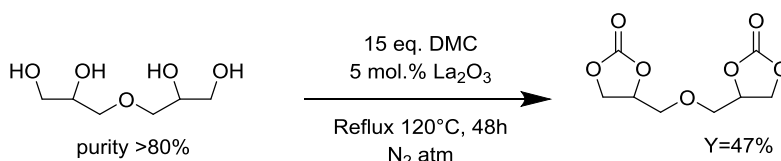
Diglycerol dicarbonate was prepared from the commercial and technical grade diglycerol from TCI chemicals (purity >80%). The low purity of this compound is explained by the possible mixture of α,α -, β,β - and α,β -diglycerol produced during glycerol etherification detailed in the Scheme 4. Triglycerol and oligomers of glycerol can also be part of the mixture.



Scheme 4 - Potential composition of diglycerol from glycerol etherification.

Interestingly, Tryznowski *et al.*⁴⁸ recently reported a new pathway to prepare pure α,α -diglycerol by carbonation of the isomers mixture, and recovery of the α,α -diglycerol dicarbonate by crystallization in ethyl acetate (79% yield). The pure DGDC was finally hydrolyzed with K_2CO_3 in methanol to recover the pure α,α -diglycerol. According to this study, such process could be of interest for the NIPU production at larger scale.

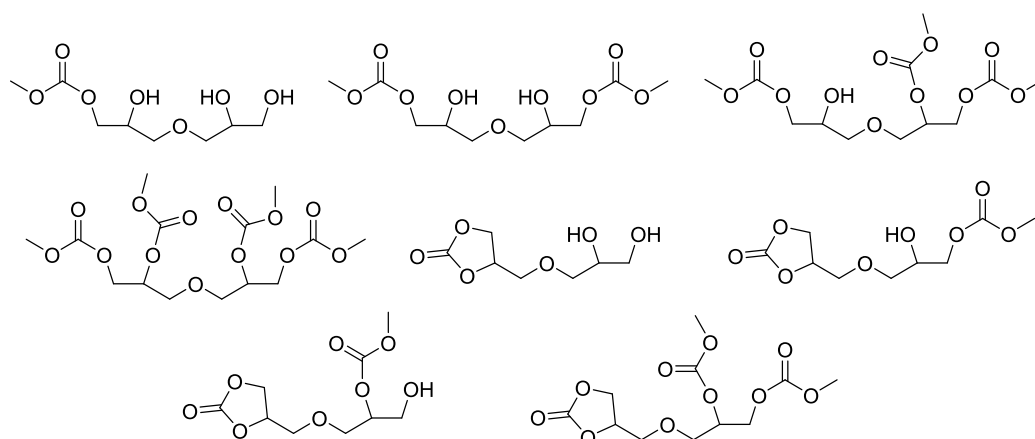
A one-step carbonation procedure patented by Solvay⁴⁹ (see Scheme 5) was applied to the isomer mixture of diglycerol, in 15 eq. dimethyl carbonate (DMC) with 5% of lanthanum oxide (La_2O_3) as a catalyst. Before the reaction, diglycerol was dried under vacuum at $90^\circ C$ in order to remove traces of water. DMC played the role of reactive solvent and was brought under reflux at $120^\circ C$ for 48h.



Scheme 5– Diglycerol carbonation procedure from the Solvay Patent WO2014009421.⁴⁹

The carbonation of such mixture of isomers results in a new mixture of mono-, bis-, linear or cyclic carbonates. An example of possible by-products obtained from α,α -diglycerol is depicted in Scheme 6. The crude mixture obtained was filtrated in order to remove the insoluble catalyst and the excess of DMC was evaporated. The targeted α,α -diglycerol dicarbonate was purified by recrystallization in cold methanol at $-80^\circ C$ and recovered by

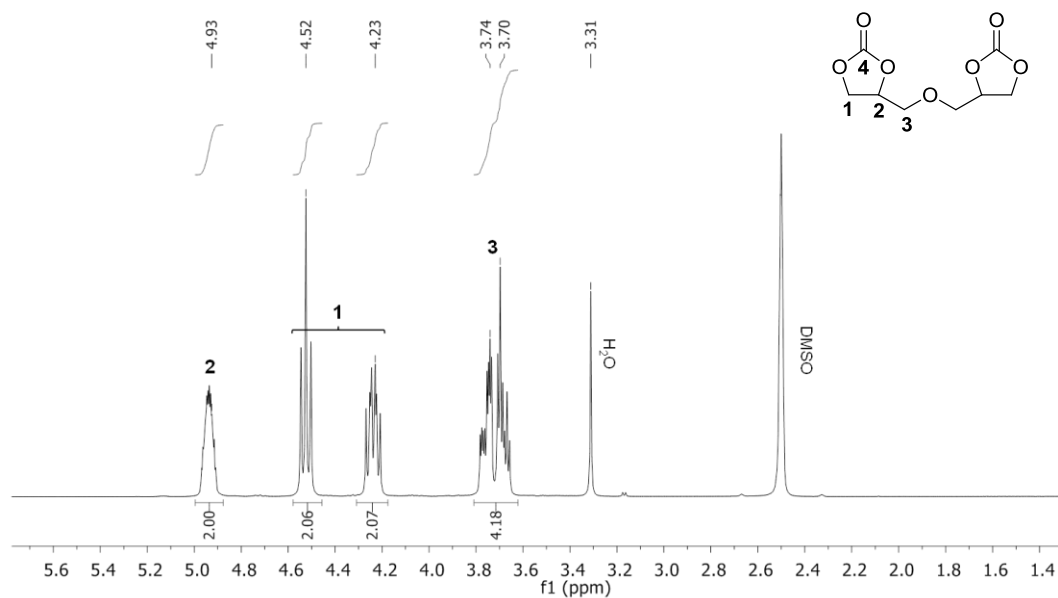
filtration. The resulting white crystal was obtained with a 46% yield thanks to three successive recrystallizations of the crude mixture.



Scheme 6 – Potential by-products from the reaction of α,α -diglycerol isomer with DMC.

2.1.2. Characterization and properties

Pure DGDC was fully characterized by 1D and 2D NMR techniques (see ESI). ^1H and ^{13}C NMR spectra are shown in Figure 15 and give no indication for the presence of impurity. The signals at 3.70 and 3.74 ppm were attributed to the protons in alpha of the ether moiety and their shape was correlated to the different isomers of DGDC conferred by its asymmetric carbons.



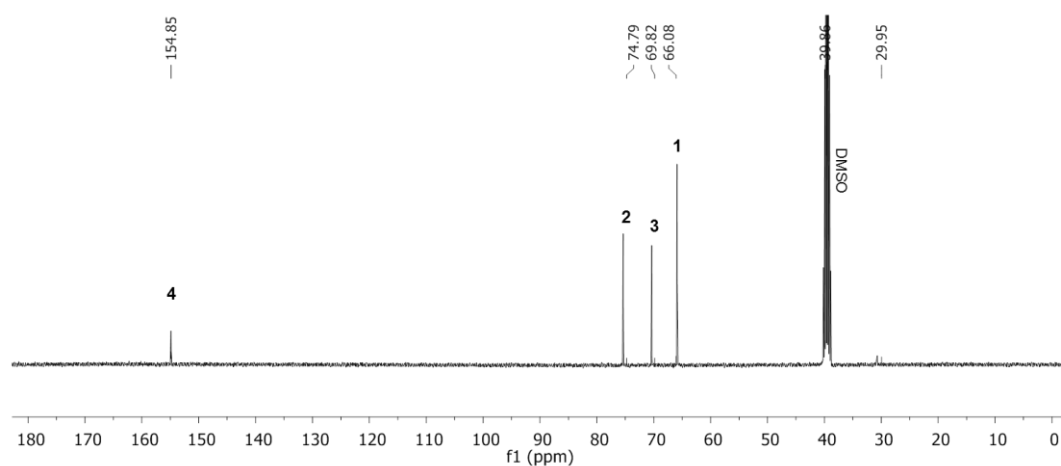


Figure 15 – ^1H and ^{13}C NMR spectra of purified DGDC (analysis performed in DMSO- d_6)

The mono-crystal obtained from the DGDC recrystallization in methanol enabled a precise analysis of the X-ray crystal structure. The DGDC crystallized in a centrosymmetric system (Pbca, (Å): $a=7.7$, $b=11.8$, $c=20.7$) including the equimolar amount of enantiomers (R,R) and (S,S) (see Figure 16) that could not be distinguished in ^1H NMR. Thus, methanol could selectively induce enantiomers crystallization from the raw mixture. A similar study was carried out at the same time by another team from Poland⁴⁸ who studied the crystallographic pattern of the DGDC, and found an identical co-crystallization of enantiomers in a centrosymmetric system when the crude DGDC was recrystallized in ethyl acetate. The melting temperature of the DGDC crystals was determined by DSC at 73°C.

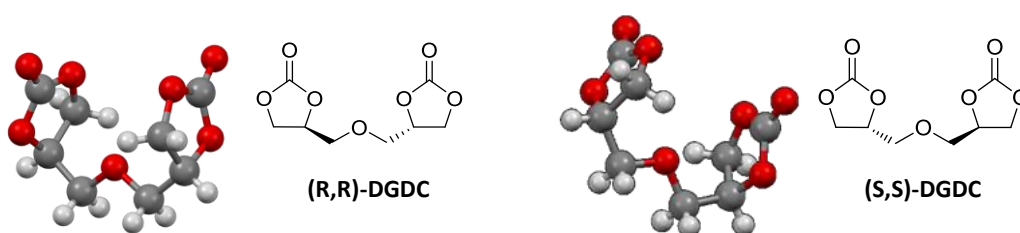


Figure 16 – X-ray structures and corresponding chemical representations of purified DGDC enantiomers.

As in the first part of the chapter, the difference in reactivity between classical 5-membered cyclic carbonates and DGDC was quantified by kinetic experiments, monitored *in situ* by ^1H NMR spectroscopy. The bifunctional ether-activated DGDC was reacted with 2 eq. of hexylamine at 50°C in DMSO- d_6 at 1 mol.L⁻¹, with trichlorobenzene (TCB) as internal reference (see Figure 17). DGDC kinetic pattern was compared to TMC and *Dec-5CC* ones

that were respectively the high and the low benchmarks. DGDC exhibited an enhanced reactivity towards primary amines in comparison with the pure aliphatic **Dec-5CC** and even with the lipidic ether-activated **UndCC-ether**. Moreover, similar reactivity to TMC and **UndCC-ester** ones was obtained and confirmed the growing interest for the DGDC as monomer for NIPU synthesis (see Figure 17).

The model reaction ^1H NMR spectrum is depicted in Figure 18. All the corresponding peaks were assigned thanks to 2D NMR. Tertiary carbons bearing primary or secondary alcohols were clearly identified at 4.67 and 3.72 ppm. Thus, a ratio of 29:71 between primary and secondary hydroxyl groups present on the so-formed hydroxyurethanes was calculated from NMR integrations and was in accordance with the values found in DGDC-based PHUs by van Velthoven *et al.*³⁰ and with the **Und-bCC-ether**-based-PHU synthesized in part 1.3 (28:72). Besides, the formation of 6% of urea (relatively to urethane functions) represented by the labile proton at 6.74 ppm was unavoidable, as it was discussed previously in the chapter.

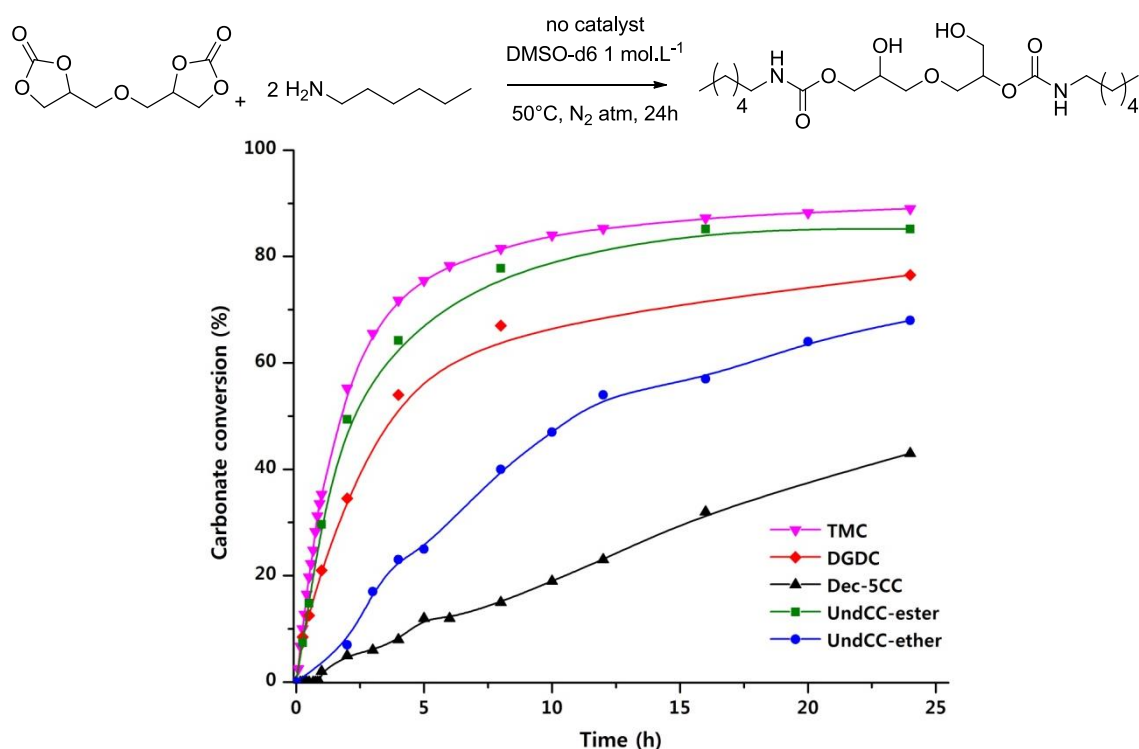


Figure 17 –Kinetic of the conversion of DGDC, TMC, UndCC-ester, UndCC-ether and Dec-5CC, in model reaction with hexylamine followed by ^1H NMR spectroscopy. (50°C , 1 mol.L^{-1} in DMSO-d_6 , ratio 1:1 except for DGDC (ratio 1:2)).

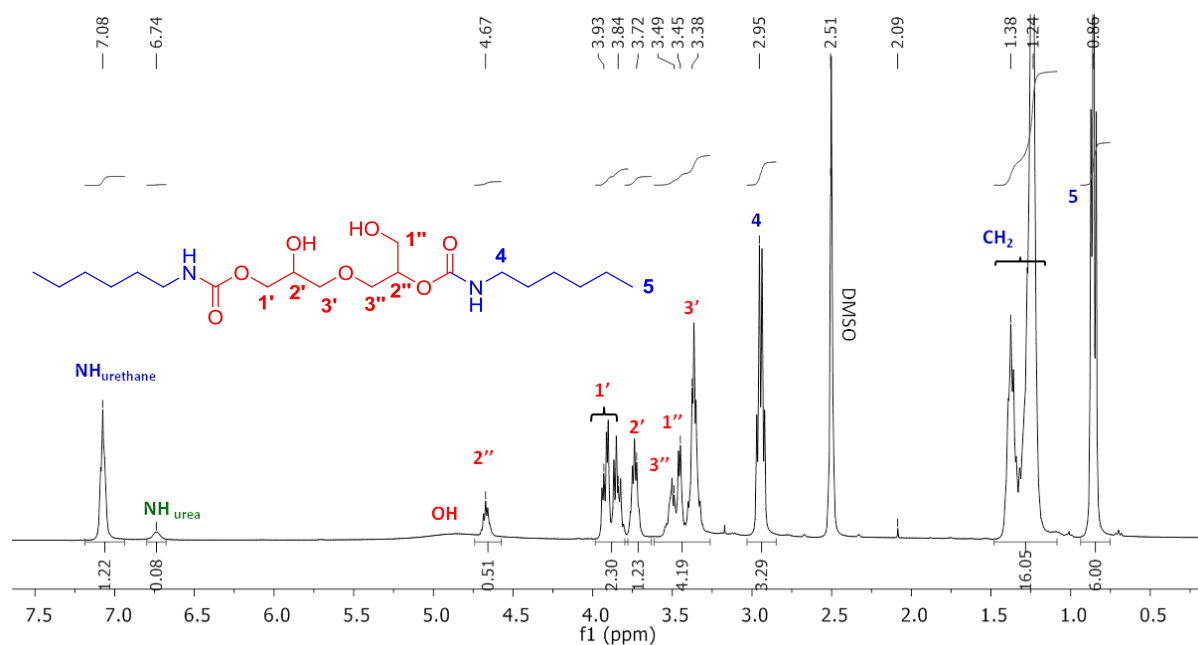


Figure 18 – ^1H NMR of the model reaction between DGDC and hexylamine in DMSO-d_6 at 1 mol.L^{-1} at 50°C .

2.2. Poly(hydroxyurethane) synthesis and applications

Three strategies were adopted to valorize the DGDC as material precursors. The first one consists in polymerizing the pure DGDC with aliphatic diamines and amine-terminated oligomers such as *Jeffamine* or PEG-2000 to determine the influence of the comonomer nature and content onto PHU's properties (T_g , $T_{d5\%}$, solubility in water, etc.). The second strategy tends to valorize the wastes from DGDC purification for PHU synthesis. The thermal properties could be tuned depending on the purity grade of the DGDC. In a third point, the DGDC was copolymerized with amine-terminated PEG-2000 and 1,12-diaminododecane (12DA) in order to study the copolymer self-assembly in water.

2.2.1. DGDC-based PHUs with tunable properties varying diamine nature

To prepare a wide range of DGDC-based PHUs, pure DGDC was engaged as rigid and polar monomer in polyaddition with six various diamines, i.e. 1,4-diaminobutane (4DA), 1,10-diaminododecane (10DA), *Und-C20-diamine* (20DA), *Priamine*[®] 1075 from CRODA, amine-terminated PEG 2000 (PEG-diNH₂) and *Jeffamine* 400 (PPG-diNH₂). The *Priamine* and *Jeffamine* were used to introduce some flexibility in the PHUs by increasing the free volume between the polymer chains and PEG-diNH₂, to introduce additional hydrophilicity to the polymer. The other diamines were employed to vary the spacer length between urethane functions. Polymerizations were monitored by ^1H NMR spectroscopy and the resulting PHUs

Polymerizations were thus performed in solution (DMF at 1 mol.L⁻¹ at 70°C for 7 days), to control the monomer reactivity and to avoid cross-linking. In addition, such conditions ease the comparison with the data already reported in the literature. In those conditions, the conversions leveled off at 80% after 24h, as shown in Figure 19 where residual monomers were identified by NMR (**PHU 5**). The low conversion obtained with PEG-diNH₂-based PHU (**PHU 8**), 65%, can be explained by the poor reactivity of this long diamine.

As expected, the molar masses displayed by the PHUs synthesized in DMF were lower in comparison with the ones prepared in bulk conditions. Taking in account the tremendous difference in reactivity between the polymerized diamines, it is essential to reason in terms of apparent polymerization degree (DP_n, calculated by SEC in DMF). For instance, **PHU 8** made from the pre-polymer PEG-diNH₂ revealed a relatively high molar mass of 13100 g.mol⁻¹ (D=1.5) that corresponds to a DP_n close to 6. Contrarily, the lowest molar mass of 7600 g.mol⁻¹ was obtained for 20DA-based PHU (**PHU 6**). However, **PHU 6** displayed a DP_n of 14, demonstrating a higher reactivity of the 20DA in comparison with the long PEG-diNH₂. The highest degrees of polymerization were achieved for **PHU 4** and **5** prepared from the reactive 4DA and 10DA, with respectively DP_n values of 33 and 31.

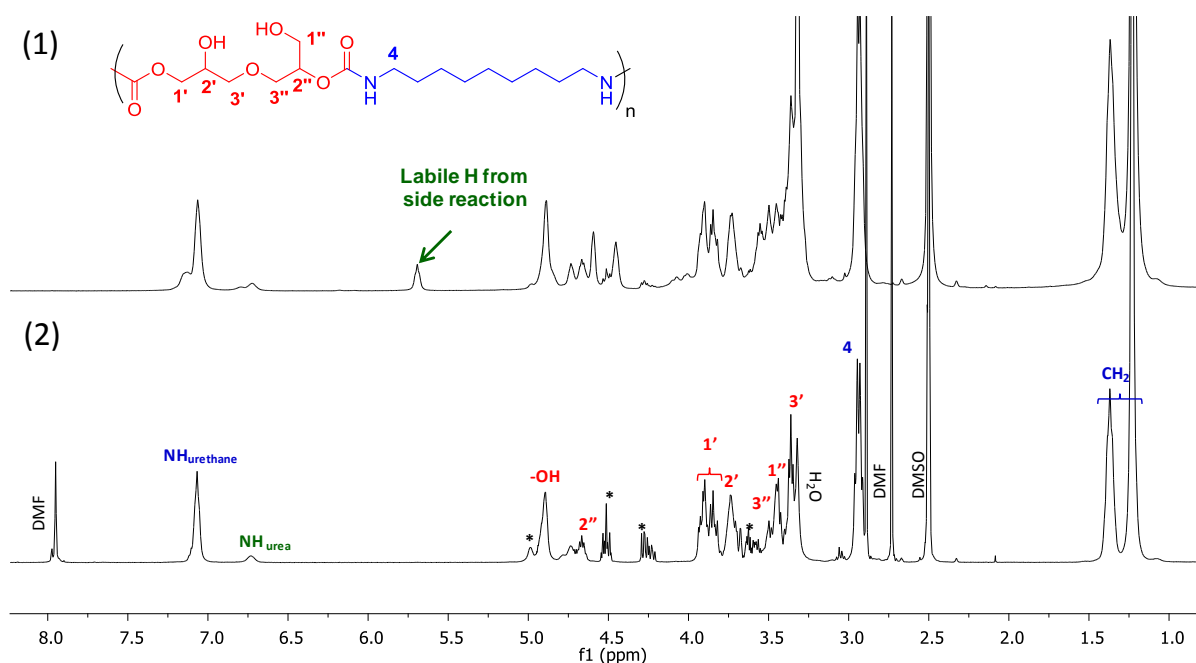


Figure 19 - Stacked ¹H NMR spectra of PHU from 10DA and DGDC (1) at 130°C in bulk (PHU 2) and (2) at 70°C in DMF at 1 mol.L⁻¹ (PHU 5) in DMSO-d₆ at 24h of polymerization (*: residual monomers/chain ends).

Meanwhile, all the proton NMR signals of the soluble polymers were assigned by means of 1D and 2D NMR techniques. Thus, the ratio between primary and secondary hydroxyl groups could be calculated considering the integration of the protons **2'** and **2''** from tertiary carbons. OH_I:OH_{II} ratios were in the range [22:78-27:73] irrespective of the reaction conditions and these values correlated with the ones obtained by NMR with DGDC model reaction (29: 71). Nevertheless, some conversions and OH_I:OH_{II} ratios were impossible to calculate due to signal overlap or poor resolution of the NMR signals.

The so-formed PHUs were then analyzed by DSC and TGA to establish the structure-properties relationship. Most of the PHUs were amorphous and this feature could be attributed to the poorly defined hard segment imparted by the two hydroxyl groups generated during the polyaddition of DGDC. The same trend was reported by van Velthoven *et al.*³⁰.

T_g values were in the range -13- 27°C depending on the diamine (see Figure 20). For instance, the flexibility was brought by the *Priamine* segments (**PHU 7**), due to the dangling aliphatic chains that act as internal plasticizers. Similarly, *Jeffamine 400* which is a soft segment prevented crystallization and conferred to **PHU 9** a low T_g value of -13°C. On the contrary, 20DA provided semi-crystalline **PHU 6** with T_g of 27°C and T_m of 92°C, in agreement with a PE-like behavior.⁴⁷ When PEG-diNH₂ was used as comonomer (**PHU 8**), no T_g value could be measured due to high crystallinity ratio imparted by the PEG segment. Indeed, PEG-diNH₂ was analyzed by DSC and exhibited an enthalpy of melting of ΔH_f= 172 J.g⁻¹ at 53°C. Regarding the **PHU 8**, the second heating cycle in DSC showed a peak of fusion at 43°C with a corresponding enthalpy of 99 J.g⁻¹. With this information, we demonstrated that PEG-diNH₂ which composes the **PHU 8** at 90 w.%, expressed only 52% of its native crystallinity with a 10°C shift in its melting temperature when copolymerized with DGDC.

The thermal stability of the PHUs was assessed using TGA analysis. An isothermal procedure at 160°C was applied for 15 min in order to remove DMF traces and the T_{d5%} were thus determined from 160°C. Consequently, the residual solvent, the water and the monomer evaporations were not taken into account in the weight loss calculation. The T_{d5%} ranged from 200 to 284°C depending on the diamine employed. **PHU 8** showed a higher T_{d5%} equal to 284°C as a result of the presence of PEG-diNH₂. Interestingly, the same PHU was fully soluble in water thanks to the PEG chain imparted by the diamine. When the hydrophobic *Jeffamine 400* was polymerized with DGDC, the resulting polymer was also soluble in water. This behavior was attributed to the high content of hydroxyl groups generated that helped the PHU hydrophilicity. None of the other prepared PHUs were water soluble.

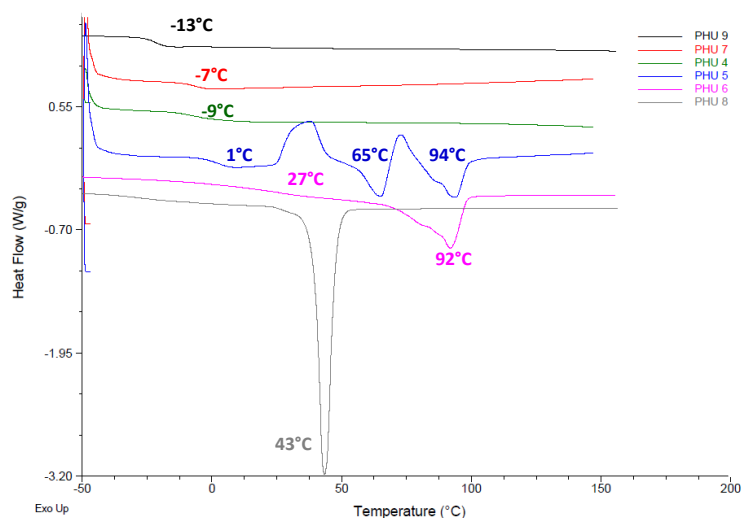


Figure 20 – DSC second heating cycle (10°C/min) of the PHU synthesized in solvent (PHU 4 to 9) to study the influence of the diamine on the PHU properties.

2.2.2. PHUs from DGDC with different purity grade

During the DGDC purification process (see part 2.1), 2 enantiomers of DGDC were isolated with 46% yield after three successive recrystallizations of the raw DGDC (**raw-DGDC**). The non-recrystallized part containing other diastereoisomers and by-products was recovered as the non-recrystallized DGDC (**N-DGDC**). In order to valorize the residues from DGDC purification and to tune the thermal properties of DGDC-based PHUs, **N-DGDC**, **raw-DGDC** and the recrystallized DGDC (**R-DGDC**) were respectively polymerized with 4DA in bulk at 70°C (after 24h). Results are detailed in Table 6.

Table 6 - Characterization of PHUs obtained from different purity grade DGDC and 4DA.

PHU	DGDC	Conditions	Conversion (%) ²	\bar{M}_n (g.mol ⁻¹) [D] ¹	T _g (°C) ^a	T _m (°C) ^a	T _{d5%} (°C) ^b
10	N-DGDC		100	4900 [1.2]	-8	-	200
11	Raw-DGDC	70°C, bulk, 24h	92	6700 [1.2]	5	-	188
12	R-DGDC		67	11400 [1.7]	20	-	227

¹: Determined at the end of the polymerization (24h) with SEC in DMF (LiBr, PS standards) ²: Determined by ¹H NMR spectroscopy; ^a: Determined by DSC at 10°C.min⁻¹ from the second cycle; ^b: Determined by TGA at 10°C.min⁻¹ under nitrogen.

PHU 10 and 11 synthesized with a low purity grade DGDC exhibited high conversions. Indeed, the presence of linear carbonates and impurities in **N-DGDC** and **Raw-DGDC** reduced the molar equivalent of cyclic carbonates (see Figure 21 and ESI) and led to a DGDC

conversion up to 100% after 24h. Higher molar mass of $11400 \text{ g}\cdot\text{mol}^{-1}$ with dispersity of 1.7 could be achieved for **PHU 12**, displaying the higher content of reactive cyclic carbonates.

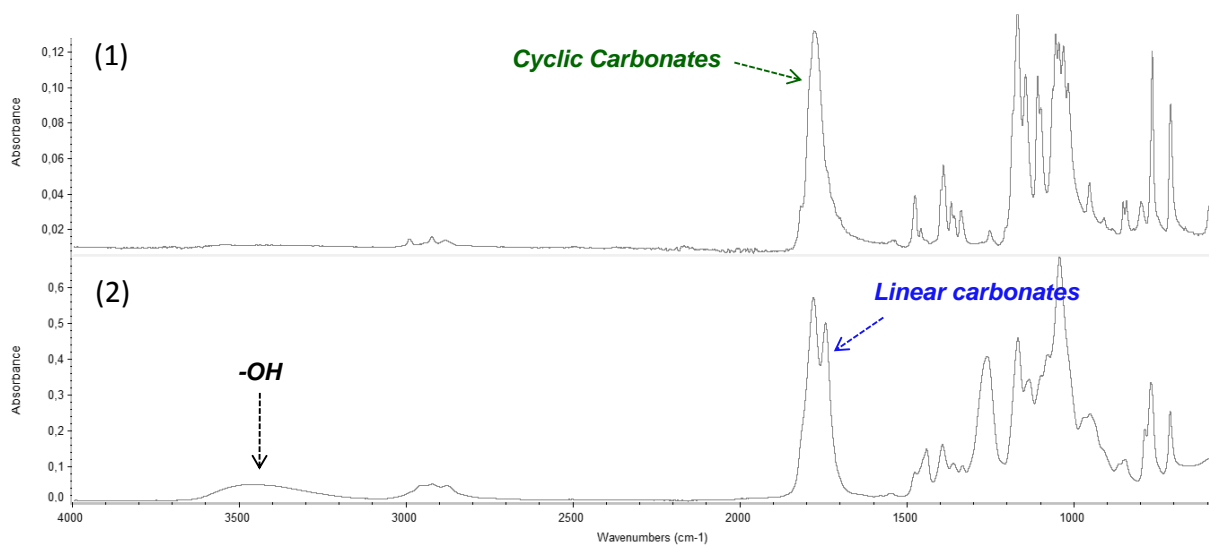


Figure 21 – Stacked FTIR of (1) R-DGDC and (2) Raw-DGDC.

As expected, the melting temperatures of the different DGDCs were depending on the purity grade. As shown in Figure 22, the higher the purity of DGDC, the higher its crystallinity. Reversibly, the lower the DGDC purity, the lower the T_g of the resulting PHUs. The presence of impurities (see Scheme 6) and linear carbonates, identified by FTIR (see Figure 21) in **Raw-DGDC** play the role of PHU plasticizers, lowering the T_g value of the PHUs; 5°C for **PHU 11** in comparison to 20°C for **PHU 12**. Accordingly, the thermal stability was also lower for **PHU 10** and **PHU 11** with $T_{d5\%}$ below 200°C in comparison to **PHU 12**. (see Table 6).

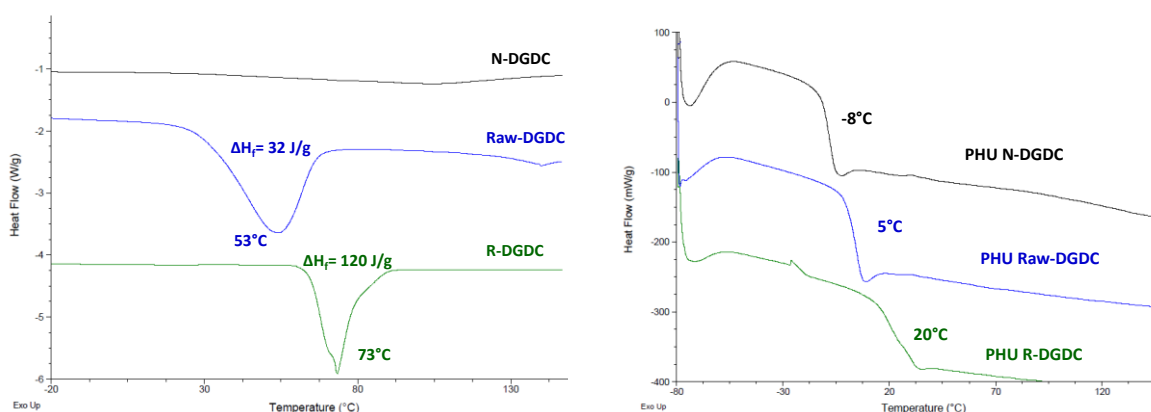
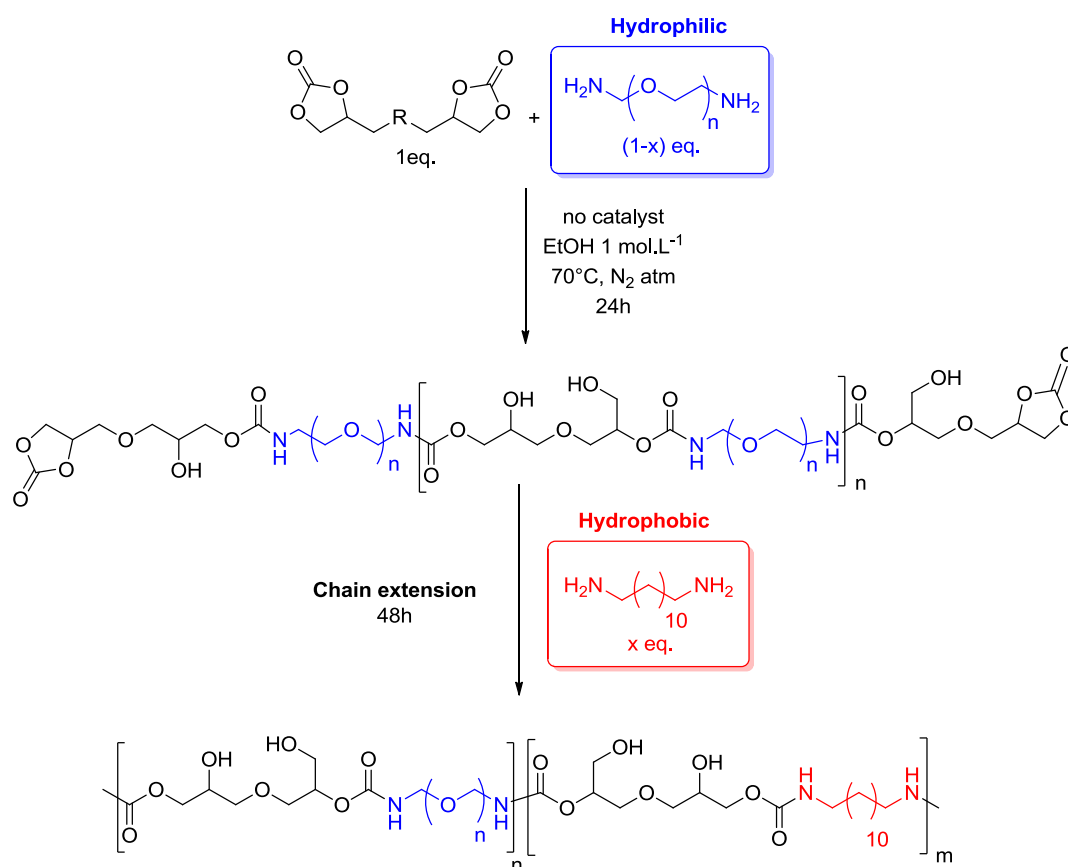


Figure 22 – DSC second heating cycle ($10^\circ\text{C}/\text{min}$) of the N-DGDC, raw-DGDC and R-DGDC and the corresponding synthesized PHUs (PHU 10, 11 and 12).

As a conclusion, PHU thermal properties could be tuned depending on the DGDC purity. Additionally, **N-DGDC** represents an attractive monomer as it is liquid and easy to handle; no purification is required and bulk polymerization can be performed without the use of toxic and high boiling point solvents. The resulting poly(hydroxyurethane)s could be used as viscosity modifiers for instance.

2.2.3. DGDC-based copolymers

As previously discussed, some DGDC-based PHUs exhibited different water solubility with respect to the diamine used as comonomer. We took advantage of this feature to evaluate the self-assembly properties of the so-formed PHUs in water. In order to study such behavior, DGDC was copolymerized with hydrophobic and hydrophilic diamines, following a chain-extension process as described in Scheme 7.



Scheme 7 – Procedure for copolymerization by chain extension of DGDC with PEG-diNH₂ and 12DA.

Several ratios between hydrophobic 12DA and hydrophilic PEG-diNH₂ diamines were tested. The polymerizations were performed by reacting first the less reactive diamine PEG-diNH₂ in

EtOH (1 mol.L⁻¹) at 70°C. Then, the hydrophobic 12DA was copolymerized with the PEG pre-polymer terminated by DGDC moieties, as depicted in Scheme 7. The copolymer characteristics are summarized in Table 7.

Table 7 - Characterization of the homo- and Copolymer PHUs obtained from PEG-diNH₂, 12DA and DGDC in EtOH (1 mol.L⁻¹) at 70°C.

PHU	Ratio PEG diNH ₂ : 12DA	Conditions	Final conversion (%) ²	\bar{M}_n (g.mol ⁻¹) [Đ] ¹	T _g (°C) ^a	T _m (°C) ^a	T _{d5%} (°C) ^b
1	1 : 0		85	10000 [1.9]	nd	42	280
2	0 : 1		97	26900 [1.6]	46	89/108	261
3	0.75 : 0.25	EtOH (1 mol.L ⁻¹)	78	9900 [1.9]	-23	42	284
4	0.5 : 0.5		91	12700 [2]	-17	41	282
5	0.25 : 0.75		100	15200 [1.9]	nd	36/68/9 5	269

nd: could not be determined because of the high cristalinity of the polymer; ¹: Determined at the end of the polymerization by SEC in DMF (LiBr, PS standards); ²: Determined by ¹H NMR spectroscopy; ^a: Determined by DSC at 10°C.min⁻¹ from the second cycle; ^b: Determined by TGA at 10°C.min⁻¹ under nitrogen.

The two homopolymers **PHU 1** and **PHU 2** justified the choice of polymerizing first the less reactive diamine (PEG-diNH₂) before chain extension with the second one, as a complete conversion and a higher molar mass were reached for the 12DA-based **PHU 2** (26900 g.mol⁻¹). Regarding the copolymers, the dispersities around 2 as well as the SEC traces (see Figure 23) support the chain extension efficiency. The molar masses obtained were higher for high content of 12DA.

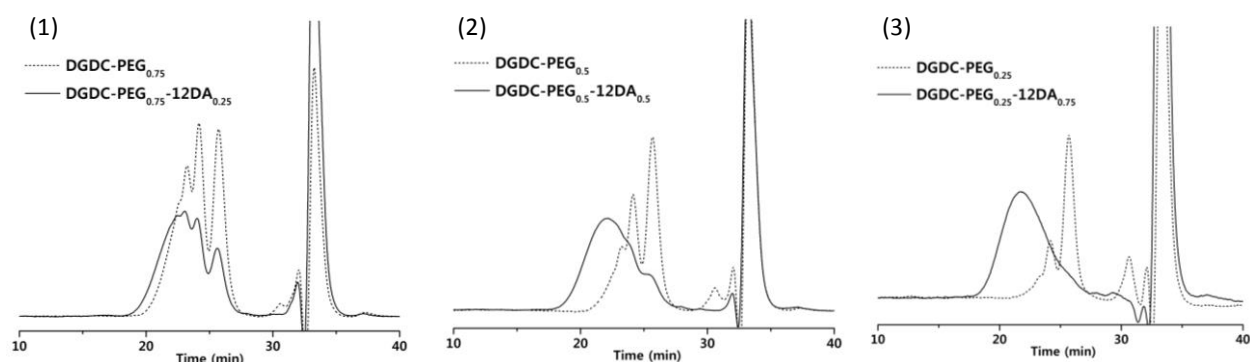


Figure 23 – SEC traces of (1) PHU 3, (2) PHU 4 and (3) PHU 5 before (dot line) and after (solid line) the chain extension process (DMF, LiBr, PS standards).

All the copolymers were semi-crystalline and exhibited low T_g, especially at high PEG-diNH₂ content. Indeed, the ether functions along the PEG backbone induced free rotation and polymer chain mobility. Several melting temperatures were observed when the amount of

12DA increased in the polymer backbone composition (**PHU 5**), suggesting a phase segregation within the copolymer. $T_{d5\%}$ were comprised between 261 and 284°C and were higher when the PEG-diNH₂ content was larger.

PHU 1, only containing PEG segments, was fully soluble in water contrarily to other PHU. The self-assembly in water of the **PHU 2, 3, 4** and **5** copolymers was thus carried out by nano-precipitation before being analyzed by dynamic light scattering (DLS). The DLS samples were deposited on TEM grids and observed through the transmission electronic microscope. The TEM and DLS results are summarized in the Figure 24.

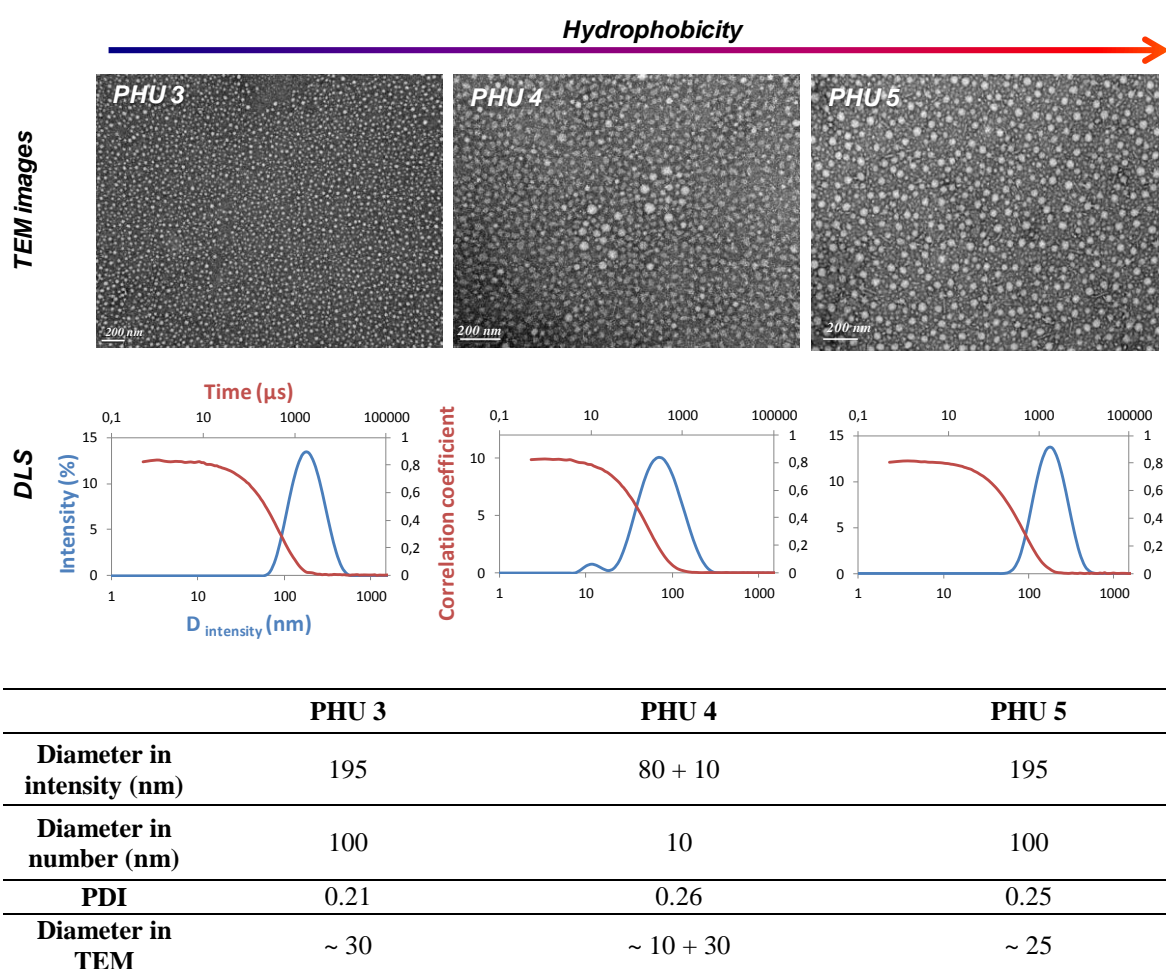


Figure 24 – TEM images, DLS traces and relative data for PHU 3, 4 and 5.

Firstly, **PHU 2** did not display any self-assembly pattern in DLS. The numerous pendant hydroxyl groups of the polymerized DGDC were not sufficient to induce self-assembly in water.

However, the TEM pictures clearly showed the self-assembly of the copolymers as particles with average diameters of 30 nm, irrespective of the hydrophobic weight fraction. However, DLS measurements indicated the presence of particles with a diameter of 195 nm (in intensity) for **PHU 3** and **PHU 5**, with PDI of 0.21 and 0.25, respectively. It is noteworthy to mention that the average diameter in intensity is not always representative of the size of aggregates present within the solution. This pattern could explain the difference between the size of particles when analyzed by DLS or TEM. Also, it could be attributed to the possible water swelling of the particles during DLS measurements, giving larger size particles than in TEM images, where the particles were dried before analysis. An exception is observed with **PHU 4** that displayed two populations by DLS with diameters in intensity of 10 and 80 nm that could also be distinguished by TEM. Thus, particle sizes could be reduced when hydrophobic and hydrophilic contents were equilibrated (50:50).

Hence, we demonstrated in this preliminary work that DGDC was an interesting building block to induce PHU self-assembly in water, taking advantage of the high hydroxyl content imparted by this cyclic carbonate when copolymerized with diamines. Nonetheless, this study would need further investigations to define the size and type of particles formed by self-assembly of these copolymers, for instance in highly diluted conditions.

Conclusions

This chapter highlights the problematic encountered with 5-membered ring cyclic carbonates from fatty acid based derivatives. Indeed, their lack of reactivity towards aminolysis, imparted by their inherent structure, is an obstacle to the enhancement of the polymerization reaction rate and to the preparation of high molar mass PHUs. In order to circumvent the above mentioned issues, reactive 5CC were synthesized from glycerol carbonate, epichlorohydrin and fatty acid derivatives, enabling the activation of the cyclic carbonate by the insertion of an ester or an ether moiety in β position nearby the cycle. Both activations were efficient to increase the CC reactivity when reacted with amines in model reaction or polymerization. Thanks to the “monomer activation”, the synthesized PHUs displayed molar masses up to $60000 \text{ g}\cdot\text{mol}^{-1}$ with dispersities comprised between 1.5 and 3.7. More precisely, the ester-activated 5CC was the most promising monomer thanks to its similar reactivity with 6CC.

Various parameters such as the chemical structure of cyclic carbonates and comonomers, the temperature, the solvent or the lipidic backbone length were crucial for the kinetic and the selectivity of the hydroxyurethane formation. For instance, the amidation side reaction occurring with ester-activated monomers could be controlled by decreasing the temperature. However, urea was formed independently of the activation used.

A second route to the synthesis of DGDC (“ether-activated monomer”) from the readily available glycerol was investigated and demonstrated the high potential of this monomer in polymerization. Indeed, DGDC exhibited a similar reactivity to ester-activated monomers when reacted with amines, and enabled the formation of PHU with high hydroxyl contents. Polymerization were performed in harsh (bulk, 130°C) conditions that led to cross-linked materials and unidentified side reactions. In soft (solvent, 70°C) conditions, thermoplastic PHUs were synthesized with molar masses up to $26900 \text{ g}\cdot\text{mol}^{-1}$. Some of them displayed water soluble properties when copolymerized with hydrophilic diamines. In the same logic, self-assembly of DGDC-based copolymers showed interesting results and would necessitate supplementary investigations.

To go further, PHU molar masses could have been improved by polymerizing in bulk activated lipidic cyclic carbonates derived from the oleic acid platform that generally present lower melting points (liquid at room temperature). In the same line, solid monomers could be polymerized using the reactive extrusion at moderate temperature, avoiding the use of solvent. Other investigations regarding the monomer reactivity and conversions as well as the PHU

molar masses, would be needed to further analyze the role of the solvent on the formation of hydroxyurethane functions, by studying the interactions between monomers, polymer chains and solvent. Furthermore, the catalysis of the synthesized 'activated monomers' would be an interesting pathway for increasing conversions and PHU molar masses (see Chapter 5).

- Carpentier, J.-F.; Guillaume, S. M. *Green Chem.* **2014**, *16* (4), 1947–1956.
- (37) Carre, C.; Bonnet, L.; Averous, L. *RSC Adv.* **2014**, *4*, 54018–54025.
- (38) Duval, C.; Kébir, N.; Jauseau, R.; Burel, F. *J. Polym. Sci. Part A Polym. Chem.* **2016**, *54* (6), 758–764.
- (39) Bigot, S.; Daghrir, M.; Mhanna, A.; Boni, G.; Pourchet, S.; Lecamp, L.; Plasseraud, L. *Eur. Polym. J.* **2016**, *74*, 26–37.
- (40) Türünç, O.; Meier, M. A. R. *Eur. J. Lipid Sci. Technol.* **2012**, *115* (1), 41–54.
- (41) Garipov, R. M.; Sysoev, V. A.; Mikheev, V. V.; Zagidullin, A. I.; Deberdeev, R. Y.; Irzhak, V. I.; Berlin, A. Al. *Dokl. Phys. Chem.* **2003**, *393* (1–3), 289–292.
- (42) Webster, D. C. *Prog. Org. Coatings* **2003**, *47* (1), 77–86.
- (43) Bürgel, T.; Fedtke, M.; Franzke, M. *Polym. Bull.* **1993**, *30* (2), 155–162.
- (44) Besse, V.; Camara, F.; Méchin, F.; Fleury, E.; Caillol, S.; Pascault, J.-P.; Boutevin, B. *Eur. Polym. J.* **2015**, *71*, 1–11.
- (45) Ochiai, B.; Yuriko, S.; Takeshi, E. *J. Polym. Sci. Part A Polym. Chem.* **2009**, *47* (18), 4629–4635.
- (46) Diakoumakos, C. D.; Kotzev, D. L. *Macromol. Symp.* **2004**, *216* (1), 37–46.
- (47) Stempfle, F.; Ortmann, P.; Mecking, S. *Chem. Rev.* **2016**, *116* (7), 4597–4641.
- (48) Tryznowski, M.; Swiderska, A.; Zolek-Tryznowska, Z.; Golofit, T.; Parzuchowski, P. G. *Polymer.* **2015**, *80*, 228–236.
- (49) Mignani, G.; Debray, J.; Da Silva, E.; Lemaire, M.; Raoul, Y. Method for producing polyglycerol poly(carbonate), WO2014009421, **2011**.

Experimental and Supporting Information

Experimental Methods

Mono-cyclic carbonate synthesis

• ***UndCC-ether synthesis*** : (i) In a round-bottom flask, 10-undecen-1-ol (10 g, 58.7 mmol) was stirred with epichlorohydrin (54.35 g, 587 mmol, 10 eq.) and TBABr (1.89 g, 5.87 mmol, 0.1 eq.) at room temperature for 30 min. NaOH was added *via* a 50 w.% concentrated aqueous solution (70 mL, 0.88 mol, 15 eq.). After 24h of reaction at room temperature, the mixture reaction was diluted with 4 volumes of distilled water. The aqueous phase was extracted 3 times with 100 mL of ethyl acetate. The organic phase was then washed twice with 75 mL of water, dried over anhydrous magnesium sulfate, filtered and the remaining epichlorohydrin was removed on rotary evaporator. The ¹H NMR spectrum revealed a conversion of 72%. The compound *Und-epoxide* was purified by flash chromatography using a mixture of cyclohexane and ethyl acetate (100:0 to 88:12) and obtained as a viscous transparent liquid. Yield: 58%. ¹H NMR (CDCl₃, 25°C, 400 MHz), δ (ppm): 5.80 (m, 1H), 4.96 (m, 2H), 3.70 and 3.37 (dd, 2H), 3.49 (m, 2H), 3.14(m, 1H), 2.78 and 2.59 (t, 2H), 2.02 (m, 2H), 1.58-1.28 (m, 14H). ¹³C NMR (CDCl₃, 25°C, 100 MHz), δ (ppm):137.9 (CH=CH₂), 113.2 (CH=CH₂), 70.7 (OCH₂-CH₂), 70.4 (CH₂O-CH₂CH₂), 49.9 (CH₂-CH-CH₂O), 43.4 (CH₂-CH-CH₂O), 32.7 (CH₂-CH=CH₂), 28.7-25.1 (CH₂). (ii) The *Und-epoxide* (7.72 g, 34.2 mmol) was first pre-mixed with the TBABr (0.24 g, 0.7 mmol, 3 w.%) in 5 mL of acetone. Then the mixture was placed in a reactor and heated up at 80°C. Once the temperature got stabilized, CO₂ was slowly introduced into the reactor until 50 bars. After 3 days, the reactor was cooled down to RT and slowly depressurized to the atmospheric pressure. The mixture was reconcentrated on rotary evaporator. The ¹H NMR of the final mixture revealed a conversion of 98%. The *UndCC-ether* was purified by flash chromatography using a mixture of cyclohexane and ethyl acetate (100:0 to 81:19), and obtained as a viscous transparent liquid. Yield: 82%. ¹H NMR (CDCl₃, 25°C, 400 MHz), δ (ppm): 5.72 (m, 1H), 4.90 (m, 2H), 4.73 (m, 1H), 4.42-4.32 (t, 2H), 3.58 (m, 2H), 3.41 (t, 2H), 1.98 (dd, 2H), 1.48 (m, 2H), 1.21 (m, 14H). ¹³C NMR (CDCl₃, 25°C, 100 MHz), δ (ppm): 155.3 (OCOO), 138.8 (CH=CH₂); 114.2 (CH=CH₂), 74.7 (CH₂-CH-CH₂O), 71.8 (CH₂O-CH₂-CH₂), 68.8 (CH-CH₂O-CH₂), 66.1 (CH₂-CH-CH₂O), 33.6 (CH₂-CH=CH₂), 28.7-26.2 (CH₂). IR (cm⁻¹): 3075, 2979, 2928, 2850, 1760.

• ***OleylCC-ether synthesis***: (i) *Oleyl-epoxide* was synthesized using the same procedure than for *Und-epoxide*, but starting from oleyl alcohol. Viscous transparent oil was obtained and no purification was applied before carbonation. Conversion: 78%. (ii) *OleylCC-ether* was

synthesized using the same carbonation procedure as in *UndCC-ether* synthesis. Conversion: 99%. Viscous transparent oil was obtained after purification by flash chromatography with a mixture of cyclohexane and ethyl acetate as eluent (100:0 to 86:14). Yield: 46%. ¹H NMR (CDCl₃, 25°C, 400 MHz), δ (ppm): 5.35 (m, 2H), 4.78 (m, 1H), 4.50 and 4.40 (t, 2H), 3.62 (m, 2H), 3.49 (t, 2H), 2.02 (m, 4H), 1.56-1.27 (m, 26H), 0.88 (t, 3H). ¹³C-NMR (CDCl₃, 25°C, 100 MHz), δ (ppm): 155.3 (OCOO), 130.1 (CH₂-CH=CH), 75.4 (CH-CH₂OCH₂), 72.10(CH₂O-CH₂-CH₂), 69.6 (CH-CH₂-OCH₂), 66.3 (CH₂-CH-CH₂O), 32.0-22.8 (CH₂), 27.3 (CH₂-CH=CH), 14.3(CH₃). IR (cm⁻¹): 3003, 2917, 2853, 1797, 1133.

• ***UndCC-ester synthesis:*** (i) Into a round-bottom flask containing 1 eq. (250 g, 1.34 mol) of undecenoic acid, thionyl chloride (271.5 g, 2.28 mol) was added dropwise under inert atmosphere at 60°C and the formed SO₂ and HCl were trapped during the reaction (with gas traps containing aqueous sodium hydroxide solution). When the conversion (determined by GC) was quantitative (> 99%), the excess of thionyl chloride was distilled out and the product was stored at -18°C. Yield: 99%. (ii) In a round-bottom flask, 1 eq. (116.7 g, 0.99 mol) of glycerol carbonate and 1.3 eq. (130.2 g, 1.29 mol) of triethylamine were diluted in 500 mL of dry THF. 1 eq. (270 g, 0.99 mol) of undecenoyl chloride was added dropwise under inert atmosphere at 0°C. The mixture reaction was left 2h at room temperature and the conversion (determined by GC) reached 96%. *UndCC-ester* was then extracted with 250 mL of ethyl acetate and washed several times with 250 mL of water before solvent reconcentration. ITERG provided 20 g of the crude *UndCC-ester*, obtained as an oily white powder that could be purified by recrystallization in 100 mL of cold heptane. 73% yield was achieved after subsequent reconcentration of the recrystallization filtrate and recrystallization. ¹H NMR (CDCl₃, 25°C, 400 MHz), δ (ppm): 5.82 (m, 1H), 5.00 (m, 2H), 4.91 (m, 1H), 4.55 (t, 1H), 4.31 (m, 3H), 2.36 (t, 2H), 2.02 (m, 2H), 1.59-1.29 (m, 14H). ¹³C NMR (CDCl₃, 25°C, 100 MHz), δ (ppm): 173.6 (CH₂-OCO-CH₂), 154.2 (OCOO), 139.2 (CH=CH₂), 114.0 (CH=CH₂), 73.5 (CH-CH₂-OCO), 65.5 (CH₂-CH-CH₂-OCO), 62.7 (CH-CH₂-OCO), 34.4 (OCO-CH₂-CH₂), 33.9 (CH₂-CH=CH₂), 31.1-29.0 (CH₂), 24.9 (OCO-CH₂-CH₂). IR (cm⁻¹): 3081, 3000, 2920, 2853, 1781, 1733.

• ***OleylCC-ester synthesis:*** *OleylCC-ester* was synthesized following the procedure (ii) used for *UndCC-ester* synthesis, but starting from oleoyl chloride. The product was purified by flash chromatography using a mixture of cyclohexane and ethyl acetate (100:0 to 80:20) and obtained as a viscous transparent liquid. Yield: 47%. ¹H NMR (CDCl₃, 25°C, 400 MHz), δ (ppm): 5.32 (m, 2H), 4.91 (m, 1H), 4.57 (t, 1H), 4.34 (m, 3H), 2.36 (t, 2H), 1.99 (m, 4H), 1.62-1.29 (m, 22H), 0.85 (t, 3H). ¹³C NMR (CDCl₃, 25°C, 100 MHz), δ (ppm): 173.4 (CH₂-

OCO-CH₂), 154.6 (OCOO), 130.1 (CH=CH), 73.8 (CH-CH₂-OCO), 66.0 (CH₂-CH-CH₂-OCO), 62.9 (CH-CH₂-OCO), 34.0 (OCO-CH₂-CH₂), 31.9-29.2 (CH₂), 27.2 (CH₂-CH=CH), 24.9 (OCO-CH₂-CH₂), 22.7 (CH₂), 14.2 (CH₃). IR (cm⁻¹): 3000, 2920, 2858, 1792, 1738.

- **Und-6CC synthesis:** Synthesis is detailed in Maisonneuve *et al.*, *RSC Adv.* **2014**, *4* (49), 25795–25803. **Und-6CC** was obtained as viscous transparent oil. Yield: 75%. Purity: 99.5%. ¹H NMR (CDCl₃, 25°C, 400 MHz), δ (ppm): 5.73 (m, 1H), 4.94 (m, 2H), 4.41 (m, 2H), 4.06 (m, 2H), 2.17 (m, 1H), 2.02 (m, 2H), 1.35-1.30 (m, 12H). ¹³C NMR (CDCl₃, 25°C, 100 MHz), δ (ppm): 148.3 (OCOO), 139.1 (CH=CH₂), 114.7 (CH=CH₂), 72.5 (CH₂-OCOO), 34.0 (CH₂-CH=CH₂), 31.4 (CH-CH₂-OCOO), 29.5-26.7 (CH₂). IR (cm⁻¹): 3075, 2979, 2928, 2850, 1760.

- **Oleyl-6CC synthesis:** **Oleyl-6CC** was synthesized following the procedure used for **Und-6CC** synthesis, but starting from methyl oleate. Viscous transparent oil was obtained after purification by flash chromatography with a mixture of cyclohexane and ethyl acetate (100:0 to 60:40). Yield: 43%. ¹H NMR (CDCl₃, 25°C, 400 MHz), δ (ppm): 5.33 (m, 2H), 4.41 (m, 2H), 4.13 (m, 2H), 2.22 (m, 1H), 2.02 (m, 4H), 1.28 (m, 22H), 0.91 (t, 3H). ¹³C-NMR (CDCl₃, 25°C, 100 MHz), δ (ppm): 148.6 (OCOO), 130.6 and 129.2 (CH=CH), 72.4 (CH₂-OCOO), 32.0 (CH₂), 31.4 (CH-CH₂-OCOO), 29.9-22.7 (CH₂). 27.3 (CH₂-CH=CH), 14.1 (CH₃). IR (cm⁻¹): 3000, 2979, 2925, 2853, 1754.

- **Dec-5CC synthesis:** The commercially available 1,2-epoxydodecane (3.02 g, 16.4 mmol) was first pre-mixed with TBABr (0.09 g, 0.28 mmol, 3 w.%) and 5 mL of acetone. Afterwards, the mixture was placed in a high-pressure autoclave and heated up at 80°C. Once the temperature got stabilized, CO₂ was slowly introduced into the reactor until 40 bars. After 3 days, the reactor was cooled down to RT and slowly depressurized to the atmospheric pressure. The ¹H NMR of the final mixture revealed a conversion of 98%. The **Dec-5CC** was purified by flash chromatography using a mixture of cyclohexane: ethyl acetate (100:0 to 88:12). The product was isolated as transparent viscous oil with a yield of 90%. ¹H NMR (CDCl₃, 25°C, 400 MHz), δ (ppm): 4.70 (m, 1H), 4.49 (t, 1H), 4.06 (t, 1H), 1.80 (m, 1H), 1.65 (1H), 1.40-1.26 (16H), 0.89(t, 3H). ¹³C-NMR (CDCl₃, 25°C, 100 MHz), δ (ppm): 155.3 (OCOO), 77.4 (CH-OCOO), 69.5 (CH₂-OCOO), 34.0 (CH₂-CH-OCOO), 31.9-22.7 (CH₂), 14.2 (CH₃). IR (cm⁻¹): 2925, 2848, 1789.

Bis-cyclic carbonate synthesis

• **Und-bCC-ether synthesis:** Into a round-bottom flask, the *UndCC-ether* (5 g, 18.5 mmol) and 1st generation Grubbs catalyst (76.2 mg, 0.093 mmol, 0.5 mol.%) were charged under nitrogen. The contents were vigorously stirred at 35°C for 24h. The equilibrium was driven thank to the removal under vacuum of the produced ethylene. The product was then purified with flash chromatography using a mixture of dichloromethane and methanol as eluent (100:0 to 95:5). *Und-bCC-ether* was obtained as a clear grey powder. Yield: 53%. ¹H NMR (CDCl₃, 25°C, 400 MHz), δ (ppm): 5.38 (m, 2H), 4.80 (m, 2H), 4.49 and 4.39 (t, 4H), 3.64 (m, 4H), 3.50 (t, 4H), 1.97 (m, 4H), 1.56 (m, 6H), 1.27 (m, 26H). ¹³C NMR (CDCl₃, 25°C, 100 MHz), δ (ppm): 154.5 (OCOO), 130.9 (CH=CH), 75.2 (CH₂-CH-CH₂O), 72.2 (CH-CH₂-OCH₂), 69.6 (CH₂-CH-CH₂O), 66.3 (CH₂CH-CH₂O), 32.7 (CH₂-CH=CH), 29.9-26.1 (CH₂). IR (cm⁻¹): 2923, 2850, 1792, 1141. T_m=54°C.

• **Seb-bCC-ether synthesis:** (i) 1,10-decanediol (20 g, 0.115 mol) was stirred with epichlorohydrin (53 g, 0.573 mol, 5 eq.) and TBABr (1.74 g, 5.39 mmol, 0.047 eq.) at room temperature for 30 min. KOH pellets were added (32.2 g, 0.574 mol, 5 eq.) and the mixture reaction was stirred overnight. The work-up was similar than for *Und-epoxide*. Conversion: 85%. *Seb-epoxide* was purified by flash chromatography using a mixture of cyclohexane and ethyl acetate (100:0 to 60:40) and obtained as a viscous transparent liquid. Yield: 31%. ¹H NMR (CDCl₃, 25°C, 400 MHz), δ (ppm): 3.61 and 3.31 (dd, 4H), 3.42 (m, 4H), 3.08 (m, 2H), 2.74 and 2.53 (t, 4H), 1.51 (m, 4H), 1.21 (m, 12H). ¹³C NMR (CDCl₃, 25°C, 100 MHz), δ (ppm): 71.9 (OCH₂-CH₂), 71.7 (CH₂O-CH₂CH₂), 50.9 (CH₂-CH-CH₂O), 44.6 (CH₂-CH-CH₂O), 29.7-26.2 (CH₂). (ii) *Seb-epoxide* was carbonated employing the same procedure of carbonation as for *UndCC-ether* obtention. Conversion: 100%. *Seb-bCC-ether* was purified by flash chromatography using a mixture of DCM and methanol (100:0 to 97:3), and obtained as a white waxy solid at room temperature. Yield: 98%. ¹H NMR (CDCl₃, 25°C, 400 MHz), δ (ppm): 4.76 (m, 2H), 4.45-4.35 (t, 4H), 3.59 (m, 4H), 3.43 (t, 4H), 1.53 (m, 4H), 1.26 (m, 12H). ¹³C NMR (CDCl₃, 25°C, 100 MHz), δ (ppm): 155.1 (OCOO), 75.2 (CH₂-CH-CH₂O), 72.5 (CH₂O-CH₂-CH₂), 69.6 (CH-CH₂O-CH₂), 66.5 (CH₂-CH-CH₂O), 29.6-25.8 (CH₂). IR (cm⁻¹): 2920, 2841, 1777, 1128, 1041. T_m=54°C.

• **Und-bCC-ester synthesis:** Into a round-bottom flask equipped with a mineral oil bubbler, the *UndCC-ester* (3 g, 5.6 mmol) was mixed with 2 mL of dichloromethane. 1st generation Grubbs catalyst (42.6 mg, 0.028 mmol, 0.5 mol.%) was then charged under nitrogen. The contents were vigorously stirred at room temperature for 24h. The ¹H NMR revealed of conversion of 80%. The product was purified by recrystallization in 10 mL of cold

dichloromethane (-80°C) followed by a filtration and a washing with 30 mL of dichloromethane. **Und-bCC-ester** was obtained as a grey powder. Yield: 44%. ¹H NMR (CDCl₃, 25°C, 400 MHz), δ (ppm): 5.36 (m, 2H), 4.92 (m, 2H), 4.55 and 4.32 (t, 4H), 4.28 (t, 4H), 2.35 (t, 4H), 1.95 (m, 4H), 1.63-1.28 (24H). ¹³C NMR (CDCl₃, 25°C, 100 MHz), δ (ppm): 173.0 (CH₂-OCO-CH₂), 154.5 (OCOO), 130.5 (CH=CH), 73.7 (CH-CH₂-OCO), 65.7 (CH₂-CH-CH₂-OCO), 62.7 (CH-CH₂-OCO), 34.2 (OCO-CH₂-CH₂), 32.0 (CH₂-CH=CH), 29.4-28.5 (CH₂), 24.5 (OCO-CH₂-CH₂). IR (cm⁻¹): 2917, 2850, 1784, 1736. T_m=111°C.

• **Seb-bCC-ester synthesis:** In a round-bottom flask, 2.6 eq. (5.14 g, 43.4 mmol) of glycerol carbonate and 4 eq. (9.02 mL, 66.8 mmol) of triethylamine were diluted in 10 mL of dry dichloromethane. 2.6 eq. (4 g, 16.7 mmol) of sebacyl chloride was slowly added under inert atmosphere at 0°C. The mixture reaction was left 2h at room temperature. Afterwards, the mixture was reconcentrated and 50 mL of petroleum ether was added to extract the **Seb-bCC-ester**. The triethylammonium salts formed during the reaction were filtered and the filtrate was washed three times with 25 mL of a 10 mol.% HCl solution, once with 25 mL of saturated NaHCO₃ solution and finally with 25 mL of brine. ¹H NMR indicated a quantitative conversion. After purification by flash chromatography using a mixture of dichloromethane and methanol (100:0 to 97:3), **Seb-bCC-ester** was obtained in 47% yield as a white powder. ¹H NMR (DMSO-d₆, 25°C, 400 MHz), δ (ppm): 5.01 (m, 2H), 4.56 and 4.25 (t, 4H), 4.29 (t, 4H), 2.31 (t, 4H), 1.53 (m, 4H), 1.25 (8H). ¹³C NMR (DMSO-d₆, 25°C, 100 MHz), δ (ppm): 173.8 (CH₂-OCO-CH₂), 154.1 (OCOO), 74.3 (CH-CH₂-OCO), 66.4 (CH₂-CH-CH₂-OCO), 62.8 (CH-CH₂-OCO), 33.3 (OCO-CH₂-CH₂), 28.5-28.2 (CH₂), 24.2 (OCO-CH₂-CH₂). IR (cm⁻¹): 2936, 2845, 1778, 1730. T_m= 84 °C.

• **b5CC synthesis :** (i) The commercially available 1,2-epoxy-9-decene (7 g, 45.4 mmol) was first pre-mixed with the TBABr (0.21 g, 0.64 mmol, 3 w.%). Then the mixture was placed in a reactor and heated up at 80°C. Once the temperature got stabilized, CO₂ was slowly introduced into the reactor until 50 bars. After 24h, the reactor was cooled down to RT and slowly depressurized to the atmospheric pressure. The ¹H NMR of the final mixture revealed a conversion of 94.5%. The product was purified by flash chromatography using a mixture of cyclohexane: ethyl acetate (100:0 to 70:30). Yield: 50%. ¹H NMR (CDCl₃, 25°C, 400 MHz), δ (ppm): 5.77 (m, 1H), 4.96 (m, 2H), 4.71 (m, 1H), 4.51 (t, 1H), 4.03 (t, 1H), 2.04 (m, 2H), 1.77 (m, 1H), 1.68 (m, 1H), 1.45-1.33 (m, 8H). ¹³C-NMR (CDCl₃, 25°C, 100 MHz), δ (ppm): 155.2 (OCOO), 139.0 (CH=CH₂), 114.5 (CH=CH₂), 77.4 (CH-OCOO), 69.5 (CH₂-OCOO), 34.0 (CH₂-CH-OCOO), 33.8 (CH₂-CH=CH₂), 29.1-28.8 (CH₂), 24.5 (CH₂-CH₂-CH-OCOO). IR (cm⁻¹): 2924, 2856, 1786. (ii) Into a round-bottom flask equipped with a mineral oil

bubbler, 5g (1 eq., 25 mmol) of the carbonated 1,2-epoxy-9-decene was mixed with 50mL of distilled dichloromethane. 3rd generation Grubbs catalyst (76 mg, 0.13 mmol, 0.5 mol.%) was then charged under nitrogen. The contents were vigorously stirred at room temperature. ¹H NMR revealed 93% of conversion in 3 days. Viscous transparent oil was obtained after purification by flash chromatography using 100% of cyclohexane as eluent. Yield: 65%. **b5CC** ¹H NMR (CDCl₃, 25°C, 400 MHz), δ (ppm): 5.37 (m, 2H), 4.69 (m, 2H), 4.49 and 4.03 (t, 4H), 1.96 (m, 4H), 1.78 and 1.66 (m, 4H), 1.46-1.34 (m, 16H). ¹³C-NMR (CDCl₃, 25°C, 100 MHz), δ (ppm): 155.2 (OCOO), 130.4 (CH=CH), 77.1 (CH-OCOO), 69.4 (CH₂-OCOO), 34.0 (CH₂-CH-OCOO), 33.8 (CH₂-CH=CH), 32.5-23.7 (CH₂). IR (cm⁻¹): 2923, 2850, 1786. T_m= -54 °C.

• **DGDC synthesis:** diglycerol (5 g, 30.1 mmol, 1 eq.) was dried under vacuum at 90°C for 2h in a 250 mL-round bottom flask. Dimethyl carbonate (40.65 g, 451.5 mmol, 15 eq.) was then added and the mixture was stirred for 10 additional minutes. Finally, La₂O₃ (0.4902 g, 1.5 mmol, 0.05 eq.) was charged and the resulting heterogeneous mixture was heated at 110°C for 48h under reflux. Conversion was impossible to determine by ¹H NMR. The resulting mixture was filtrated to remove the insoluble catalyst and reconcentrated. The crude product was purified by recrystallization in cold methanol at -80°C and obtained as a white powder, after filtration and evaporation of dimethyl carbonate. Successive recrystallizations could lead to an improved yield of 46%. ¹H NMR (DMSO-d₆, 25°C, 400 MHz), δ (ppm): 4.93 (m, 2H), 4.52 and 4.23 (t, 4H), 3.74 (t, 4H). ¹³C NMR (DMSO-d₆, 25°C, 100 MHz), δ (ppm): 154.9 (OCOO), 74.8 (CH-CH₂-O-CH₂), 69.8 (CH-CH₂-O-CH₂), 66.1 (CH₂-CH-CH₂-O-CH₂). IR (cm⁻¹): 2925, 1773, 1476, 1401, 1165. T_m=73 °C.

• **General procedure for kinetic experiments:** The kinetic experiments were performed in NMR tube at 1 mol.L⁻¹ in DMSO-d₆, generally at 50°C and with a ratio 1:1 between cyclic carbonate and hexylamine. All reagents were dried on molecular sieves or distilled before the reaction. Hexylamine was dried under CaH₂ and distilled of after drying. The cyclic carbonate was directly dried overnight in a NMR tube capped with a septum, under vacuum. 0.5 mL of dried DMSO-d₆ and 12.5 μL of TCB were added *via* the septum and homogenized with the mixture. The hexylamine (66 μL, 0.5 mmol, 1 eq.) was then added just before putting the tube in the NMR apparatus. In the case of DGDC *in situ* kinetic measurements, 2 eq. of hexylamine were used due to the monomer bifunctionality. The reaction mixture was then heated at the reaction temperature. The reaction was monitored with ¹H NMR spectroscopy with the disappearance of the cyclic carbonate protons for 2 days.

• **General procedure for polymerizations :** PHUs were prepared from the *b5CC*, *Und-bCC-ether*, *Und-bCC-ester*, *Seb-bCC-ether* and *Seb-bCC-ester* with 1,10-diaminodecane (10DA), *Und-C20-diamine* (20DA), 1,6-diaminohexane (6DA), 1,3-cyclohexanebis(methylamine) (6cDA) and N,N'-dimethyl-1,6-hexanediamine (m-6DA) as comonomers with a molar ratio 1 : 1. PHU syntheses were performed in DMF (1 mol.L⁻¹) at 70°C into a schlenk tube under magnetic stirring and nitrogen atmosphere for 7 days. Some polymerizations were also achieved in EtOH at 1 mol.L⁻¹ at 70°C under ambient atmosphere. No catalysts were added for the polymerization reactions. Conversions were determined by ¹H NMR spectroscopy after 24h and 7 days of polymerization, following the disappearance of CC protons.

• **General procedure for DGDC polymerization:** DGDC-based PHUs were prepared using 1,4-diaminobutane (4DA), 1,10-decanediamine (10DA), 1,12-dodecanediamine (12DA), *Und-C20-diamine* (20DA), Priamine[®] from CRODA, Jeffamine 400, and Poly(ethylene glycol) (2000 g.mol⁻¹) diamine terminated as comonomers with a molar ratio 1 : 1. Polymerizations were processed in bulk (at 70 or 130°C) or in DMF (1 mol.L⁻¹) at 70°C into a schlenk tube under magnetic stirring and nitrogen atmosphere for several days. Some polymerizations were also achieved in EtOH at 1 mol.L⁻¹ at 70°C. Conversions were determined by ¹H NMR spectroscopy after 24h.

• **General procedure for nano-precipitation:** The polymer was dissolved in 1 mL of THF at 10 mg/mL and the resulting solution was added drop-wise to 10 mL of water under magnetic stirring. Then, THF was evaporated under the fume hood for 2 days before being analyzed by dynamic light scattering (DLS). The samples were filtered through a 1µm filter before DLS analysis.

• **General procedure for TEM grid preparation:** TEM grids were prepared by depositing the filtered solution used for DLS onto a copper grid and the excess solution was removed with a filter paper before being dried under ambient air for 1.5 min. For negative stained, a drop of an uranyl acetate solution (1 w.%) was placed on the grid and dried for 1.5 min after removal of the excess with a filter paper.

Supporting Information

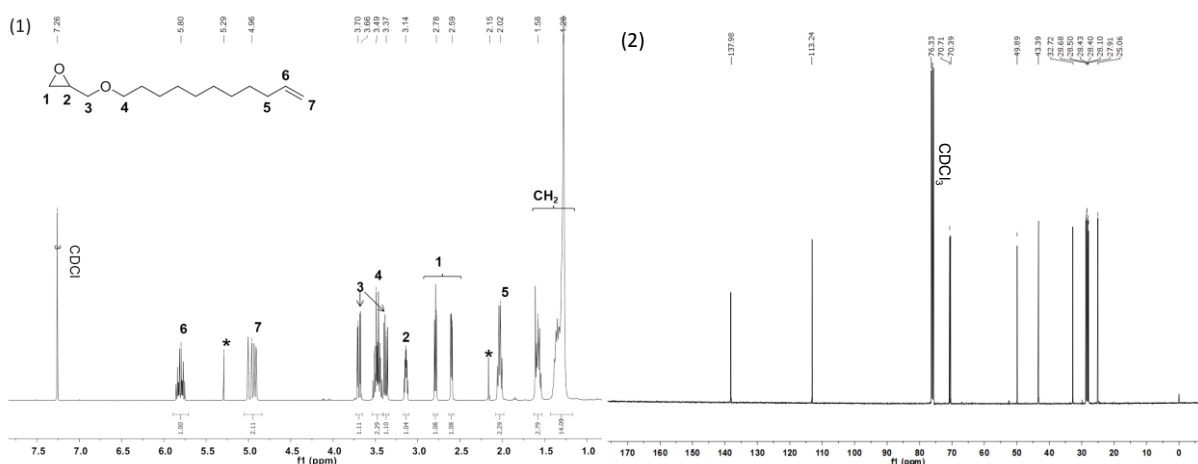


Figure ESI 1 - Evidence of the formation of Und-epoxide: (1) ¹H NMR and (2) ¹³C NMR. (Analysis performed in CDCl₃, *: residual solvents)

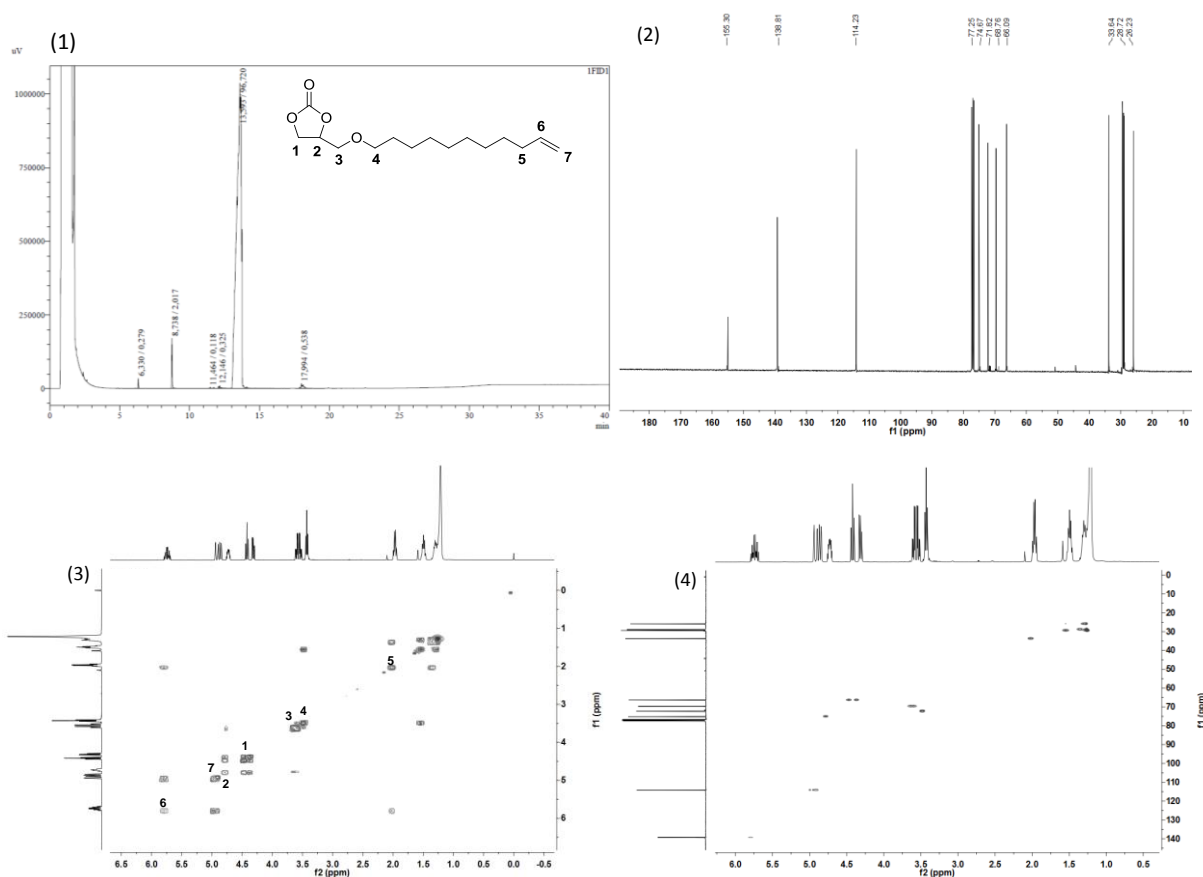


Figure ESI 2- Characterization of UndCC-ether (1) Gas chromatography (96.7% purity), (2) ¹³C NMR, (3) ¹H-¹H COSY NMR and (4) ¹H-¹³C HSQC-NMR. (Analysis performed in CDCl₃)

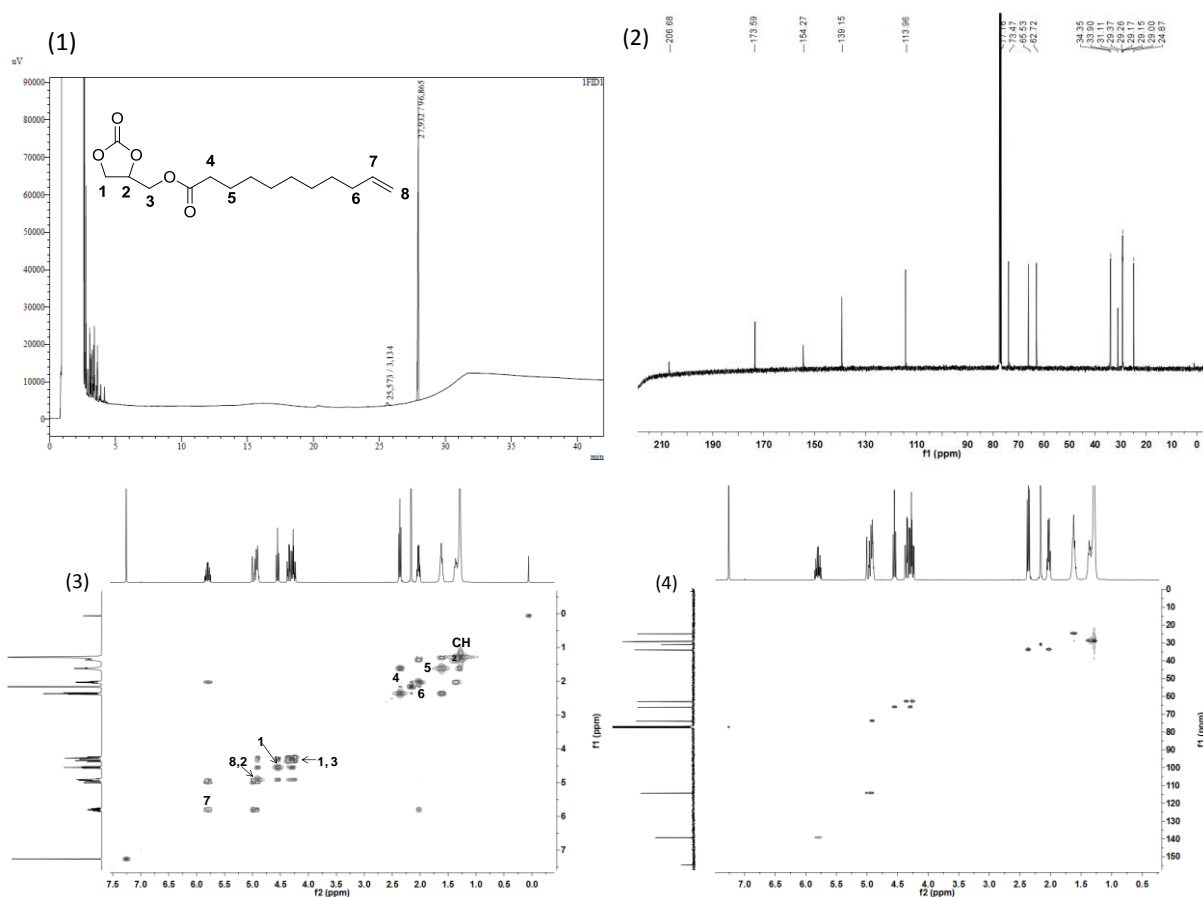
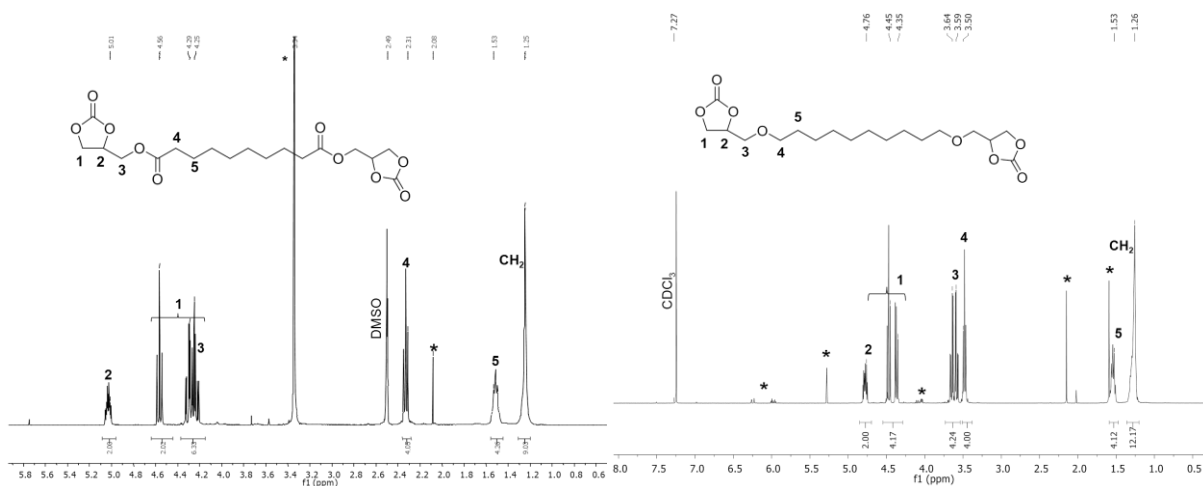


Figure ESI 3- Purified UndCC-ester (1) Gas Chromatography (96.8 % purity), (2) ¹³C NMR, (3) ¹H-¹H COSY NMR and (4) ¹H-¹³C HSQC-NMR. (Analysis performed in CDCl₃, *: residual solvents)



ESI Figure 4- ¹H NMR spectrum of Seb-bCC-ester in DMSO-d₆. (left) and Seb-bCC-ether in CDCl₃. (*: residual solvents and impurities)

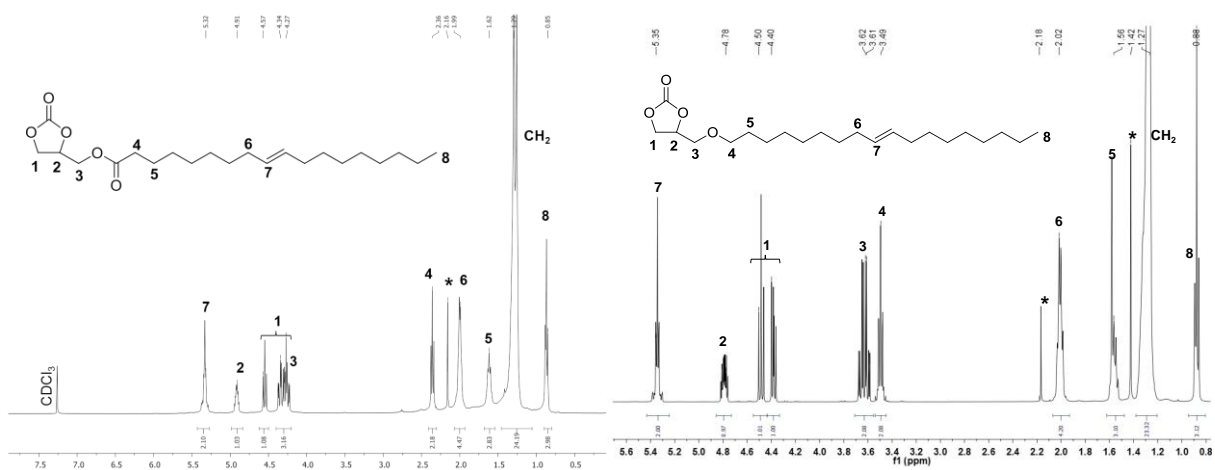


Figure ESI 5- ¹H NMR spectrum of OleylCC-ester (left) and OleylCC-ether (right) (Analysis performed in CDCl₃, *: residual solvents).

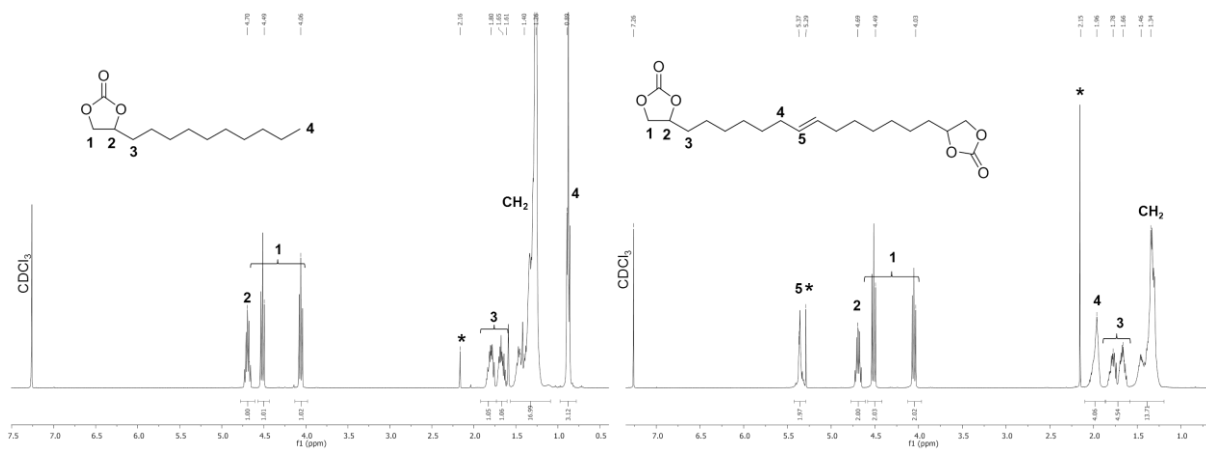
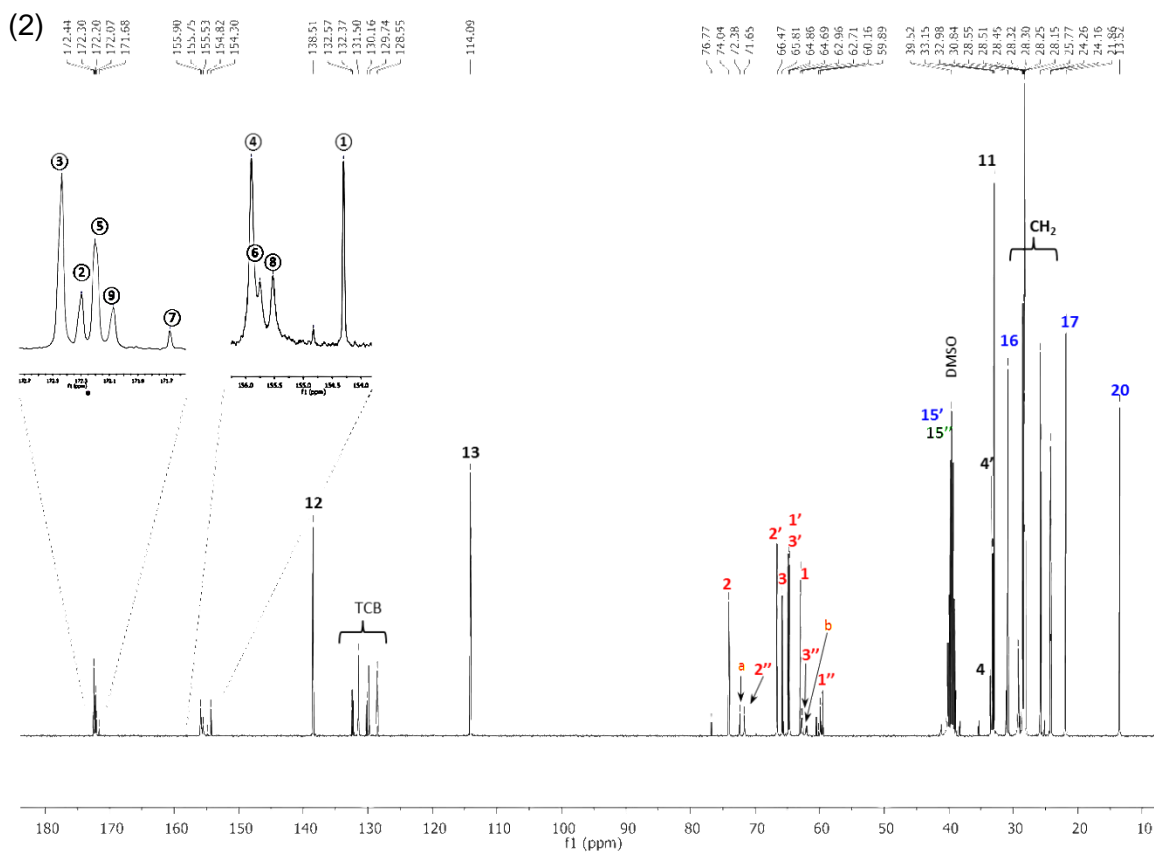
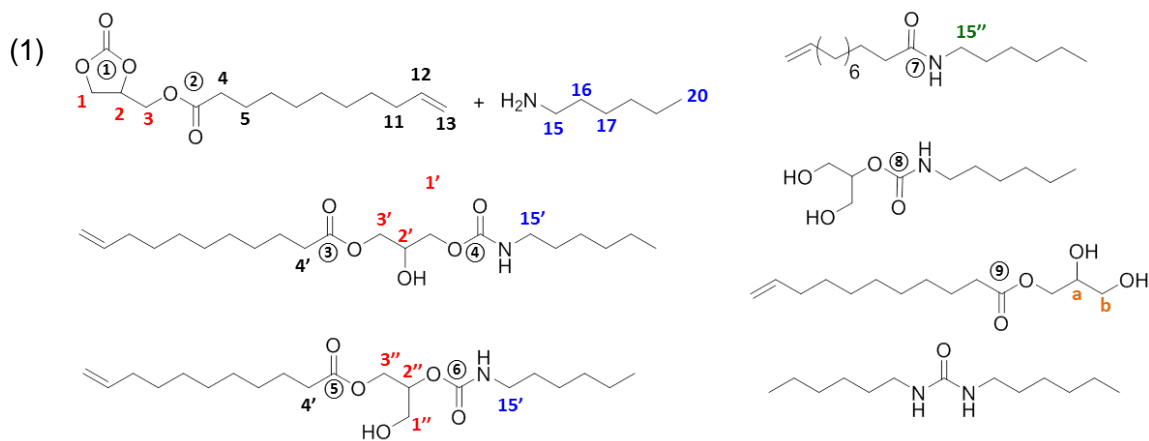


Figure ESI 6 - ¹H NMR spectrum of Dec-5CC (left) and b5CC (right) (Analysis performed in CDCl₃, (* : residual solvents)



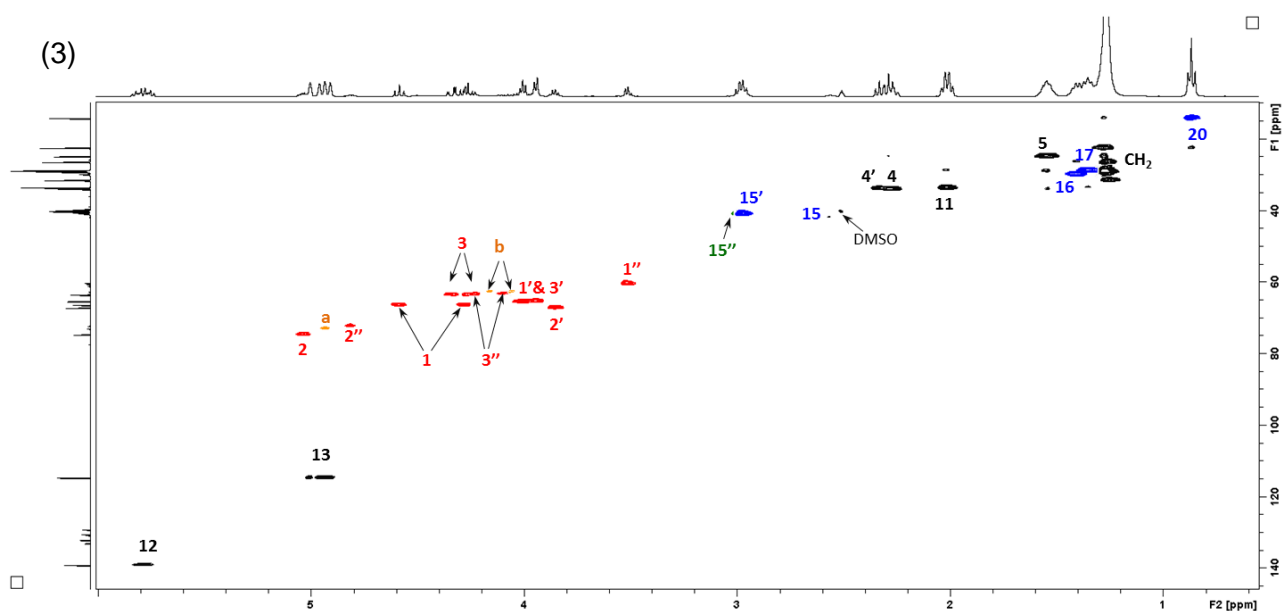


Figure ESI 7 – (1) Scheme of the different molecules identified by (2) ^{13}C and (3) ^1H - ^{13}C HSQC during the model reaction between UndCC-ester and hexylamine (ratio 1:1, in DMSO- d_6 at 50°C).

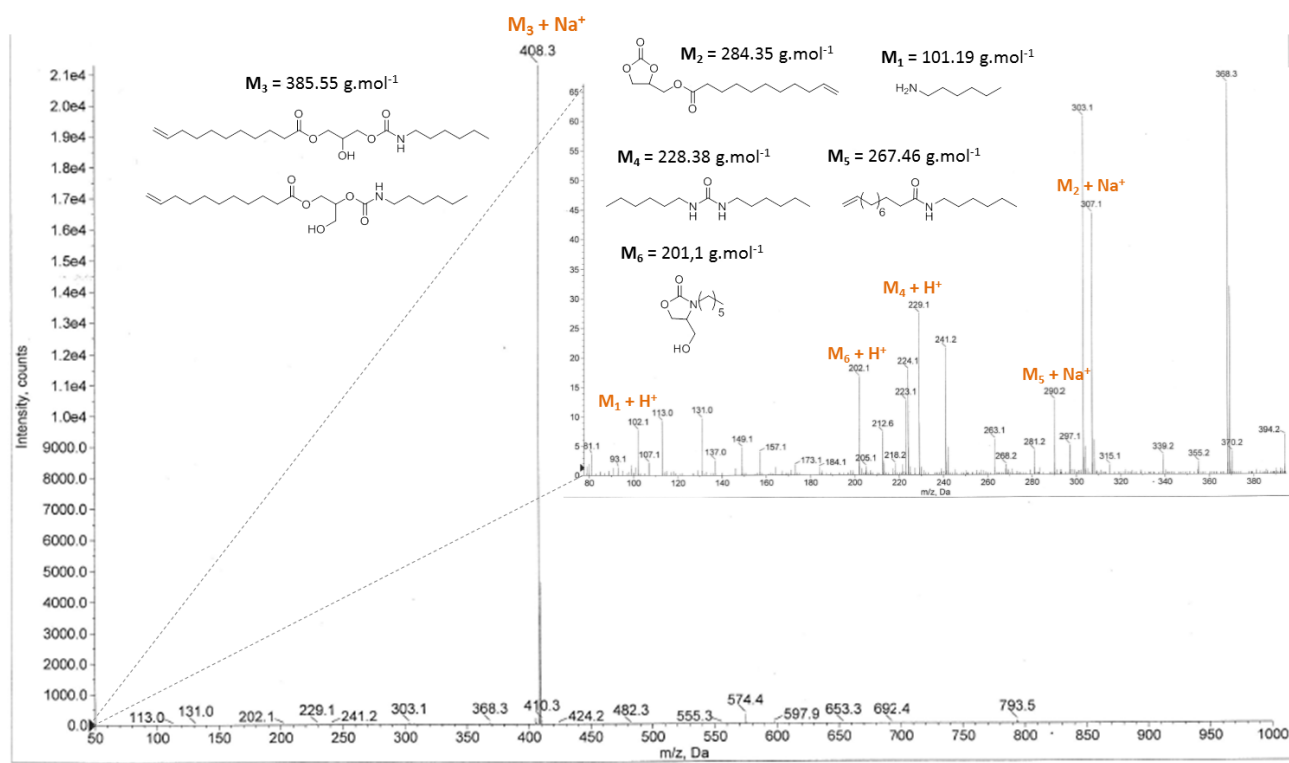


Figure ESI 8 – Mass spectrum (obtained by ESI) of the reaction between UndCC-ester and hexylamine at 50°C in bulk, with a ratio 1:1.

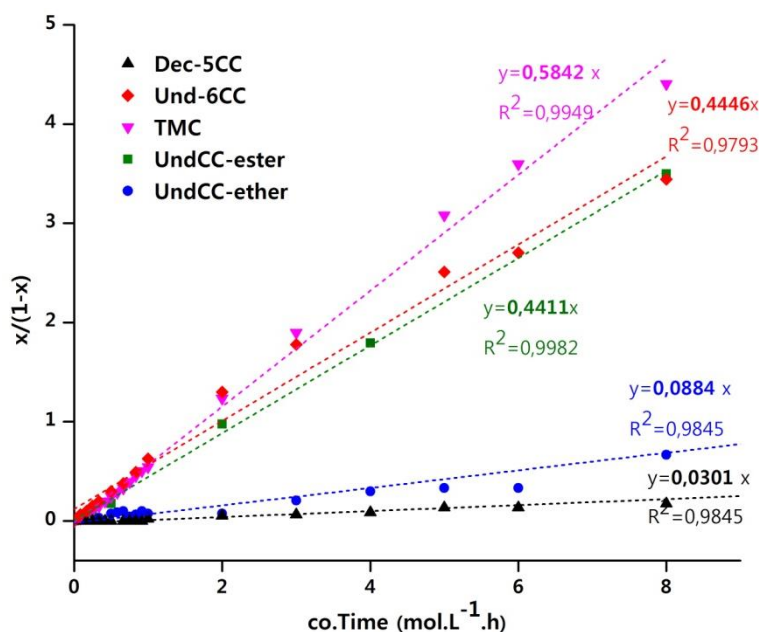


Figure ESI 9- 2nd order Kinetic law: Time-(x/(1-x)) relationships for the reactions of cyclic carbonates with hexylamine, at 50°C and in DMSO-d6 (1 mol.L⁻¹).

$$\% \text{ Urea} = \frac{\int H_{\text{urea}}}{\int H_{\text{urea}} + \int H_{\text{amide}} + \int H_{\text{urethane}}} \quad (E)$$

$$\% \text{ Amide} = \frac{\int H_{\text{amide}}}{\int H_{\text{urea}} + \int H_{\text{amide}} + \int H_{\text{urethane}}} \quad (E')$$

$$\% \text{ Urethane} = \frac{\int H_{\text{urethane}}}{\int H_{\text{urea}} + \int H_{\text{amide}} + \int H_{\text{urethane}}} \quad (E'')$$

Formula ESI 1 - Formula used for the calculation of % of urea, amide and urethane formed during kinetic measurements and polymerization, using ¹H NMR integrations of labile protons (H_{urea}, H_{amide} and H_{urethane}) in DMSO-d6 .

$$k_{app} = A_{app} \cdot e^{\frac{Ea}{RT}}$$

Note: The activation energy is not the only parameter to take into account in kinetic analysis. In the Arrhénius equation, A_{app} is the pre-exponential factor that indicates the rate of efficient collision. The bigger A_{app}, the more reactive the monomer is. A_{app} was calculated for 5CC and 6CC synthesized by Endo and coll.¹⁵ and for *UndCC-ester*.

$$A_{app} (6CC) = 13570 \text{ L}\cdot\text{mol}^{-1}\cdot\text{h}^{-1};$$

$$A_{app} (5CC) = 1.72 \text{ L}\cdot\text{mol}^{-1}\cdot\text{h}^{-1};$$

$$A_{app} (\text{UndCC-ester}) = 10282 \text{ L}\cdot\text{mol}^{-1}\cdot\text{h}^{-1}.$$

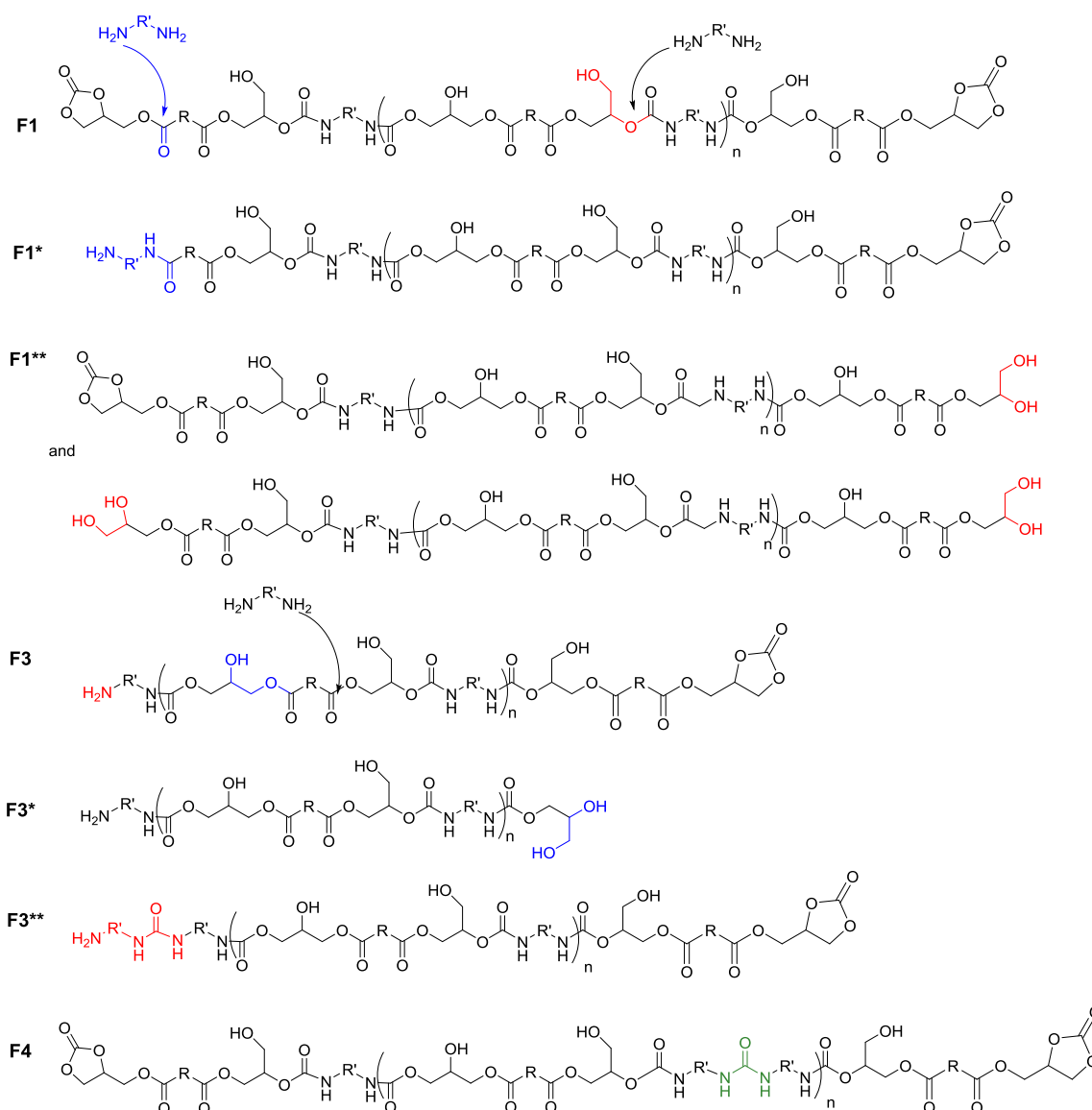
Formula ESI 2 – Arrhénius equation and calculation of A_{app} for 5CC, 6CC (Endo and coll.) and UndCC-ester.

PHU families	Description	Reaction	PHU 1 ($M_{\text{unit}}=712.49 \text{ g}\cdot\text{mol}^{-1}$)
F1	C-(C _{n-1} -A _n)-C	Polyaddition : urethane formation	$n^*(M_{\text{unit}})+M_{\text{C}}+M_{\text{Na}}$
F2	C-(C _n -A _{n-1})-A	Polyaddition : urethane formation	$n^*(M_{\text{unit}})+M_{\text{A}}+M_{\text{Na}}$
F3	A-(C _n -A _n)-C	Polyaddition : urethane formation	$(n+1)^*(M_{\text{unit}})+M_{\text{Na}}$
F4	C-(C _{n-1} -U ^A -A _n)-C	1 Urea linkage within the chain	$n^*(M_{\text{unit}})+M_{\text{C}}+M_{\text{urea}}+M_{\text{Na}}$
F5	C-(C _{n-1} -U ^A -U ^A -A _n)-C	2 Urea linkages within the chain	$n^*(M_{\text{unit}})+M_{\text{C}}+2M_{\text{urea}}+M_{\text{Na}}$
F1*	A _{amide} -(C _{n-1} -A _n)-C	Transamidation at the chain end or by cyclisation	$n^*(M_{\text{unit}})-M_{\text{GC}}+M_{\text{amine}}+M_{\text{Na}}$
F3*	A-(C _n -A _n)-C _{GC}	Transamidation intra-chain	$(n+1)^*(M_{\text{unit}})+M_{\text{GC}}+M_{\text{Na}}$
F1**	C-(C _{n-1} -A _n)-C ^{OH} C ^{OH} -(C _{n-1} -A _n)-C ^{OH}	Urea formation intra-chain resulting in the formation of hydroxyl groups at the chain-end	$n^*(M_{\text{unit}})+M_{\text{C}}-M_{\text{C=O}}+2M_{\text{H}}+M_{\text{Na}}$ $n^*(M_{\text{unit}})+M_{\text{C}}-2M_{\text{C=O}}+4M_{\text{H}}+M_{\text{Na}}$
F3**	U ^A -(C _n -A _n)-C	Urea formation at the chain end	$(n+1)^*(M_{\text{unit}})+M_{\text{urea}}+M_{\text{Na}}$

*amide formation

** urea formation

Abbreviations are as followed: C=*Und-bCC-ester* with $M_{\text{C}}=540.29 \text{ g}\cdot\text{mol}^{-1}$; A=decane-1,10-diamine with $M_{\text{A}}=172.19 \text{ g}\cdot\text{mol}^{-1}$; U^A=urea linkage on A with $M_{\text{urea}}=M_{\text{A}}+M_{\text{C=O}}-2M_{\text{H}}=198.19 \text{ g}\cdot\text{mol}^{-1}$; GC=glycerol carbonate and equivalents in mass, with $M_{\text{GC}}=118.3 \text{ g}\cdot\text{mol}^{-1}$; C^{OH}: chain end produced by urea formation: $M_{\text{COH}}=M_{\text{C}}-M_{\text{C=O}}+2M_{\text{H}}=514.29 \text{ g}\cdot\text{mol}^{-1}$



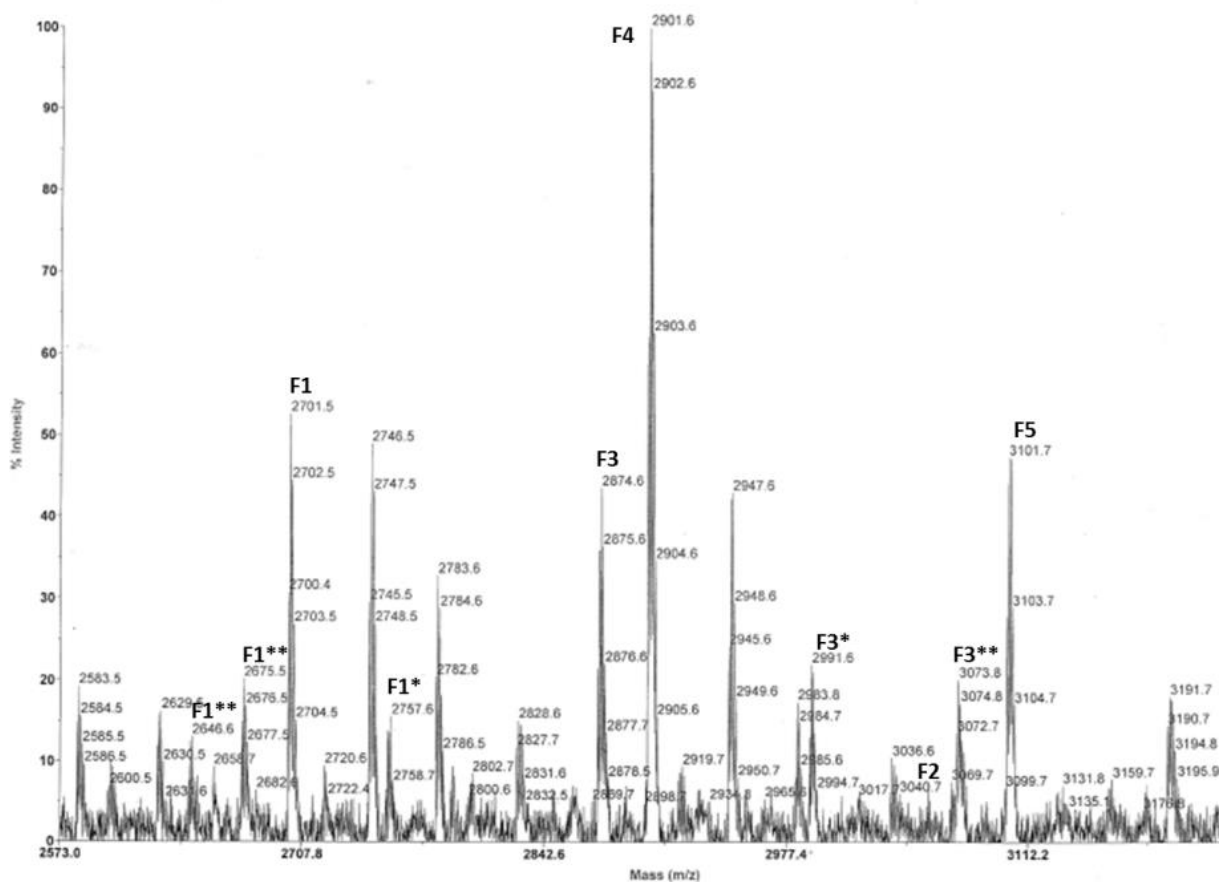
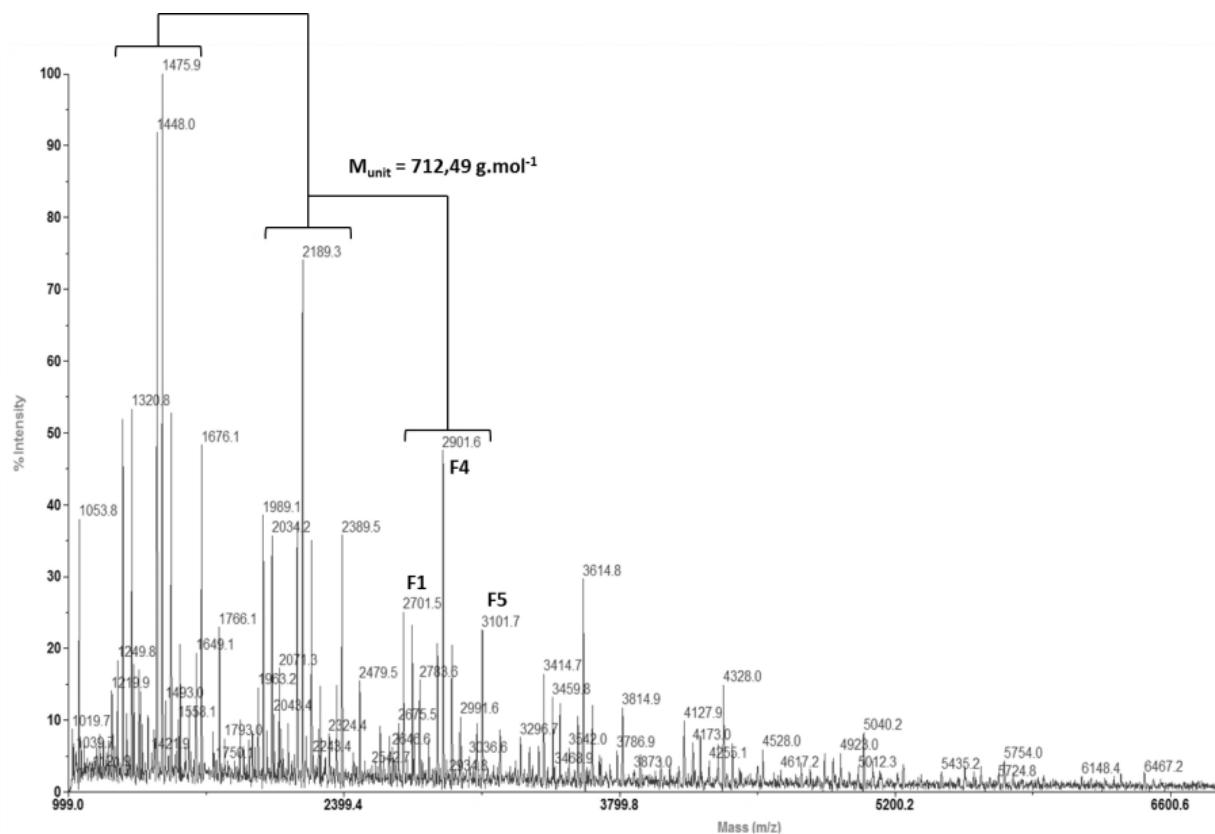


Figure ESI 10 – Different PHU families in the sample PHU 4 visible in mass spectrometry (technique MALDI-TOF) (Polymer synthesized in part 1.3.).

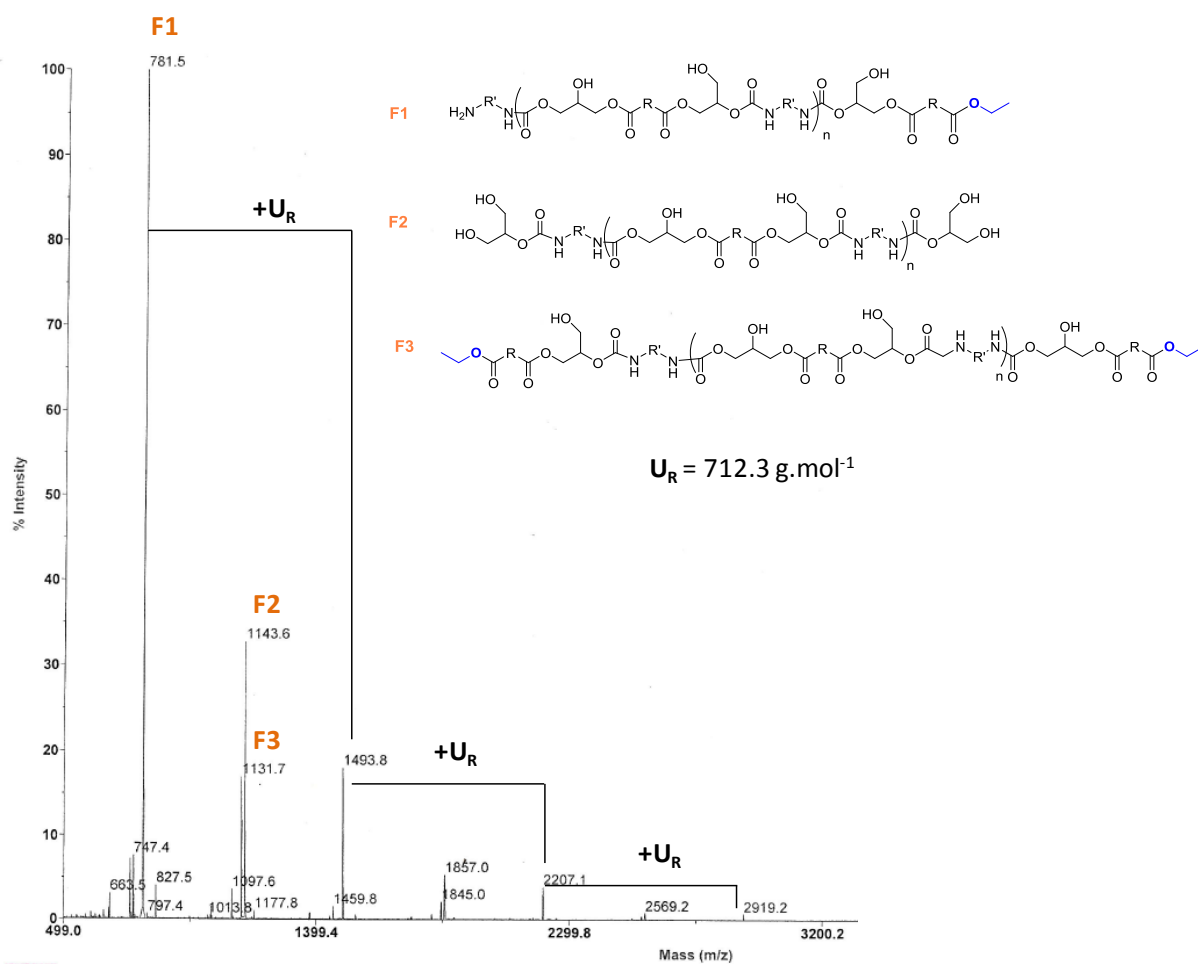


Figure ESI 11 – Different PHU families in the sample PHU 5 visible in mass spectrometry (technique MALDI-TOF) (Polymer synthesized in part 1.3.).

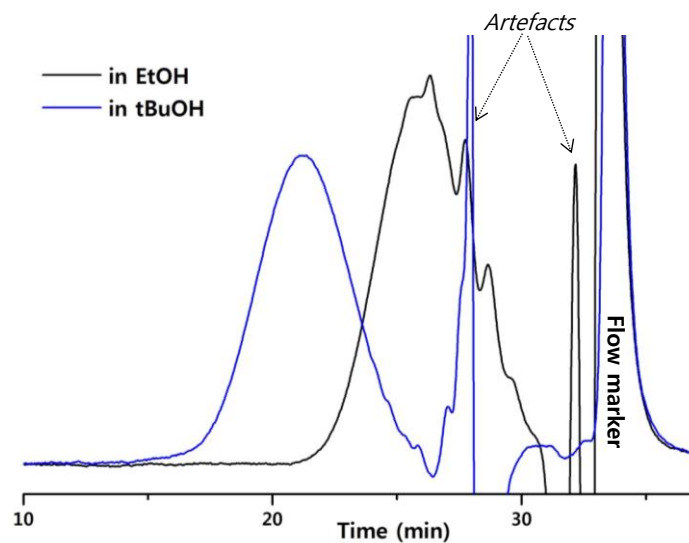


Figure ESI 12 –SEC traces of PHUs synthesized from Und-bCC-ester and 10DA in EtOH and tBuOH at 70°C for 7 days and 24h respectively (SEC in DMF, LiB, PS standards).

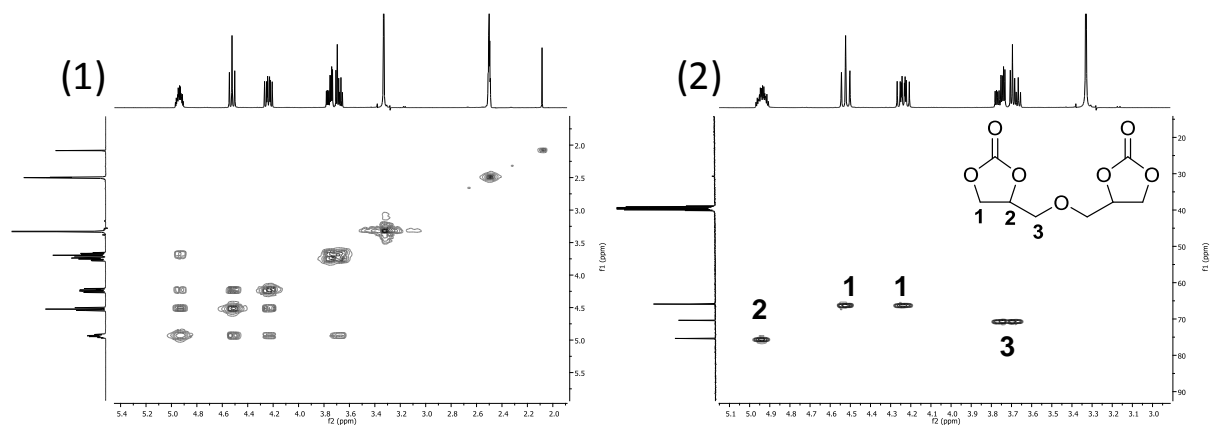


Figure ESI 13- Purified DGDC (1) ^1H - ^1H COSY NMR and (2) ^1H - ^{13}C HSQC-NMR.
(Analysis performed in DMSO- d_6 .)

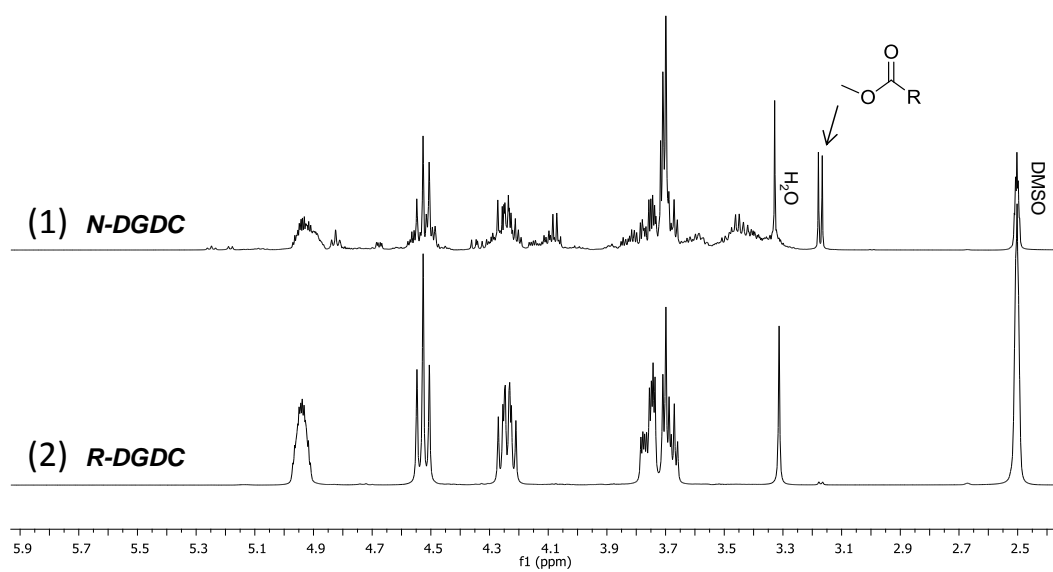


Figure ESI 14 – Stacked ^1H NMR spectra of (1) N-DGDC and (2) R-DGDC in DMSO- d_6 .

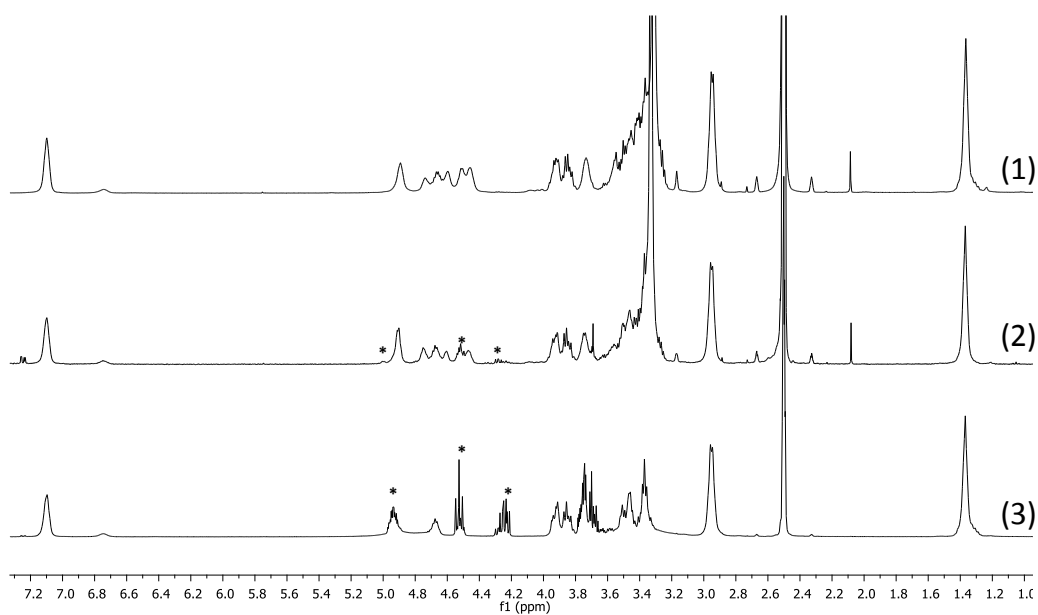


Figure ESI 15 – Stacked ^1H NMR spectra of (1) PHU 10 from N-DGDC, (2) PHU 11 from Raw-DGDC and (3) PHU 12 from R-DGDC in DMSO- d_6 (Polymers synthesized in part 2.2.2.,*: residual monomers).

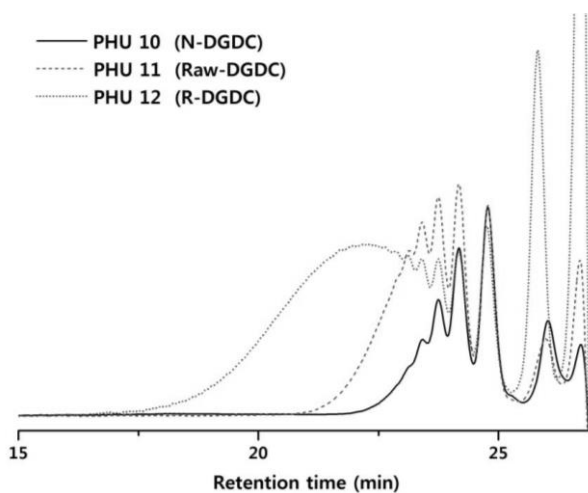


Figure ESI 16 – SEC traces of PHU 10 from N-DGDC, PHU 11 from Raw-DGDC and PHU 12 from R-DGDC (Polymers synthesized in part 2.2.2., SEC in DMF, LiBr, PS standards).

Chapter 4

Fatty acid-based sulfur-activated cyclic carbonates via thiol-ene “click” chemistry towards PHUs and post-functionalization.

Keywords: Thiol-ene, activated cyclic carbonates, fatty acid, poly(hydroxyurethane)s, post-functionalization, sulfone, sulfonium salts.

Mots-clés: Thiol-ene, carbonates cycliques activés, ester d'acides gras, poly(hydroxyuréthane)s, post-fonctionnalisation, sulfone, sels de sulfonium.

Table of contents

Introduction	193
1. Sulfur-activated cyclic carbonate synthesis and characterization	195
1.1. Sulfur-activated lipidic 5CC synthesis	195
1.2. Reactivity of sulfur-activated cyclic carbonates	198
1.3. Sulfone-activated CC and reactivity toward aminolysis	200
2. PHUs from sulfur-activated monomers: synthesis and post-functionalization	203
2.1. PHUs from sulfur activated monomers	203
2.2. Post-functionalization of sulfur-containing PHUs	207
2.2.1. Sulfonation	208
2.2.2. Sulfonium salts synthesis	211
Conclusions	214
References	215
Experimental and Supporting Information	216

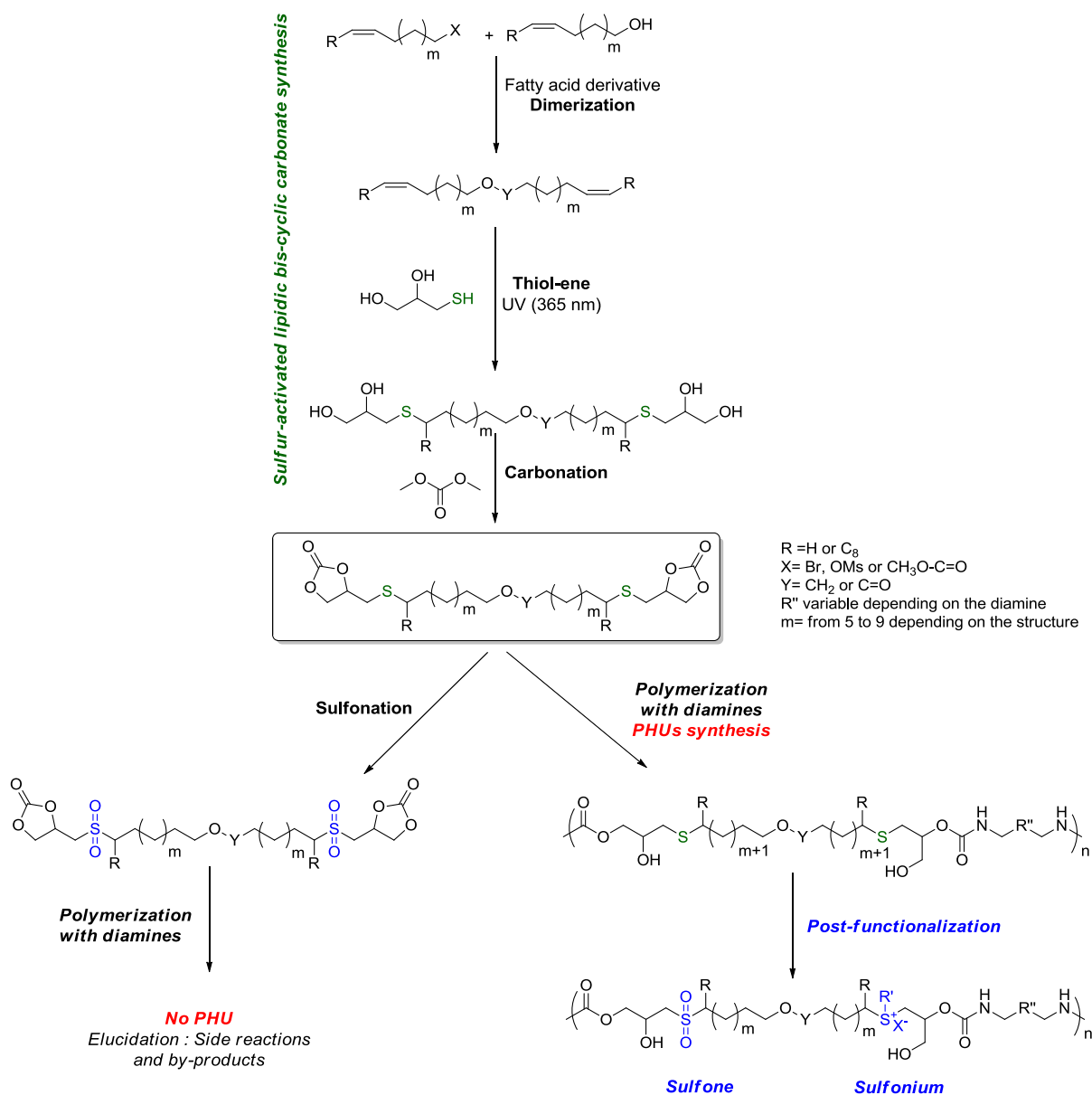
Introduction

The previous chapter described the development of a versatile platform of ether- and ester-activated cyclic carbonate monomers for poly(hydroxyurethane)s synthesis as a competitive route in comparison to the alcohol/isocyanate one towards thermoplastic PUs.

The present work is dedicated to the design of novel sulfur-activated cyclic carbonates from thioglycerol and fatty acid derivatives. In this methodology, the sulfur atom is introduced in β position of the 5-membered ring cyclic carbonate by thiol-ene “click” coupling reaction on fatty acid-based dienes already described in the Chapter 2. The so-formed monomers were characterized by FTIR, NMR spectroscopies, HPLC and DSC. The reactivity of a sulfur-activated mono-cyclic carbonate was assessed by the kinetic study of its model reaction with hexylamine. Furthermore, the derivatization of such sulfur-based cyclic carbonate in its corresponding sulfone was achieved. The fast reaction between sulfone-activated cyclic carbonate and amine was studied and characterized by NMR and ESI.

Fatty acid-based sulfur-activated bCC were polymerized with diamines in solvent without employing catalyst. FTIR, NMR, SEC, DSC and TGA were performed to investigate the PHUs chemical structure, molar masses and thermal properties. Finally, the so-formed PHUs were post-functionalized by introducing sulfone and sulfonium moieties. The impact of these chemical modifications was mostly studied on their solubility and thermal stability. The Scheme 1 summarizes the strategy employed in the present Chapter.

Strategy adopted in Chapter 4



Scheme 1 - Strategy adopted for cyclic carbonate activation by a sulfur atom in β position nearby the cycle.

1. Sulfur-activated cyclic carbonate synthesis and characterization

Only few works already reported the synthesis of sulfur-based cyclic carbonates towards PHU syntheses.¹⁻⁵ Among them, only one research team synthesized bis-cyclic carbonates displaying a sulfur atom in β position nearby the carbonate by reacting a tosylated glycerol carbonate with several dithiols.³

In this chapter, a new route towards sulfur-activated cyclic carbonates has been set up *via* the thiol-ene coupling of thioglycerol with dimerized fatty acid derivatives, followed by a transcarbonation of the resulting tetraols using dimethyl carbonate (DMC). To the best of our knowledge, this is the first time that the synthesis of bio-based cyclic carbonates with a sulfur atom in β position nearby the cycle was conducted following this pathway.

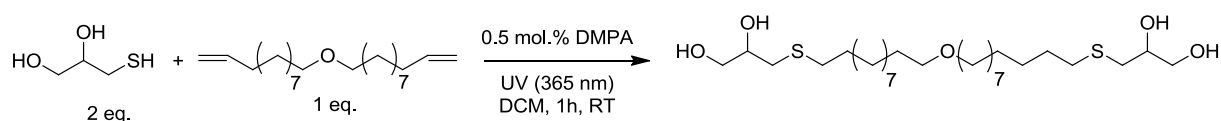
1.1. Sulfur-activated lipidic 5CC synthesis

Thioglycerol, which is derived from the main by-product of triglyceride transesterification (glycerol) appears as an interesting building-block to design sulfur-activated cyclic carbonates. Indeed, the latter was coupled to fatty acid-based dienes using thiol-ene “click” chemistry, widely used in the last decade as a green methodology.⁶

Und(ether)-tetraol, *Oleyl(ether)-tetraol* and *Und(ester)-tetraol* were respectively synthesized from *Und(ether)-diene*, *Oleyl(ether)-diene* and *Und(ester)-diene* with 2 eq. of thioglycerol in a UV reactor (365 nm) at room temperature in DCM, using DMPA as photoinitiator (see Scheme 2). The diene syntheses are detailed in the Supporting Information of the Chapter 2 as the fatty acid-based dienes were already coupled by thiol-ene with cysteamine hydrochloride for aliphatic primary amine preparation.

The conversion of dienes was followed by ¹H NMR with the disappearance of the characteristic protons from the external and internal double bonds at respectively 4.96-5.73 ppm and 5.33 ppm (see Figure 1, (1) and (2)). The terminal unsaturated *Und(ether)-diene* and *Und(ester)-diene* were completely converted into their corresponding tetraols after 1h with 0.5 mol.% of DMPA, and yielded at 99% after a washing procedure. Besides, the isomerization product resulting from the Markovnikov addition was detected by ¹H NMR for *Und(ether)-tetraol* with the characteristic CH₃ shifts below 1 ppm.

With regard to the internal unsaturated *Oleyl(ether)-diene*, 90% conversion into the corresponding tetraol was reached after 48h with higher amount of DMPA (1.5 mol.%). As *Oleyl(ether)-tetraol* is a viscous liquid, the purification was made by flash column chromatography and only 30% yield could be achieved. Thus, the tetraols obtained from castor oil were easily obtained through a green methodology that necessitates a simple purification step leading to high yields. Noteworthy, Meier and coll.⁷ and Li and coll.⁸ have already used this strategy for an AB₂-type monomer synthesis from thioglycerol and methyl undecenoate that was used in self-polycondensation to give linear or hyperbranched polymers.



Scheme 2 - Standard conditions for thiol-ene coupling of fatty acid-based dienes (here Und(ether)-diene) with thioglycerol under UV irradiation (365 nm).

The last step leading to the cyclic carbonate formation was conducted in dimethyl carbonate (15 eq./tetraol) as reactive solvent. The reaction proceeded at 70°C under reflux for 4h with 3 mol.%/diol of K₂CO₃ as catalyst. Indeed, the transcarbonation strategy using linear carbonates to produce cyclic carbonate moieties has been extensively employed.⁹⁻¹¹ However, to the best of our knowledge, this is the first time that a cyclic carbonate originated from thioglycerol was synthesized using the transcarbonation pathway.

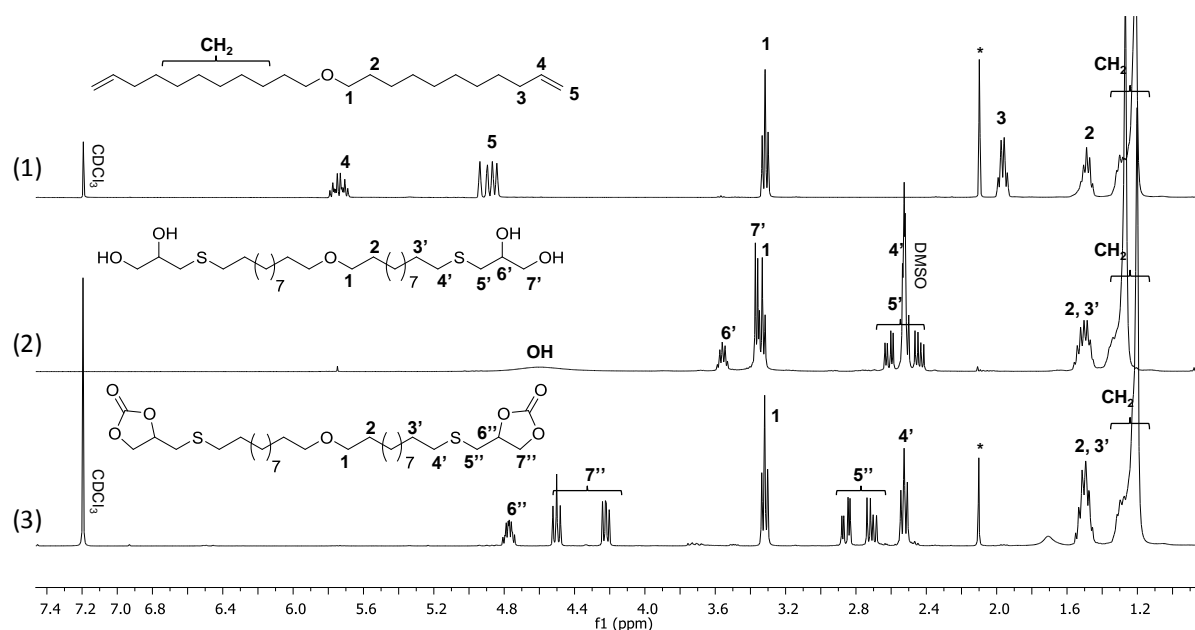


Figure 1 - Stacked ¹H NMR spectra of (1) Und(ether)-diene in CDCl₃ (2) Und(ether)-tetraol in DMSO-d₆ and (3) Und(ether)-bCC-S in CDCl₃ (* impurities or solvent traces).

The reaction was monitored by ^1H NMR, following the appearance of the multiplet at 4.8 ppm and the triplets around 4.2-4.5 ppm that characterize the cyclic carbonate moieties (see Figure 1, (2) and (3)). FTIR measurement could confirm the cyclic carbonate formation with the appearance of a band in the range $1795\text{-}1775\text{ cm}^{-1}$, corresponding to the carbonyl vibration of the cycle (see ESI). After 4h reaction, almost full conversion was attained for all the fatty acid-based tetraols. The crude mixtures were washed three times with brine to remove the excess of thioglycerol, before being dried and reconcentrated. The tetraol purities were determined by HPLC and were comprised between 88.9% and 98.5% without any purification process. Although, the purification by column flash chromatography was tested on *Und(ester)-bCC-S* in the purpose of improving its purity grade (88.9%). However, an extremely poor yield of 2% was obtained since the affinity between sulfur compounds and silica gel is high. Taking in account the low yields obtained after flash chromatography, we decided to use the monomers without further purification.

The ^1H NMR spectra of the sulfur-activated cyclic carbonates after the work-up with the peak assignments are given in Figure 2.

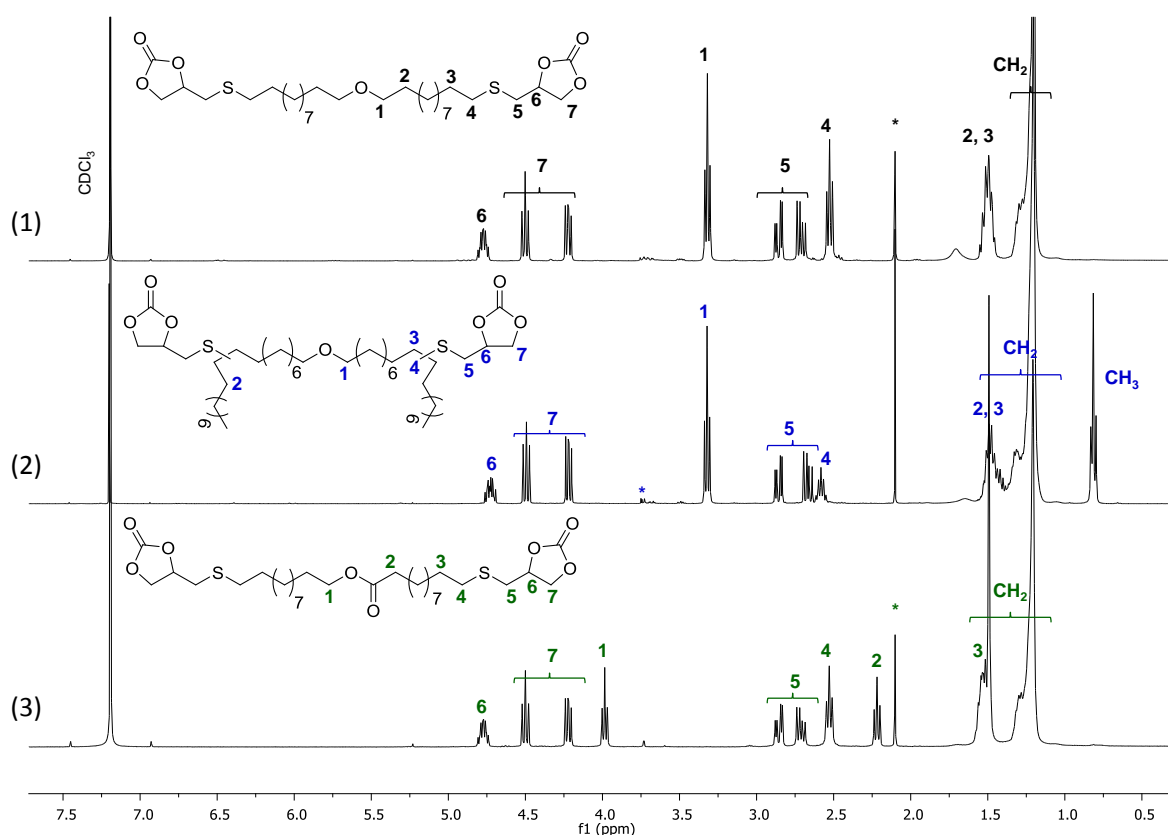
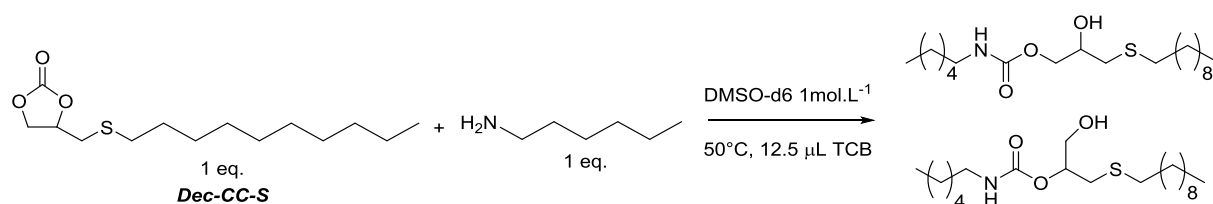


Figure 2 - Stacked ^1H NMR spectra of (1) *Und(ether)-bCC-S* in CDCl_3 (2) *Und(ester)-bCC-S* in CDCl_3 and (3) *Oleyl(ether)-bCC-S* in CDCl_3 (* impurities or solvent traces).

The respective purity and melting points of the monomers, as well as the ^{13}C NMR, ^1H - ^1H COSY NMR, ^1H - ^{13}C HSQC analyses are given in Supporting Information. While bringing flexibility with pendant chains to the central block, a low glass transition temperature of -59°C was displayed by *Oleyl(ether)-bCC-S*. Nonetheless, no significant difference was observed between *Und(ether)-bCC-S* and *Und(ester)-bCC-S* melting temperatures (T_m of 93 and 89°C respectively).

1.2. Reactivity of sulfur-activated cyclic carbonates

In order to quantify the effect brought by the sulfur atom, a sulfur-activated mono-cyclic carbonate was synthesized from 1-decene using the strategy presented in the previous part. The detailed synthesis is reported in Supporting Information and the chemical structure is presented in Scheme 3 (*Dec-CC-S*). *Dec-CC-S* was then reacted with hexylamine in DMSO- d_6 and the model reaction was monitored *in situ* by ^1H NMR for 2 days at 50°C . Trichlorobenzene (TCB) was injected in the NMR tube as external reference.



Scheme 3 – Model reaction of Dec-CC-S aminolysis with hexylamine in DMSO- d_6 (1 mol.L^{-1}) at 50°C .

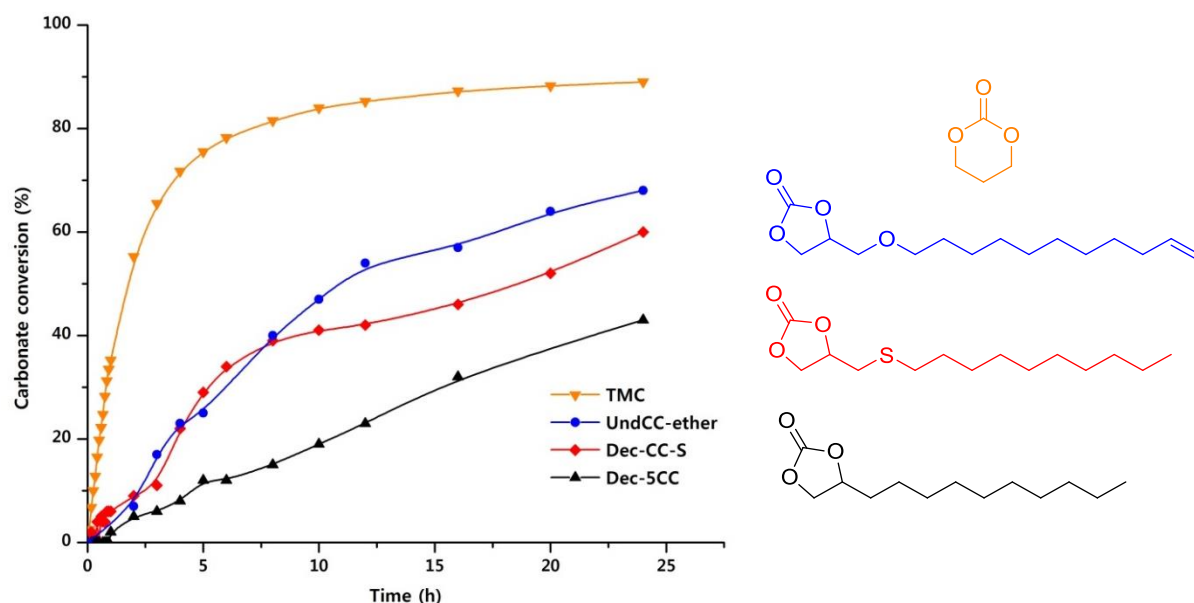
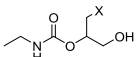
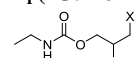


Figure 3 - Effect of various cyclic carbonate activations on the kinetic of the reactions with hexylamine followed by ^1H NMR spectroscopy. (50°C , 1 mol.L^{-1} in DMSO- d_6 , ratio 1:1).

The cyclic carbonate conversions were calculated following the disappearance of the multiplet at 4.8 ppm. The Figure 3 shows the conversion of *Dec-CC-S* as a function of time and its reactivity could be compared with high (TMC) and low (*Dec-5CC*) benchmarks and with *UndCC-ether* synthesized in the Chapter 3. The graphs demonstrated also that ether- and sulfur- cyclic carbonate activations were almost equivalent towards aminolysis. This statement can be correlated to the DFT calculations showing an enthalpy of hydroxyurethane formation $\Delta H_f = -53.76 \text{ kJ}\cdot\text{mol}^{-1}$ close to the one calculated for ether-activated cyclic carbonate in Chapter 3 (see Table 1). The k_{app} were calculated upon the 6 first hours from the kinetic results using Equation 1 in Chapter 3. *Dec-CC-S* exhibited a $k_{app} = 0.08 \text{ L}\cdot\text{mol}^{-1}\cdot\text{h}^{-1}$ in the same range than *UndCC-ether* k_{app} ($0.09 \text{ L}\cdot\text{mol}^{-1}\cdot\text{h}^{-1}$, see Table 1). Additionally, the ratio between primary and secondary alcohols was equal to 22:78 (calculated at 50% of cyclic carbonate conversion) and was in agreement with the one obtained for *UndCC-ether*. Lastly, the percentage of urea formed during aminolysis was higher for a sulfur-activated cyclic carbonate than for *UndCC-ether*, but still in the same order of magnitude.

Table 1 - Kinetic, selectivity and DFT data for ether- and sulfur-activated monocyclic carbonates.

<i>Kinetic and selectivity *</i>		
	<i>UndCC-ether</i>	<i>Dec-CC-S</i>
Urea (%) ¹	2.9	5.9
Urethane (%) ¹	97.1	94.1
Ratio OH _I :OH _{II} ¹	28 : 72	22 : 78
k_{app} (L.mol ⁻¹ .h ⁻¹)	0.09	0.08
<i>DFT Calculations</i>		
-X	-OMe	-SMe
Bond length (Å) 	1.358	1.359
Bond length (Å) 	1.363	1.362
ΔH_f (kJ.mol⁻¹) 	-27.36	-26.19
ΔH_f (kJ.mol⁻¹) 	-55.90	-53.76

*: Determined after 50% of CC conversion; ¹: Proportions calculated with the Equations in ESI[†] of Chapter 3.

1.3. Sulfone-activated CC and reactivity toward aminolysis

The enthalpy of hydroxyurethane formation (ΔH_f) was calculated at $-72.34 \text{ kJ}\cdot\text{mol}^{-1}$ when a sulfone was positioned in β nearby the cyclic carbonate. Thus, the reactivity of *Dec-CC-S* would be enhanced by oxidizing the sulfur atom into sulfone.

To that purpose, *Dec-CC-S* was oxidized using *m*-chloroperbenzoic acid (mCPBA) as oxidative agent. In a first protocol, 2 eq. of mCPBA per sulfur atom were reacted with *Dec-CC-S* in DCM at room temperature for 3h (see Figure 4 conditions (A)). As it is depicted in Figure 4, the ^1H NMR spectrum (2) displayed the presence of sulfoxide traces. Thus, by reacting 3 eq. of mCPBA in DCM at room temperature for 24h, full conversion of sulfur atom in its most oxidized state was achieved (see Figure 4 conditions (B)).

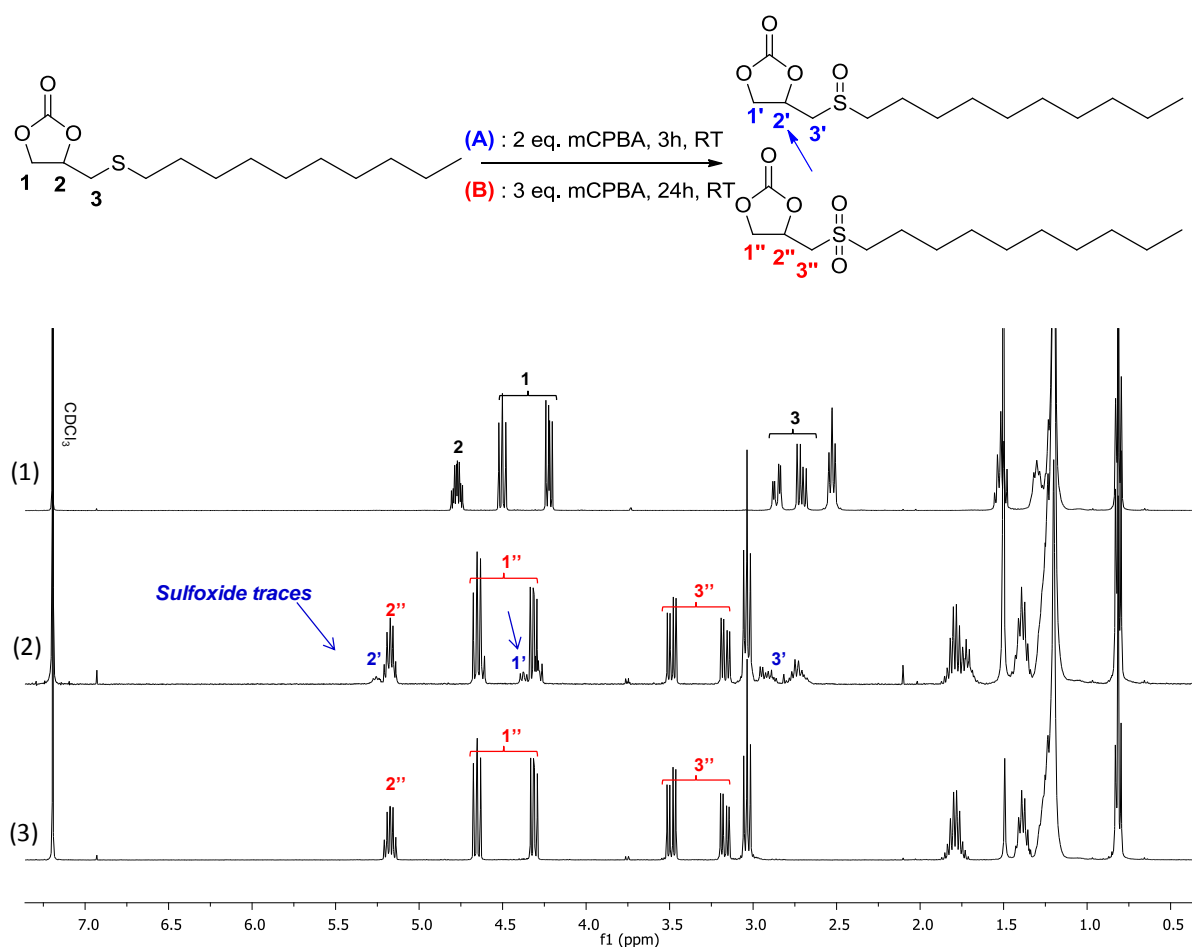
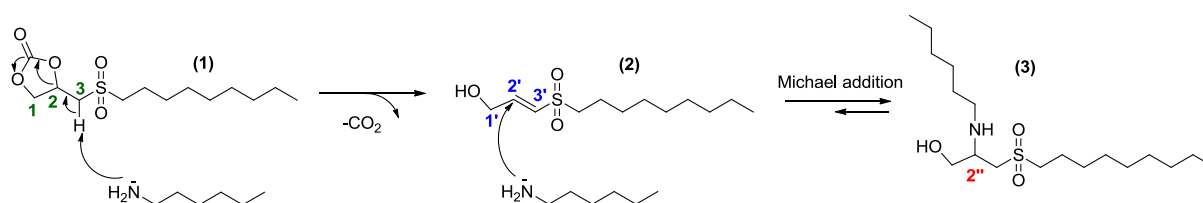


Figure 4 - (A) Reaction conditions for sulfur oxidation of *Dec-CC-S* and (B) optimized conditions for complete sulfonation. Stacked ^1H NMR spectra in CDCl_3 of (1) the starting material, (2) at the end of the reaction in conditions (A) and (3) at the end of the reaction in optimized conditions (B).

The ^1H NMR spectrum (3) in Figure 4 demonstrated the shift of cyclic carbonate signals due to the sulfone function. During the reaction, the acidic form of mCPBA precipitated in DCM and was filtered out before applying several washing (Na_2SO_3 , NaHCO_3 and brine). The sulfone-activated cyclic carbonate called *Dec-CC-sulfone* was recovered as a white powder at

42% yield with a purity of 100% (determined by HPLC). *Und(ester)-bCC-S* was also oxidized into *Und(ester)-bCC-sulfone* using the optimized conditions in order to study its polymerization with diamines (see part 2.1).

In order to quantify the sulfone impact on cyclic carbonate reactivity toward aminolysis, the reaction between *Dec-CC-sulfone* and hexylamine (ratio 1:1) was carried out in DMSO at 70°C for 24h. As soon as the hexylamine was inserted, the immediate disappearance of the cyclic carbonate moiety was observed by ¹H NMR (see Figure 5, (2)) in favour of signals between 6.5 and 7 ppm, characteristic of double bonds. The ESI analysis of the resulting mixture was performed and demonstrated the presence of the major compounds (2) and (3) schematized in Scheme 4 as well as the minor hydroxyurethane product formed by the cyclic carbonate aminolysis (see ESI).



Scheme 4 - Possible side reactions occurring with Dec-CC-sulfone in presence of hexylamine.

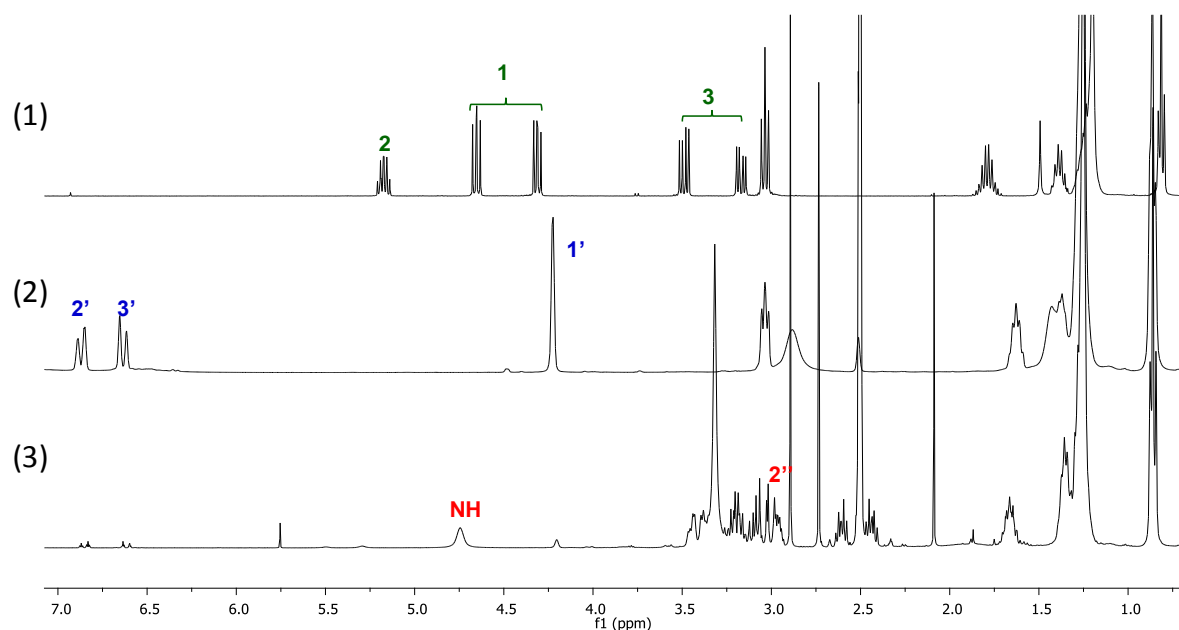


Figure 5 - Stacked ¹H NMR spectra of (1) the starting material in CDCl₃ and the steps (2) and (3) (respectively in CDCl₃ and DMSO-d₆)

The major by-product (**2**) was formed after an immediate deprotonation by hexylamine of the labile proton between the cycle and the sulfone moiety, inducing the formation of a vinyl sulfone that provoked a decarboxylation. This major reaction was confirmed by identifying shifts of the product (**2**) using 1D and 2D NMR spectroscopies and by the observation of bubbling in the reaction media. The ESI analysis suggested the presence of the by-product (**3**) arising from a second attack of the hexylamine on the double bond through a Michael addition. To confirm this result, an additional equivalent of hexylamine was inserted in the mixture after a complete consumption of cyclic carbonates, in order to drive the equilibrium toward the formation of the adduct. The ^1H NMR spectrum (**3**) of the Figure 5 testified the occurrence of the Michael addition on the unsaturation of the vinyl sulfone thanks to the disappearance of the signals at 6.5 and 7 ppm and the appearance of the labile -NH proton at 4.7 ppm. The reactivity of such sulfone towards amines (especially primary ones) following a Michael addition has already been used by Pathak and co-workers¹² on vinyl sulfone modified carbohydrates. More recently, Cruz *et al.*¹³ employed vinyl sulfone as a “click” function for ‘coupling-and-decoupling’ chemistry through a Michael addition of alcohols, amines or thiols, followed by the cleavage step *via* nucleophilic substitutions.

For a better understanding, aniline, that is a less reactive amine with respect to hexylamine, was reacted with *Dec-CC-sulfone* and no reaction occurred as proved by ^1H NMR (see ESI). Contrarily, the presence of basic and non-nucleophilic triethylamine in the mixture reaction enabled the formation of (**2**) (see ESI). Thus, the highly acidic proton located between the cycle and the sulfone is subjected to a deprotonation by the attack of amines. Consequently, such sulfonated monomers are not suitable monomers for thermoplastic PHU synthesis as the cyclic carbonate aminolysis is unfavorable.

We aimed at conducting similar kinetic studies on a mono-cyclic carbonate activated by a sulfonium salt in β position. The alkylation of *Dec-CC-S* was performed in DMF at 80°C overnight using bromobutane as alkylating agent. Unfortunately, the resulting product could not be isolated and purified for a further kinetic experiment. Therefore, the post-functionalization strategy was preferred for the insertion of sulfonium salt moieties into the PHU backbone.

2. PHUs from sulfur-activated monomers: synthesis and post-functionalization

2.1. PHUs from sulfur activated monomers

The polyadditions of the sulfur-activated bis-cyclic carbonates *Und(ether)-bCC-S*, *Und(ester)-bCC-S*, *Oleyl(ether)-bCC-S* and *Und(ester)-bCC-sulfone* with 1,10-diaminodecane (10DA) and *Priamine*[®] 1075 from CRODA as comonomers were carried out in order to investigate the relation between monomer structures and PHU properties. The polymerizations were performed in DMF at 1 mol.L⁻¹ and 70°C under nitrogen atmosphere without any catalyst. The PHUs obtained were further characterized by ¹H NMR, SEC, DSC and TGA without prior quenching and precipitation after 7 days. All the data are reported in Table 2. Some values could not be calculated due to insolubility issues in DMSO-d6 or ¹H NMR signal overlaps.

PHUs formation was followed by ¹H NMR with the disappearance of the signals in α -position nearby the cycle in the ranges 4.2-4.6 ppm, and with the presence of the characteristic protons nearby the nitrogen atom of the urethane linkage at 2.98 ppm (see Figure 6).

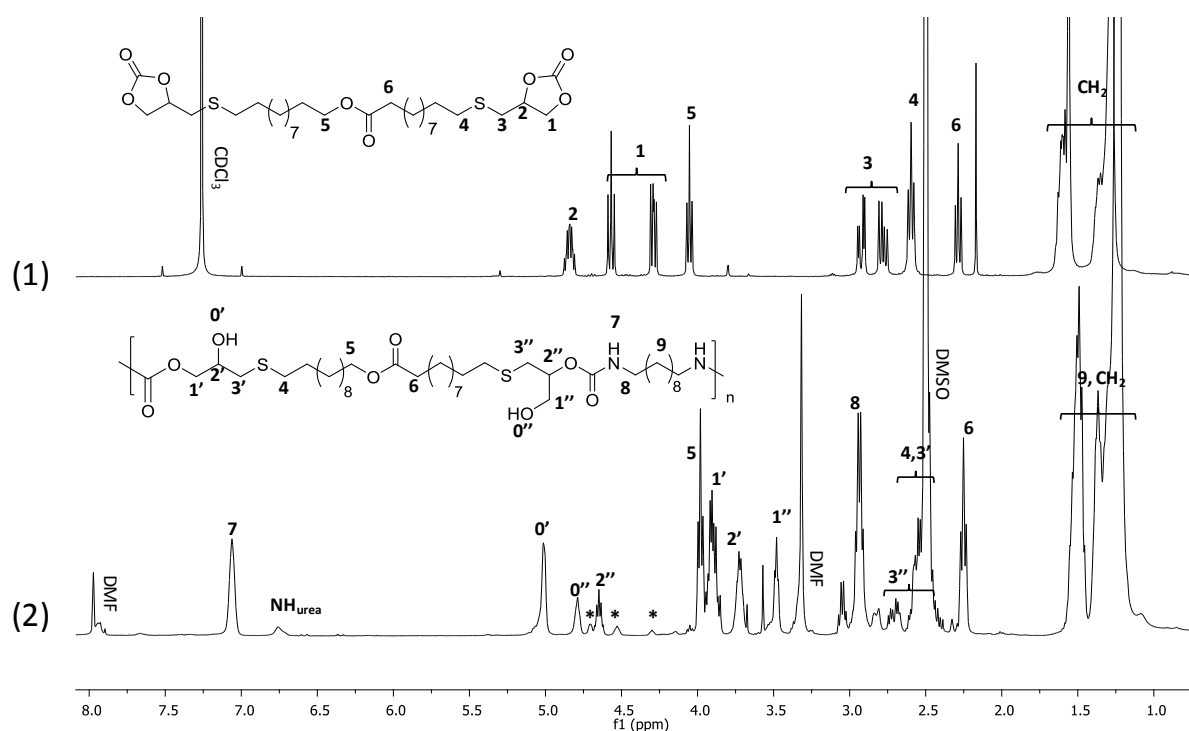


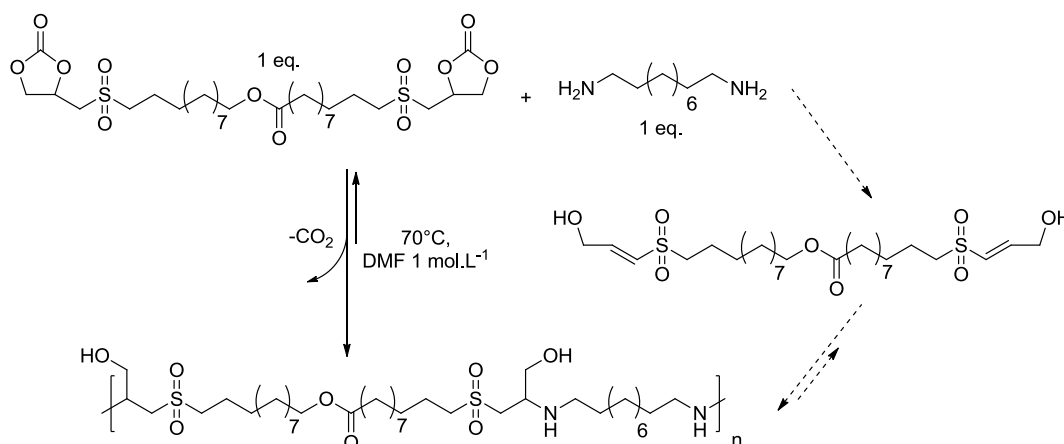
Figure 6 - Stacked ¹H NMR spectra of (1) Und(ester)-bCC-S in CDCl₃ and (2) PHU 5 in DMSO-d₆, (* residual monomers/chain ends).

ones displayed for ether-activated CC-based PHUs reported in Chapter 3 ($\text{OH}_I:\text{OH}_{II} \approx 30:70$). Besides, urea signals were detected by ^1H NMR with the shift of the labile proton at 6.8 ppm and were obtained in the same proportion ($\approx 10\%$) than for PHUs made from ether-activated monomers (Chapter 3).

Besides, no amide functions from side-reactions with the ester-containing monomer were identified in **PHU 5** and **6**. This feature could be assigned to the chemical structure of the monomer that presents electron-stabilizing aliphatic chains nearby the ester function.

Depending on the diamine employed, SEC were performed in DMF (LiBr, PS standards) or in THF (PS standards) for *Priamine*-based PHUs. Relatively high molar masses ranging from 10900 to 14900 $\text{g}\cdot\text{mol}^{-1}$ (\mathcal{D} : 1.67-1.86) in DMF and from 6300 to 11700 $\text{g}\cdot\text{mol}^{-1}$ (\mathcal{D} : 2.05-2.15) in THF were obtained after 7 days of polymerization at 70°C in DMF.

When the particular sulfonated-monomer *Und(ester)-bCC-sulfone* was polymerized with 10DA, ^1H NMR spectroscopy showed a complete disappearance of carbonate signals after 24h. However, typical signals of urethane linkages as well as the labile protons of the urethane function were not visible. The ^1H NMR spectrum presented in ESI † showed the presence of unsaturations attributed to the deprotonation of the acidic proton in α of the sulfone. A polymer of 5300 $\text{g}\cdot\text{mol}^{-1}$ molar mass with a dispersity of 1.33 was detected by SEC in DMF. We assume that the bis-unsaturated monomers formed *in situ* by the above-mentioned deprotonation/decarboxylation of *Und(ester)-bCC-sulfone* reacted with diamines through a Michael addition (see Scheme 5).



Scheme 5 - Polymerization of *Und(ester)-bCC-sulfone* *via* Michael addition of diamines.

As the 10DA:bCC ratio was 1:1, the double bonds were not all reacted after their formation, leading to a low molar mass polymer (see Table 2, **PHU 7**). Moreover, amines could be reacted with the *in situ* produced CO₂, leading to unactive amine salts and subsequently to low conversions and molar masses. The converted insaturations could be increased by processing the polymerization under vacuum or by flushing the material with nitrogen.

Hence, the synthesis of an unexpected polysulfone with new properties was driven by a favored reactivity of acid protons nearby the sulfone towards amine. This polymerization could be used in foam production with tri-functional monomers, taking advantage of the *in situ* decarboxylation of sulfone-activated cyclic carbonates.

As in Chapter 3, the thermal properties of the synthesized PHUs were correlated to their chemical structures. DSC second heating cycles and corresponding TGA traces are displayed in Figure 7. Amorphous PHUs were obtained with *Oleyl(ether)-bCC-S* due to the long alkyl dangling group present in this monomer. When copolymerized with 10DA, the latter enabled the formation of **PHU 3** with a low T_g of -29°C. The additional effect of plastification brought by the pendant alkyl chains of the *Priamine* permitted to lower the T_g to -34°C (**PHU 4**). Similarly, the semi-crystalline 10DA-based **PHU 5** demonstrated a T_g of -8°C that was decreased to -26°C when *Priamine* was used as comonomer (**PHU 6**). As a general trend, all PHUs exhibited low glass transition temperatures imparted by the sulfur atoms and by the long aliphatic chains that introduce flexibility to the polymer chains. Most of the PHUs were semi-crystalline thanks to the well-defined monomer structure with ether or ester linkages on the backbone that could form crystalline clusters by hydrogen bonding with pendant hydroxyl groups and urethane carbonyl moieties. However, in the case of **PHU 1** and **PHU 5**, several melting peaks appeared revealing different crystallization modes or a possible segregation between soft and hard segments. In the case of **PHU 2** and **6**, melting temperatures were lowered when *Priamine* was used and only one crystallization mode was observed.

With regard to PHU thermal stability, 5 w.% loss degradation temperatures in the range 258 to 286°C were achieved, except for the “**PHU**” **7** synthesized with *Und(ester)-bCC-sulfone*. The latter demonstrated a T_{d5%} of 205°C, likely due to its lower molar mass and to the presence of sulfone moieties in the backbone of the polymer in comparison to the thio-ether-containing PHU (see Figure 7). Indeed, considering the equilibrium displayed in the Scheme 5, an easy depolymerization can occur by a retro-Michael addition, favoring a faster degradation of the PHU. Nonetheless, it can be mentioned that the residue percentage after 500°C is above 5% only in the case of the sulfonated polymer. **PHU 4** made from monomers

with aliphatic pendant chains exhibited the highest resistance to temperature with a $T_{d5\%}$ of 286°C.

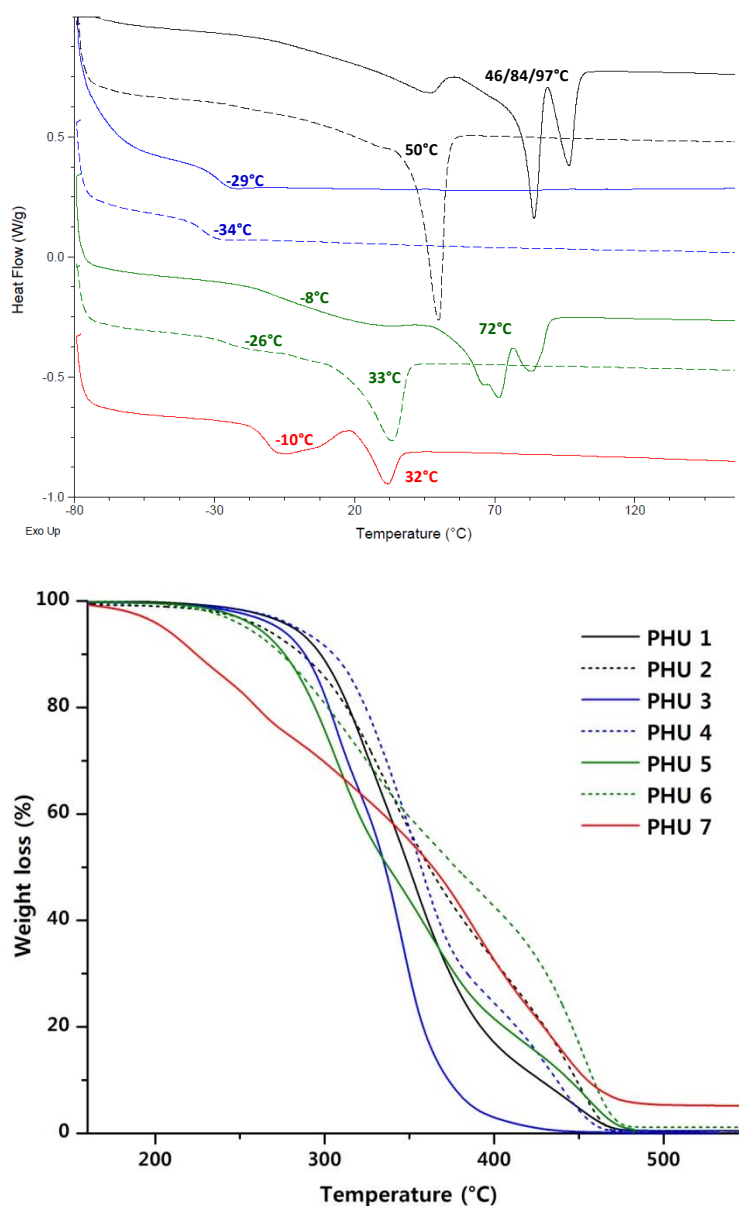


Figure 7 - DSC second heating cycle(10°C/min) of PHU 1 to PHU 7 and corresponding TGA traces from 160°C to 550°C (after an isothermal procedure of 15 min at 160°C to remove the residual DMF).

2.2. Post-functionalization of sulfur-containing PHUs

Taking advantage of the presence of sulfur atoms contained in the PHU backbones, post-functionalizations were performed on **PHU 5**, by selective oxidation of the thio-ether groups to sulfone or by sulfonium salt synthesis, in order to tune the final properties and to subsequently broaden applications.

The sulfonation (or sulfoxidation) of polymeric materials has already been described on linear fatty acid-based polymers^{14,15} but has never been attempted on PHUs. In these studies, the thio-ether oxidation was reported to impact solubility of the post-functionalized polymers as well as their thermal stability and crystallinity. As an example, Cadiz and coworkers¹⁵ post-functionalized a fully bio-based triblock copolymer derived from PLA and castor oil derivatives that exhibited enhanced thermal stability and lower crystallinity.

Besides, post-functionalization of polypeptides through sulfonium salt synthesis has already been described by Deming and coll.^{16,17} but on unhindered methionine pendant group. To do so, functionalized epoxides were reacted with thio-ether compounds in acetic acid. Nonetheless, this technique has not been applied on PHU containing hindered sulfur atoms in a polymer backbone.

Hence, the following study was carried out on **PHU 5** ($\bar{M}_n = 14900 \text{ g.mol}^{-1}$, $\bar{D} = 1.86$) prepared by polyaddition of *Und(ester)-bCC-S* and 10DA in the previous part (2.1). The post-functionalized **PHU 5-sulfone** and **PHU 5-sulfonium** were analyzed either by NMR, FTIR, DSC and TGA and the results are reported in Table 3.

Table 3 - Characterization of PHU 5, post-functionalized PHU 5-sulfone and PHU 5-sulfonium.

PHU	Monomers	$\bar{M}_n \text{ (g.mol}^{-1}\text{)} [\bar{D}]^1$	$T_g \text{ (}^\circ\text{C)}^a$	$T_m \text{ (}^\circ\text{C)}^a$	$T_{d5\%} \text{ (}^\circ\text{C)}^b$
PHU 5		14900 [1.86]	-8	72	258
PHU 5-sulfone	<i>Und(ester)-bCC-S</i> and 10DA	2900 [1.43]	4	92	213
PHU 5-sulfonium		RI detector: 5200 [1.62] UV detector : 4000 [2.3]*	4	71	241

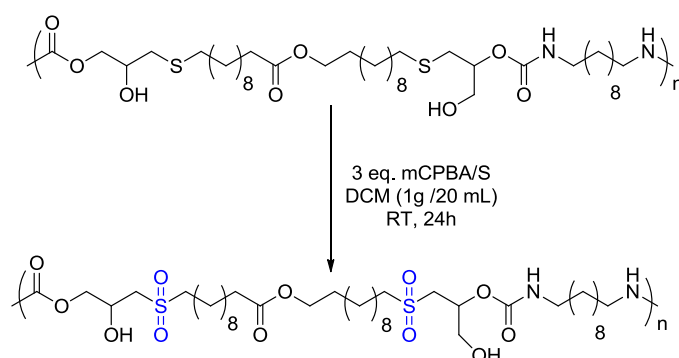
^a: Determined by DSC at $10^\circ\text{C.min}^{-1}$ from the second cycle; ^b: Determined by TGA at $10^\circ\text{C.min}^{-1}$ under nitrogen; *UV detector used for SEC in DMF.

2.2.1. Sulfonation

As demonstrated in the part 1.3, it was impossible to polymerize sulfone-activated bis-cyclic carbonate to form a sulfonated PHU due to the side reactions undergone by such carbonates during aminolysis. Therefore, post-functionalization was the best compromise for bringing the sulfone moiety in the PHU backbone.

The oxidation of **PHU 5** in its polysulfone analogue (**PHU 5-sulfone**) was carried out in DCM at room temperature in the presence of 3 equivalents of mCPBA per sulfur atoms. To avoid staying at the first oxidation state of the sulfur atom (sulfoxide), the mixture reaction

was left 24h (see Scheme 6). After having applied a filtration and a washing procedure (see ESI), a yield of 60% was achieved. The polymer turned from a clear yellow to a white powder after thio-ether oxidation.



Scheme 6 - Experimental procedure for PHU 5 sulfonation.

FTIR certified the formation of sulfones with the presence of two bands of absorption at 1127 cm^{-1} and 1387 cm^{-1} . However, no new band in between 1030 and 1070 cm^{-1} characterizing sulfoxides was detected (see wavenumbers in ESI). The fine chemical structures of **PHU 5** and **PHU 5-sulfone** were elucidated thanks to ^1H , ^{13}C NMR and 2D NMR (COSY, HSQC) as illustrated in Figure 8.

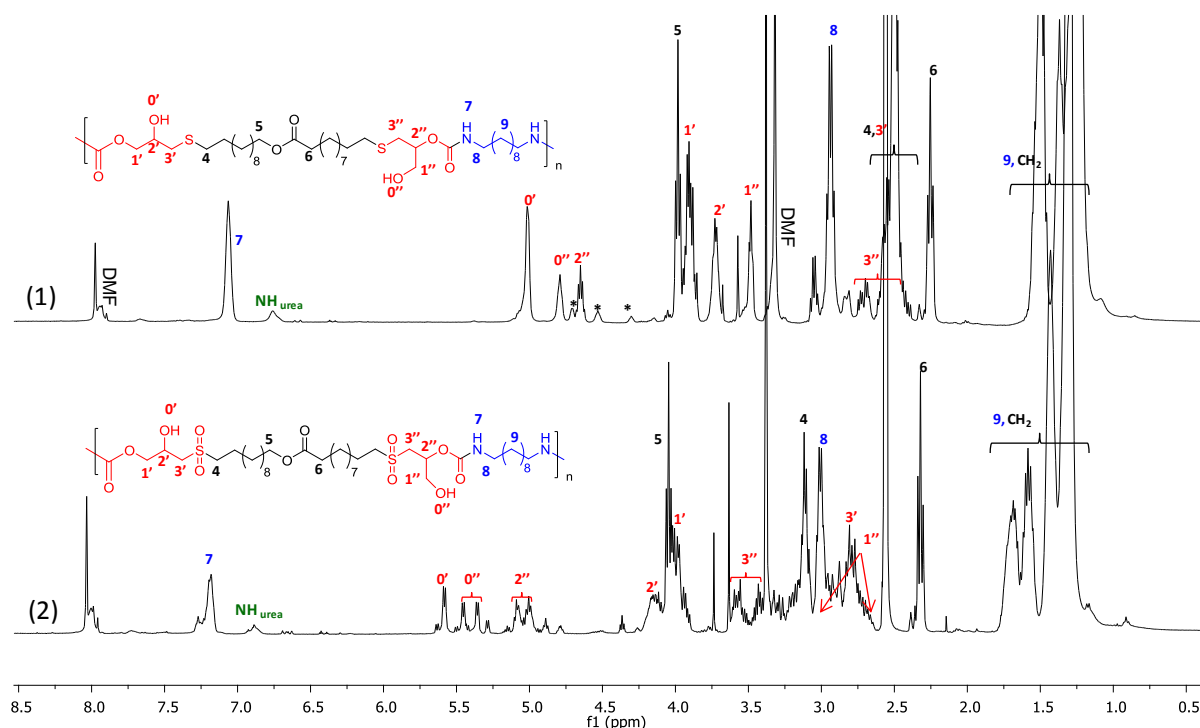


Figure 8 - Stacked ^1H NMR spectra of (1) PHU 5 (sulfur based PHU) in DMSO-d6 and (2) the post-functionalized PHU5-sulfone in DMSO-d6. (* residual monomers/chain ends).

All the signals initially present nearby the sulfur atom in **PHU 5** (see spectra (1), Figure 8, **1'** to **3'**, **1''** to **3''** and **4**) were shifted downfield of the ^1H NMR spectra due to the electronic effects imparted by the sulfone. More specifically, the sulfonation was confirmed by the downfield signals of the protons adjacent to the sulfur atom (**3'**, **3''** and **4**) to 3.5-2.75 ppm.

The average number molar mass of **PHU 5-sulfone** was measured by SEC in DMF (LiBr, PS standards) at $2900 \text{ g}\cdot\text{mol}^{-1}$ and was decreased by 5 in comparison to **PHU 5**. The dispersity was also noticed to be lowered from 1.86 to 1.43 after thio-ether oxidation. The SEC traces before and after post-functionalization are presented in Figure 9 and clearly displayed a significant loss of molar mass with the appearance of oligomers at higher retention times. Several parameters could be taken in consideration to explain such results. The depolymerization of **PHU 5-sulfone** could have occurred but this theory was not brought to light. Secondly, the chemical modifications on a polymer can impact the shape of the polymer random coil, inducing a change of its hydrodynamic volume and of its subsequent apparent molar mass. But the most probable theory is a lack of solubility of **PHU 5-sulfone** in DMF due to the presence of sulfone moieties along the backbone as it has already been observed in the literature for other polymers.¹⁵ Indeed, the longest functionalized polymer chains were not solubilized in DMF and therefore not analyzed. As a consequence, the SEC chromatogram only displayed the soluble oligomers present in the filtered SEC solution.

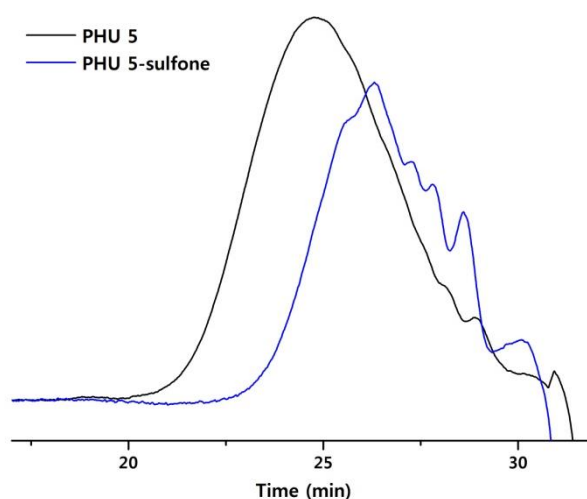


Figure 9 - SEC traces of PHU 5 and of PHU5-sulfone after post-functionalized (DMF, LiBr, PS standards, RI detector).

Thermal properties of **PHU 5-sulfone** were investigated by DSC and TGA and the results are reported in Table 3.

Similarly to the starting raw material (**PHU 5**), the oxidized homologue was semi-crystalline, but showed higher glass transition and melting temperatures of respectively 4°C and 92°C. However, the thermal decomposition at 5 w.% loss was decreased from 258°C to 213°C. These results were in contrast to what have been previously reported in the literature regarding fatty acid-based polysulfones.^{14,15}

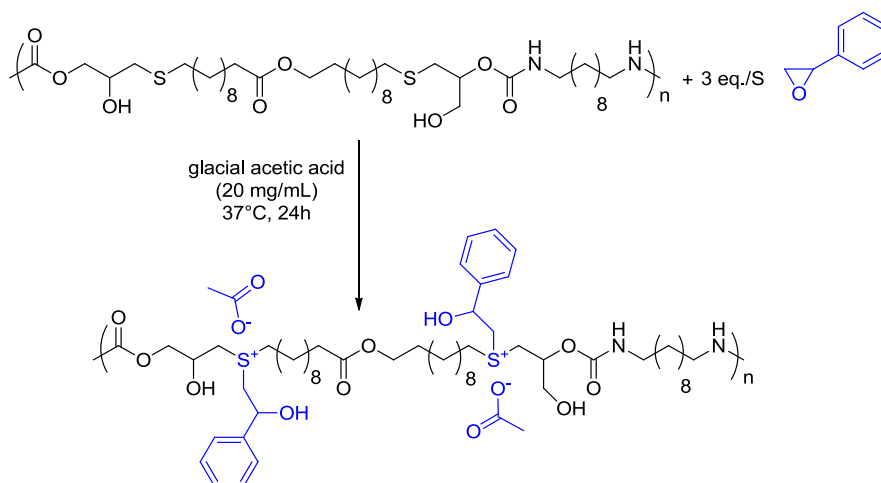
Lastly, we tried to solubilize **PHU 5-sulfone** in water, taking advantage of the high hydrogen bonding ability of the sulfone moiety. Nevertheless, the polysulfone could not be solubilized in water because of the high amount of hydrophobic segments within the polymer backbone.

2.2.2. Sulfonium salts synthesis

The introduction of dangling alkyl groups varying the chain length is a practical route to tune thermal properties of polymers. The introduction of other functional groups *via* sulfonium salt synthesis can also be an advantage for certain applications such as biomedical or pharmaceutical ones. The sulfonium salts can be prepared by thio-ether alkylation either using alkyl halides or functionalized epoxides. Deming and co-workers^{16,17} used both strategies on methionine-based polypeptides but only the second strategy¹⁷ was successful on our starting material that displays intrachain hindered thio-ethers.

As proof of concept, epoxy styrene was chosen to perform the alkylation of thio-ethers, in order to facilitate the analysis by ¹H NMR spectroscopy and SEC (UV detector).

PHU 5 was reacted with 3 eq. of epoxy styrene per sulphur atom in glacial acetic acid for 24h at 37°C. (see Scheme 7). A part of epoxy styrene was consumed by the acetic acid (ring-opening), explaining the excess of epoxides used. After work-up and precipitation in toluene, the polymer was recovered at 31% yield as a sharp yellow and sticky polymer.



Scheme 7 - Experimental procedure for post-functionalization of PHU 5 via sulfonium salt synthesis.

The sulfonium salt synthesis was confirmed by the disappearance of the epoxide signals between 2.8 and 3.9 ppm and by the presence of benzylic proton signals on ^1H NMR at 7.3 ppm (see ESI) and by their corresponding FTIR band at 3061 cm^{-1} . Moreover, the hydroxyl groups were not reacted with epoxy styrene as shown by the remaining proton shifts at 5.1 ppm and 4.8 ppm. The best confirmation was given by the SEC trace obtained with UV detector (260 nm) (see Figure 10). Indeed, as the initial raw material **PHU 5** was not responding with this detector, **PHU 5-sulfonium** exhibited a visible molar mass of $4000\text{ g}\cdot\text{mol}^{-1}$ (\mathcal{D} : 2.3) thanks to the UV-sensitive aromatic ring, originate from the post-functionalization. The molar masses obtained with the RI and the UV detectors were slightly different with respectively $\bar{M}_n = 5200\text{ g}\cdot\text{mol}^{-1}$, $\mathcal{D} = 1.62$ and $\bar{M}_n = 4000\text{ g}\cdot\text{mol}^{-1}$, $\mathcal{D} = 2.3$. The mass weight distributions were coherent with an homogeneous grafting of epoxy styrene on the PHU chain.

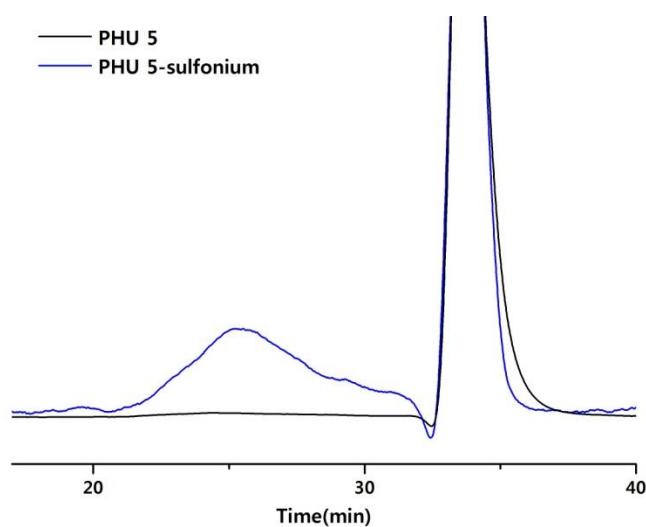


Figure 10 - SEC traces of PHU 5 and of PHU5-sulfonium after post-functionalized (DMF, LiBr, PS standards, UV detector).

Thermal properties of **PHU 5-sulfonium** were assessed by DSC and TGA. The glass transition temperature was increased to 4°C, keeping the same melting temperature (71°C). Contrarily to the polysulfone synthesized previously, **PHU 5-sulfonium** kept the thermal stability displayed by the raw material with a $T_{d5\%}$ of 241°C. The presence of aromatic rings as pendant groups can explain this observation. Moreover, the solubility pattern of this polymer was not changed from the initial one. Apolar solvent such as toluene as well as water were not solubilizing **PHU 5-sulfonium**.

This part of our research was initiated as a proof of concept but needs further investigations and derivatizations for tuning sulphur-based PHU properties.

Conclusions

In conclusion, sulfur activated 5-membered cyclic carbonates were synthesized by thiol-ene coupling of thioglycerol and fatty acid-based dienes obtained from castor and canola oils. In model reaction with hexylamine, sulfur-activated monomers displayed a similar reactivity than ether-activated cyclic carbonates synthesized in the Chapter 3. The sulfone-activated ones obtained by oxidation of sulfur-activated CC was found to be highly reactive towards amines. Unfortunately, the side reaction between the amine and the acidic protons nearby the sulfone was favored and hydroxyurethanes could not be prepared from such cyclic carbonates. The lipidic sulfur-based cyclic carbonates were then successfully polymerized leading to PHUs with molar masses up to $14900 \text{ g}\cdot\text{mol}^{-1}$. Depending on the diamine employed, PHU properties could be tuned with T_g in the range -34 to -8°C and $T_{d5\%}$ in between 258 and 286°C . However, the polymerization of sulfonated bCC resulted in a semi-crystalline polymer with low thermal stability and molar mass and with a chemical structure that differed from the PHU one.

To go further, one sulfur-based PHU was post-functionalized taking advantage of the sulfur content within the polymer backbone. Sulfone moieties as well as sulfonium salts were synthesized following respectively an oxidation process and an alkylation using epoxides. Such modifications were shown to increase the glass transition temperatures of the polymer and to increase the melting temperature in the case of the sulfonation process. However, polymer solubility was not radically impacted by the post-functionalization as it was expected.

This study has demonstrated the possibility of inserting a sulfur atom in β position nearby the cyclic carbonate moiety *via* a simple thiol-ene reaction, taking advantage of the higher reactivity of such carbonates as well as the possibility of post-functionalizing the resulting polymers using sulfur atoms. Nonetheless, the last-mentioned part was a proof of concept that requires deep investigations, especially in terms of polymer properties.

References

- (1) Tomita, H.; Sanda, F.; Endo, T. *J. Polym. Sci. Part A Polym. Chem.* **2001**, *39* (6), 860–867.
- (2) Tomita, H.; Sanda, F.; Endo, T. *J. Polym. Sci. Part A Polym. Chem.* **2001**, *39* (23), 4091–4100.
- (3) Besse, V.; Foyer, G.; Auvergne, R.; Caillol, S.; Boutevin, B. *J. Polym. Sci. Part A Polym. Chem.* **2013**, *51* (15), 3284–3296.
- (4) Benyahya, S.; Desroches, M.; Auvergne, R.; Carlotti, S.; Caillol, S.; Boutevin, B. *Polym. Chem.* **2011**, *2* (11), 2661–2667.
- (5) Maisonneuve, L.; Wirotius, A.-L.; Alfos, C.; Grau, E.; Cramail, H. *Polym. Chem.* **2014**, *5*, 6142–6147.
- (6) Türünç, O.; Meier, M. A. R. *Eur. J. Lipid Sci. Technol.* **2012**, *115* (1), 41–54.
- (7) Türünç, O.; Meier, M. A. R. *Macromol. Rapid Commun.* **2010**, *31* (20), 1822–1826.
- (8) Bao, Y.; He, J.; Li, Y. *Polym. Int.* **2013**, *62* (10), 1457–1464.
- (9) Pyo, S.-H.; Persson, P.; Mollaahmad, M. A.; Sörensen, K.; Lundmark, S.; Hatti-Kaul, R. *Pure Appl. Chem.* **2012**, *84*, 411–860.
- (10) Mouloungui, Z.; Yoo, J.-W.; Gachen, C.-A.; Gaset, A.; Vermeersch, G. Process for the preparation of glycerol carbonate from glycerol and ethylene or propylene carbonates, EP19960390003, **1996**.
- (11) Mignani, G.; Debray, J.; Da Silva, E.; Lemaire, M.; Raoul, Y. Method for producing polyglycerol poly(carbonate), WO2014009421, **2011**.
- (12) Bhattacharya, R.; Kesharwani, M. K.; Manna, C.; Ganguly, B.; Suresh, C. G.; Pathak, T. *J. Org. Chem.* **2010**, *75* (2), 303–314.
- (13) Cruz, C. M.; Ortega-Muñoz, M.; López-Jaramillo, F. J.; Hernández-Mateo, F.; Blanco, V.; Santoyo-González, F. *Adv. Synth. Catal.* **2016**.
- (14) Van Den Berg, O.; Dispinar, T.; Hommez, B.; Du Prez, F. E. *Eur. Polym. J.* **2013**, *49* (4), 804–812.
- (15) Beyazkilic, Z.; Lligadas, G.; Ronda, J. C.; Galià, M.; Cádiz, V. *Polymer*. **2015**, *68* (0), 101–110.
- (16) Kramer, J. R.; Deming, T. J. *Biomacromolecules* **2012**, *13* (6), 1719–1723.
- (17) Gharakhanian, E. G.; Deming, T. J. *Biomacromolecules* **2015**, *16* (6), 1802–1806.

Experimental and Supporting Information

Experimental Methods

• **General procedure for thiol-ene coupling:** Dimerized bis-unsaturated fatty acids were reacted with thioglycerol in DCM using DMPA as photoinitiator. The reaction was carried out in a UV reactor (365 nm) for 1h, or 48h in the case of the *Oleyl(ether)-tetraol* synthesis.

Dec-diol synthesis: 1-decene (1 eq., 2 g, 14.3 mmol), thioglycerol (1 eq., 1.54 g, 14.3 mmol) were reacted in 2 mL of DCM for 1h in a UV reactor, with 0.5 w.% of DMPA (10 mg) as photoinitiator. Conversion: 100%. The solvent was evaporated under reduced pressure and the product was obtained as a transparent oil after purification by flash chromatography (eluent: DCM:methanol from 100:0 to 95:5). Yield: 78%. ¹H NMR (DMSO-d₆, 25°C, 400 MHz), δ (ppm): 3.78 (m, 1H), 3.73 and 3.56 (q, 2H), 2.77 and 2.61 (dd, 2H), 2.53 (t, 2H), 1.58 (m, 2H), 1.26 (m, 14H), 0.85 (t, 3H). ¹³C NMR (DMSO-d₆, 25°C, 100 MHz), δ (ppm): 69.7 (CH-OH), 65.2 (CH₂-OH), 35.8 (CH-CH₂-S), 32.8 (S-CH₂-CH₂), 31.8-22.6 (CH₂), 14.0 (CH₃).

Und(ether)-tetraol synthesis: *Und(ether)-diene* (1 eq., 2 g, 6.2 mmol), thioglycerol (2 eq., 1.34 g, 12.4 mmol) were reacted in 2 mL of DCM for 1h in a UV reactor, with 0.5 w.% of DMPA (10 mg) as photoinitiator. Conversion: 100%. The heterogeneous mixture obtained was filtered and the resulting white powder was abundantly washed with petroleum ether. Yield: 99%. ¹H NMR (DMSO-d₆, 25°C, 400 MHz), δ (ppm): 4.58 (m, 4H), 3.57 (m, 2H), 3.35 (t, 4H), 3.33 (t, 4H), 2.62 and 2.43 (dd, 4H), 2.53 (t, 4H), 1.52-1.27 (m, 34H). ¹³C NMR (DMSO-d₆, 25°C, 100 MHz), δ (ppm): 71.2 (CH-OH), 69.8 (CH₂-O-CH₂), 64.7 (CH₂-OH), 35.2 (CH-CH₂-S), 32.1 (S-CH₂-CH₂), 29.3-25.7 (CH₂).

Oleyl(ether)-tetraol synthesis: *Oleyl(ether)-diene* (1 eq., 2.5 g, 4.82 mmol), thioglycerol (2 eq., 1.04 g, 9.6 mmol) were reacted in 2 mL of DCM for 48h in a UV reactor, with 1.5 w.% of DMPA (38 mg) as photoinitiator. Conversion: 90%. The solvent was evaporated and the crude product was purified by flash column chromatography (eluent: DCM:methanol from 100:0 to 90:10) to obtain a transparent viscous liquid. Yield: 30%. ¹H NMR (DMSO-d₆, 25°C, 400 MHz), δ (ppm): 4.68 (d, 2H), 4.51 (t, 2H), 3.51 (m, 2H), 3.35 (t, 4H), 3.33 (t, 4H), 2.59 (m, 2H), 2.54 and 2.37 (dd, 4H), 1.45-1.25 (m, 60H), 0.88 (t, 6H). ¹³C NMR (DMSO-d₆, 25°C, 100 MHz), δ (ppm): 71.4 (CH-OH), 69.7 (CH₂-O-CH₂), 64.3 (CH₂-OH), 45.2 (S-CH-CH₂), 33.4 (CH-CH₂-S-CH), 33.9-21.9 (CH₂), 13.7 (CH₃).

Und(ester)-tetraol synthesis: *Und(ester)-diene* (1 eq., 3 g, 8.9 mmol), thioglycerol (2 eq., 1.93 g, 17.8 mmol) were reacted in 2 mL of DCM 1h in a UV reactor, with 0.5 w.% of DMPA

(15 mg) as photoinitiator. Conversion: 100%. The heterogeneous mixture obtained was filtered and the resulting white powder was abundantly washed with petroleum ether. Yield: 99%. ^1H NMR (CDCl_3 , 25°C, 400 MHz), δ (ppm): 4.07 (t, 2H), 3.78 (m, 2H), 3.75 and 3.35 (q, 4H), 2.73 and 2.69 (dd, 4H), 2.62 (t, 4H), 2.30 (m, 6H), 1.60-1.27 (m, 34H). ^{13}C NMR (CDCl_3 , 25°C, 100 MHz), δ (ppm): 174.2 ($\text{CH}_2\text{-}\underline{\text{C}}=\text{O-O-}$), 69.9 (CH-OH), 65.5 ($\text{CH}_2\text{-OH}$), 64.8 ($\text{O=C-O-}\underline{\text{C}}\text{H}_2$), 35.9 ($\text{CH-}\underline{\text{C}}\text{H}_2\text{-S}$), 34.3 ($\underline{\text{C}}\text{H}_2\text{-C=O-O-CH}_2$), 32.3 ($\text{S-}\underline{\text{C}}\text{H}_2\text{-CH}_2$), 31.8-24.5 (CH_2).

• **General procedure for carbonation:** Fatty acids tetraols were dried under vacuum and were subsequently reacted under nitrogen atmosphere with an excess of anhydrous dimethylcarbonate (DMC, 15 eq.), using 3 mol.% of K_2CO_3 per diol as transesterification catalyst. The reaction was carried out for 4h at 70°C under reflux.

Dec-CC-S synthesis: *Dec-diol* (1 eq., 1 g, 7 mmol), DMC (15 eq., 8.5 mL, 105 mmol), K_2CO_3 (0.03 eq., 29 mg, 0.21 mmol). Conversion: 100%. DCM was added to the crude mixture and washed with brine three times. The organic phase was dried with magnesium sulfate and reconcentrated using a rotary evaporator. The product was obtained as a transparent viscous liquid after purification by flash column chromatography (eluent: DCM:methanol from 100:0 to 95:5). Yield: 30%. Purity: 90.1% (HPLC). ^1H NMR (CDCl_3 , 25°C, 400 MHz), δ (ppm): 4.84 (m, 1H), 4.55 and 4.31 (t, 2H), 2.94 and 2.77 (dd, 2H), 2.59 (t, 2H), 1.58 (m, 2H), 1.37-1.26 (m, 14H), 0.86 (t, 3H). ^{13}C NMR (CDCl_3 , 25°C, 100 MHz), δ (ppm): 154.5 (O-C=O-O), 75.6 ($\text{CH}_2\text{-}\underline{\text{C}}\text{H-CH}_2$), 68.7 ($\text{O-}\underline{\text{C}}\text{H}_2\text{-CH}$), 34.7 ($\text{CH}_2\text{-CH-}\underline{\text{C}}\text{H}_2\text{-S}$), 33.2 ($\text{S-}\underline{\text{C}}\text{H}_2\text{-CH}_2$), 32-23 (CH_2), 14.4 (CH_3). IR (cm^{-1}): 2954, 2919, 1769, 1190, 1167, 718.

Und(ether)-bCC-S synthesis: *Und(ether)-tetraol* (1 eq., 1 g, 1.86 mmol), DMC (15 eq., 2.34 mL, 28 mmol), K_2CO_3 (0.06 eq., 15 mg, 0.11 mmol). Conversion: 100%. DCM was added to the crude mixture and washed with brine three times. The organic phase was dried with magnesium sulfate and reconcentrated using a rotary evaporator. The product was obtained as a white powder. Yield: 88%. Purity: 95.4% (HPLC). ^1H NMR (DMSO-d_6 , 25°C, 400 MHz), δ (ppm): 4.82 (m, 2H), 4.57 and 4.27 (t, 4H), 3.37 (t, 4H), 2.91 and 2.75 (dd, 4H), 2.57 (t, 4H), 1.56-1.27 (m, 34H). ^{13}C NMR (DMSO-d_6 , 25°C, 100 MHz), δ (ppm): 154.6 (O-C=O-O), 75.6 ($\text{CH}_2\text{-}\underline{\text{C}}\text{H-CH}_2$), 71.2 ($\underline{\text{C}}\text{H}_2\text{-O-CH}_2$), 68.8 ($\text{O-}\underline{\text{C}}\text{H}_2\text{-CH}$), 34.9 ($\text{CH-}\underline{\text{C}}\text{H}_2\text{-S}$), 33.2 ($\text{S-}\underline{\text{C}}\text{H}_2\text{-CH}_2$), 30-26.1 (CH_2). IR (cm^{-1}): 2918, 2849, 1769, 1115, 718. $T_m=93^\circ\text{C}$.

Oleyl(ether)-bCC-S synthesis: *Oleyl(ether)-tetraol* (1 eq., 0.75 g, 1 mmol), DMC (15 eq., 1.26 mL, 15 mmol), K_2CO_3 (0.06 eq., 8.3 mg, 0.11 mmol). Conversion: 97%. DCM was added to the crude mixture and washed with brine three times. The organic phase was dried

with magnesium sulfate and reconcentrated using a rotary evaporator. The product was obtained as a viscous transparent liquid. Yield: 71%. Purity: 98.5% (HPLC). ^1H NMR (CDCl_3 , 25°C , 400 MHz), δ (ppm): 4.78 (m, 2H), 4.53 and 4.28 (t, 4H), 3.38 (t, 4H), 2.90 and 2.72 (dd, 4H), 2.12 (m, 2H), 1.60-1.26 (m, 60H), 0.87 (t, 6H). ^{13}C NMR (CDCl_3 , 25°C , 100 MHz), δ (ppm): 154.9 (O-C=O-O), 75.7 ($\text{CH}_2\text{-CH-CH}_2\text{-S}$), 71.4 ($\text{CH}_2\text{-O-CH}_2$), 68.5 (O- $\text{CH}_2\text{-CH}$), 47.3 (S- CH-CH_2), 32.9 ($\text{CH-CH}_2\text{-S-CH}$), 35-22.8 (CH_2), 14.1 (CH_3). IR (cm^{-1}): 2919, 2851, 1794, 1114, 717. T_m =nd, T_g =-59°C.

Und(ester)-bCC-S synthesis: *Und(ester)-tetraol* (1 eq., 0.75 g, 1.36 mmol), DMC (15 eq., 1.71 mL, 20.4 mmol), K_2CO_3 (0.06 eq., 11 mg, 0.08 mmol). Conversion: 99%. DCM was added to the crude mixture and washed with brine three times. The organic phase was dried with magnesium sulfate and reconcentrated using a rotary evaporator. The product was obtained as a white powder. Yield: 90%. Purity: 88.9% (HPLC). ^1H NMR (CDCl_3 , 25°C , 400 MHz), δ (ppm): 4.83 (m, 2H), 4.75 and 4.29 (t, 4H), 4.04 (t, 2H), 2.94 and 2.79 (dd, 4H), 2.60 (t, 4H), 2.29 (t, 2H), 1.58-1.28 (m, 34H). ^{13}C NMR (CDCl_3 , 25°C , 100 MHz), δ (ppm): 174.2 ($\text{CH}_2\text{-C=O-O-}$), 154.8 (O-C=O-O), 75.7 ($\text{CH}_2\text{-CH-CH}_2$), 68.6 (O- $\text{CH}_2\text{-CH}$), 64.5 (O=C-O- CH_2), 34.9 ($\text{CH-CH}_2\text{-S}$), 34.7 ($\text{CH}_2\text{-C=O-O-CH}_2$), 33.3 (S- $\text{CH}_2\text{-CH}_2$), 29.9-28.9 (CH_2). IR (cm^{-1}): 2918, 2849, 1769, 1725, 1286, 718. T_m =89°C.

• **General procedure for sulfonation:** 1 eq. of sulphur-activated cyclic carbonate was reacted with 3 eq. of m-chloroperbenzoic acid (mCPBA) per sulphur atom in DCM (1 g / 20 mL) during 24h at room temperature. The reaction mixture was then cooled up at 0°C to ensure the precipitation in DCM of the acidic form of mCPBA that was subsequently filtrated. The resulting organic phase was washed 4 times with Na_2SO_3 saturated solution, three times with NaHCO_3 saturated solution and rinsed with deionized water in order to remove residual mCPBA. The organic phase was dried over magnesium sulphate and reconcentrated using rotary evaporator. No further purification was required. This procedure was applied to PHU post-functionalization.

Dec-CC-sulfone synthesis: *Dec-CC-S* (1 eq., 2 g, 7.3 mmol) and mCPBA (3 eq., 3.79 g, 22 mmol) were reacted in 40 mL of DCM. Conversion: 100%. The product was obtained after the work up as a white powder. Yield: 42%. Purity: 100% (HPLC). (CDCl_3 , 25°C , 400 MHz), δ (ppm): 5.24 (m, 1H), 4.71 and 4.36 (t, 2H), 2.56 and 3.26 (dd, 2H), 3.10 (t, 2H), 1.85 (m, 2H), 1.46-1.27 (m, 14H), 0.86 (t, 3H). ^{13}C NMR (CDCl_3 , 25°C , 100 MHz), δ (ppm): 153.1 (O-C=O-O), 70.7 ($\text{CH}_2\text{-CH-CH}_2$), 68.7 (O- $\text{CH}_2\text{-CH}$), 55.5 ($\text{CH-CH}_2\text{-SO}_2$), 55.1 ($\text{SO}_2\text{-CH}_2\text{-CH}_2$), 31.9-21.9 (CH_2), 14.1 (CH_3). IR (cm^{-1}): 2954, 2919, 1769, 1303, 1132.

Und(ester)-bCC-sulfone synthesis: *Und(ester)-bCC-S* (1 eq., 1 g, 1.65 mmol) and mCPBA (6 eq., 1.55 g, 9.9 mmol) were reacted in 20 mL of DCM. Conversion: 100%. The product was obtained after the work up as a white powder. Yield: nd. Purity: 63.2% (HPLC). ^1H NMR (CDCl_3 , 25°C, 400 MHz), δ (ppm): 5.26 (m, 2H), 4.73 and 4.42 (t, 4H), 4.04 (t, 2H), 3.35 and 3.22 (dd, 4H), 3.08 (t, 4H), 2.27 (t, 2H), 1.85-1.29 (m, 34H). ^{13}C NMR (CDCl_3 , 25°C, 100 MHz), δ (ppm): 174.5 ($\text{CH}_2\text{-}\underline{\text{C}}=\text{O-O-}$), 153.9 (O-C=O-O), 71.2 ($\text{CH}_2\text{-}\underline{\text{C}}\text{H-CH}_2$), 69.1 ($\text{O-}\underline{\text{C}}\text{H-CH}$), 64.8 ($\text{O=C-O-}\underline{\text{C}}\text{H}_2$), 55.9 ($\text{CH-}\underline{\text{C}}\text{H}_2\text{-SO}_2$), 55.4 ($\text{SO}_2\text{-}\underline{\text{C}}\text{H}_2\text{-CH}_2$), 34.9 ($\underline{\text{C}}\text{H}_2\text{-C=O-O-CH}_2$), 31.4-22.2 (CH_2). IR (cm^{-1}): 2918, 2849, 1769, 1725, 1286, 1130.

- **General procedure for kinetic experiments:** The kinetic experiments were performed in NMR tube at 1 mol.L⁻¹ in DMSO-d₆, at 50°C and with a ratio 1:1 between cyclic carbonate and hexylamine. All reagents were dried on molecular sieves or distilled before the reaction. Hexylamine was dried under CaH₂ and distilled of after drying. The cyclic carbonate was directly dried overnight in a NMR tube capped with a septum, under vacuum. 0.5 mL of dried DMSO-d₆ and 12.5 μL of TCB were added *via* the septum and the mixture was homogenized. The hexylamine (66 μL , 0.5 mmol, 1 eq.) was then added just before putting the tube in the NMR apparatus. The reaction was monitored with ^1H NMR spectroscopy with the disappearance of the cyclic carbonate protons for 2 days.

- **General procedure for polymerizations:** PHUs were prepared from *Und(ether)-bCC-S*, *Und(ester)-bCC-S*, *Oleyl(ether)-bCC-S* and *Und(ester)-bCC-sulfone* with 1,10-diaminodecane (10DA) and *Priamine* as comonomers with a molar ratio 1:1. PHU syntheses were performed in DMF (1 mol.L⁻¹) at 70°C into a schlenk tube under magnetic stirring and nitrogen atmosphere for 7 days. No catalysts were added for the polymerization reactions. Conversions were determined by ^1H NMR spectroscopy after 24h and 7 days of polymerization.

PHU 5: IR (cm^{-1}): 3328, 2918, 2850, 1725, 1687, 1534, 1281, 1248, 1108, 1048, 1012.

- **Sulfonation of sulphur-based PHU 5 (PHU 5-sulfone):** See ‘General procedure for sulfonation’ described above. Yield: 60%. IR (cm^{-1}): 3328, 2919, 2850, 1725, 1687, 1534, 1387, 1281, 1247, 1117, 1127, 1048, 1009.

• **Post-functionalization of sulphur-based PHU 5 with epoxy styrene (PHU 5-sulfonium):**
PHU 5 (1 eq., 0.25 g, 0.643 mmol of sulphur atom) was reacted with epoxy styrene (3 eq./ sulphur atom, 0.23 g, 1.93 mmol) in glacial acetic acid for 24h at 37°C. Half of the acetic acid was then evaporated using the rotary evaporator. The remained reaction mixture was then precipitated in toluene. The polymer was recovered by filtration and was abundantly washed with toluene before being dried under vacuum. Yield: 31%. IR (cm⁻¹): 3329, 3061, 2918, 2850, 1726 1667 1535.

Supporting Information

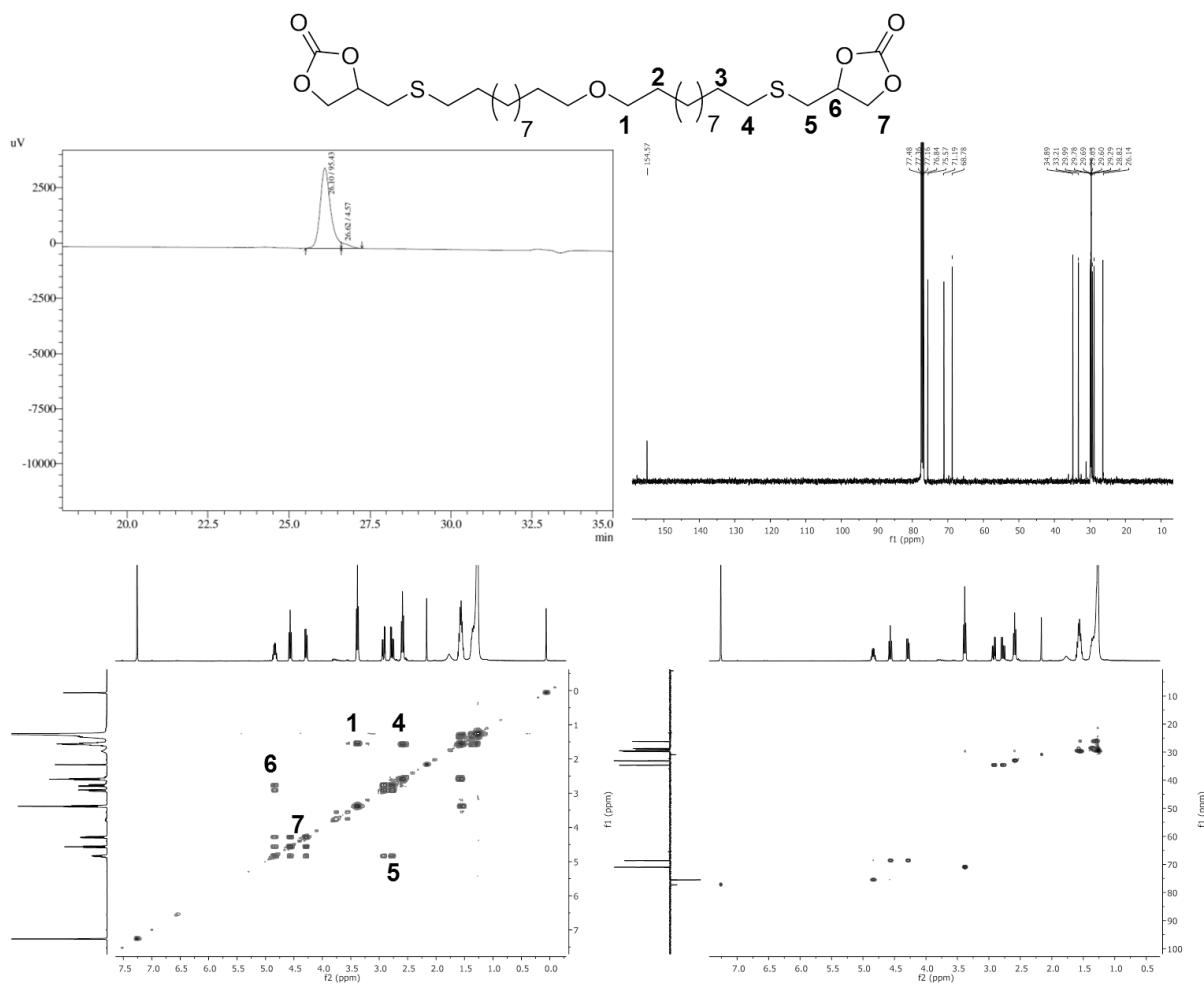


Figure ESI 1 - Characterization of Und(ether)-bCC-S (1) HPLC (95.4% purity), (2) ^{13}C NMR, (3) ^1H - ^1H COSY NMR and (4) ^1H - ^{13}C HSQC-NMR (Analysis performed in CDCl_3).

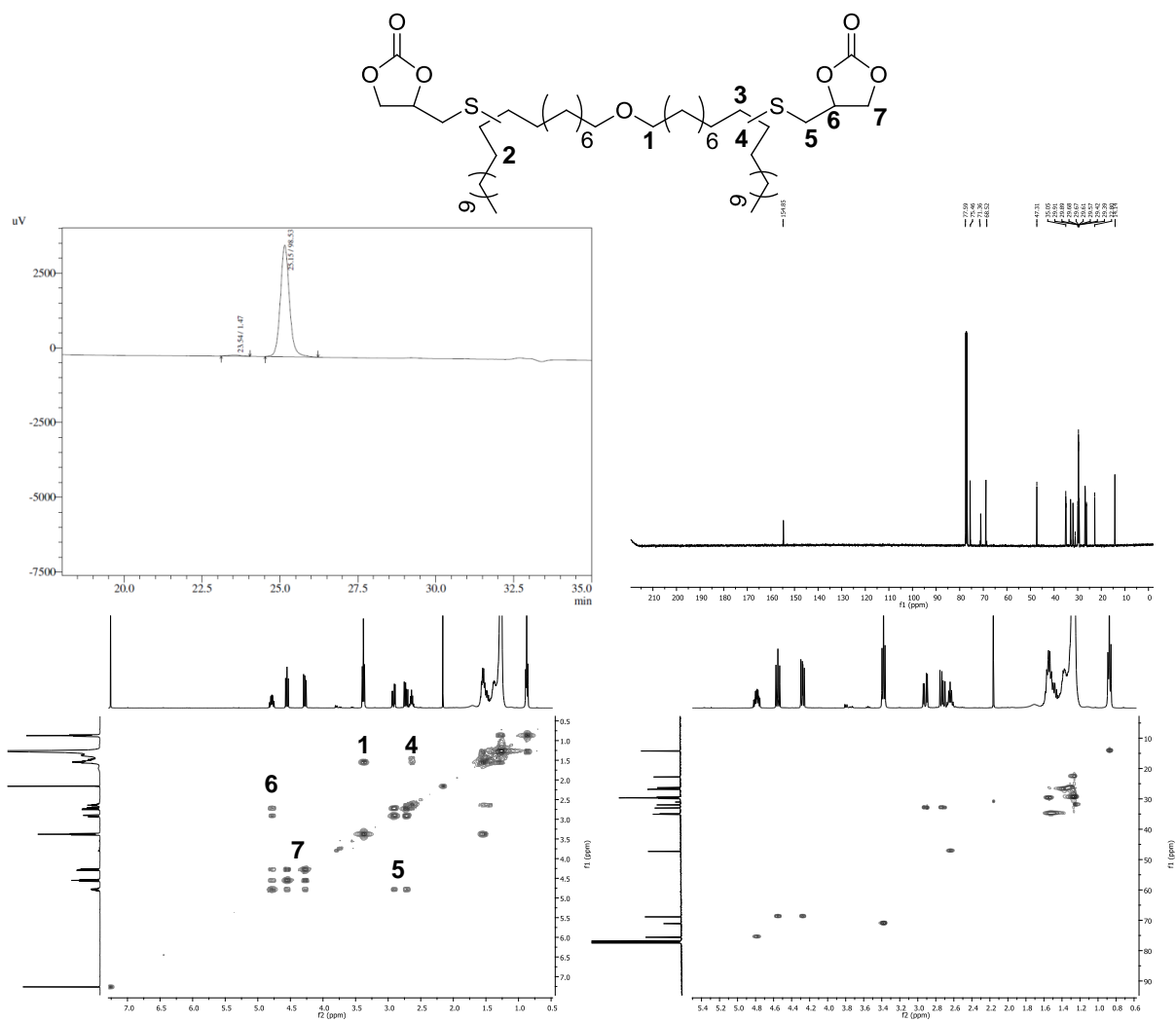


Figure ESI 2 - Characterization of Oleyl(ether)-bCC-S (1) HPLC (98.5% purity), (2) ^{13}C NMR, (3) ^1H - ^1H COSY NMR and (4) ^1H - ^{13}C HSQC-NMR (Analysis performed in CDCl_3).

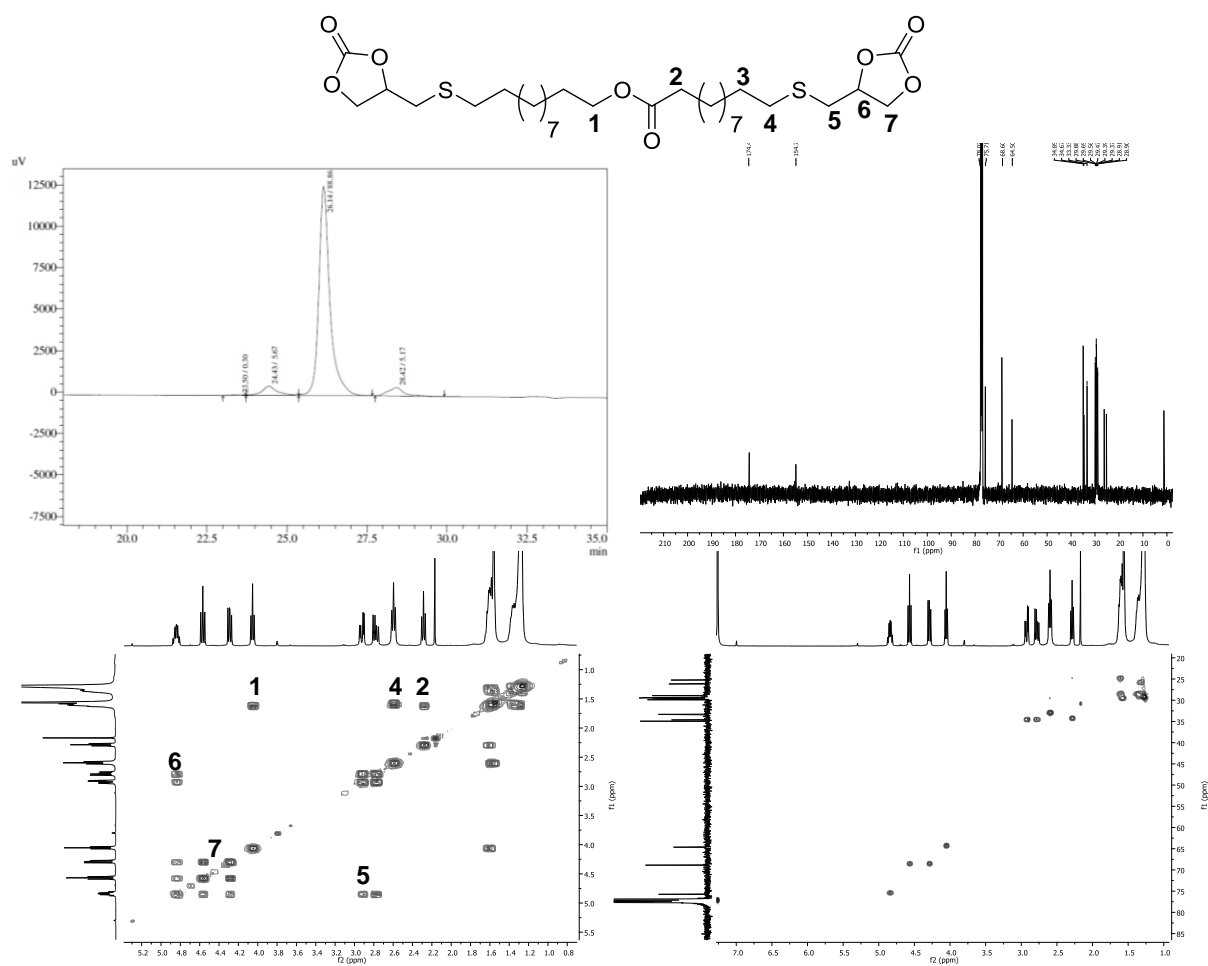


Figure ESI 3 - Characterization of Und(ester)-bCC-S (1) HPLC (88.9% purity), (2) ^{13}C NMR, (3) ^1H - ^1H COSY NMR and (4) ^1H - ^{13}C HSQC-NMR (Analysis performed in CDCl_3).

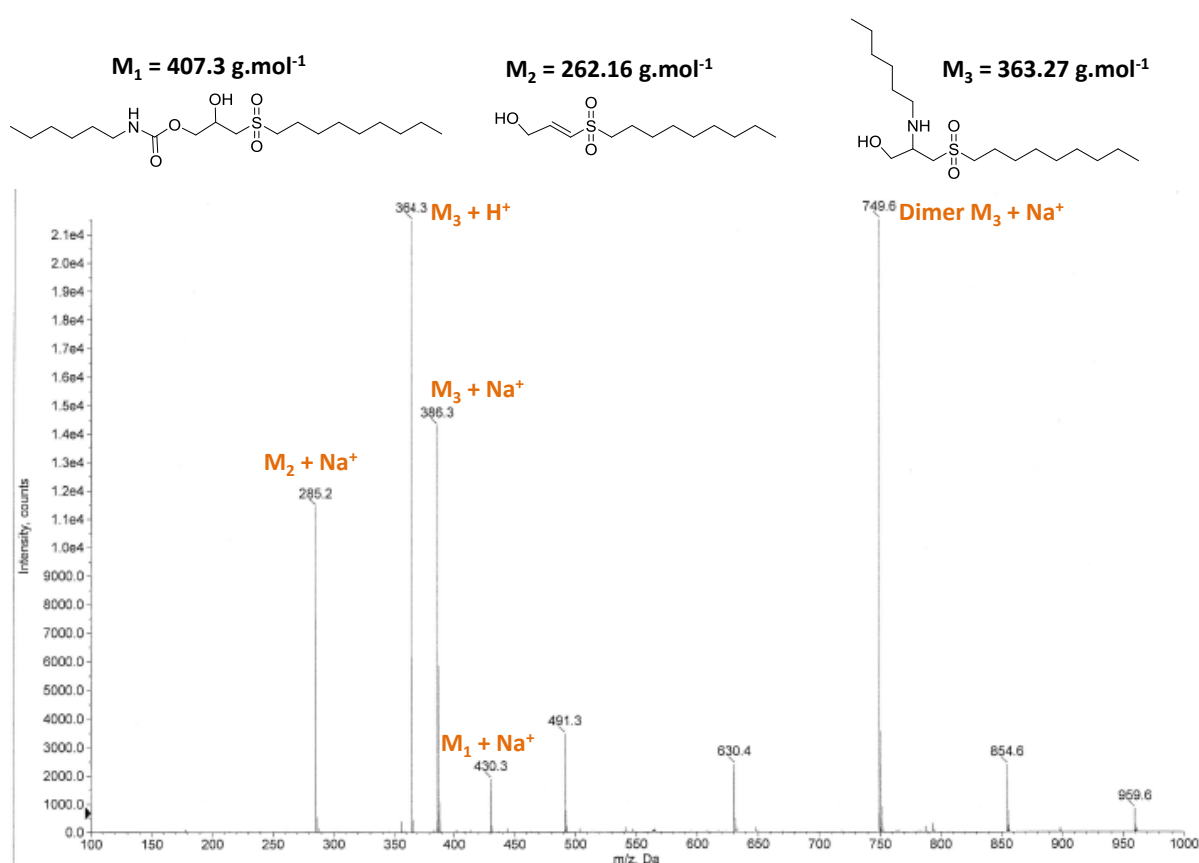


Figure ESI 4 – Mass spectrum (obtained by ESI) of the reaction between Dec-CC-sulfone and hexylamine at 50°C in DMSO (1mol.L⁻¹), with a ratio 1:1.

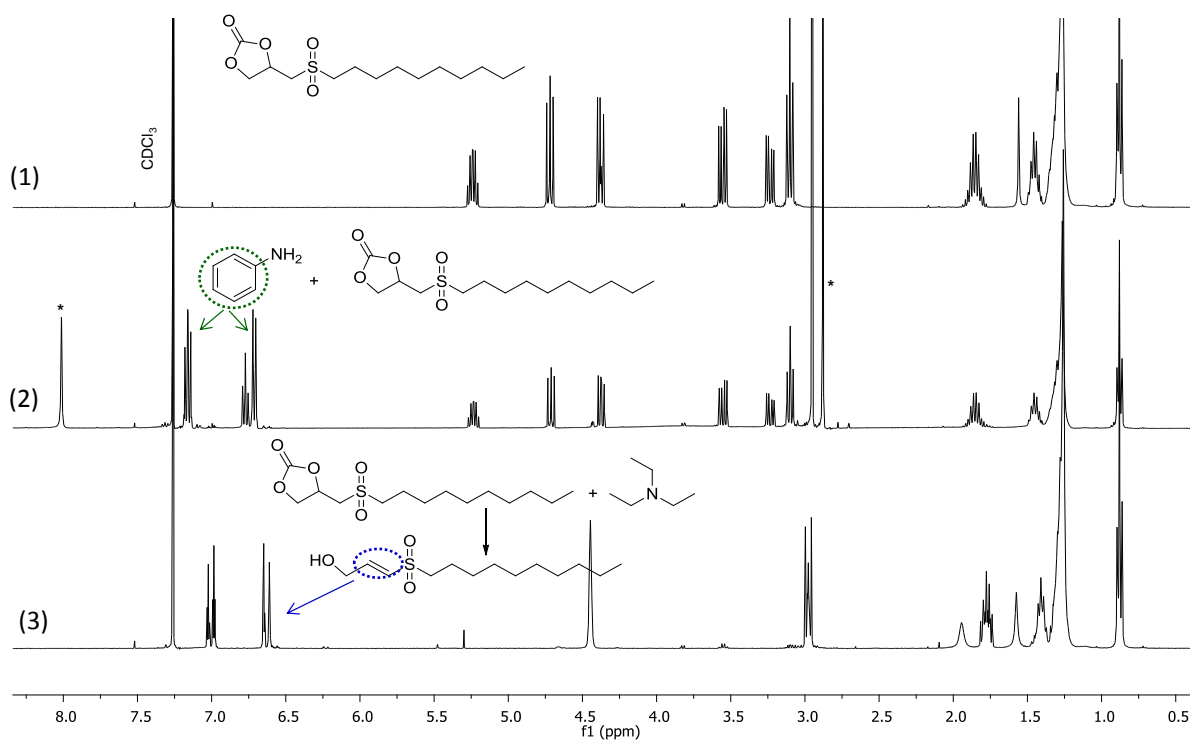


Figure ESI 5 - Stacked ¹H NMR spectra of (1) Dec-CC-sulfone, (2) the reaction between aniline and Dec-CC-sulfone of (3) the reaction between triethylamine and Dec-CC-sulfone (analysis performed in CDCl₃, *: residual solvents).

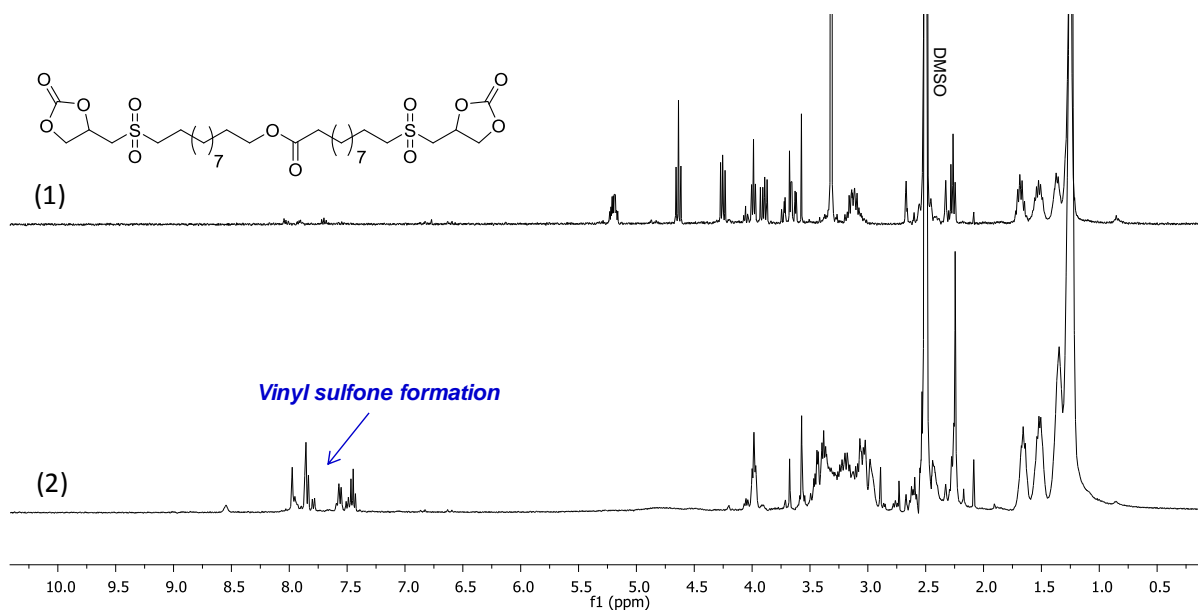


Figure ESI 6 - Stacked ^1H NMR spectra of (1) Und(ester)-bCC-sulfone and (2) the resulting polymer PHU 7 when polymerized with 10DA (analysis performed in DMSO- d_6).

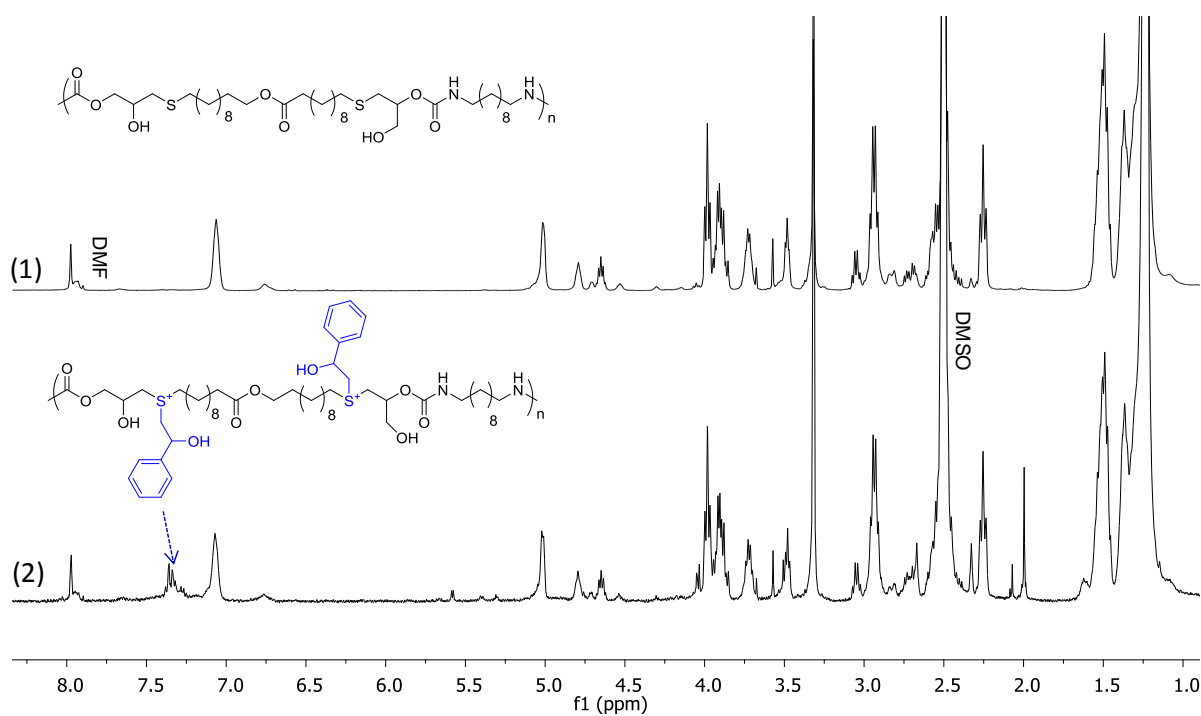


Figure ESI 7 - Stacked ^1H NMR spectra of (1) PHU 5 and (2) PHU 5-sulfonium after post-functionalization with epoxy styrene (analysis performed in DMSO- d_6).

Chapter 5

Potential solutions for the enhancement of cyclic carbonate reactivity towards amines: Catalysis and 'ultra'-activated monomers

Keywords: Reactive cyclic carbonate, methyl acrylate, poly(hydroxyurethane)s, thermosets, catalysis.

Mots-clés: Carbonate cyclique réactif, acrylate de méthyle, poly(hydroxyuréthane)s, thermosets, catalyse.

Table of contents

Introduction	229
1. Towards the catalysis of the cyclic carbonate-amine polyaddition	230
1.1. Screening of catalysts on the system DGDC-6cDA.....	230
1.2. Catalysis applied on lipidic activated-CC	235
2. ‘Ultra’-activated methyl acrylate-based cyclic carbonates towards PHUs and Poly(hydroxyurethane-amide-ester)s	236
2.1. Cyclic carbonates synthesis from methyl acrylate	237
2.1.1. <i>GECA synthesis</i>	237
2.1.2. <i>GECA and fatty acid-based monomer synthesis</i>	238
2.2. Kinetic study on GECA-based cyclic carbonate and side reactions.....	241
2.3. Polymerization of GECA and derivatives	245
2.3.1. <i>PHUs synthesis from GECA-based monomers</i>	245
2.3.2. <i>Poly(hydroxyurethane-amide-ester)s from GECA</i>	246
Conclusions	252
References	253
Experimental and Supporting Information	254

Introduction

The previous chapters described the development of reactive 5-membered cyclic carbonates through the insertion of ether, ester or sulfur moieties in β position nearby the cycle, with the aim of increasing their reactivity towards amines. Although the PHUs molar masses obtained with these monomers were improved in comparison to the ones achieved with non-substituted cyclic carbonates, efforts are still required to increase the kinetic of polymerization as well as the resulting PHU molar masses.

The present work constitutes a preliminary investigation into potential solutions for the enhancement of the 5-membered ring cyclic carbonate reactivity towards aminolysis. Besides, one of the main goals is to reach the maximum conversion for the obtention of high molar mass PHUs with strengthened thermo-mechanical properties. For that purpose, two strategies have been adopted in this Chapter: (i) the use of additives for the catalysis of the polyaddition and (ii) the modification of the monomer structure.

On the one hand, several catalysts such as LiCl, TBD and thioureas have been tested during the polyaddition between DGDC and the 1,3-cyclohexanebis(methylamine) (6cDA) in order to select the most efficient additives. Various catalytic systems were then applied on the fatty acid-based monomers synthesized in the Chapter 3, with the aim of analyzing the combined effect of the catalysis and of the monomer activation.

On the other hand, in the same perspective than the previous chapters, ‘ultra’-activated monomers were synthesized by epoxidation/carbonation of methyl acrylate, enabling the positioning of the ester moiety in α position. The negative inductive effect induced by the proximate ester destabilized the cycle that was much more reactive during aminolysis. A fatty-acid derivative could be coupled by enzymatic transesterification to the carbonated methyl acrylate (**GECA**) in order to obtain a lipidic and ‘ultra’-activated bis-cyclic carbonate that can be polymerized with diamines. The high reactivity of such monomers induced amidation side reactions that could be used for the synthesis of hybrid Poly(hydroxyurethane-amide)s when **GECA** was directly polymerized with diamines in presence of TBD.

Strategy adopted in Chapter 5

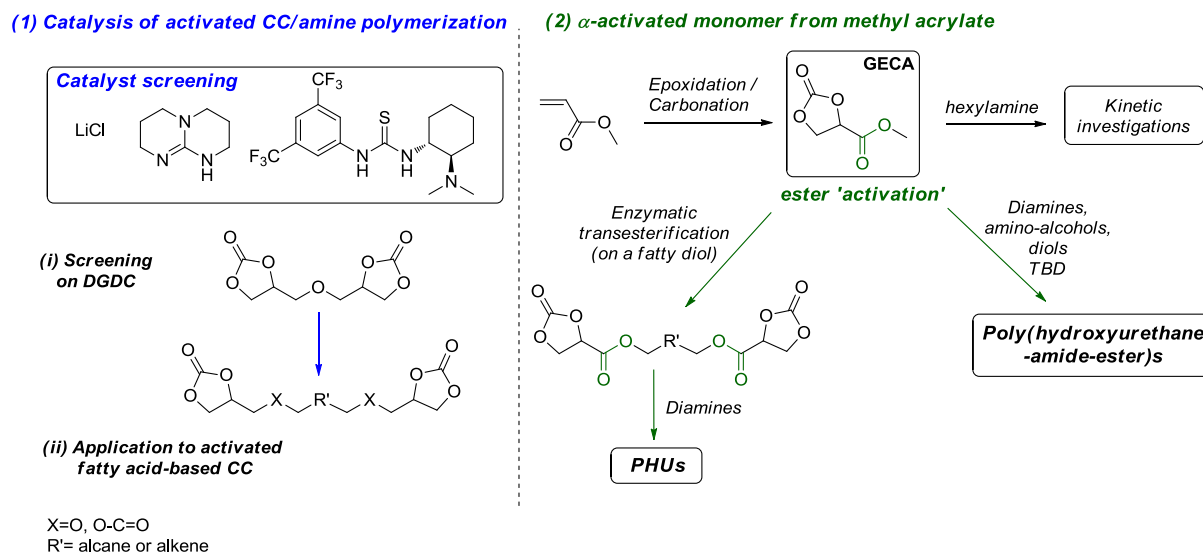


Figure 1 – Strategy adopted to further enhance CC reactivity towards aminolysis.

1. Towards the catalysis of the cyclic carbonate-amine polyaddition

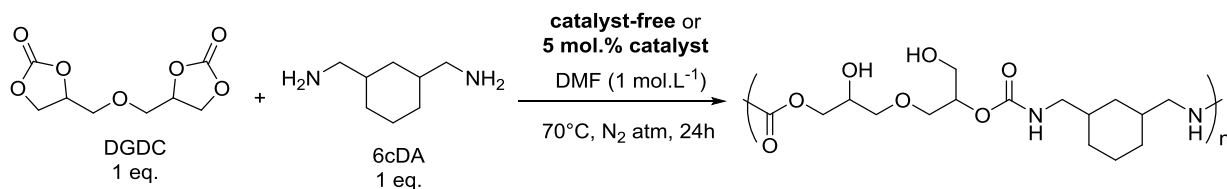
A potential solution for the improvement of the 5CC reactivity towards amines is the use of catalysts. Various additives already tested in previous works¹⁻⁹ were employed to polymerize our bio-based cyclic carbonates, in order to see the effect of the combined monomer activation and the presence of a catalyst. A screening of catalysts was first carried out on the polyaddition between DGDC and 6cDA. Then, some catalytic systems were selected to polymerize some of the lipidic reactive cyclic carbonates synthesized in Chapter 3.

1.1. Screening of catalysts on the system DGDC-6cDA

The catalyst screening was conducted on the polymerization of diglycerol dicarbonate (DGDC) as it is readily available from the one-step reaction between diglycerol and dimethyl carbonate (see Chapter 3). 6cDA was used as comonomer because of its lower reactivity in comparison to the aliphatic diamines such as 10DA. The effect of the catalyst would be consequently highlighted.

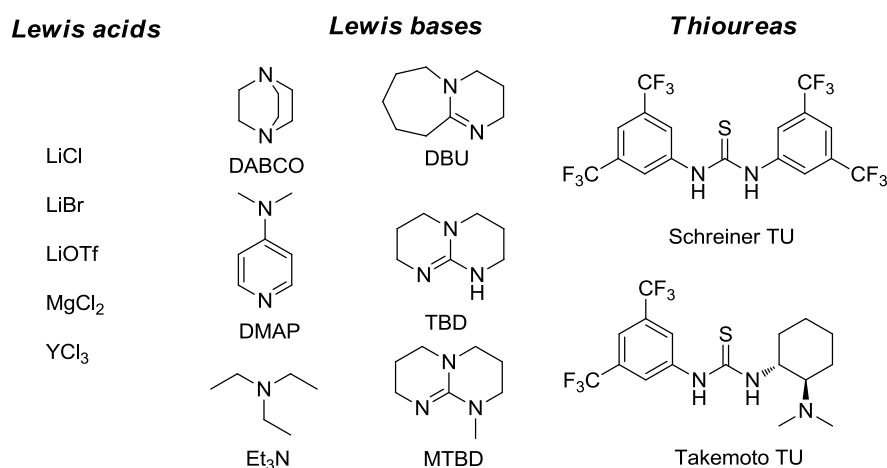
The polymerizations were performed in DMF (1 mol.L⁻¹) at 70°C under nitrogen for 24h (see Scheme 1). In the purpose of following the DGDC conversion kinetic into urethane functions,

aliquots were taken at $t=0\text{h}$, 0.5h, 1h, 3h, 5h, and 24h and analyzed by means of ^1H NMR spectroscopy, following the disappearance of the cyclic carbonates signals between 4.95 and 3.70 ppm (see Figure 2).



Scheme 1 -Procedure for catalyst-free or catalyzed-polymerizations between DGDC and 6cDA.

Firstly, the catalyst-free polymerization of DGDC and 6cDA was carried out and used as a benchmark for further comparison with catalyzed polyadditions. Then, several catalysts represented in Scheme 2 were tested on the DGDC/6cDA system. Cooperative catalysis, that has been reported to be efficient to catalyze the hydroxyurethane formation,¹⁰ was also achieved. The resulting PHU properties (molar mass, $T_{d5\%}$) were analyzed and correlated to the catalyst employed. All the results are presented in Table 1.



Scheme 2 - Catalysts used for the synthesis of PHU from DGDC and 6cDA

The Figure 3 depicted the kinetic of the catalyst-free as well as the catalyzed polymerizations over 24h. **PHU 0** synthesized without the use of catalyst displayed a DGDC conversion of 91% after 24h. With respect to the kinetic profiles shown in Figure 3, some additives such as LiOTf exhibited a slower polyaddition kinetic than the catalyst-free polymerization one. Contrarily, both thioureas enhanced the DGDC conversions during and at the end of the

polyaddition (around 95%). In all cases, the kinetic profile of the DGDC conversion tends to reach a plateau from the beginning of the reaction (0.5 h). However, the ^1H NMR analyses of the aliquots were performed after 2 days of DMF evaporation at room temperature. Additionally, the polyadditions were not quenched because, as demonstrated by Maisonneuve *et al.*¹¹, the quenching procedure with a primary amine such as hexylamine induced the formation of urea and a subsequent decrease in PHU molar masses. Consequently, the conversions were over-estimated and were not representative of the actual kinetic of the DGDC conversion.

Hence, the effect of the catalyst on the kinetic of the polymerization was not investigated. Besides, a particular attention was given to the catalyst effect on the degradation temperature and the molar masses of the resulting PHUs.

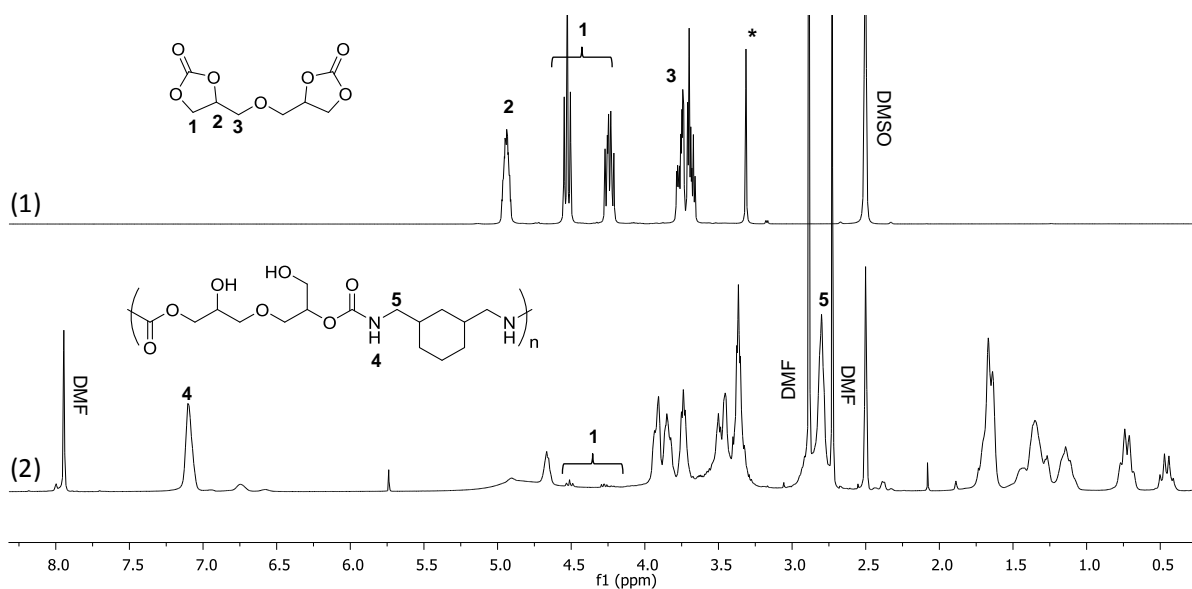


Figure 2 - Stacked ^1H NMR spectra of (1) DGDC and (2) PHU 0 after 24h (*: impurities or residual solvents. Analysis performed in DMSO-d₆)

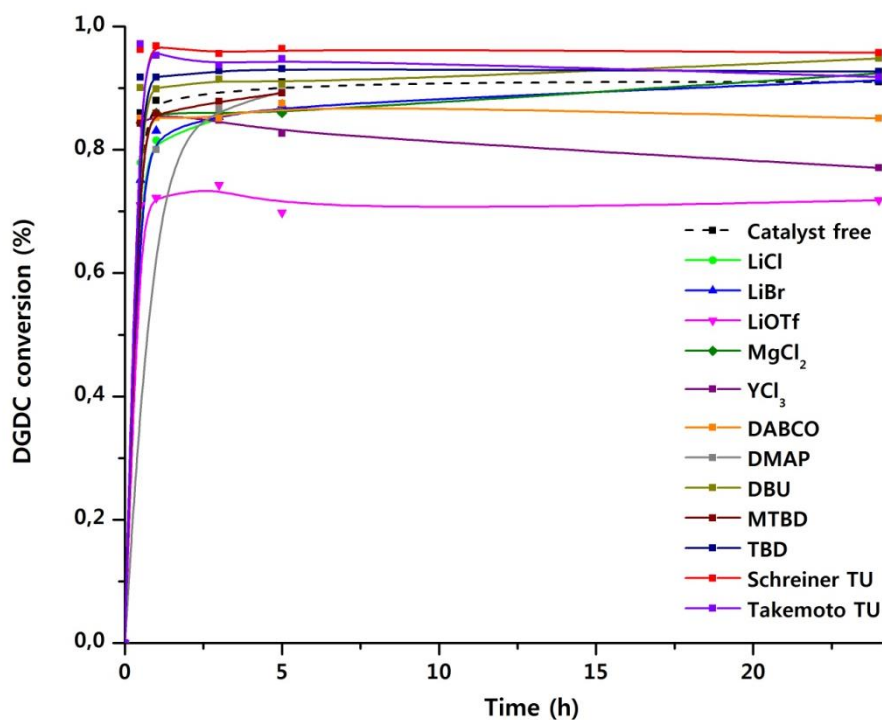


Figure 3 – Kinetic profiles of the catalyst-free and catalyzed DGDC/6cDA polymerizations over 24h.

Table 1 – Catalyst screening on the polyaddition between DGDC and 6cDA.

PHU	Catalyst	$\bar{M}_n(\text{g}\cdot\text{mol}^{-1})^1$	\bar{D}^1	$T_{d5\%}(\text{°C})^a$
0	-	3800	2	231
1	LiCl	8100	1.7	243
2	LiBr	6400	1.8	226
3	LiOTf	5800	1.5	228
4	MgCl ₂	3200	1.9	220
5	YCl ₃	2400	1.7	220
6	DABCO	3900	2.5	215
7	DMAP	5000	1.7	205
8	Et ₃ N	10700	1.3	219
9	DBU	8400	1.6	199
10	MTBD	2300	2	217
11	TBD	4950	1.9	195
12	Schreiner TU	2400	2.1	224
13	Takemoto TU	2600	1.8	232
14	LiCl/DBU	5200	2.3	201
15	LiCl/ Et ₃ N	10400	1.8	223

¹: Determined at the end of the polymerization (24h) by SEC in DMF (LiBr, PS Std); ^a: Determined by TGA at 10°C.min⁻¹ under nitrogen.

A catalyst is commonly employed to lower the activation energy of the polymerization. This pattern has a direct consequence on the depolymerization that is eased in the presence of the same catalyst. Its efficiency can thus be apprehended by a TGA analysis. With regard to the temperature of degradation at 5% weight loss, values below 220°C were achieved when polymerizations were carried out using Lewis bases as catalyst. TBD and DBU were the most efficient additives for decreasing the polymer thermal stability below 200°C and favoring the depolymerization. Such strong bases have already been reported in the literature to be the most suitable catalysts for the PHU synthesis.¹⁻⁵

On the other hand, catalysts impacted significantly the PHU molar masses. Indeed, the highest one was obtained for **PHU 8** with 10700 g.mol⁻¹ when triethylamine (Et₃N) was used as catalyst. Besides, **PHU 1** synthesized with LiCl as additive displayed a relatively high molar mass of 8100 g.mol⁻¹ even though the thermal stability of the polymer was conserved.

Cooperative catalysis has been reported to be one of the most efficient solutions to catalyze the CC/amine polyaddition,¹⁰ thanks to the combine effect of an acid and a base. In the reported mechanism, the Lewis acid enhances the electrophilicity of the CC carbonyl group, favoring the attack of the co-catalyst (Lewis base). Such strategy was tested on DGDC/6cDA, taking the most suitable Lewis acid (5 mol.% of LiCl) and several efficient Lewis bases (5 mol.%), following the procedure used in the previous part (see Scheme 1).

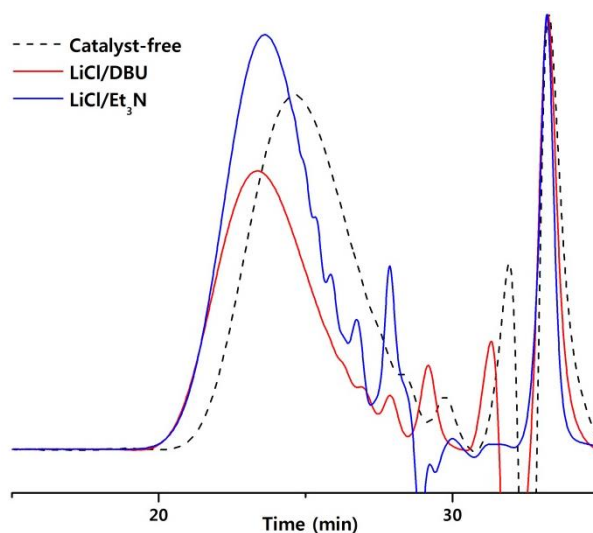


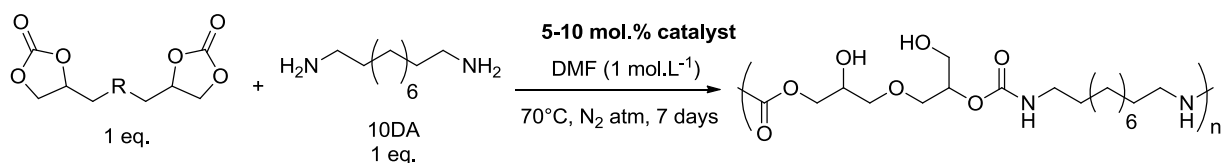
Figure 4 - SEC traces (DMF, LiBr, PS standards) of PHU 0, 14 and 15, in order to see the effect of the co-catalysis on the PHU molar masses in comparison to the catalyst-free one.

SEC traces in Figure 4 clearly demonstrate the benefits brought by the cooperative catalyses on the PHU molar masses. The most promising result was obtained for **PHU 15** by combining

LiCl and Et₃N in the same catalytic system, enabling the preparation of a higher molar mass PHU (10400 g.mol⁻¹, Đ=1,8). However, no significant difference in molar mass was observed on the resulting PHU when Et₃N or the cooperative catalytic system LiCl/ Et₃N were utilized.

1.2. Catalysis applied on lipidic activated-CC

The most common catalysts as well as the best catalytic systems investigated in the previous part were used to polymerize ether- and ester-activated cyclic carbonates (*Und-bCC-ether* and *Und-bCC-ester*) synthesized in the Chapter 3. The polymerizations were performed in DMF (1 mol.L⁻¹) at 70°C under nitrogen for 7 days using 0, 5 or 10 mol.% of catalyst (see Scheme 3). The resulting PHU were analyzed by ¹H NMR spectroscopy, SEC and TGA (see Table 2).



Scheme 3 - Procedure for catalyst-free or catalyzed-polymerizations between lipidic activated-bCC and 10DA.

Interestingly, the Schreiner TU as well as the bases TBD and DBU were not selective of the ester-activated CC ring-opening. Indeed, such catalysts are commonly used for transesterifications and were able, in our case, to catalyze the transamidation reaction of 10DA onto the ester moieties present in *Und-bCC-ester*. This side reaction resulted in the random cleavage of the polymer backbone, reducing the molar masses and increasing the dispersities. Consequently, dispersities in between 2.5 and 3.1 and molar masses in the ranges 4160-6730 g.mol⁻¹ were achieved using these catalysts. This pattern is confirmed by the higher amount of amide functions exhibited by **PHU 18** and **19**. Thus, the combined effect of catalysis and monomer activation was disadvantageous in the case of ester-activated cyclic carbonates, and led to PHU with lowered properties.

With regard to the catalysis of *Und-bCC-ether*, all the catalysts (except TBD) were favoring the preparation of higher molar mass PHU in comparison to **PHU 20** synthesized without catalyst. 5 mol.% of LiCl/DBU was found to be the best suited catalytic system to achieve **PHU 25** with a molar mass of 15300 g.mol⁻¹. The high catalytic effect of this cooperative catalysis was confirmed by the decrease of the temperature of degradation at 5 w.% from 270 to 227°C. Interestingly, the TBD and DBU were more selective towards the cyclic carbonate

aminolysis, as less ureas were generated during the polymerization. However, none of the catalyst was significantly impacting the selectivity between OH_I: OH_{II}.

Therefore, the polymerization of ether-activated CC such as DGDC and *Und-bCC-ether* with diamines can be catalyzed by a co-catalytic system, including a Lewis base and a Lewis acid. In the case of ester-activated cyclic carbonates, the tested catalysts were not selective to aminolysis and resulted in an increase of transamidation side reaction.

Table 2 – Catalysis of the polymerization between lipidic activated-bCC and 10DA.

PHU	bCC	Catalyst (10 mol.%)	Ratio OH _I :OH _{II} ¹	Ratio Urea /Amide/Urethane ¹	\bar{M}_n (g.mol ⁻¹) ²	\bar{D} ²	T _{d5%} (°C) ^a
16		-	41:59	9.6/2.6/87.8	12000	1.9	274
17	<i>Und-bCC- ester</i>	Schreiner TU	36:64	11/7/82	6730	2.5	266
18		TBD	39:61	2/5/86	4430	3.1	214
19		DBU	42:58	5/6/89	4160	3.1	242
20		-	28:72	12/0/88	7500	1.7	270
21	<i>Und-bCC- ether</i>	Schreiner TU	28:72	11/0/89	8300	1.6	257
22		TBD	26:74	7/0/93	3730	1.9	210
23		DBU	24:76	7/0/93	10070	1.6	257
24		Et ₃ N *	28:72	11/0/89	15500	1.5	272
25		LiCl/DBU*	28:72	11/0/89	15300	1.5	227
26		LiCl/ Et ₃ N *	31:69	10/0/90	11900	1.4	239

*: 5 mol.% of catalyst. ¹: Determined by ¹H NMR spectroscopy at the end of the polymerization (7 days); ²: Determined by SEC in DMF (LiBr, PS Std); ^a: Determined by TGA at 10°C.min⁻¹ under nitrogen.

2. 'Ultra'-activated methyl acrylate-based cyclic carbonates towards PHUs and Poly(hydroxyurethane-amide-ester)s

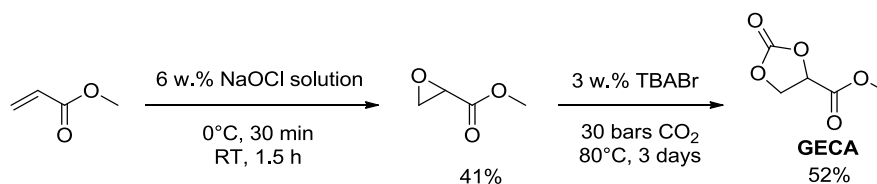
As seen in the previous chapters, the cyclic carbonates from fatty acid derivatives were specifically designed by inserting ether, ester and sulfur moieties in β position nearby the cycle, in order to improve their reactivity towards amines. In this part of the chapter, methyl acrylate was used as a building block to design α-activated cyclic carbonates. The latter have not been synthesized and described in the academic research field. Nonetheless, two interesting patents from the same group ^{12,13} protected the syntheses of α-activated cyclic

carbonates from methyl acrylate, with an ester or amide as “activating groups”. The latter exhibit an exacerbated reactivity towards amine, making them attractive for the synthesis of poly(hydroxyurethane)s.

2.1. Cyclic carbonates synthesis from methyl acrylate

Here, the epoxidation/carbonation strategy was applied on the methyl acrylate to obtain the carbonated methyl acrylate called 4-methoxycarbonyl-2-oxo-1,3-dioxolane or **GECA** (see Scheme 4). The latter was then coupled by enzymatic transesterification to *Und-C20-diol*, to develop a reactive fatty acid-based bis-cyclic carbonate.

2.1.1. GECA synthesis



Scheme 4- Synthesis of GECA from methyl acrylate with corresponding yields.

Methyl acrylate was first epoxidized with a sodium hypochlorite solution following a procedure reported by Stevenson *et al.*¹⁴ The crude product was extracted with DCM and purified by evaporation using the rotary evaporator. However, due to the high volatility of methyl acrylate and of its epoxidized homologue, the conversion could not be calculated. The yield was evaluated at 41% after a complete evaporation of the unreacted methyl acrylate. The formation of the desired product was confirmed by means of ¹H NMR spectroscopy with the signals at 3.42 ppm and 2.93 ppm characterizing the epoxide function (see Figure 5).

From an industrial point of view, it could be interesting to increase the yield of the epoxidation step. The close boiling points of the reagent and the product make the selective distillation difficult. Temperature was decreased from 30 to 20°C during the solvent evaporation but no significant improvement on the yield was observed. However, the latter could be dramatically increased using specific distillation equipments (fractional distillation).

A second strategy consisted in using heavier acrylate such as methyl methacrylate or tertbutyl acrylate to prevent the evaporation of the epoxidized product. Nonetheless, the epoxidation of

those hindered acrylates could not be achieved under the conditions mentioned in Scheme 4. The strategy was thus set aside.

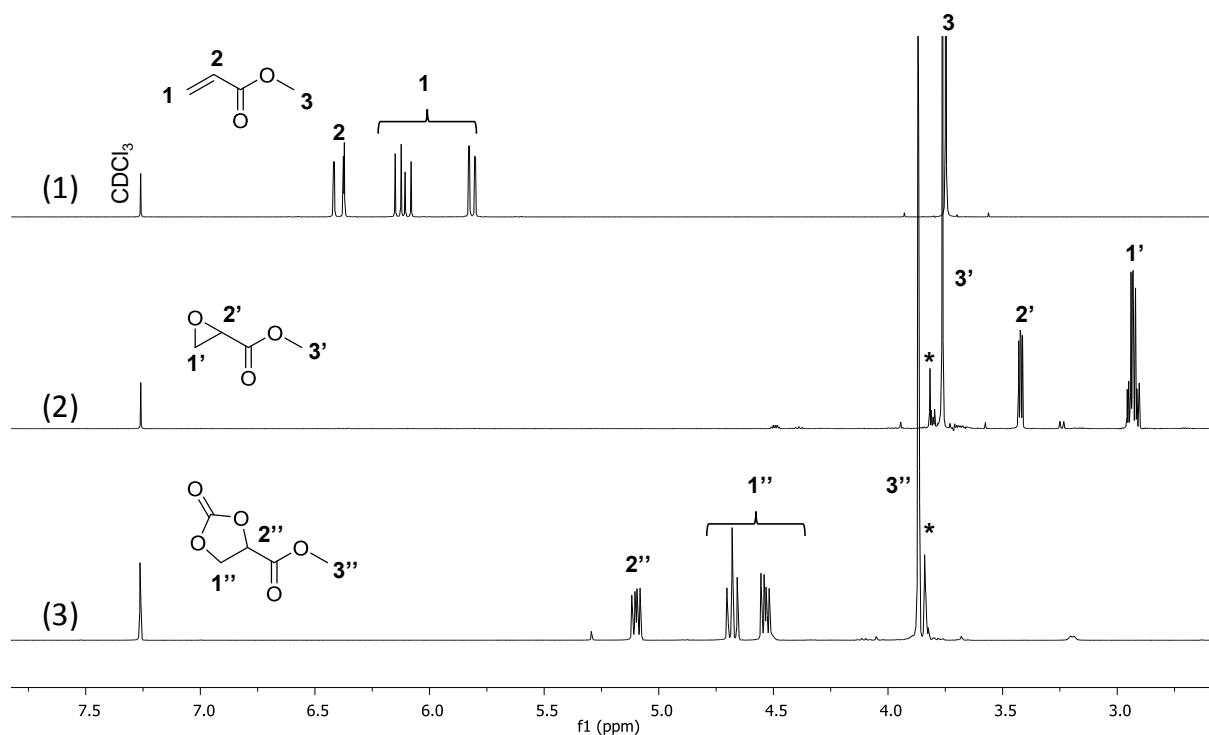


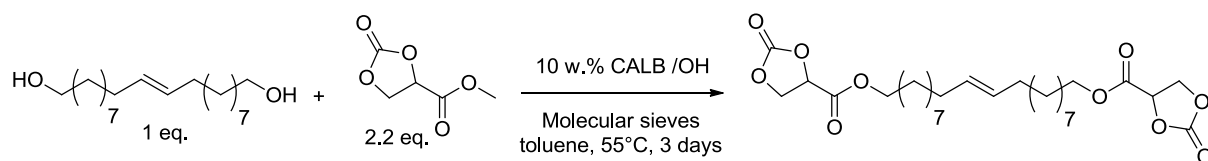
Figure 5- Stacked ¹H NMR spectra of (1) methyl acrylate, (2) epoxidized methyl acrylate and (3) GECA. (All analyses were performed in CDCl₃,*: impurities)

In a second step, the carbonation of the epoxidized methyl acrylate was performed under pressurized CO₂ using TBABr as catalyst. After 24h, the conversion was below 50%. Consequently, the reaction was conducted upon 3 days to reach full conversion. The **GECA** formation was confirmed by ¹H NMR spectroscopy with the appearance of the proton 2'' (see Figure 5) at 5.08 ppm, attributed thanks to 2D NMR spectroscopies (see ESI). **GECA** was obtained as a clear yellow liquid at 52% yield after purification by flash chromatography. This synthesis was performed at the gram scale with more than 30 g of **GECA** synthesized in the course of this study. This process can be transferred at the industrial scale but requires specific distillation equipments to be reliable.

2.1.2. **GECA and fatty acid-based monomer synthesis**

In the purpose of providing a reactive fatty acid-based bis-cyclic carbonate, the **GECA** building block was coupled to *Und-C20-diol* by enzymatic transesterification using the supported-enzyme *Candida Antarctica* Lipase B (CALB). Such synthesis has already been

described in a patent ¹³ that provides an enzymatic process for the preparation of **GECA**-based compounds.



Scheme 5- Synthesis of bisGECA-C₂₀ by enzymatic transesterification.

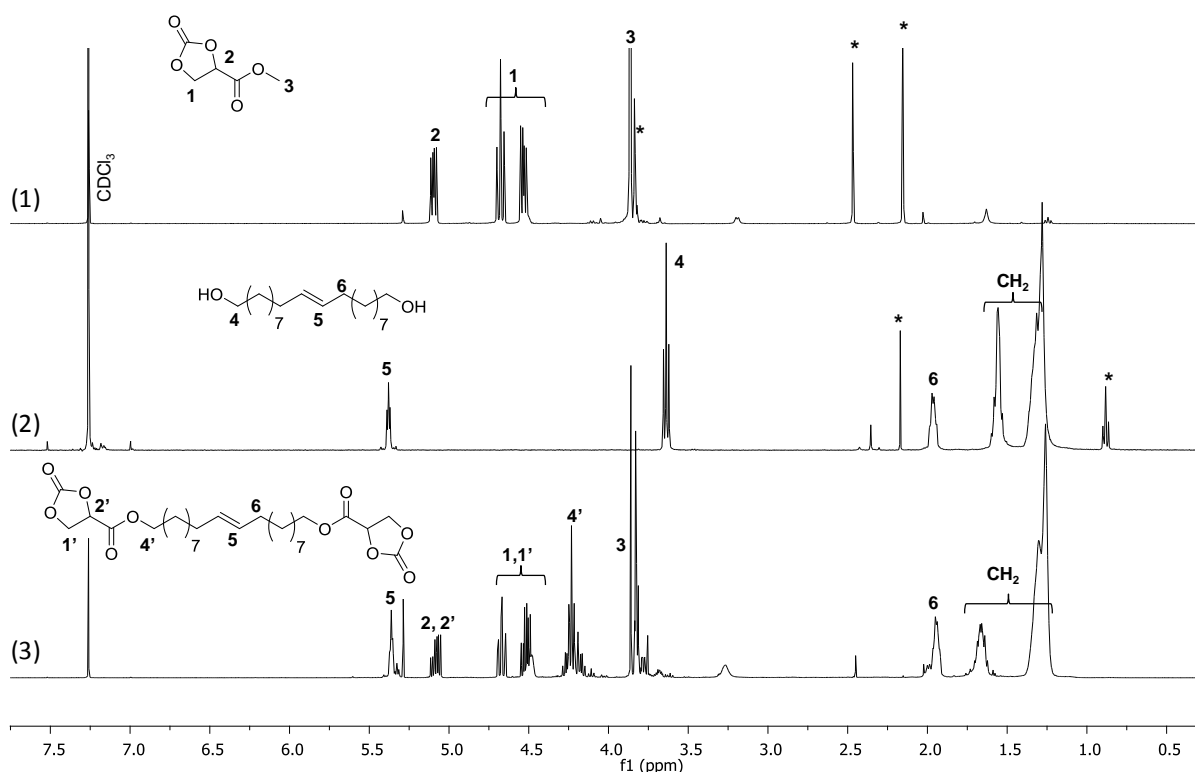
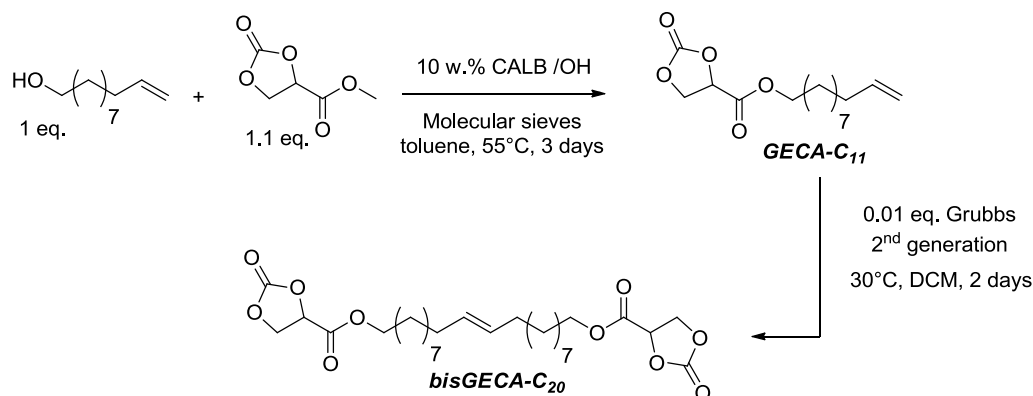


Figure 6- Stacked ¹H NMR spectra of (1) GECA, (2) Und-C₂₀-diol and (3) bisGECA-C₂₀ after flash chromatography. (All analyses were performed in CDCl₃.) (*: impurities)

The *bisGECA-C₂₀* whose synthesis is illustrated in the Scheme 5 was obtained after 3 days of an enzymatic transesterification between *Und-C₂₀-diol* and **GECA**. The reaction was performed in the presence of activated molecular sieve (4Å) in order to drive the equilibrium towards the formation of the product. Moreover, the enzyme was used on a support to ease the purification process. The formation of the product was confirmed by ¹H NMR spectroscopy with the disappearance of the protons at 3.6 ppm nearby the alcohol functions and the appearance of the characteristic signals of the cyclic carbonate at 5.09, 4.65 and 4.53 ppm (see Figure 6). The product was not purified as the residual **GECA** could not be separated from *bisGECA-C₂₀* by flash chromatography (see Figure 6 and column chromatogram in ESI).

Another strategy was conducted for the synthesis of *bisGECA-C₂₀*, performing first the transesterification between **GECA** and 10-undecen-1-ol, followed by a self-metathesis reaction of the so-formed mono-cyclic carbonate (see Scheme 6).



Scheme 6- Synthesis of *bisGECA-C₂₀* by *GECA-C₁₁* self-metathesis.

The transesterification step was assessed by means of ¹H NMR with the disappearance of the signals at 3.6 ppm corresponding to the protons in alpha of the alcohol function and with the characteristic signals of the **GECA** building block at 5.07, 4.67 and 4.52 ppm. The so-formed *GECA-C₁₁* was purified by flash chromatography and obtained with a yield of 65%. The product was subsequently dimerized by a self-metathesis reaction using a 2nd generation Grubbs catalyst. After 2 days of reaction, the conversion was estimated by ¹H NMR with the disappearance of the typical signals of the external double bonds (5.80 and 4.92 ppm), in favor of the protons corresponding to the formation of internal unsaturations at 5.37 ppm (see Figure 7). After a recrystallization in cold DCM, *bisGECA-C₂₀* was obtained at 26% yield and was fully characterized by means of 1D and 2D NMR spectroscopies (see ESI).

The synthesis of *bisGECA-C₂₀* via the *GECA-C₁₁* self-metathesis was preferred over the first method, as the final product was easier to purify by recrystallization and was consequently more likely to be used in polymerization. Indeed, the purification of *bisGECA-C₂₀* synthesized from the first method could not be recrystallized as the co-crystallization of the *Und-C₂₀-diol* was occurring.

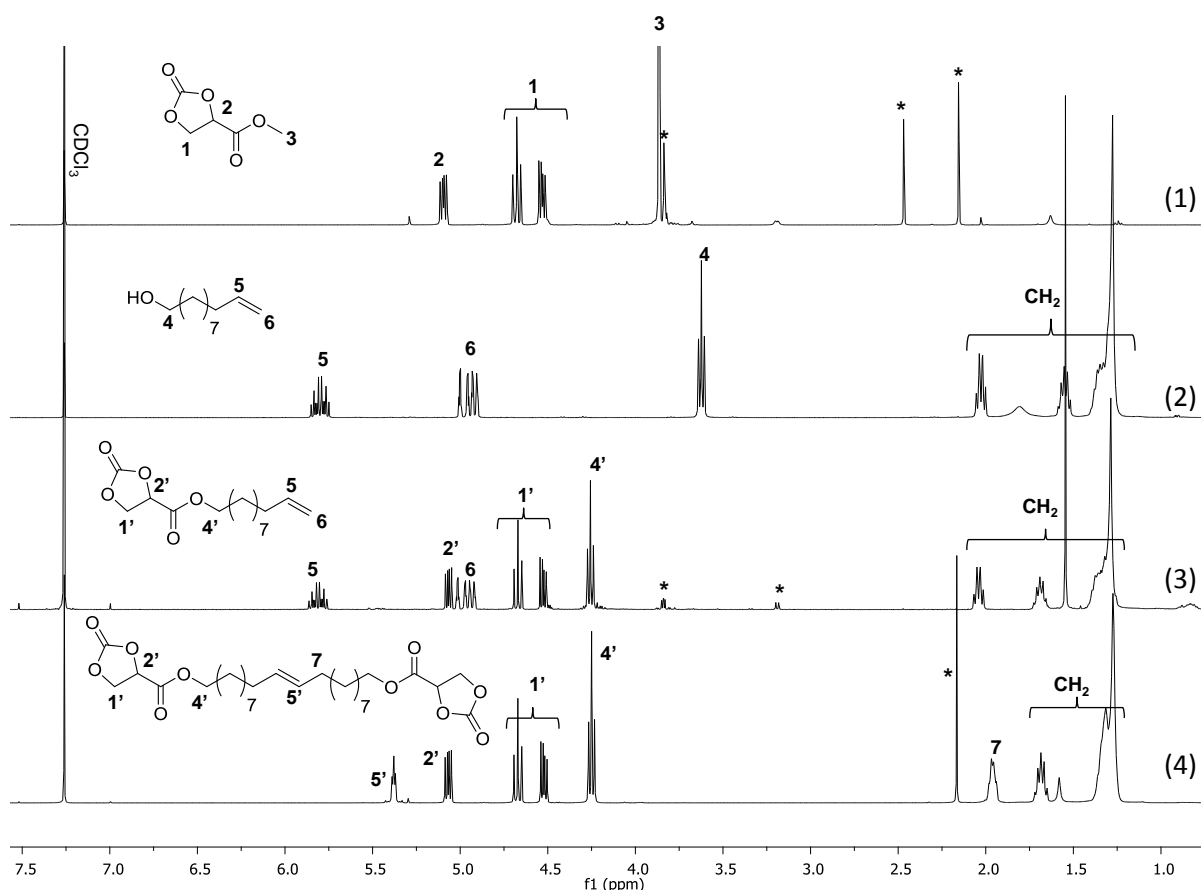
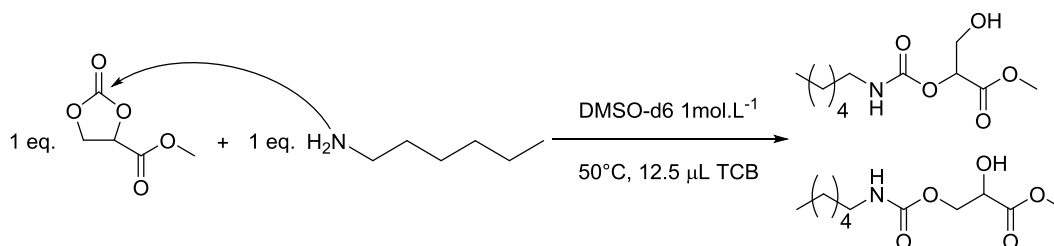


Figure 7- Stacked ^1H NMR spectra of (1) GECA, (2) 10-undecen-1-ol, (3) GECA- C_{11} and (4) bisGECA- C_{20} . (All analyses were performed in CDCl_3 .) (*: impurities)

2.2. Kinetic study on GECA-based cyclic carbonate and side reactions

In order to quantify the reactivity of the α -activated cyclic carbonates, kinetic experiments were monitored *in situ* by ^1H NMR spectroscopy. GECA and GECA- C_{11} were reacted with hexylamine at 50°C in DMSO-d_6 at $1\text{ mol}\cdot\text{L}^{-1}$ for 24h, with trichlorobenzene (TCB) as internal reference (see Scheme 7).



Scheme 7- Model reaction between GECA and hexylamine.

The GECA conversion was followed *in situ* by ^1H NMR for 24h, thanks to the disappearance of the CC protons between 4.6 and 5.4 ppm and to the appearance of the protons in alpha of the urethane function at 2.98 ppm (see Figure 8). The conversion was plotted as a function of

time (see Figure 9). The **GECA** displayed a high reactivity towards hexylamine since a conversion close to 100% was reached after 10 min of reaction. **GECA-C₁₁** demonstrated a conversion of 75% after 10 min, supporting the lower reactivity of such lipid-based cyclic carbonate. In comparison, the reactive TMC and **UndCC-ester** displayed a conversion below 10% after the same time. This results indicates that the insertion of an ester moiety in alpha of the cyclic carbonates generate ‘ultra’-reactive monomers towards aminolysis. The Table 3 showing the DFT calculation, demonstrated the high reactivity of **GECA**, thanks to the longer bond length between the oxygen and the cyclic carbonate carbonyl (1.368 Å), in comparison to the **UndCC-ester** one (1.361 Å). Unfortunately, the k_{app} of **GECA** and **GECA-C₁₁** could not be calculated because of the high reactivity over the five first minutes.

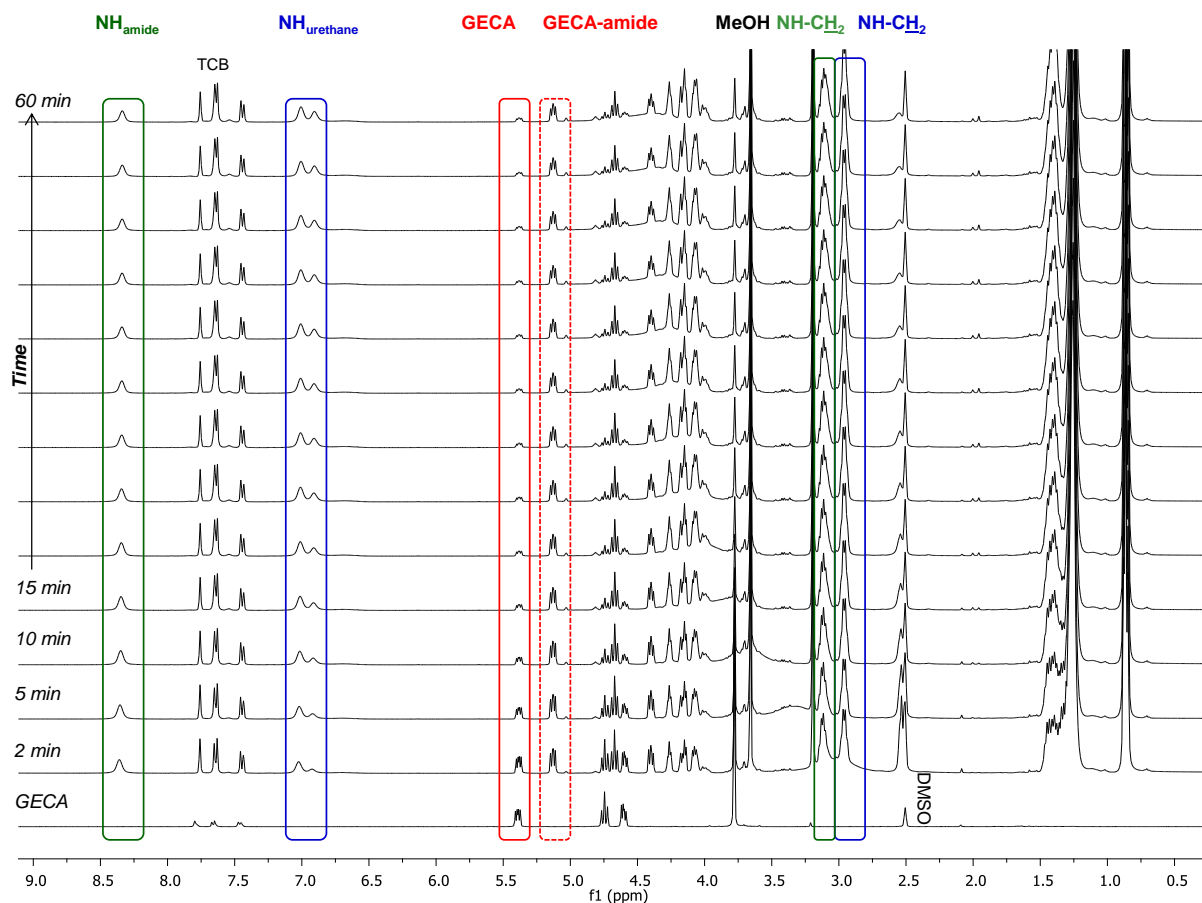


Figure 8- Stacked ¹H NMR monitoring of the reaction between GECA and hexylamine at 50°C in DMSO-d₆ (1 mol.L⁻¹), with a ratio 1:1.

The stacked ¹H NMR spectra of the model reaction between **GECA** and hexylamine in Figure 8 revealed the formation of amide functions from the beginning of the reaction, with the appearance of the labile protons at 8.4 ppm and of the protons in α of the amide at 3.1 ppm. After 60 min, 23% of amides were visible by ¹H NMR (see Table 3). The presence of amides

is related to the transamidation of the methyl ester function of the **GECA** with hexylamine. The resulting **GECA-amide** (see Scheme 8) was identified by ^1H NMR with the proton present on the tertiary carbon of the cyclic carbonate at 5.1 ppm, as well as with the appearance of methanol released during the reaction at 3.16 ppm. As depicted in Scheme 8, this reaction can occur on the hydroxyurethanes formed by the ring-opening of **GECA** with hexylamine, resulting in the formation of a hydroxyurethane-amide. ESI analysis presented in Supporting Information, confirmed the formation of both hydroxyurethane and hydroxyurethane-amide. Moreover, the formation of **GECA-amide** intermediate was immediate after the insertion of the amine as demonstrated by the ^1H NMR spectrum after 2 min of reaction. Consequently, the **GECA-amide** that presents an amide function in α of the cycle was more reactive towards aminolysis compared to **GECA**. Noteworthy, no urea function was detected, probably due to the quick hexylamine consumption through hydroxyurethane and amide formations.

With respect to **GECA-C₁₁**, its lower reactivity could be related to the presence of a long carbon chain nearby the ester function. Indeed, the transamidation reaction is more hindered and the aliphatic chain possibly stabilizes the carbonyl function.

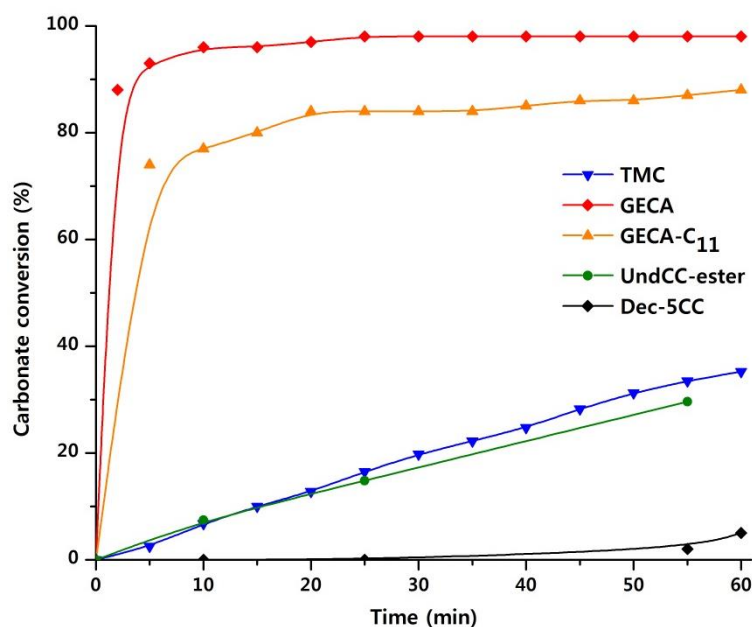
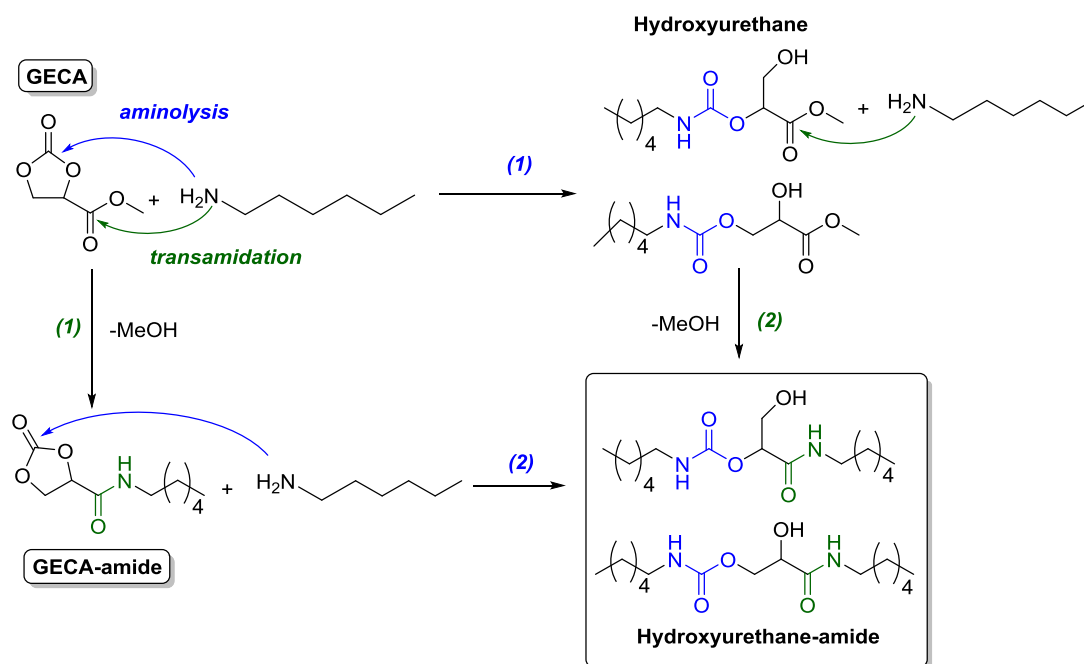


Figure 9- Kinetic of the reaction of **GECA**, **GECA-C₁₁**, **TMC**, **UndCC-ester** and **Dec-5CC** with hexylamine, followed *in situ* by ^1H NMR spectroscopy. (50°C, 1 mol.L⁻¹ in DMSO-d₆, ratio 1:1)



Scheme 8- Two major reactions occurring between GECA and hexylamine, identified by ^1H NMR spectroscopy and ESI analysis.

Table 3 – Kinetic, selectivity and DFT data for UndbCC-ester, GECA and GECA- C_{11} .

<i>Kinetic and selectivity*</i>			
	<i>UndCC-ester</i>	<i>GECA</i>	<i>GECA-C₁₁</i>
Urethane (%) ¹	95.2	77	67
Amide (%) ¹	2.1	23	33
Urea (%) ¹	2.7	0	0
Ratio OH _I :OH _{II}	23:77	nd	nd
<i>DFT Calculations</i>			
-X	<i>-CH₂-OC=OMe</i>	<i>-C=OOMe</i>	
Bond length (Å) 	1.361	1.368	
Bond length (Å) 	1.363	1.355	
ΔH_f (kJ.mol⁻¹) 	-57.96	-22.79	
ΔH_f (kJ.mol⁻¹) 	-62.83	-56.57	

*: Determined after 60 min of model reaction; ¹: Proportions calculated with the Equations in ESI† of Chapter 3.

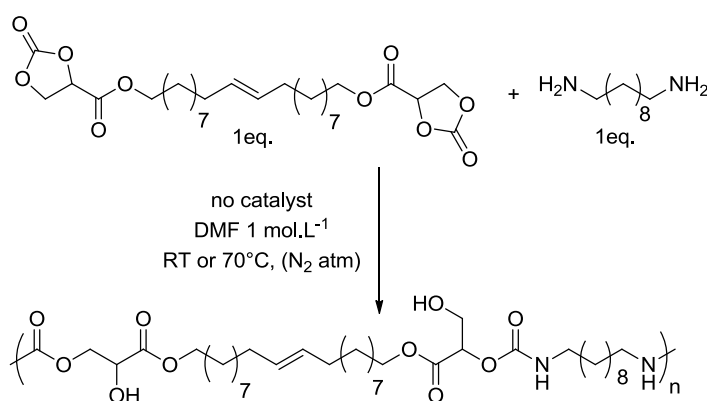
The presence of ester functions in α -position nearby the cyclic carbonate dramatically increases its reactivity when reacted with amines. Nonetheless, the unavoidable transamidation side reaction leads to hybrid molecules containing both hydroxyurethane and

amide functions. **GECA** can consequently be considered as an AA*-monomer that will be polymerized with diamines in the part 1.3.2, for the preparation of hybrid materials.

2.3. Polymerization of GECA and derivatives

2.3.1. PHUs synthesis from GECA-based monomers

The *bisGECA-C₂₀* was polymerized with 10DA for 7 days following the methodology illustrated in Scheme 9, in order to evaluate the possibility of preparing PHUs from such activated monomer. Two temperatures were tested to see the impact on the conversions, side reactions and molar masses of the polymer. The results are presented in Table 4.



Scheme 9- Polymerization of bisGECA-C₂₀ and 10DA in DMF (1 mol.L⁻¹) at different temperatures.

Table 4- Characterization of PHUs obtained from bisGECA-C₂₀ and 10DA.

PHU	Reaction conditions	Conversion 24h/7d (%) ¹	Ratio urethane/amide/urea ^{1,2}	\bar{M}_n (g.mol ⁻¹) [D] ³	T _g (°C) ^a	T _m (°C) ^a	T _{d5%} (°C) ^b
1	DMF 1 mol.L ⁻¹ 70°C	92/92	75 / 16 / 9	5200 [1.62]	-6	39/69	230
2	DMF 1 mol.L ⁻¹ RT	90/91	85 / 7 / 8	3500 [1.58]	nd	nd	nd

¹:Determined by ¹H NMR spectroscopy; ²: Determined using the relations (E), (E') and (E'') (see ESI, Chapter 3); ³:Determined by SEC in DMF (LiBr, PS Std); ^a: Determined by DSC at 10°C.min⁻¹ from the second cycle. ; ^b: Determined by TGA at 10°C.min⁻¹ under nitrogen.;

The conversions were determined by means of ¹H NMR spectroscopy, following the disappearance of the *bisGECA-C₂₀* signals (see Figure 10). The conversion of cyclic carbonates reached 90% in 24h, regardless the temperature of polymerization. The ¹H NMR spectra of the resulting polymer after 24h and 7 days of polymerization exhibit the presence of

labile protons characterizing urethanes, as well as amides and ureas generated by side reactions. As demonstrated in the previous part, the formation of amide is inevitable due to ester functions present within the *bisGECA-C₂₀*. When the latter was polymerized, the ratio between urethanes, amides and ureas tends to vary with the temperature. Indeed, the amide formation was driven by the increase of the temperature with 16% of amide functions formed at 70°C instead of 7% at room temperature. Conversely, the proportion of ureas was independent of the temperature.

Molar masses of 5200 g.mol⁻¹ and 3500 g.mol⁻¹ were obtained after polymerizations at respectively 70°C and room temperature. These low values were attributed to the transamidation occurring between 10DA and the ester functions in α of the hydroxyurethane moieties. Consequently, the synthesized poly(hydroxyurethane-amide)s cannot reach high molar masses as the above-mentioned side reaction cleave the polymer chain.

With regard to the thermal properties, the thermal stability of the poly(hydroxyurethane-amide)s was lower than for classical PHU ones with a $T_{d5\%}$ of 230°C. This pattern could be related to the low molar masses exhibited by these polymers.

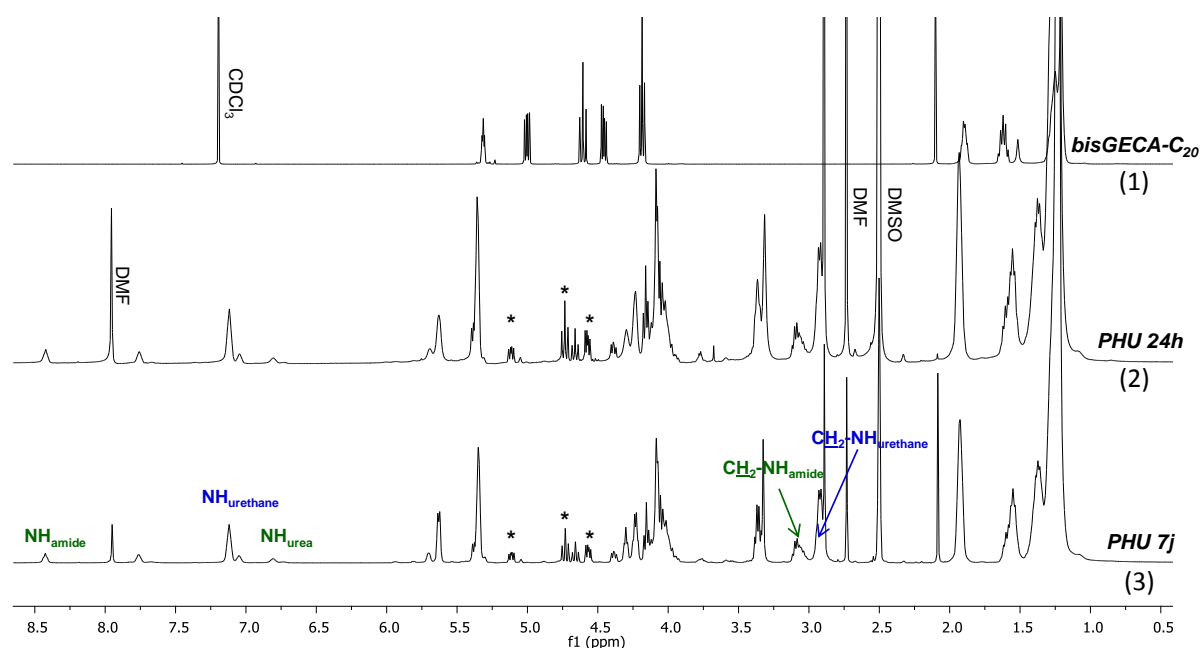


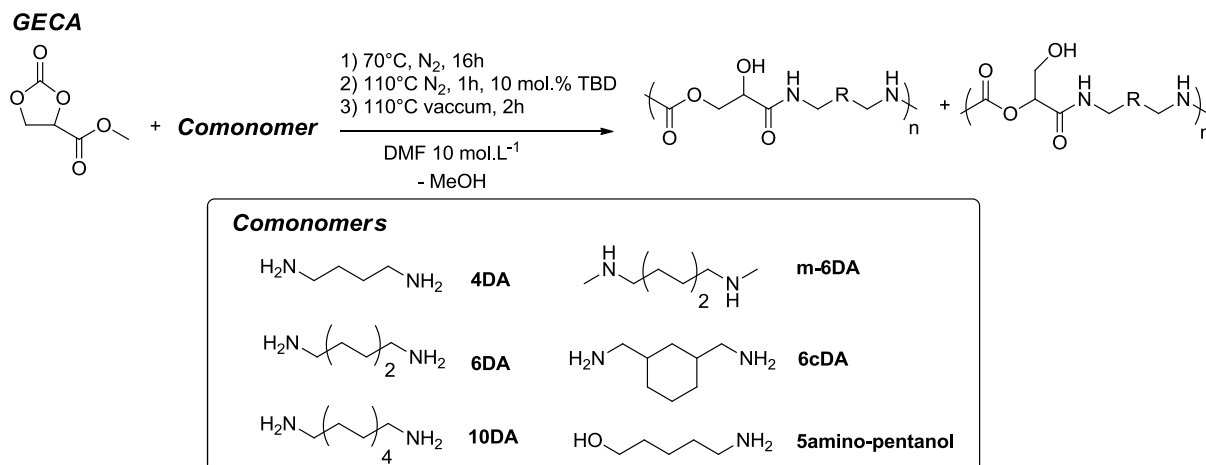
Figure 10- Stacked ¹H NMR spectra of (1) *bisGECA-C₂₀* in CDCl₃, (2) PHU 1 after 24h in DMSO-d₆ and (3) PHU 1 after 7 days in DMSO-d₆. (*: residual monomers / chain ends)

2.3.2. Poly(hydroxyurethane-amide-ester)s from GECA

In this part, the synthesis of linear and cross-linked hybrid poly(hydroxyurethane-amide-ester)s was conducted by polymerizing the AA* monomer **GECA** with various diamines (or

amino-alcohol), taking advantage of the ineluctable transamidation side reaction occurring with this ‘ultra’-activated monomer.

A specific three-step procedure was applied by first reacting **GECA** and the comonomer at 70°C. The mixture reaction was heated up and 10 mol.% of TBD was inserted to catalyze the transamidation step. Vacuum was finally applied to drive the reaction towards the polymer formation by removing the methanol (see Scheme 10).



Scheme 10- Polymerization of GECA and various diamines as comonomers.

Various comonomers comprising linear, cyclic, primary and secondary diamines as well as amino-alcohol (4DA, 6DA, 10DA, m-6DA, 6cDA and 5-amino pentanol) were employed to tune the polymer properties. As demonstrated by Tomita *et al.*,¹⁵ the mentioned comonomers exhibited different reactivities towards cyclic carbonates and can impact in our case, the inherent structure of the polymer (linear or cross-linked material). The conversion of **GECA** was calculated by means of ¹H NMR spectroscopy and the final materials were characterized by SEC, TGA and DSC. When cross-linking was observed, the swelling properties of the network were measured.

It can be noticed from the Table 5 that the conversions were total at the end of the polymerization. The stacked ¹H NMR spectra showed in Supporting Information confirmed the disappearance of the characteristic protons of the **GECA** after the three-step procedure.

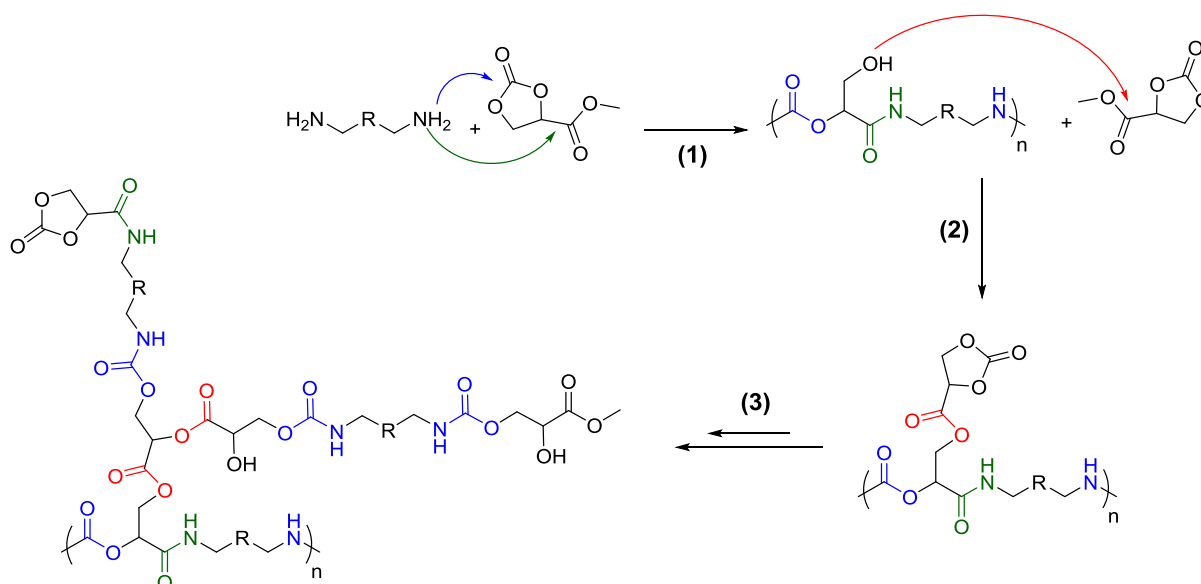
SEC data which are exposed in Table 5 were collected for linear polymers soluble in DMF and indicate that the molar masses were in the range 1800 to 2600 g.mol⁻¹. However, polymers **P1**, **P2**, **P3** and **P5** were partially cross-linked and could not be analyzed by SEC. Indeed, the 3D network formation was explained by the transesterification occurring between

the methyl function of the **GECA** and the hydroxyl pendant groups formed by the **GECA** ring-opening. This hypothesis was confirmed when 1,10-decanediol and **GECA** were polymerized and resulted in the formation of **PHU 7**, exhibiting a molar mass of $3000 \text{ g}\cdot\text{mol}^{-1}$. As a result, the thermosets displayed hydroxyurethane, amide and ester functions in their backbone as depicted in Scheme 11.

Table 5- Characterization of Poly(hydroxyurethane-amide)s obtained from GECA and various diamines.

Polymer	Diamine	Conversion (%) ¹	Soluble (%)	Swelling (%)	\bar{M}_n (g.mol ⁻¹) [D] ²	T _g (°C) ^a	T _m (°C) ^a	T _{d5%} (°C) ^b
P1	4DA	100	72	456	nd	61	-	216
P2	6DA	100	72	764	nd	52	-	222
P3	10DA	100	60	596	nd	32	-	235
P4	6cDA	100	100	-	2600 [1.82]	74	-	218
P5	m-6DA	100	88*	94*	nd	26	-	204
P6	5amino-pentanol	100	100	-	1800 [1.38]	-20	-	206
P7	1,10-decanediol	100	100	-	3000 [2.19] [⊙]	-24	-	202

¹: Determined by ¹H NMR spectroscopy at the end of the polymerization; ²: Determined by SEC in DMF (LiBr, PS Std); ^a: Determined by DSC at 10°C.min⁻¹ from the second cycle. ; ^b: Determined by TGA at 10°C.min⁻¹ under nitrogen.;*: Determined on a mass below 6 mg. [⊙]: Molar mass calculated by detection with the UV detector in SEC DMF.



Scheme 11- Supposed mechanism of cross-linking between GECA and diamines.

The swelling properties of the thermosets were measured by weighting the sample (m_D) that was immersed in DMF for 24h. The swollen networks were then dried between sheets of paper and weighted again (m_S). They were subsequently dried in an oven at 70°C for 2 days

under vacuum and weighted again (m_{DO}). The swelling percentage was calculated from the difference in weight between dried and swollen networks.¹⁶

$$\text{Swelling (\%)} = \frac{m_S - m_{DO}}{m_{DO}} * 100$$

The soluble part was calculated from the difference in weight between dried sample and dried network.

$$\text{Soluble (\%)} = 100 * \left(1 - \frac{m_{DO}}{m_D}\right)$$

It is noteworthy to mention that the swelling percentage calculated for the synthesized polymers are particularly high. Indeed, the swelling percentage is related to the degree of cross-linking and lower cross-linking density usually results in higher distances between network nodes, enabling a higher solvent absorption. With regard to polymers **P1**, **P2** and **P3**, the lowest swelling percentage (456%) was displayed by the polymer **P1** synthesized from 4DA. This pattern could be justified by the small size of the diamine that induces a high hydroxyl density within the polymer chain. Thus, the occurrence of cross-linking is increased, as the latter comes from the transesterification between hydroxyl moieties and **GECA**; the density of cross-linking is consequently higher. However, low percentages of insoluble are exhibited by these polymers, testifying a partial cross-linking.

Thermal properties of the **GECA**-based polymers were elucidated by DSC (see Figure 11). As expected, all polymers were amorphous because of the random attack of the diamine onto methyl esters or cyclic carbonates, inducing the irregularities within the polymer backbone. The glass transition temperatures ranging from -20 to 74°C were relatively high, especially for the cross-linked materials. As expected, the reduction of the number of carbons of the diamines resulted in an increase of the T_g . For instance, **P1** synthesized with 4DA displayed a T_g of 61°C contrarily to the 10DA-based **P3** that showed a T_g of 32°C. Besides, the cyclic diamine 6cDA conferred rigidity to the linear polymer **P5** as a T_g of 74°C was obtained. The lowest T_g of -20°C exhibited by the **P6** synthesized with 5-amino-1-pentanol was induced by the formation of oligomers, coming from the difference in reactivity between alcohol and amine moieties.

Thermal stabilities in between 204 and 235°C were achieved and were in correlation with the high amount of thermally degradable functionalities (urethane, amide, ester) existing within the polymer chain (see Figure 11).

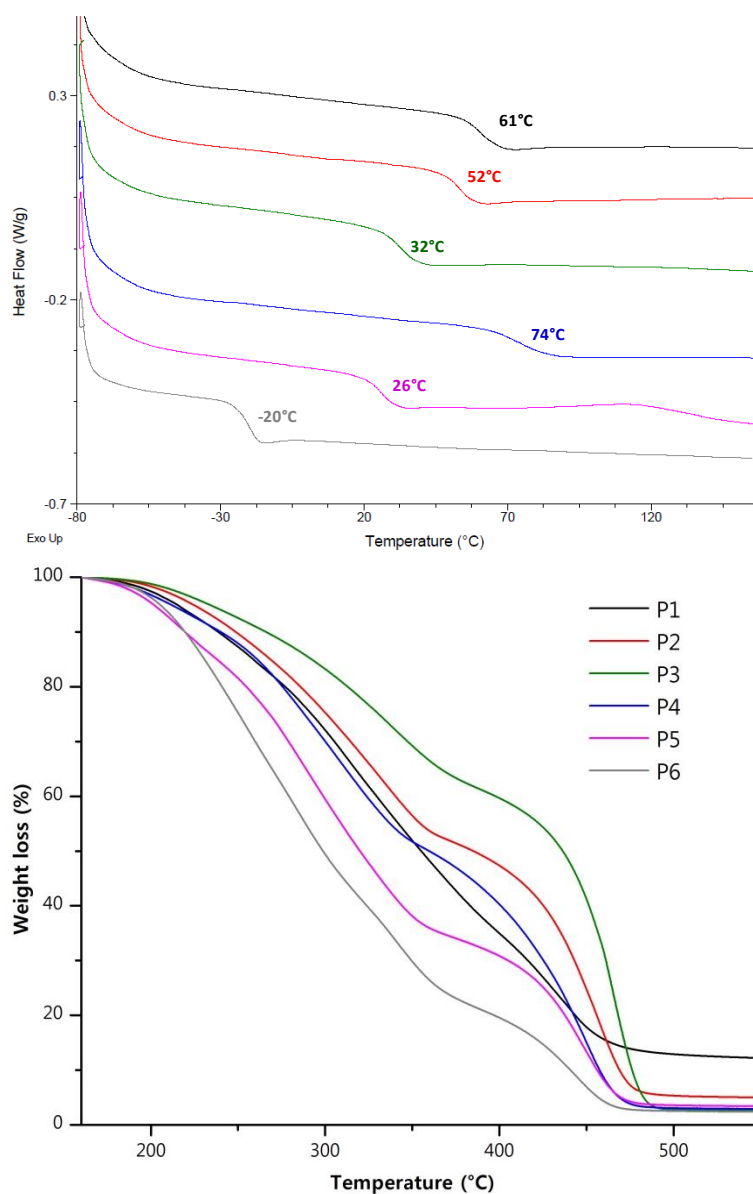


Figure 11- Second heating cycle (10°C/min) of P1 to P6 and corresponding TGA traces from 160°C (after DMF removal) to 550°C.

Interestingly, the polymers synthesized from **GECA** (clear yellow liquid) and diamines or amino alcohols (colorless liquids or white powders) were colored (orange, red or purple, see Figure 12). Many tests were conducted in order to determine the origin of the coloration. The latter was not induced by the presence of impurities, charges or radicals as quench tests were performed on the polymers. Besides, no solvent or catalyst effect was observed. Notably, the coloration appeared when the comonomer was inserted in the mixture reaction. Besides, it was noticed that the nature of the comonomer influences the coloration; for instance, **P1** synthesized with 4DA was orange whereas the cyclic diamine-based **P4** was purple. Unfortunately, no rational explanation was found to explain this phenomenon.



Figure 12- Picture of the synthesized polymers (P1 to P6) showing the coloration (orange, red and purple).

To conclude this part, the ‘ultra’-activated cyclic carbonate **GECA** was easily prepared from methyl acrylate and exhibited high reactivity towards amines. The lipidic-based bCC synthesized from the **GECA** building-block was polymerized with 10DA, but the resulting PHU exhibited limited properties due to the transamidation side reaction. Taking advantage of the latter, the highly reactive **GECA** was directly used in polymerization with diamines and amino alcohol, combining cyclic carbonate ring-opening, transamidation and transesterification. Interestingly, linear or cross-linked colored polymers were obtained.

Conclusions

In this chapter, preliminary investigations into potential solutions for the enhancement of the cyclic carbonate reactivity towards aminolysis were conducted.

First, the catalysis of the polyaddition between cyclic carbonates and amines was investigated in order to analyze the combined effect of activation of the monomer and catalysis on the CC reactivity. A screening study was performed with commercially available additives and demonstrated that Lewis bases were more suitable to catalyze the PHU synthesis, especially when a Lewis acid was employed as co-catalyst. We also demonstrated that the catalysis of ether-activated monomers was effective contrarily to the ester-activated CC, that were subject to increased transamidation side reactions when a Lewis base was employed.

The second strategy consisted in the structure modification of the cyclic carbonate in order to decrease its stability and consequently to ease the amine attack. Hence, the cyclic carbonate synthesized from methyl acrylate (**GECA**) was an interesting building block that enables the insertion of an ester moiety in α position of lipidic cyclic CC, *via* the enzymatic transesterification on fatty acid-based alcohols. These activated carbonates exhibited a high reactivity but no selectivity towards aminolysis, as the transamidation was favored. The **GECA** building block was thus polymerized directly with diamines (or amino-alcohol), taking advantage of the main side reaction occurring with the methyl ester function. The resulting materials displayed interesting properties as they were cross-linked, colored and more or less rigid depending on the monomer used.

Therefore, further investigations are required to design specific and selective catalysts towards the aminolysis of the 5-membered cyclic carbonates, taking in account the monomer structure. Reversibly, it could be interesting to synthesize activated cyclic carbonates with amide in α position nearby the cycle. This would ensure the preparation of reactive cyclic carbonates with a more stable 'activating' function towards transamidation, keeping its electron-withdrawing ability.

References

- (1) Webster, D. C.; Crain, A. L. *Prog. Org. Coatings* **2000**, *40* (1–4), 275–282.
- (2) Honel, M.; Sprenger, W.; Wendt, W.; Ziegler, P. Carrier resin for pigment pastes, preparation and use thereof, US5055542, 1991.
- (3) Fleischer, M.; Blattmann, H.; Mulhaupt, R. *Green Chem.* **2013**, *15* (4), 934–942.
- (4) Lambeth, R. H.; Henderson, T. J. *Polymer*. **2013**, *54* (21), 5568–5573.
- (5) Blain, M.; Jean-Gerard, L.; Auvergne, R.; Benazet, D.; Caillol, S.; Andrioletti, B. *Green Chem.* **2014**, *16* (9), 4286–4291.
- (6) Holen, J. V. Process using a cyclic carbonate reactant and a beta-hydroxyurethanes thereby obtained, US0236119, 2004.
- (7) Holen, J. Van. Process using a cyclic carbonate reactant, US0113594, 2005.
- (8) Ochiai, B.; Inoue, S.; Endo, T. *J. Polym. Sci. Part A Polym. Chem.* **2005**, *43* (24), 6613–6618.
- (9) Blain, M.; Yau, H.; Jean-Gérard, L.; Auvergne, R.; Benazet, D.; Schreiner, P. R.; Caillol, S.; Andrioletti, B. *ChemSusChem* **2016**, *9* (16), 2269–2272.
- (10) Lombardo, V. M.; Dhulst, E. A.; Leitsch, E. K.; Wilmot, N.; Heath, W. H.; Gies, A. P.; Miller, M. D.; Torkelson, J. M.; Scheidt, K. A. *European J. Org. Chem.* **2015**, *2015* (13), 2791–2795.
- (11) Maisonneuve, L.; Wirotius, A.-L.; Alfos, C.; Grau, E.; Cramail, H. *Polym. Chem.* **2014**, *5*, 6142–6147.
- (12) Woelfle, H.; Whalther, B.; Kholer, M.; Putzien, S. 2-oxo-1,3-dioxolane-4-carboxamides, their preparation and use, WO2013092011, 2011.
- (13) Lengsfeld, C. S.; Shoureshi, R. A. 2-oxo-1, 3-dioxolane-4-carboxylic acid and derivatives thereof, their preparation and use, US20100311130, 2008.
- (14) Stevenson, C.; Nielsen, L.; Jacobsen, E. *Org. Synth.* **2009**, *83* (2006), 162–169.
- (15) Diakoumakos, C. D.; Kotzev, D. L. *Macromol. Symp.* **2004**, *216* (1), 37–46.
- (16) Kristufek, T. S.; Kristufek, S. L.; Link, L. A.; Weems, A. C.; Khan, S.; Lim, S.-M.; Lonneck, A. T.; Raymond, J. E.; Maitland, D. J.; Wooley, K. L. *Polym. Chem.* **2016**, *7* (15), 2639–2644.

Experimental and Supporting Information

Experimental Methods

Catalysis

- **General procedure for catalyst-free polymerizations:** PHUs were prepared from diglycerol dicarbonate (DGDC), *Und-bCC-ether* and *Und-bCC-ester* with 1,3-cyclohexanebis (methylamine) (6cDA) and 1,10-diaminodecane (10DA) as comonomers with a molar ratio 1:1. These polymerizations were performed in DMF (1 mol.L⁻¹) at 70°C into a schlenk tube under magnetic stirring and nitrogen atmosphere for 24h. Aliquots were taken at t=0h, 0.5h, 1h, 3h, 5h, and 24h. The resulting PHUs were characterized by RMN, SEC and TGA.
- **General procedure for catalyzed polymerizations:** The catalyzed polymerizations were performed following the same procedure than previously mentioned, but adding the catalyst once the monomers were completely dissolved in DMF.

Synthesis of GECA and GECA derivatives

- **General procedure for GECA synthesis:** (i) Into a round bottom flask, 470 mL of a 6% NaOCl solution were stirred at 0°C for 30 min. Then, 29.25 g of methyl acrylate (340 mmol) was added to the basic solution that was vigorously stirred for 30 min at 0°C. The mixture was reacted for an additional 1.5h at room temperature and turned from a clear yellow to a white turbid solution. As the reaction is exothermic, the flask was cooled down to room temperature before processing to the work-up. The aqueous phase was extracted 4 times with 75 mL of DCM and was subsequently dried over MgSO₄. The organic phase was reconcentrated with the rotary evaporator at 20°C for 20 min. The remaining unreacted methyl acrylate was thus removed from the epoxidized product (conversion could not be calculated for this reason) that was obtained as a pure incolor liquid. Yield: 41%. ¹H NMR (CDCl₃, 25°C, 400 MHz), δ (ppm): 3.76 (s, 3H), 3.42 (dd, 1H), 2.93 (m, 2H). ¹³C NMR (CDCl₃, 25°C, 100 MHz), δ (ppm): 169.7 (O-C=O), 52.5 (CH₃), 47.3 (CH-C=O), 46.3 (CH₂). (ii) The epoxidized methyl acrylate (14.26 g, 140 mmol) and 3 w.% of TBABr (0.428 g) was dissolved in 10 mL of acetone and introduced in a 250 mL-autoclave equipped with a mechanical stirring. The reactor was pressurized with 30 bars of CO₂ and heated up at 80°C. The mixture was reacted for 3 days before being cooled and reconcentrated. Conversion:

100%. The **GECA** was obtained as a clear yellow liquid after purification by flash chromatography (eluent: DCM). Yield: 52%. Purity: 90.5% (determined by GC). ^1H NMR (CDCl_3 , 25°C , 400 MHz), δ (ppm): 5.08 (dd, 1H), 4.67 (t, 1H), 4.51 (dd, 1H), 3.87 (s, 3H). ^{13}C NMR (CDCl_3 , 25°C , 100 MHz), δ (ppm): 172.1 ($\text{CH}_3\text{-O-C=O}$), 153.6 (O-C=O-O), 72.6 (CH-C=O), 67.2 (CH_2), 53.9 (CH_3).

• **General procedure for GECA enzymatic transesterification:** Into a round bottom flask containing dry molecular sieves (4\AA), 1 eq. of alcohol, 1.1 eq. of **GECA** /OH function and 10 w.% of supported-enzyme *Candida Antarctica Lipase B* (CALB) /OH function were stirred in dry toluene under inert atmosphere for 72 h at 55°C . The crude mixture was filtered and the filtrate was reconcentrated. When required, the product was purified by flash chromatography (eluent: DCM:MeOH).

GECA- C_{11} synthesis: 1 eq. of 10-undecen-1-ol (9.32 g, 55 mmol), 1.1 eq. of **GECA** (8.8 g, 60 mmol), 932 mg of CALB, 55 mL of toluene. Conversion: 80%. Transparent oil obtained after purification by flash chromatography (eluent: DCM:MeOH, 100:0 to 97:3). Yield: 65%. Purity: 98.5% (determined by GC). ^1H NMR (CDCl_3 , 25°C , 400 MHz), δ (ppm): 5.80 (m, 1H), 5.07 (dd, 1H), 4.92 (dd, 2H), 4.67 and 4.52 (t, dd, 2H), 4.21 (t, 2H), 2.01 (q, 2H), 1.65 (t, 2H), 1.27 (m, 12H). ^{13}C NMR (CDCl_3 , 25°C , 100 MHz), δ (ppm): 171.3 ($\text{CH}_2\text{-CH}_2\text{-O-C=O}$), 153.8 (O-C=O-O), 139.4 (CH=CH_2), 114.3 (CH=CH_2), 72.8 ($\text{CH}_2\text{-CH-C=O}$), 67.1 ($\text{CH}_2\text{-CH-C=O}$), 66.8 ($\text{O-CH}_2\text{-CH}_2$), 34.0 ($\text{CH=CH}_2\text{-CH}_2$), 29.6-25.9 (CH_2).

bisGECA- C_{20} synthesis: 1 eq. of *Und-C20-diol* (7 g, 22.4 mmol), 2.2 eq. of **GECA** (7.19 g, 49.2 mmol), 1.4 g of CALB, 45 mL of toluene. Conversion: 69%. As residual **GECA** and **bisGECA- C_{20}** were not well separated by flash chromatography, the product was not purified (see the next part for the NMR shifts of the **bisGECA- C_{20}**).

• **Metathesis reaction of GECA- C_{11} for bisGECA- C_{20} synthesis:** Into a dry round bottom flask, 1 eq. of **GECA- C_{11}** (9 g, 31.7 mmol) was dried under vacuum before being dissolved in 22 mL of dry DCM. Then, 0.01 eq. of the 2nd generation Grubbs catalyst (0.26 g) was added under inert atmosphere and the flask was connected to a gas bubbler for the ethylene removal. The self-metathesis was carried out for 2 days at 30°C to reach 88% conversion. The product was recovered by an overnight recrystallization in cold DCM (-20°C). Yield: 26%. ^1H NMR (CDCl_3 , 25°C , 400 MHz), δ (ppm): 5.37 (t, 2H), 5.09 (dd, 2H), 4.65 and 4.53 (t, dd, 4H), 4.25 (t, 4H), 1.96 (m, 4H), 1.67 (t, 4H), 1.27 (m, 24H). ^{13}C NMR (CDCl_3 , 25°C , 100 MHz), δ

(ppm): 167.7 ($\text{CH}_2\text{-CH}_2\text{-O-C=O}$), 153.8 (O-C=O-O), 130.5 (CH=CH), 72.5 ($\text{CH}_2\text{-CH-C=O}$), 67.2 ($\text{O-CH}_2\text{-CH}_2$), 67.0 ($\text{CH}_2\text{-CH-C=O}$), 32.7 (CH=CH-CH_2), 31.1-25.9 (CH_2).

- **General procedure for kinetic experiments:** The kinetic experiments were performed in a NMR tube at 1 mol.L^{-1} in DMSO-d₆, at 25 or 50°C and with a ratio 1:1 between cyclic carbonate and hexylamine. All reagents were dried on molecular sieves or distilled before the reaction. Hexylamine was dried under CaH₂ and distilled after drying. The cyclic carbonate was directly dried overnight in a NMR tube capped with a septum, under vacuum. 0.5 mL of dried DMSO-d₆ and 12.5 μL of TCB were added *via* the septum and the mixture was homogenized. The hexylamine (66 μL, 0.5 mmol, 1 eq.) was then added just before putting the tube in the NMR apparatus. The reaction was monitored with ¹H NMR spectroscopy with the disappearance of the cyclic carbonate protons for 2 days.

- **Procedure for PHU synthesis:** PHU was prepared from *bisGECA-C₂₀* and 1,10-diaminodecane (10DA) as comonomer with a molar ratio 1 : 1. PHU synthesis was performed in DMF (1 mol.L^{-1}) at 70°C (or room temperature) into a schlenk tube under magnetic stirring and nitrogen atmosphere for 7 days. No catalysts were added for the polymerization reactions. Conversions were determined by ¹H NMR spectroscopy after 24h and 7 days of polymerization.

- **General procedure for Poly(hydroxyurethane-amide-ester)s synthesis:** GECA was reacted with several co-monomers: 1,4-diaminobutane (4DA), 1,6-diaminohexane (6DA), N,N'-dimethylhexylamine (m-6DA), 1,10-diaminodecane (10DA), 1,3-cyclohexanebis(methylamine) (6cDA) and 5-amino-1-pentanol (5amino-pentanol). The two monomers were first mixed and reacted in DMF (10 mol.L^{-1}) at room temperature for 16h under nitrogen atmosphere. Then, 10 mol.% of TBD was added to the solution and the reaction mixture was heated up to 110°C and stirred for 1h. Vacuum was finally applied for 2h in order to remove the methanol and drive the transesterification towards the polymer formation.

Supporting Information

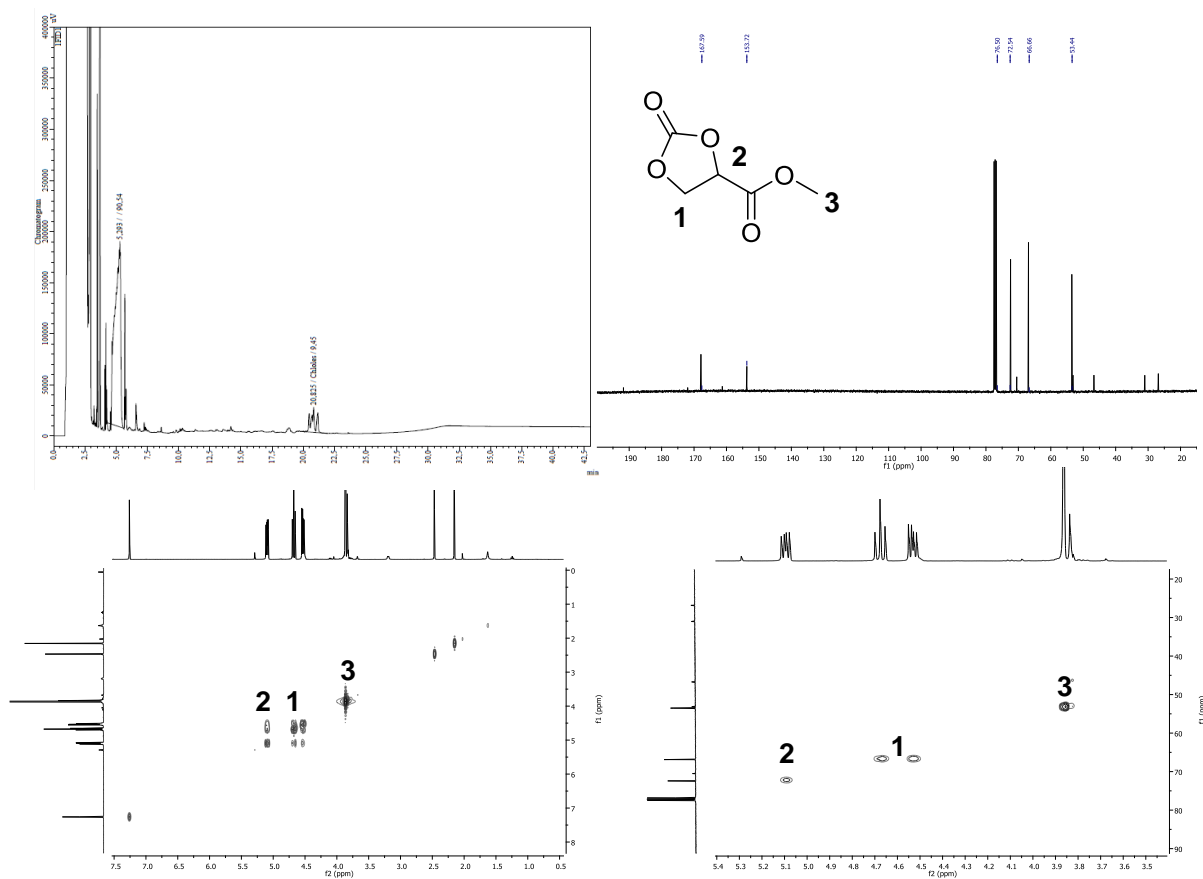


Figure ESI 1 - Characterization of GECA: (1) GC (90.5% purity), (2) ^{13}C NMR, (3) ^1H - ^1H COSY NMR and (4) ^1H - ^{13}C HSQC-NMR (Analysis performed in CDCl_3)

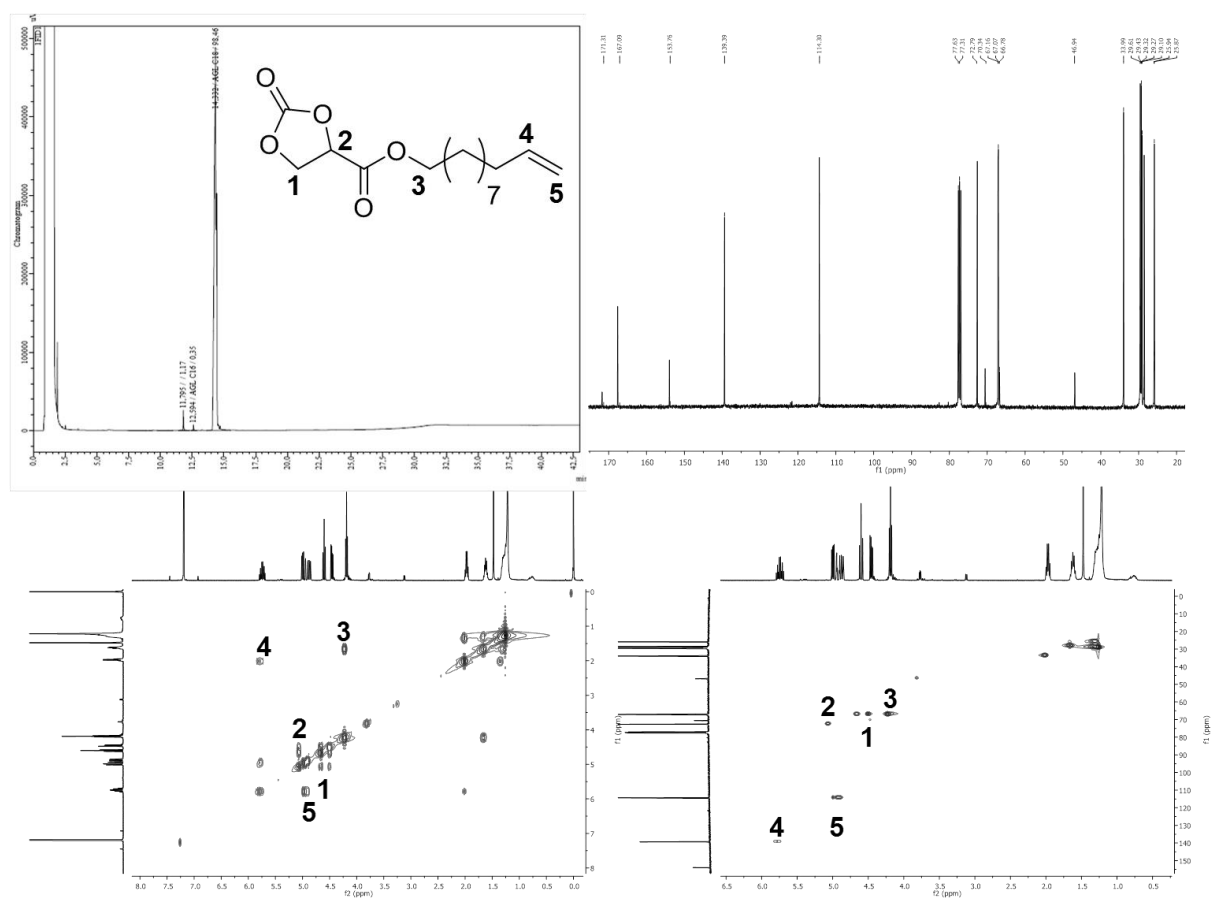


Figure ESI 2 - Characterization of GECA-C₁₁: (1) GC (98.5% purity), (2) ¹³C NMR, (3) ¹H-¹H COSY NMR and (4) ¹H-¹³C HSQC-NMR (Analysis performed in CDCl₃)

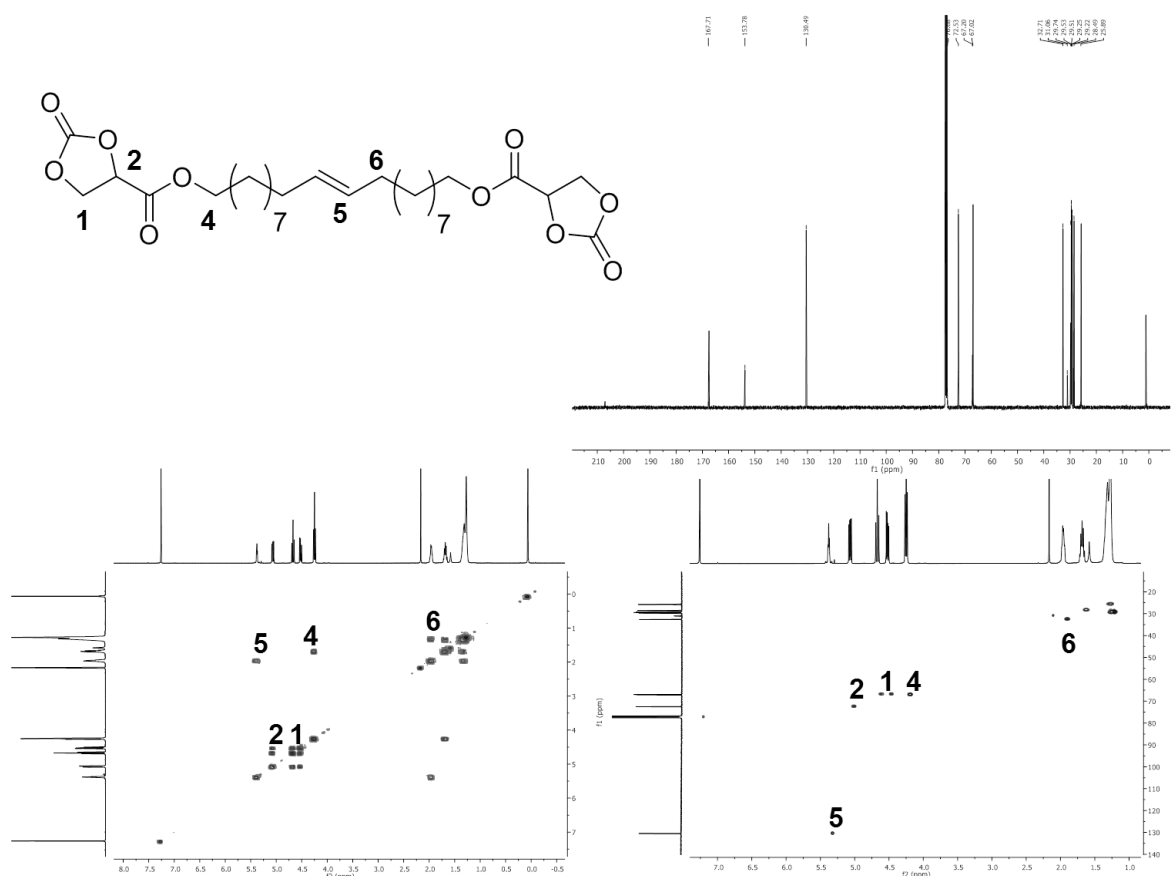


Figure ESI 3 - Characterization of bisGECA-C₂₀: (1) ¹³C NMR, (2) ¹H-¹H COSY NMR and (3) ¹H-¹³C HSQC-NMR. (Analysis performed in CDCl₃)

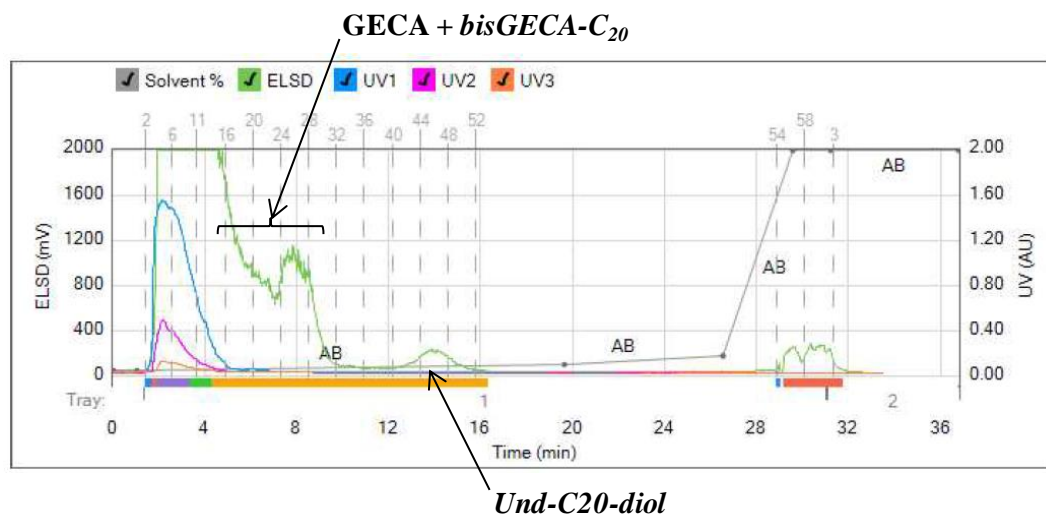


Figure ESI 4 – Flash chromatography trace obtained during the purification of bisGECA-C₂₀ with DCM:MeOH as eluent.

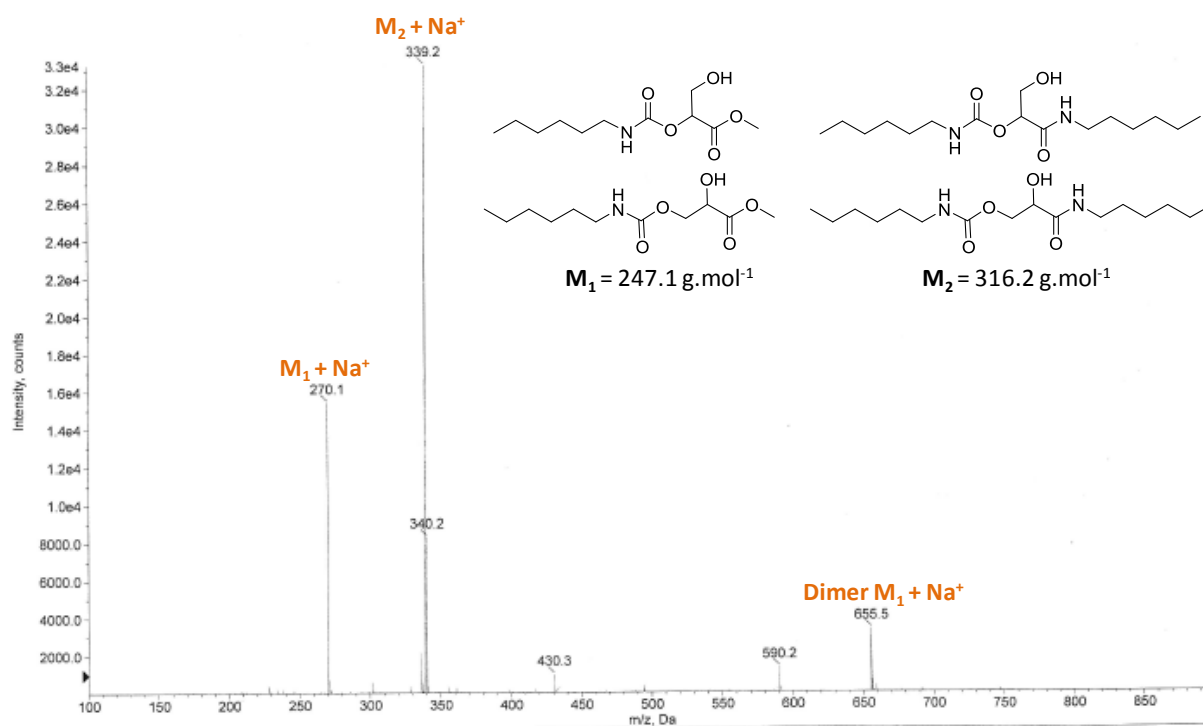


Figure ESI 5 – Mass spectrum (obtained by ESI) of the reaction between GECA and hexylamine.

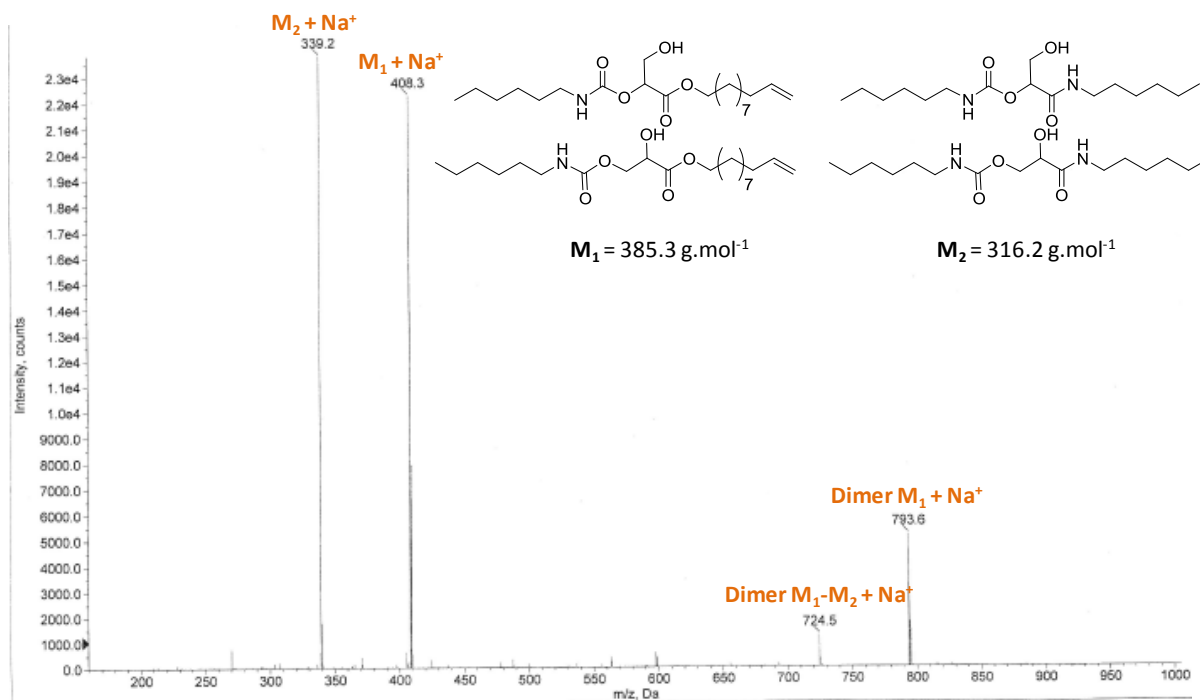


Figure ESI 6 – Mass spectrum (obtained by ESI) of the reaction between GECA-C₁₁ and hexylamine.

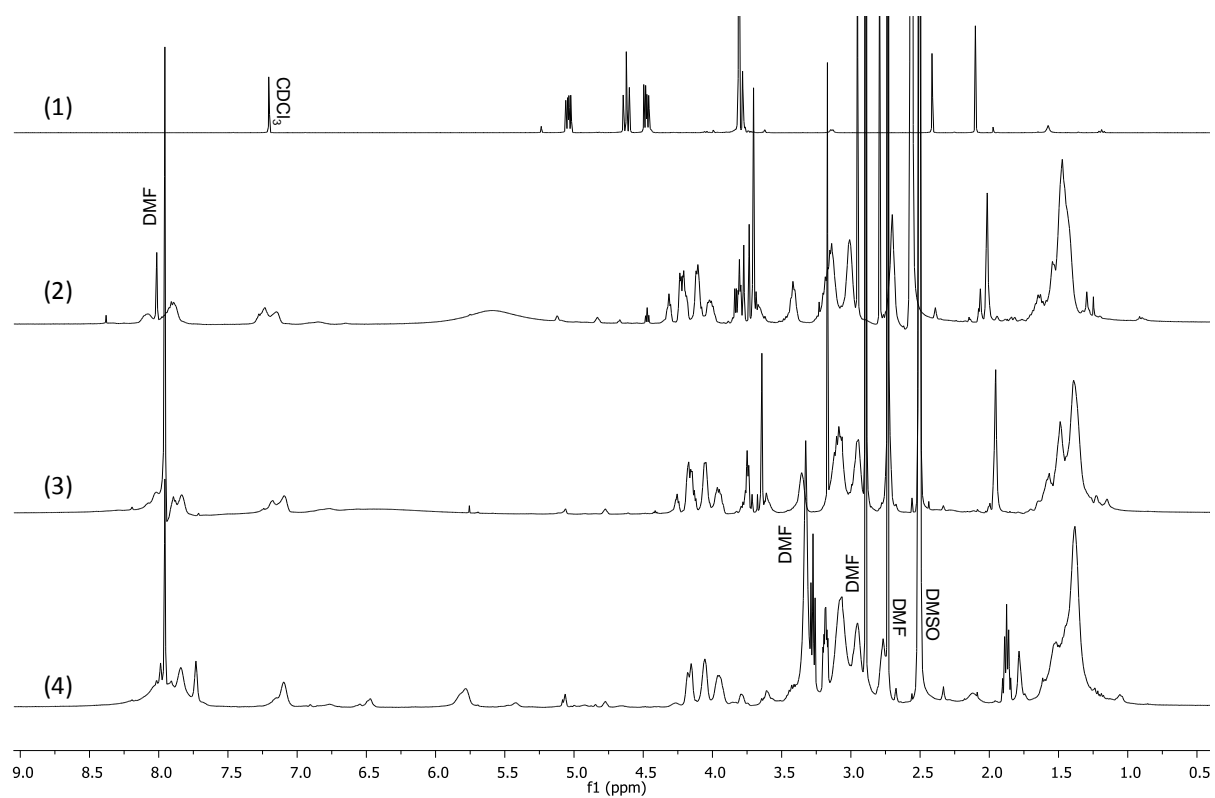


Figure ESI 7 - Stacked ¹H NMR spectra of (1) GECA and of the PHU resulting from the polymerization between GECA and 4DA after (2) the first step (3) the second step and (4) the last step of the procedure. (Analyses performed in CDCl₃ or DMSO-d₆).

General Conclusions and Perspectives

Two key challenges appeared to be essential in the progress of renewable PHUs preparation from the carbonate/amine polyaddition route:

- The lack of commercially available bio-based aliphatic amines and
- The lack of reactive 5-membered cyclic carbonates, especially the fatty acid-based ones.

Meeting these challenges are the objectives of this thesis. First, mild and simple routes to aliphatic bio-based amines were investigated. The synthesis of amines was realized through the preparation of nitrile intermediates in mild conditions. To that purpose, the copper-TEMPO mediated aerobic oxidation of alcohols into nitriles was studied and optimized. We were able to adapt this well-known technology to aliphatic bio-based and fatty acid-based substrates, in order to prepare the corresponding aliphatic amines. The process was optimized under air and the catalytic system was then heterogeneized *via* the use of supported-TEMPO or *via* the addition of Cu(0) in the media. Long aliphatic diamines were also prepared using thiol-ene “click” coupling reaction between cysteamine hydrochloride and fatty acid-based dienes. Both routes were versatile and transferable to many other bio-based alcohols and unsaturated compounds.

The second objective was addressed by playing with the chemical structure of 5-membered cyclic carbonates, in order to render these substrates more reactive towards aminolysis. The insertion of various functional groups, i.e. ether, ester and sulfur nearby the cycle was achieved enabling an activation of the cyclic carbonate. Various routes, some of them being already explored in industry or academy, were investigated to prepare these cyclic carbonates. Glycerol derivatives including glycerol carbonate, epichlorohydrin, diglycerol and thioglycerol were reacted in one or several steps, with fatty acid-based alcohols, acyl chlorides, brominated and mesylated substrates.

Model reactions and polymerizations with (di)amines were implemented and demonstrated the effect of the carbonate structure on kinetics and PHUs properties. Amorphous and semi-crystalline PHU with average molar mass up to $60000 \text{ g}\cdot\text{mol}^{-1}$ and T_g ranging from -34 to 27°C were obtained. As presented on the Figure 1, the presence of a function in beta position

of the aliphatic CC structure led to an increase of its reactivity with amines in comparison to the non-substituted 5CC and to the uncatalyzed alcohol/isocyanate addition.

Ether and sulfur moieties positioned in beta of the carbonate cycle conferred to the CC an improved reactivity towards aminolysis, but the best results were achieved when an ester function was located either in α or β nearby the CC. However, the ester-activated CCs were subject to transamidation and other non-identified side reactions that consequently modified the stoichiometry between CC and amine, leading to low molar mass PHUs. Moreover, side reactions inducing cross-linking were also observed when bulk polymerizations were performed at high temperature. Taking advantage of the transamidation side reaction, the carbonated methyl acrylate (**GECA**) was polymerized with various comonomers to prepare cross-linked poly(hydroxyurethane-amide-ester)s. The resulting materials exhibited high T_g up to 74°C and swelling ratios in the range 90-764%.

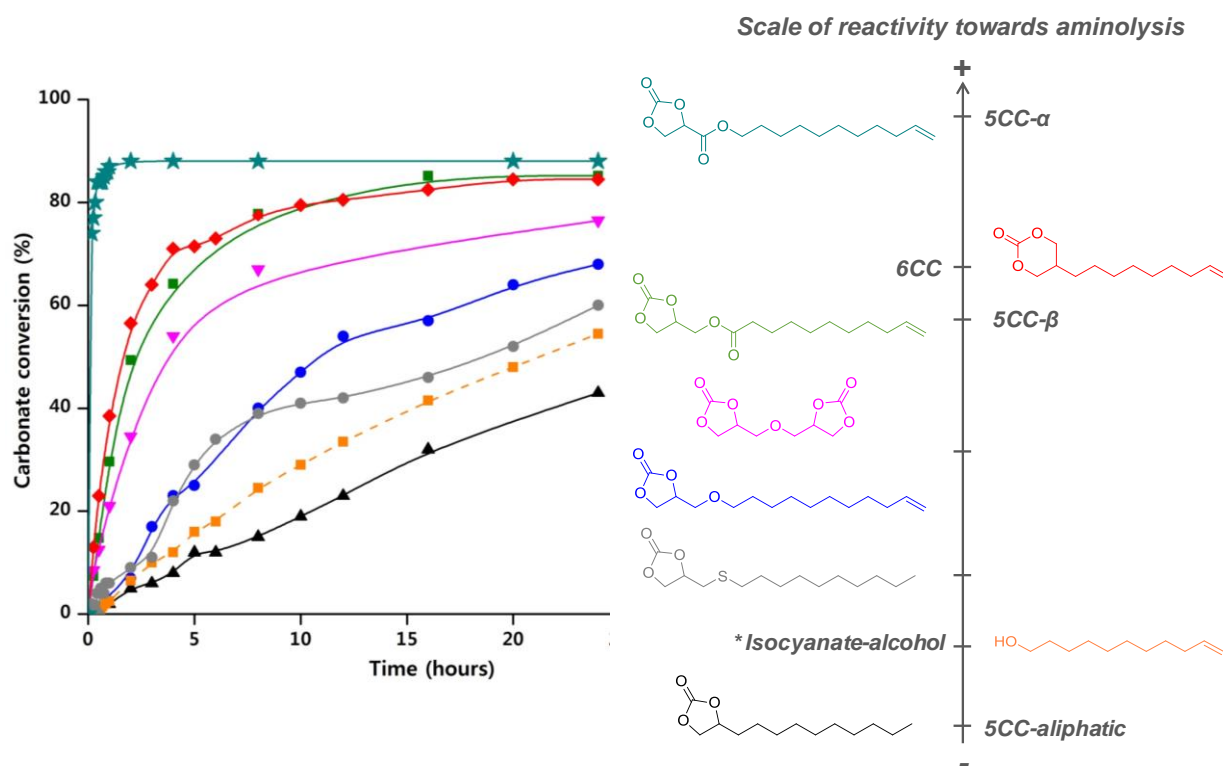


Figure 1 - Kinetics and related reactivity scale of the different “activated” cyclic carbonates and comparison with the *alcohol: isocyanate addition.

Taking advantage of the sulfur-based PHU synthesized in Chapter 4, original materials were prepared by sulfur derivatization into sulfonium and sulfone moieties. These preliminary investigations demonstrated the possibility of tuning PHU properties by grafting a plethora of functions *via* the epoxy chemistry. The particular DGDC presented in Chapter 3 appeared evenly as an interesting CC to tune the PHU properties (solubility, self-assembly...) thanks to

its valuable reactivity and to the high density of hydroxyl group generated when polymerized with diamines. For instance, hydrosoluble PHUs were obtained from DGDC and PEG-diNH₂ polymerization whereas self-assembly in water was observed when the same bCC was copolymerized with both hydrophobic and hydrophilic diamines.

From a kinetic point of view, we demonstrated the viability of the carbonate/amine route in comparison with the classical urethane preparation. Nonetheless, the major issue remains the relatively low molar masses achieved because of incomplete conversions and uncontrolled side reactions. Thus, parameters such as monomer structure and reactivity, solvent and temperature were found to be crucial to improve conversions and PHU molar masses. Many efforts are still required to make the polymerization process more competitive to ensure its industrialization.

Since the carbonate/amine route is more and more studied, research perspectives in this subject are numerous. The major lines of potential developments are summarized below.

- Knowing the occurrence of many **side reactions** during the polyaddition between cyclic carbonates and amines, the **design of selective catalysts** to reduce by-products and make the process more competitive compared to the classical synthetic pathway is highly required. Indeed, in the industrial isocyanate chemistry, most of the processes involve a fast curing at room temperature using specific catalysts such as dibutyltin dilaurate (DBTL). Many years of research could enable the control of side reactions as well as the kinetic of the isocyanate/alcohol polyaddition, permitting the preparation of complex materials such as solid PU foams. The industrial growth of the carbonate/amine route towards non-isocyanate polyurethanes lies in the development of analog selective catalysts (metallic, organometallic, organic or enzymatic ones) that could significantly accelerate the polyaddition rate even at room temperature.
- An important key-challenge in this field is **the optimization of the polymerization process**. Indeed, the use of solvents such as DMF or DMSO is an obstacle to the industrialization of the process. **Bulk polymerizations at room temperature** would circumvent the use of such toxic and heavy solvents and would enhance the reaction rate. However, the process requires to be performed near room temperature as side reactions and cross-linking occur in bulk at high temperature. To tackle the needs, low melting point monomers from renewable resources needs to be designed. For instance, longer fatty acids such as oleic acid could help for the

synthesis of flexible bis-cyclic carbonates. Besides, when a bulk polymerization is conducted, the viscosity increase imparted by the important hydrogen-bonding prevents to reach high conversions and PHU molar masses. Therefore, progress in using **specific tools** such as **reactive extruder** or **mechanical stirrers** is highly recommended for the development of such processes. Moreover, the stoichiometry between CC and amine has to be taken into account as side reactions involving amines are frequently observed during polymerizations.

- **PHU thermo-mechanical properties** need to be deeply investigated and compared to the corresponding PU ones. Indeed, the discrepancy between PUs and PHUs coming from the presence of pendant hydroxyl groups, strongly impact thermo-mechanical properties and polymer morphologies. Moreover, the role of OH- functions in the solubility patterns and the self-assembly properties deserves to be clarified. Taking advantage of these dangling groups, cross-linking and post-functionalization could be performed to broaden the application fields. Meanwhile, PHUs are more and more valorized in the synthesis of **new materials** such as elastomers, segmented PHUs, hybrid materials, thermosets or copolymers. Furthermore, PHU thermo-mechanical properties can be tuned by using other bio-sourced building-blocks such as isosorbide or vanillin for monomer preparation, opening new range of applications.

Materials and Methods

Materials

Copper(II) bromide (CuBr₂, 99%), tetrakisacetonitrile copper(I) triflate (Cu(MeCN)₄OTf), copper(II) acetate (Cu(Oac)₂, 98%), 4-carboxy-2,2,6,6-tetramethylpiperidine 1-oxyl (4-carboxy-TEMPO, 97%), Raney Nickel (50 w.% slurry in water), copper (I) chloride (CuCl, > 99.9%), (S)-(-)-β-citronellol (> 99%), copper turnings, sodium hydrate (NaH) (60% dispersion in mineral oil), sodium hydroxide (NaOH, pellet), potassium carbonate (K₂CO₃, 98%), tetrabutylammonium bromide (TBABr, 99%), ethyl chloroformate (97%), Grubbs 1st generation metathesis catalyst, Grubbs 3rd generation metathesis catalyst, hexylamine (99%), dimethyl carbonate (DMC, 99%), 1,2,4-trichlorobenzene (TCB, 99%), oleoyl chloride (>80%), 1,2-epoxydodecane (90%), hydrochloric acid (33 w.% solution), 1,5,7-triazabicyclodec-5-ene (TBD, 98%), phytol (97%), cysteamine hydrochloride (Cys.HCl, 98%), 2,2-bis(hydroxymethyl)propionic acid (DMPA, 98%), trifluoroacetic acid (TFA, 99%), ammonium chloride (99.5%), sodium sulfate (Na₂SO₃, magnesium sulfate (MgSO₄), sodium carbonate (NaHCO₃), hexylisocyanate (97%), N,N'-methylhexylamine (m-6DA, 98%), 1,3-cyclohexanebis(methylamine) (6cDA, 99%), *Jeffamine* (400 g.mol⁻¹), 1,8-diazabicyclo[5.4.0]undec-7-ene (DBU), 7-methyl-1,5,7-triazabicyclo[4.4.0]dec-5-ene (MTBD, >95.0%), 1,3-bis[3,5-bis(trifluoromethyl)phenyl]thiourea (Schreiner TU, >98.0%), lithium bromide (LiBr, 99%), lithium trifluoromethanesulfonate (LiOTf, 99.995%), magnesium chloride (MgCl₂, powder 98%), magnesium bromide (MgBr₂, 98%), 1,4-diazabicyclo[2.2.2]octane (DABCO, 98%), 4-dimethylaminopyridine (DMAP, 99%), potassium tert-butoxide (sublimed KOtBu, 99.9%), 1-thioglycerol (>99%), 1-decene (94%), *meta*-chloroperbenzoic acid (mCPBA, 77%), glacial acetic acid, sodium hypochlorite (NaOCl 10 w.%), methyl acrylate (99%), *Candida Antarctica* Lipase B (CALB, polymer-bound) and 5-amino-1-pentanol (95%) were obtained from Sigma-Aldrich.

Triethylamine (Et₃N, 99%), sebacyl chloride (97%), 1,2-epoxy-9-decene (96%), tetramethylethylenediamine (TMEDA, 99%), copper iodide (CuI, 98%), ammonium hydroxide 28 w.%, 1-bromo-10-undecene (96%), lanthanum (III) oxide (La₂O₃, 99.99%), lithium chloride (LiCl, 99%), 1,6-diaminohexane (6DA, >99%) and aniline (99%) were purchased from Alfa Aesar.

1,10-decanediol (98%), 2,2,6,6-tetramethyl-1-piperidinyloxy, free radical (TEMPO, 98%) sublimated before using, TEMPO polymer-bound (1,0 mmol/g loading, TEMPO-PS),

TEMPO covalently bound on silica gel (0,70 mmol/g loading, TEMPO-Si), 1,1,4,7,10,10-hexamethyltriethylenetetramine (HMTETA, 97%), 4,4'-dimethyl-2,2'-dipyridyl, (99%), 4,4'-dinonyl-2,2'-dipyridyl (97%), pyridine (>99%), 2,2'-bipyridyl (bipyridine, >98%), copper turnings (Cu(0)), copper(I) bromide (CuBr, 98%), 10-undecen-1-ol (>98%), 4,4'-dimethoxy-2,2'-bipyridyl (>98%), 4,4'-dimethyl-2,2'-bipyridyl (p-(Me)bpy, 99%), 6,6'-dibromo-2,2'-bipyridyl (>95%), copper(II), trifluoromethanesulfonate (Cu(OTf)₂, >98%), copper(I) acetate (CuOac, >93%), methyl 10-undecenoate (>96.0%), 10-undecen-1-ol (99%), 1,10-decanediamine (10DA, >98%), glycerol 1,2-carbonate (glycerol carbonate, >90%), 1,3-dioxane-2-one (trimethylene carbonate, TMC, >98%), lithium aluminum hydride (LiAlH₄, 95%), epichlorohydrin (>99%), 1,4-diaminobutane (4DA, >98%), 1,10-diaminodecane (10DA, >97%), 1,12-diaminododecane (12DA, >98%) and diglycerol (DG, >80%), were supplied by TCI, Europe.

Copper (II) chloride (CuCl₂, 99%) and epoxy styrene (98%) were purchased from Acros Organics.

Yttrium chloride (YCl₃, anhydride 99.9%), 1-[3,5-Bis(trifluoromethyl)phenyl]-3-[(1S,2S)-(+)-2-(dimethylamino)cyclohexyl]thiourea and 1-[3,5-Bis(trifluoromethyl)phenyl]-3-[(1S,2S)-(+)-2-(dimethylamino)cyclohexyl]thiourea (Takemoto TU,>98%) were supplied by STREM.

Priamine[®] 1075 was kindly supplied by CRODA.

Uranyl acetate dehydrate was supplied by TAAB.

Oleyl alcohol (99.9%), oleyl methanesulfonate (>99%) and methyl oleate (99%) were purchased from Nu-Check-Prep.

ITERG kindly provided 20 g of *UndCC-ester*. All products and solvents (reagent grade) were used as received except otherwise mentioned. The solvents were of reagent grade quality and were purified wherever necessary according to the methods reported in the literature.

Methods

Nuclear Magnetic Resonance (NMR)

^1H and ^{13}C -NMR spectra were recorded on Bruker Avance 400 spectrometer (400.20 MHz or 400.33 MHz and 100.63 MHz for ^1H and ^{13}C , respectively) by using CDCl_3 or DMSO-d_6 as a solvent at room temperature, except otherwise mentioned. ^{13}C DEPT (Distortionless Enhancement of Polarisation Transfer) and Two-dimensional analyses such as ^1H - ^1H COSY (CORrelation SpectroscopY), ^1H - ^1H TOCSY (TOtal Correlation SpectroscopY), ^1H - ^{13}C HSQC (Heteronuclear Single Quantum Spectroscopy) and ^1H - ^{13}C HMBC (Heteronuclear Multiple Bond Correlation) were also performed.

Fourier Transformed Infra-Red-Attenuated Total Reflection (FTIR)

Infrared spectra were obtained on a Bruker-Tensor 27 spectrometer, equipped with a diamond crystal, using the attenuated total reflection mode. The spectra were acquired from 400 to 4000 cm^{-1} using 16 scans at a resolution of 4 wavenumbers.

Flash chromatography

Flash chromatography was performed on a Grace Reveleris apparatus, employing silica cartridges from Grace. Cyclohexane: ethyl acetate and dichloromethane: methanol gradients were used as eluents depending on the products. The detection was performed through ELSD and UV detectors at 254 nm and 280 nm.

Gas chromatography (GC)

The gas chromatography analyses were performed by ITERG using a Shimadzu GC equipped with: Flame ionization detectors (FID, 380°C) and Zebron ZB-5HT (5% phenyl - 95% dimethylpolysiloxane) 15 m x 0.25 mm ID, 0.1 μm thickness capillary column. The carrier gas was hydrogen. The column temperature was initially set at 60°C (volume injected: 1 μl), then increased to 370°C at a rate of $10^\circ\text{C}\cdot\text{min}^{-1}$ and held isothermally for 10 min.

High-Performance Liquid Chromatography (HPLC)

HPLC was performed at the ITERG using a Shimadzu instrument fitted with an Agilent PLgel 5 μm MIXED-D column (300 mm, 7.5 mm diameter) and compounds were detected by a RID detector at 40°C . The samples were diluted in THF at $10\text{ mg}\cdot\text{L}^{-1}$ and filtered before injection in the column. The analyses were performed with THF as eluent at 40°C .

Size Exclusion Chromatography in DMF and THF (SEC)

Size Exclusion Chromatography analyses were performed in DMF (25°C) on a PL-GPC50 plus integrated GPC from Polymer laboratories-Varian with a series of three columns from Polymer Laboratories (PLgel: PLgel 5µm Guard (guard column 7.5 mm ID x 5.0 cm L); PLgel 5µm MIXED-D (7.5 mm ID x 30.0 cm L) and PLgel 5µm MIXED-D (7.5 mm ID x 30.0 cm L)).

Size Exclusion Chromatography analyses were performed in THF (25°C) on a PL GPC50 and with four TSK columns: HXL-L (guard column), G4000HXL (particles of 5 mm, pore size of 200A, and exclusion limit of 400000 g/mol), G3000HXL (particles of 5 mm, pore size of 75A, and exclusion limit of 60000 g/mol), G2000HXL (particles of 5 mm, pore size of 20 A, and exclusion limit of 10000 g/mol) at an elution rate of 1 mL/min.

In both cases, the elution times of the filtered samples were monitored using UV and RI detectors and SEC were calibrated using polystyrene standards.

Differential Scanning Calorimetry (DSC)

Differential scanning calorimetry thermograms were measured using a DSC Q100 apparatus from TA instruments. For each sample, two cycles from -80 to 160°C at 10°C.min⁻¹ (additional isotherm of 15 min at 160°C at the end of the first cycle to remove the residual DMF when necessary) were performed and then the glass transition and melting temperatures were calculated from the second heating run.

Thermogravimetric analysis (TGA)

Thermogravimetric analyses were performed on TGA-Q50 system from TA instruments at a heating rate of 10 °C.min⁻¹ under nitrogen atmosphere from room temperature to 600°C, with an isotherm at 160°C for 15 min to remove the residual DMF, when required.

X-Ray diffraction

The data for the crystal structure of DGDC was collected on a Bruker microstar X8 PROTEUM with a classical kappa geometry and Platinum135 CCD camera. All the statistics are compiled in table SX. The structure was solved by the AB-initio method implemented in SHELXD and refined with SHELXL (Sheldrick, G.M. Acta Cryst. A64, 2008, 112-122). Full-matrix least-squares refinement was performed on F^2 for all unique reflections, minimizing $w(F_o^2 - F_c^2)^2$, with anisotropic displacement parameters for non-hydrogen atoms. The positions

of the H atoms were deduced from coordinates of the non-H atoms. The non-H atoms were refined with anisotropic temperature parameters.

Time-Of-Flight Mass Spectrometer with ElectroSpray Ionization (ESI-TOF MS)

Mass spectra were performed by the Centre d'Etude Structurale et d'Analyse des Molécules Organiques (CESAMO) on a QStar Elite mass spectrometer (Applied Biosystems). The instrument is equipped with an ESI source and spectra were recorded in the negative/positive mode. The electrospray needle was maintained at 4500 V and operated at room temperature. Samples were introduced by injection through a 20 μL sample loop into a 400 $\mu\text{L}/\text{min}$ flow of methanol from the LC pump. Sample was dissolved in DCM at 1 mg/ml, and then 10 μl of this solution was diluted in 1 mL of methanol.

Time-Of-Flight Mass Spectrometer with Matrix-Assisted Laser Desorption/Ionization (MALDI-TOF MS)

MALDI-MS spectra were performed by the *Centre d'Etude Structurale et d'Analyse des Molécules Organiques (CESAMO)* on a Voyager mass spectrometer (Applied Biosystems). The instrument is equipped with a pulsed N_2 laser (337 nm) and a time-delayed extracted ion source. Spectra were recorded in the positive-ion mode using the reflectron and with an accelerating voltage of 20 kV. Samples were dissolved DMF at 10 mg/mL. The DHB matrix (2,5-dihydroxybenzoic acid) solution was prepared by dissolving 10 mg in 1 mL of DMF. A methanol solution of cationisation agent (NaI, 10 mg/mL) was also prepared. The solutions were combined in a 10:1:1 volume ratio of matrix to sample to cationisation agent. One to two microliters of the obtained solution was deposited onto the sample target and vacuum-dried.

Copolymer self-assembly by nano-precipitation

The self-assembly in water of the copolymers was carried out by nano-precipitation. Copolymers were dissolved in 1 mL of THF at 10 mg/mL and the resulting solution was added drop-wise to 10 mL of water under magnetic stirring. Then, THF was evaporated under the fume hood for 2 days before being analyzed by dynamic light scattering (DLS).

Dynamic Light Scattering (DLS)

Dynamic Light Scattering (DLS) measurement was carried out at 25°C with a Malvern Instrument Nano-ZS equipped with a He-Ne laser (1/4 632.8 nm). Samples (1 $\text{g}\cdot\text{L}^{-1}$) were

introduced into cells (pathway: 10 mm) after filtration through 1 μm nylon microfilters. The measurements were performed at a scattering angle of 90° .

Transmission Electron Microscopy (TEM)

TEM images of copolymer were recorded on a HitachiH7650 microscope working at 80 kV equipped with a GATAN Orius 10.5 Megapixel camera (Bordeaux Imaging Center, Bordeaux, France). Samples were prepared by depositing a 1 g.L^{-1} solution in water of the polymeric aggregates onto a copper grid (200 mesh coated with carbon). The excess solution was removed with a filter paper and the grid was dried under ambient air for 1.5 min. For negative stained, a drop of a uranyl acetate solution (1 w.%) was placed on the grid and dried for 1.5 min after removal of the excess with a filter paper.

UV Optic Fiber

Thiol-ene coupling were performed using a UV Optic fiber from HAMAMATSU equipped with a LC8 lamp (full power of 4000 mW.cm^{-1}) and an A9616-05 filter transmitting in the range 350-400 nm, avoiding the heating of the mixture reaction.

Elementary analyses

Elementary analyses were performed by the Institut des Sciences Analytiques (ISA) of Villeurbanne, France.

DFT Calculation

DFT calculations were done using GAUSSIAN09 with the B3LYP hybrid functional and a high quality 6-311++G(d) basis set.

Reference : M. J. Frisch, G. W. Trucks, H. B. Schlegel, G. E. Scuseria, M. A. Robb, J. R. Cheeseman, G. Scalmani, V. Barone, B. Mennucci, G. A. Petersson, H. Nakatsuji, M. Caricato, X. Li, H. P. Hratchian, A. F. Izmaylov, J. Bloino, G. Zheng, J. L. Sonnenberg, M. Hada, M. Ehara, K. Toyota, R. Fukuda, J. Hasegawa, M. Ishida, T. Nakajima, Y. Honda, O. Kitao, H. Nakai, T. Vreven, J. A. Montgomery Jr., J. E. Peralta, F. Ogliaro, M. J. Bearpark, J. Heyd, E. N. Brothers, K. N. Kudin, V. N. Staroverov, R. Kobayashi, J. Normand, K. Raghavachari, A. P. Rendell, J. C. Burant, S. S. Iyengar, J. Tomasi, M. Cossi, N. Rega, N. J. Millam, M. Klene, J. E. Knox, J. B. Cross, V. Bakken, C. Adamo, J. Jaramillo, R. Gomperts, R. E. Stratmann, O. Yazyev, A. J. Austin, R. Cammi, C. Pomelli, J. W. Ochterski, R. L. Martin, K. Morokuma, V. G. Zakrzewski, G. A. Voth, P. Salvador, J. J. Dannenberg, S. Dapprich, A. D. Daniels, Ö. Farkas, J. B. Foresman, J. V. Ortiz, J. Cioslowski and D. J. Fox, Gaussian, Inc., Wallingford, CT, USA, 2009.

Conception de carbonates cycliques originaux et d'amines issus d'huiles végétales pour la synthèse de Poly(hydroxyuréthane)s

Résumé: Cette thèse porte sur la conception de carbonates cycliques originaux et d'amines dérivés des huiles végétales dans le but de synthétiser des poly(hydroxyuréthane)s entièrement bio-sourcés. D'une part, deux voies d'accès à des amines dérivées d'acides gras utilisant des conditions douces ont été étudiées. La première consiste en l'oxydation sous air d'alcools aliphatiques en nitriles en présence de TEMPO supporté sur silice, suivi par une hydrogénation des dinitriles en diamines. Egalement, des diènes dérivés d'acides gras ont été couplés à la cystéamine *via* une chimie thiol-ène, permettant l'accès à des diamines aliphatiques bio-sourcées. D'autre part, des carbonates cycliques substitués à 5 chaînons ont été synthétisés à partir de dérivés d'acides gras et de glycérol, dans le but d'augmenter leur réactivité vis-à-vis de l'aminolyse. En insérant un groupement fonctionnel éther, thio-éther ou ester en position α ou β des carbonates cycliques, la réactivité de ces derniers vis-à-vis des amines a pu être ajustée. L'étude de la sélectivité, des réactions secondaires et de la catalyse de la voie carbonate/amine a été menée afin de mieux appréhender cette voie d'accès à des polyuréthanes sans isocyanates. Des poly(hydroxyuréthane)s entièrement oléo-sourcés ont été synthétisés avec succès, montrant des propriétés physico-chimiques contrôlables selon la structure des monomères.

Mots clés: *Amines, Carbonates cycliques, Huiles végétales, Acides gras, Glycerol, Polyurethanes sans isocyanate, Poly(hydroxyuréthane)s.*

Design of original vegetable oil-based cyclic carbonates and amines towards Poly(hydroxyurethane)s

Abstract: In this thesis, vegetable oils were used as a platform to design original cyclic carbonates and amines with the goal to synthesize fully bio-based poly(hydroxyurethane)s. On the one hand, two routes to fatty acid-based amines were implemented in mild conditions. First, the oxidation of aliphatic alcohols into nitriles was performed under air in the presence of supported TEMPO on silica, followed by hydrogenation of nitrile compounds into corresponding amines. Second, thiol-ene chemistry was performed on unsaturated fatty acid substrates to design original aliphatic bio-based diamines. On the other hand, substituted 5-membered cyclic carbonates were designed from fatty acids and glycerol derivatives to enhance their reactivity towards aminolysis. By inserting ether, thio-ether or ester functionalities in α - or β -position of the cyclic carbonates, their reactivity towards amines could be tuned. Investigations on the selectivity, side reactions and catalysis of the carbonate-amine reaction were carried out to apprehend this route to non-isocyanate polyurethanes. Fully vegetable oil-based PHUs with tunable physico-chemical properties with respect to the monomer structures could be easily achieved.

Keywords: *Amines, Cyclic carbonates, Vegetable oils, Fatty acids, Glycerol, Non-Isocyanate Polyurethanes, Poly(hydroxyurethane)s.*

Laboratoire de Chimie des Polymères Organiques
16 Avenue Pey-Berland
F-33607 Pessac

